uOttawa

L'Université canadienne
Canada's university

FACULTÉ DES ÉTUDES SUPÉRIEURES ET POSTOCTORALES

uOttawa

L'Université canadienne
Canada's university

FACULTY OF GRADUATE AND POSDOCTORAL STUDIES

Stacey A. Santi
AUTEUR DE LA THÈSE / AUTHOR OF THESIS

Ph.D. (Biochemistry)
GRADE / DEGREE

Department of Biochemistry, Microbiology and Immunology
FACULTÉ, ÉCOLE, DÉPARTEMENT / FACULTY, SCHOOL, DEPARTMENT

The Characterization and Regulation of the AKT Isoforms in Breast Cancer
TITRE DE LA THÈSE / TITLE OF THESIS

Hoyun Lee
DIRECTEUR (DIRECTRICE) DE LA THÈSE / THESIS SUPERVISOR

Jonathan Lee
CO-DIRECTEUR (CO-DIRECTRICE) DE LA THÈSE / THESIS CO-SUPERVISOR

EXAMINATEURS (EXAMINATRICES) DE LA THÈSE / THESIS EXAMINERS

Christina Addison

Jim Dimitroulakos

Christine Pratt

James Woodget

Gary W. Slater
Le Doyen de la Faculté des études supérieures et postdoctorales / Dean of the Faculty of Graduate and Postdoctoral Studies

THE CHARACTERIZATION AND REGULATION OF THE AKT ISOFORMS IN BREAST CANCER

by

STACEY A. SANTI

A thesis submitted to The Faculty of Graduate and Postdoctoral Studies
In partial fulfillment of the requirements for the degree of

DOCTOR OF PHILOSOPHY

Department of Biochemistry, Microbiology and Immunology
University of Ottawa
Ottawa, Ontario, Canada

Your file Votre référence
ISBN: 978-0-494-61226-2
Our file Notre référence
ISBN: 978-0-494-61226-2

ABSTRACT

Akt/PKB (protein kinase B) is a serine-threonine kinase involved in the regulation of many cellular processes, such as proliferation, metabolism, and cell survival. The elevated activation of the PI3K-Akt (phosphatidylinositol-3 kinase/Akt) pathway has been associated with tumor progression and increased tumour aggressiveness. Akt consists of three isoforms; Akt1, Akt2 and Akt3 (PKBα, PKBβ, and PKBγ, respectively) which share high similarity at the amino acid level (~80%). Due to their similarity, it is generally assumed that the three isoforms regulate the same cellular processes, as well as signal to the same downstream substrates with similar preference. However, accumulating lines of evidence now suggest that the isoforms may regulate different cellular processes and are not functionally redundant. To further study the Akt isoforms and the role they play in the progression of tumorigenesis, a model of breast cancer (MDA-MB231 cell line) was employed. The Akt isoforms were first characterized through the examination of their subcellular localization to discern if differences in functional regulation can be inferred through their localization. The data obtained from this work demonstrated that the isoforms displayed differential subcellular localizations. Specifically, Akt2 was found co-localized with the mitochondria, while Akt3 resided in the nucleus, thereby challenging the accepted notion that the isoforms are localized only in the cytoplasm. Next, studies were undertaken to determine which isoform is most important for cancer cell survival. Akt2 was found to be the most important isoform for survival in MDA-MB231 cells. Targeted ablation of each isoform using siRNA showed that Akt2 regulated cancer cell proliferation specifically by promoting cell cycle progression via the regulation of Cdk2, p27 and cyclin D. In addition, Akt2 ablation inhibited activation of the mTOR pathway through the downregulation of p70S6K. Prolonged

inhibition of Akt2 altered mitochondrial morphology and eventually led to autophagy of the mitochondria (mitophagy). Collectively, the results of these studies impart a distinct role for Akt2 in cancer cell progression and survival and provide evidence that Akt2 may be a relevant target for future cancer therapies.

ACKNOWLEDGEMENTS

First, I would like to thank my supervisor, Dr. Hoyun Lee for the opportunity to work in his research lab. When I first met Dr. Lee I had no molecular biology experience—just a large learning curve to conquer and a promise to him that I would work very hard. I learned so much about science from Dr. Lee. I will always be indebted to you for the training I received. Your patience as both a supervisor and a teacher and your passion for science are truly admirable and I sincerely thank you.

I would also like to thank Dr. Robert Lafrenie who is as fascinated by signal transduction research as I am. Thank you for the many hours you spent with me talking to me about Akt and assisting myself and Dr. Lee with troubleshooting. Your excellent suggestions, advice and encouragement were always welcomed and sincerely appreciated. Early, in the beginning of my PhD studies, you told me to trust my instincts about my data—it turned out to be some of the best advice I was given. Thank you for being both a mentor and a friend.

I would like to thank my co-supervisor, Dr. Jonathan Lee, and my committee members, Dr. Ian Lorimer, Dr. Bruce McKay, and Dr. Joanne Dillon. Your guidance and suggestions throughout the course of this work were invaluable.

I wish to acknowledge the members of Dr. Lee's research group (past and present) for a great working atmosphere: Paul Guerin, Changkun Hu, Byung Ju Kim, So-Young Kim, Michelle Leonard, Ningning Li, and Catharine Song. Special thanks to Renee Borkovich for being my own personal science experiment as a summer student and making me laugh. I would also like to thank Dr. Stanislav Naryzhny for your experimental guidance, helpful suggestions and a never-ending supply of dark chocolate—you are right—chocolate *can* make me forget about a bad day.

I was extremely fortunate to work in an environment where individuals were passionate about science and willing to assist you achieve your goals. There were many people who had suggestions, shared protocols and made my time at the University of Ottawa and the Northeastern Ontario Regional Cancer Centre an amazing experience: Dr. Baoqing Gao, Lisa Falcioni, Stacey Hembruff, Monique Laberge, Dr. Carita Lanner, Nina Maki, David Villeneuve, Andrew Young, Helen Zhao. Thank you for your help.

Very special thanks to Jane Vanderklift and Carol Ann Kelly. Thank you Jane, for everything you do around the lab to make life as easy as possible for students. Carol Ann: thank you for all of your help at the Department of BMI and helping make the distance between Sudbury and Ottawa so much easier.

One of the best outcomes from my PhD studies were the friends that I made: Julia Romero-how can I thank you? It is an honour and a pleasure to stand beside you at the lab bench every day. To Ken and Cory Steinberg: our friendship has endured since we first met at NEORCC. Thank you for letting myself and Chris be a part of your family.

Lastly, I would like to thank my family: my sister Lori and my husband Chris. Words cannot express how much I love you or how grateful I am for everything you both have done for me. To my mother and my father: Thank you for always being there for me. Your constant support, love and guidance have made me who I am today. Dad-you have demonstrated to me what real strength is in the face of life's adversities and always remained the optimist. A special thank you to my best friend Kristin Schafer-we have been through many roads together. I am grateful to have you as a best friend; you are a part of my family. Thank you to my grandmother, Assunta- you are still one of the most remarkable women I have ever known. This is for every candle you used to light for me when I was studying and writing exams. I wish you were still here to see this.

TABLE OF CONTENTS

LIST OF ABBREVIATIONS

ADP	adenosine diphosphate
AO	acridine orange
AMPK	AMP-activated protein kinase
ANOVA	analysis of variance
ATP	adenosine triphosphate
BCA	bicinchoninic acid
BrdU	bromodeoxyuridine
BSA	bovine serum albumin
Cdk	cyclin-dependent kinase
DMSO	dimethyl sulfoxide
DNA-PK	DNA-dependent protein kinase
ER	endoplasmic reticulum
ERK	extracellular signal-related kinase
FACS	flow assisted cell sorting
FBS	fetal bovine serum
FITC	fluorescein isothiocyanate
FoxO	Forkhead family of transcription factors
FTI	farnesyl protein transferase inhibitor
GSK-3α/β	glycogen synthase kinase-3 alpha/beta isoform
HEK	human embryonic kidney
IGF-1	insulin-like growth factor-1
ILK	interleukin kinase
IP/W	immunoprecipitation-Western blot analysis
LC3	light chain 3
LSM	laser scanning microscope/microscopy
MDC	monodansylcadaverine or danyslcadaverine
MEFs	murine embryonic fibroblasts
mRNA	messenger RNA
MTT	thiazolyl blue tetrazolium bromide
Na_2VO_3	sodium orthovanadate
NaF	sodium fluoride
NaN_3	sodium azide
NO	nitric oxide
eNOS	endothelial nitric oxide synthase
ORF	open reading frame
PAGE	polyacrylamide gel electrophoresis
PBS	phosphate-buffered saline
PCR	polymerase chain reaction
PDI	protein disulfide isomerase
PDK1	phosphoinositide-dependent kinase-1
PEPCK	phosphoenolpyruvate carboxykinase
PGC-1α	peroxisome proliferator-activated receptor-coactivator 1α
PHLPP	PH-domain leucine-rich repeat protein
PI	propidium iodide

$PI(3,4,5)P_3$	phosphatidylinositol-3,4,5-triphosphate
$PI(4,5)P_2$	phosphatidlyinositol-4,5-bisphosphate
PI3K	phosphatidylinositol-3 kinase
PKB	protein kinase B
PMSF	phenylmethylsulfonyl fluoride
PTEN	phosphatase and tensin homologue deleted on chromosome 10
PVDF	polyvinylidene difluoride
q-PCR	quantitative PCR (polymerase chain reaction)
ROS	reactive oxygen species
RTKs	receptor tyrosine kinases
rhEGF	recombinant human epidermal growth factor
SDS	sodium dodecyl sulfate
shRNA	short-hairpin RNA
siRNA	small interfering RNA
Skp2	S-phase kinase associated protein 2
TBS	tris-buffered saline
TGN38	trans-golgi network protein 2
VDAC1	voltage-dependent anion-selective channel protein 1

LIST OF FIGURES

LIST OF TABLES

CHAPTER 1.0

INTRODUCTION

1.0 INTRODUCTION

The PI3K/Akt axis regulates many cellular functions in mammalian systems, making it one of the most extensively studied protein kinase signaling pathways in molecular biology. Signaling through the axis regulates the delicate balance between cellular life and death by controlling processes such as cellular metabolism, proliferation, cell cycle progression, and protein synthesis, as well as apoptosis and autophagy (reviewed in Bellacosa, et al., 2005; Manning and Cantley, 2007; Nicholson and Anderson, 2002). Akt consists of three highly conserved and highly similar isoforms, Akt1, Akt2 and Akt3 (also referred to as PKBα, PKBβ, and PKBγ). The functional differences in isoform regulation are obscured by the fact that many published findings examine total Akt (although this is most likely Akt1). Frequently, these studies employ the use of inhibitors that block upstream activation of Akt such as LY294002 and wortmannin that act on PI3K. This effectively inhibits all Akt activation and Akt-specific signaling to all downstream substrates, suggesting that the Akt isoforms are functionally redundant. However, accumulating lines of evidence citing differential regulation of the Akt isoforms in glucose metabolism have begun to underscore the fact that the regulation of Akt may occur in a more finely-controlled manner than previously thought (Stambolic and Woodgett, 2006). It is increasingly evident that the three kinases regulate different cellular processes, demonstrated *in vitro* and *in vivo* through knockout mice studies (Cho et al., 2001a; Cho et al., 2001b; Dummler et al., 2006), and may have preferential downstream signaling substrates thereby calling the assumption of functional redundancy into question.

Due to the importance of the cellular processes that PI3K regulates, it seems logical that the PI3K/Akt axis would be an attractive candidate for therapeutic cancer treatments,

since many substrates of PI3K, and PI3K itself are frequently deregulated in many types of cancer. For example, amplification or alteration of the gene that encodes the p110α subunit of PI3K (*PIK3CA)* (Shayesteh et al., 1999) have been observed, as have deletions or mutations in PTEN, the phosphatase that negatively regulates the signaling pathway. Thus, alterations in either PI3K, or mutations in PTEN constitutively activate the Akt signaling pathway. However, the individual contribution of the Akt isoforms in cancer and the role they play in cancer progression is not currently known.

1.1 The hypothesis and objectives of the study

The rationale of the current study was to investigate the widely-cited premise that the Akt isoforms are functionally redundant. The PI3K/Akt pathway plays an important role in the activation and promotion of oncogenesis. These studies examined the role played by each of the Akt isoforms on oncogenesis in an aggressive model of breast cancer. The hypothesis of the thesis was that the different Akt isoforms would show distinct effects in the regulation of breast cancer and that one isoform is more important in regulating breast cancer cell survival.

The overall objectives of the studies included in this thesis were to investigate the regulation of the Akt isoforms, and determine the mechanism(s) that contribute to breast cancer cell survival. Specifically, the objectives of the study were to:

1. Determine if there is differential subcellular localization of the Akt isoforms that would contribute to their function and regulation in breast cancer; and
2. Determine which isoform is most important for cell survival and the mechanisms involved in this process in an aggressive breast cancer cell line.

1.2 BACKGROUND

1.2.1 Discovery of the Akt kinases

The Akt serine/threonine kinase is found downstream of phosphatidylinositol-3 kinase (PI3K), and has a central role in the regulation of many cell processes. Through a series of activating or inhibitory phosphorylations, Akt regulates many crucial cell functions, such as survival and metabolism. This fact makes Akt an integral protein to study in tumorigenesis and the study of Akt has produced a plethora of literature (approximately 17,000 English publications on Akt are presently cited in the PubMed database). Historically, Akt (then called AKT8) was isolated from a T-cell lymphoma (discovered by Staal et al., 1977; reviewed in Bellacosa et al., 2005). Subsequent cloning analyses revealed similarities in homology between AKT1 and protein kinase A and C (reviewed in Bellacosa et al., 2005; Coffer et al., 1998; Nicholson and Anderson, 2002). Thus, early reports labeled Akt1 as PKBα, or RAC-PKα (Related to PKA and PKC) (Coffer and Woodgett, 1991; Jones et al., 1991, reviewed in Bellacosa et al., 2005). Akt2, also known as PKBβ, was cloned shortly thereafter and found to be overexpressed in both ovarian cancer cell lines and tumours (Cheng et al., 1992). The discovery of Akt3 came much later and three labs reported the cloning of human Akt3 in close succession (Brodbeck et al., 1999; Masure et al., 1999; Nakatani et al., 1999a).

1.2.2 Structure of the Akt isoforms

The three Akt kinases have been mapped to separate genes: 14q32 for Akt1, 19q13.1-q13.2 for Akt2 (Coffer et al., 1998), and 1q43-44 for Akt3, respectively (Masure et al., 1999). Despite the fact that they are encoded by different genes, the Akt isoforms are highly

conserved with all three isoforms consisting of an N-terminal pleckstrin homology (PH) domain, a catalytic or kinase domain, and a regulatory domain, also referred to as the C-terminal extension region. Both the kinase and regulatory domain share similarity with PKA and PKC explaining their early nomenclature (Coffer et al., 1998). The isoforms are highly similar, displaying approximately 80% amino acid identity in the PH domains, 90% in the catalytic domains, and 70% in the C-terminal extension region (Nicholson and Anderson, 2002; Kumar and Madison, 2005). Divergences in their composition occur in the linker region (LR) that joins the PH domain to the catalytic domain (Kumar and Madison, 2005). The catalytic or kinase domain includes the threonine 308 (T308) phosphorylation site that is required for activation of Akt, while the second Akt phosphorylation site, serine 473 (S473) is found in the C-terminal extension region. Full activation of Akt requires phosphorylation at both of these sites.

A splice variant has been reported for Akt3, and is referred to as Akt3-v1 (Akt3 variant 1) (Brodbeck et al., 2001). Akt3-v1 lacks the C-terminal S472 phosphorylation site. The mechanism of how the Akt3 splice is generated is not currently known. Further, little is known regarding how the Akt3 splice variant functions *in vitro* and *in vivo*, given that full activation of the kinase does not occur with the missing phosphorylation site. Two papers have reported on the function of Akt3-v1 (Brodbeck et al., 2001, Taniyama et al., 2005). Brodbeck et al. (2001) found that Akt3-v1 showed lower kinase activation than full length-Akt3 and kinase activation was not induced by stimuli normally shown to activate PI3K/Akt, such as insulin. Instead, Akt3-v1 reacted to treatment with pervanadate, which is interesting given that pervanadate is insulin mimetic. Taniyama et al., (2005) overexpressed the splice variant in the hearts of transgenic mice. They determined that the splice was functional, and in the short-term, was cardioprotective. However, long term overexpression of the splice was

pathological, with the transgenic mice displaying cardiac hypertrophy. Further studies are required to ascertain the physiological function of the Akt3 splice variant. A schematic of the Akt kinases is presented in Fig. 1.1. For a comparative analysis of the amino acid and nucleotide homology, please see Appendix I, Fig. A1-A2. To date, only the crystal structure of the kinase domain of Akt2 is known (Huang et al., 2003).

1.2.3 Activation and regulation of the Akt Isoforms

Stimulation of receptor tyrosine kinases (RTKS) or G-protein coupled receptors initiates the activation of PI3K/Akt. Activation occurs at the cell membrane through a myriad of stimuli such as growth factors, DNA damage, chemotherapy, and environmental stressors. Activation of RTKs produces a series of lipid phosphorylations at the cell membrane catalyzed by PI3K, most importantly, the conversion of phosphatidylinositol-4,5-bisphosphate ($PI(4,5)P_2$) to phosphatidylinositol-3,4,5-triphosphate ($PI(3,4,5)P_3$). These lipid phosphorylations promote the translocation of Akt from the cytosol to the membrane and promote binding of the PH domain to PIP_3. The localization of Akt at the cell membrane prompts membrane-localized PDK1 (phosphoinositide-dependent kinase-1) to phosphorylate Akt at T308 in the T-loop or, activation loop (Bellacosa et al., 2005) in the catalytic domain. Full activation of Akt is achieved by the subsequent phosphorylation of the second phosphorylation site in the C-terminus at S473. Published reports have indicated that the phosphorylation at T308 more potently activates Akt ($\sim$ 100-fold) compared to S473 phosphorylation ($\sim$10-fold) (Alessi et al., 1996). Regardless, for full activation of Akt, both sites must be phosphorylated. For a schematic of Akt activation, please refer to Fig. 1.2.

The kinase responsible for the S473 phosphorylation site has been controversial and hotly debated for years in the literature. Various candidates have been proposed, such as

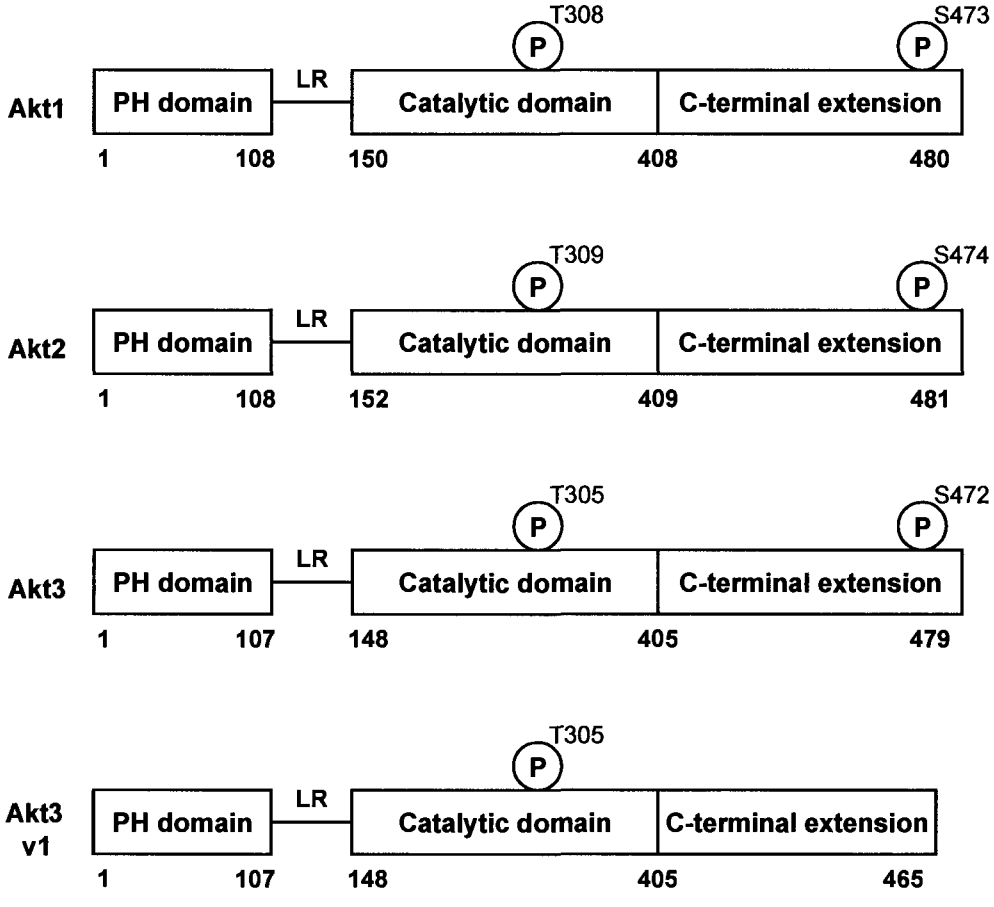
T308
S473
P
P
Akt1
PH domain
LR
Catalytic domain
C-terminal extension
1
108
150
408
480
T309
S474
P
P
Akt2
PH domain
LR
Catalytic domain
C-terminal extension
1
108
152
409
481
T305
S472
P
P
Akt3
PH domain
LR
Catalytic domain
C-terminal extension
1
107
148
405
479
T305
P
Akt3
v1
PH domain
LR
Catalytic domain
C-terminal extension
1
107
148
405
465

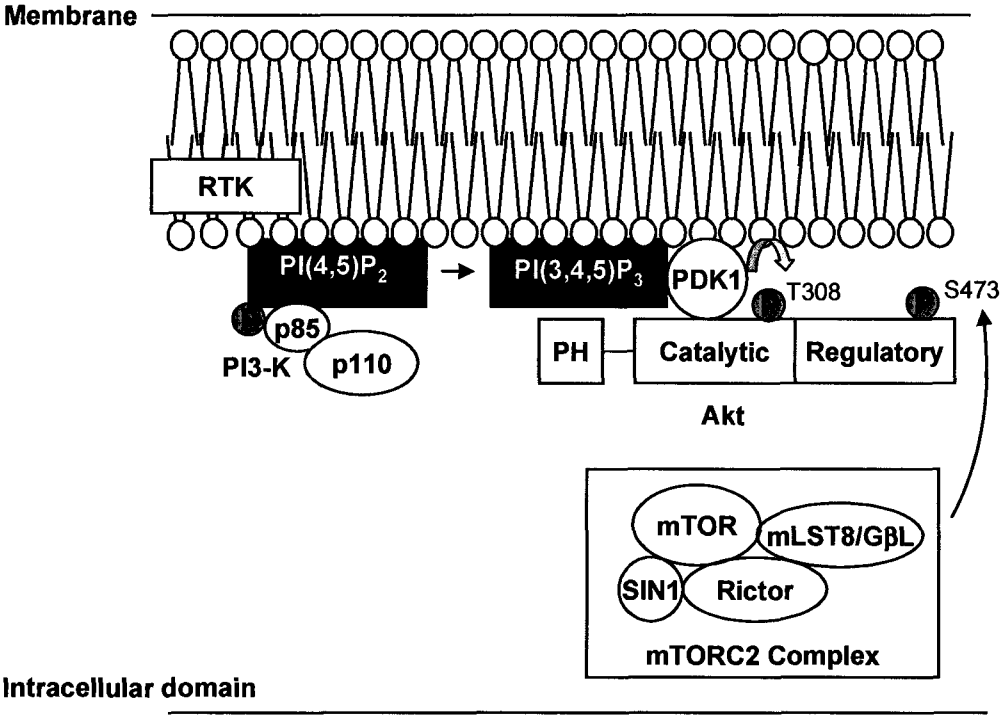
Membrane
RTK
PI(4,5)P2
PI(3,4,5)P3
PDK1
T308
S473
p85
PI3-K
p110
PH
Catalytic
Regulatory
Akt
mTOR
mLST8/GβL
SIN1
Rictor
mTORC2 Complex
Intracellular domain

DNA-PK (Feng, et al., 2004), PDK1 (Balendran et al., 1999), ILK (Troussard et al. 2003), autophosphorylation by Akt itself (Toker and Newton, 2000), and a yet-to-be identified PDK2. It has recently been discovered that the elusive S473 site is most likely Rictor, which exists within the mTORC2 protein complex that regulates the mammalian target of rapamycin (mTOR) (Hresko and Mueckler, 2005; Sarbassov et al., 2005). mTOR, complexed with Rictor in mTORC2, is not sensitive to rapamycin, and is purported to be involved in cytoskeletal organization, as well as Akt phosphorylation (Schieke and Finkel, 2006). In contrast, when mTOR is complexed in mTORC1 which contains Raptor, mTOR is sensitive to rapamycin-treatment and regulates protein synthesis through downstream targeting of p70S6K and 4E-BP1 (Schieke and Finkel, 2006). mTOR was originally proposed to be a downstream target of Akt, however the discovery of the S473 regulation, places it both up- and downstream in the Akt signaling pathway, revealing additional layers of complexity in the regulation of the protein kinase. For a schematic of mTOR regulation downstream of Akt activation, please see Fig. 1.3.

Activation of the isoforms is regulated through the two serine and threonine phosphorylation sites indicated above, T308/S473 for Akt1. The parallel activation sites for the remaining two isoforms are T309/S474 for Akt2, and T305/S472 for Akt3 (reviewed in Nicholson and Anderson, 2002). It is currently hypothesized that the activation of the three Akt kinases proceeds in the same manner as what is known for Akt1, since there is no contrary evidence to indicate otherwise.

Akt activation is constrained by the tumour suppressor PTEN, which dephosphorylates PIP_3. Recently, Brognard et al. (2007) found that PHLPP (PH-domain leucine-rich repeat protein) dephosphorylated the S473 Akt phosphorylation site (Fig. 1.3).

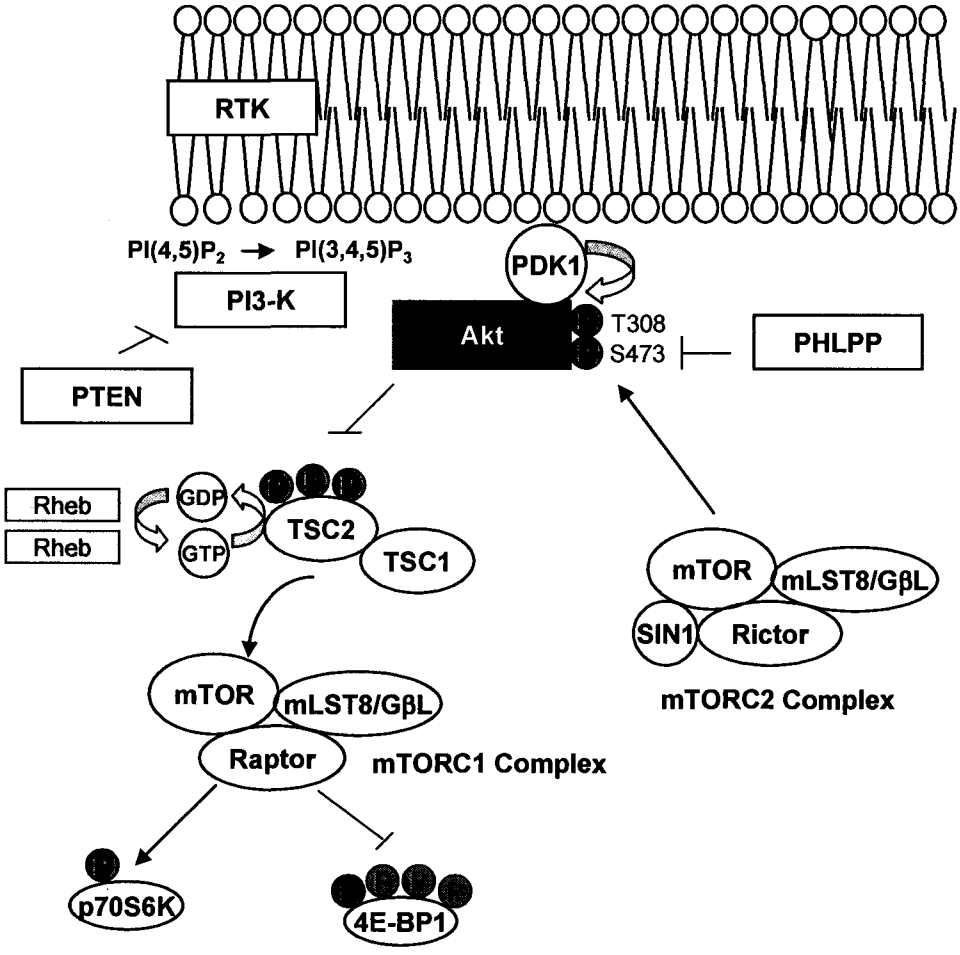
RTK
PI(4,5)P2
PI(3,4,5)P3
PDK1
PI3-K
Akt
T308
S473
PHLPP
PTEN
Rheb
Rheb
GDP
GTP
TSC2
TSC1
mTOR
mLST8/GβL
SIN1
Rictor
mTORC2 Complex
mTOR
mLST8/GβL
Raptor
mTORC1 Complex
p70S6K
4E-BP1

1.2.4 Akt signaling to downstream substrates

Akt mediates activation of target substrates through phosphorylation(s) of downstream proteins with the 'phospho-Akt substrate' (PAS) motif, RXRXX(S/T), where "X" represents any amino acid (Manning and Cantley, 2007). Phosphorylation by Akt is either an activating phosphorylation, or an inhibitory one, and it is the phosphorylation(s) of target downstream substrates that regulate the cell processes defined by Akt. Complicating the matter further, however, is the fact that Akt often displays 'dual' regulation for many of its downstream substrates. For instance, Akt phosphorylates and inhibits activation of the Forkhead transcription factors (FoxO family) which ultimately prevents the transcription of pro-apoptotic genes. However, Akt phosphorylation of the FoxO family also regulates the transcription of genes involved in cell metabolism and gluconeogenesis. Figure 1.4 presents a schematic of the more important and well-known downstream Akt substrates, while Table 1.1 lists the substrates targeted by Akt, and indicates the type of phosphorylation and level of regulation mediated by the kinase.

Since the three Akt isoforms are activated in the same manner (i.e., via phosphorylation at the two regulatory sites), their affinity for downstream substrates is assumed to be the same. There are few studies that have shown differential substrate specificity among the Akt isoforms. However, this tenet is mostly due to technical constraints—phosphorylated antibodies to Akt consistently recognize all isoforms. As well, the unavailability of isoform-specific antibodies that were not cross-reactive has confounded both the analysis and examination of isoform-specific downstream targeting until very recently. Recent studies utilizing siRNA technology and transgenic mice (discussed in Section 1.3, below) have revealed that the different Akt isoforms may regulate specific functions.

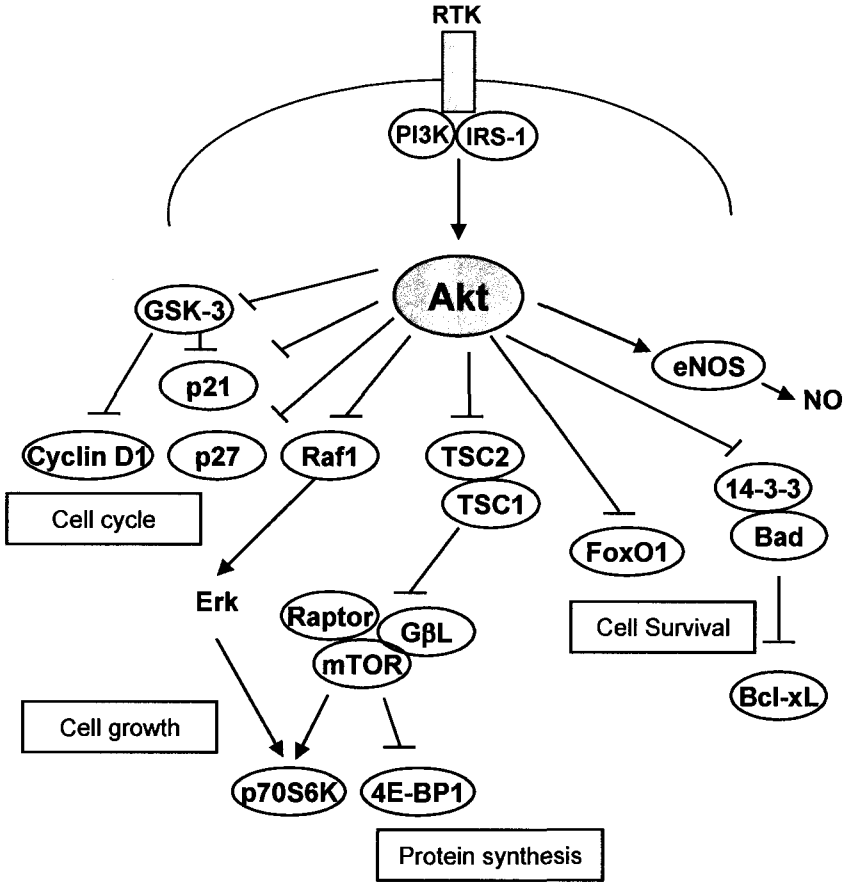
RTK
PI3K
IRS-1
Akt
GSK-3
p21
eNOS
NO
Cyclin D1
p27
Raf1
TSC2
TSC1
14-3-3
Bad
Cell cycle
FoxO1
Erk
Raptor
GβL
mTOR
Cell Survival
Bcl-xL
Cell growth
p70S6K
4E-BP1
Protein synthesis

Table 1.1. The downstream substrates regulated by Akt. Phosphorylations are either activating or inhibitory. The substrates included within this table is not exhaustive, but an overview of well-known and studied Akt substrates [Table adapted from Manning and Cantley, 2007; Nicholson and Anderson, 2002]

Substrate	Phosphorylation Site(s)	Type	Cell Process	Regulation
Bad	S136	Inhibitory	Survival	Promotes binding of pro-apoptotic Bad to 14-3-3 in the cytoplasm to prevent the activation of apoptosis
eNOS	S1177	Activation	Cardiovascular Regulation	Production of nitric oxide (NO), stimulates angiogenesis
FoxO1 FoxO3A, FoxO4/AFX	T24, S256, S319 T32, S253, S315 T32, S197, S262	Inhibitory	Survival	Inhibits transcription of FasL, Bim (proapoptotic genes)
			Metabolism	Regulates transcription of genes involved in gluconeogenesis (PGC-1α)
GSK-3	S9, S21	Inhibitory	Metabolism	Glycogen synthesis
			Cell cycle	Stabilization of cyclin D1
			Survival	Regulation of Mcl-1
IκB kinase	T23	Activation	Survival	Activates NF-κB
Mdm2	S166, S186	Activation	Survival	Inhibit p53
p21	T145	Inhibitory	Cell cycle	Cell cycle progression
p27	T157, T198	Inhibitory	Cell cycle	Cell cycle progression and autophagy
Raf-1	S259	Inhibitory	Proliferation	Activation of Erk kinase
TSC2	S939, T1462	Inhibitory	Metabolism Cell growth Translation Ribosome biogenesis	Regulation of mTOR

1.3 THE AKT ISOFORMS: REGULATION AND FUNCTION

A clear understanding of the regulation and function of the Akt isoforms has been elusive to date. One reason for this, as indicated above, was due to the lack of commercially available antibodies that can selectively target the isoforms. Because of this, the majority of published studies in the literature do not delineate the contribution of the individual isoforms in their studies, choosing instead to study pan-Akt, and total phosphorylated-Akt (usually the S473 residue), which measures the active phosphorylation of all three kinases. In point of this, a search of the PubMed database indicates that there are approximately 17, 000 articles that referenced Akt. When the isoforms are delineated, there are approximately 4000 references on Akt1 (of these, 1205 are cancer-specific), 338 citations for Akt2, and 129 for Akt3. Studies that examined all of the isoforms, in tandem total 78. Further, when the isoforms are examined individually, and the use of cross-reactive antibodies is overlooked, it becomes clear that there are conflicting findings with respect to the functions of the Akt isoforms. This is most likely due to the system studied. For example, a majority of the published reports in the literature employ Hek293, 293T and 3T3-L1 adipocytes to examine the individual functions of the isoforms. In the case of 3T3-L1 adipocytes which are mainly used to study Akt2 regulation in diabetes, this is understandable, however, Akt isoform function in the other cell lines may not be applicable to other biological systems, such as cancer. In short, the findings from the literature can only be interpreted in the original system in which they were studied.

Nonetheless, a clear picture of isoform specificity and regulation has emerged from studies that have selectively targeted the isoforms. The evidence from these reports (discussed below) has revealed specific functions of the isoforms in terms of both normal physiology as well as tumour biology.

1.3.1 Differential tissue distribution of the Akt isoforms

The Akt isoforms appear to display preferential mRNA expression in tissues. While Akt1 is found ubiquitously expressed, Akt2 mRNA expression is highest in tissues that regulate glucose metabolism, such as brown fat, liver, and skeletal muscle (Altomare et al., 1998). Akt3 expression levels are highest in the brain and in urogenital tissues such as the testes, prostate, and uterus (Brodbeck et al., 1999a), although the tissue distribution of Akt3 varies slightly in neonatal mouse samples compared to the mRNA analysis of adult samples (Yang et al., 2005). It is likely that the differential tissue distribution displayed by the isoforms is indicative of the *in vivo* regulation performed by the isoforms in tissues. In the case of Akt2 and the role it plays in the regulation of glucose uptake, this is certainly true.

1.3.2 *In vivo* regulation of the Akt isoforms and knockout mice studies

1.3.2.1 Single Akt isoform deletions

Akt1: Differences in the individual functions of the Akt isoforms have been observed from studies conducted in transgenic knockout mice, where one or two isoforms have been selectively deleted and the resulting phenotypes examined. A study conducted by Chen et al. (2001) noted that Akt1 knockout mice were smaller in overall size relative to the controls and displayed increased levels of apoptosis in the thymus and in the testes resulting in decreased spermatogenesis. In addition, the Akt1-/- mice did not display any differences in glucose or insulin regulation compared to the controls. Results published shortly thereafter by Cho et al. (2001b), confirmed the results of Chen's study also finding that the Akt1 knockout mice were reduced in size, and in concurrence with Chen, finding no alterations in glucose metabolism. However, whereas Chen et al. (2001) found that Akt1 mice were

'viable', Cho et al. (2001b) found that the deletion of the Akt1 gene was 'partially lethal'—Akt1 pups died within three days post-parturition. However, surviving mice maintained the smaller size into adulthood (Cho et al., 2001b). Both studies, however, were in agreement that Akt1 and Akt2 displayed differential regulation of glucose homeostasis, with the Akt2 isoform, playing the predominant role.

Isoform-specific functions of Akt1 have also been associated with ischemia and angiogenesis. A targeted deletion of Akt1 and Akt2 in mice revealed that Akt1-/- mice displayed defects in vascular endothelial growth factor-mediated angiogenesis and ischemia—effects not observed in Akt2-/- mice (Ackah et al., 2005).

Akt2: In contrast, to the Akt1 knockout mice described above, Akt2-knockout mice displayed pathological defects in insulin regulation and glucose homeostasis (Cho et al., 2001a). The transgenic mice in this study displayed a 'mild, but statistically significant fasting hyperglycemia', and were found to be 'slightly glucose intolerant', likely caused by pathological defects in glucose uptake (Cho et al., 2001a). Thus, Akt2-/- mice were insulin resistant. Further, the authors concluded that these features were specific to regulation by Akt2, as Akt1 and Akt3, still present in the knockout mice, were obviously not compensating for the function of the missing isoform (Cho et al., 2001a). For the most part, a follow-up study conducted by Garofalo et al. (2003) confirmed the findings reported by Cho et al. However, the authors noted that the Akt2-/- mice in their study also displayed a growth deficiency similar to what had been reported for Akt1 mice, although the defects in glucose metabolism were still the main phenotypic difference (Garofalo et al., 2003).

Akt3: Given the differential tissue distribution of Akt3, it is not surprising that Akt3 knockout mice displayed decreased brain sizes (~20%) compared to the controls (Easton et al., 2005). This is in contrast to Akt1-targeted deletions, where the whole size of the animal

was reduced. When the brains of Akt1-/- mice were compared with Akt3-/- mice, it was found that the Akt1 deletion caused a reduction in overall cell number, whereas the targeted deletion of Akt3 caused both fewer cell numbers and smaller cell size (Easton et al., 2005). Analyses of the downstream pathways in the Akt3-/- mice revealed a decrease in mTOR signaling, likely explaining the smaller cell size observed in the mice (Easton et al., 2005). Likewise for the findings in Akt1 knockout mice, Akt3-deleted mice also displayed normal glucose metabolism (Easton et al., 2005), lending credence to the specific role of glucose regulation by Akt2. Findings published one month later by Hemmings' group confirmed these findings for Akt3-/- mice (Tschopp et al., 2005). Taken together, the results from single Akt isoforms in knockout mice delineate organ-specific regulation for both Akt2 and Akt3, while the deletion of Akt1 is ubiquitous.

1.3.2.2 Double Akt isoform deletions

Akt1/Akt2 deletion: In most cases, a double deletion of two of the Akt isoforms is lethal (either embryonic, or a few days after birth) and almost all combinations display extreme growth deficiencies. For example, a combined Akt1/Akt2 knockout mouse was 50% smaller than age-matched controls; displayed decreased cell proliferation which resulted in extremely thin, translucent skin; and muscle atrophy and abnormal bone development (Peng et al., 2003). In addition, these Akt1/Akt2 double-knockout mice displayed decreased levels of adipogenesis, via defective activation of PPARγ-1α (peroxisome-proliferation-activated receptor-γ; also known as PGC-1α). The inactivation of PGC-1α, and decreased adipogenesis in these cells was attributed to the inactivation of Forkhead transcription factors (Peng et al., 2003). Further, these mice die within a few hours of birth, most likely due to

some type of respiratory failure (the authors observed labored breathing in the newborn mice) (Peng et al., 2003).

Akt1/Akt3 deletion: The combined deletion of both Akt1 and Akt3 (Akt1-/-Akt3-/-) in knockout mice was lethal at embryonic day E11-E12. These mice displayed developmental defects in both the heart and nervous system (Yang et al., 2005). Mice with a complete Akt1 deletion, but with a single Akt3 allele (Akt1-/-Akt3+/-) also die shortly after birth. However, double knockout mice left with a single Akt1 allele (Akt1+/-Akt3-/-) survive. Thus, the combined deletion of Akt1 and Akt3 underscored the role that Akt1 plays in development.

Akt2/Akt3 deletion: Similarly, Akt2/Akt3 knockout mice were viable, but displayed the same defects in glucose metabolism as the single Akt2 knockout mouse. Consistent with the findings observed for the Akt3 knockout mouse, these mice also displayed reduced brain size (Dummler et al., 2006). One very interesting result from this study indicated that mice with a single allele of Akt1 (i.e., Akt1+/-Akt2-/-Akt3-/-) survived, although they still displayed growth deficiencies. Thus, the authors concluded that Akt1 was the most important isoform for both development and survival (Dummler et al., 2006).

Collectively, the results of the studies generated with transgenic knockout mice indicate that Akt1 and Akt3 are required for growth and development, while Akt2 strictly regulates glucose metabolism. Further, mice can survive without Akt2 and Akt3, providing that a single allele of Akt1 remains.

1.3.3 Isoform specific roles in glucose regulation: Results from the diabetes literature

Despite the differences observed in the developmental/physiological functions regulated by the Akt isoforms *in vivo* in knockout mice (discussed above), the question of

whether or not the Akt isoforms are functionally redundant is still a major issue of debate within the literature (Bellacosa et al., 2004). Some of the most enlightening and interesting studies have examined the isoform-specific roles of Akt1 and Akt2 with respect to glucose metabolism. For the most part, the results from these studies indicated that while Akt2 has an essential role in glucose uptake and transport, there is some overlap observed with Akt1. Thus, it appears that when Akt2 function is compromised, Akt1 appears to compensate—at least partially—to maintain glucose homeostasis within the cell. The results from these studies are discussed below in more detail.

Jiang et al. (2003) suggested that functional redundancy was present between Akt1 and Akt2 based on the results obtained from their study. Adipocytes transfected with siRNA to both Akt1 and Akt2 displayed decreases in glucose uptake. However, the magnitude of the effect was slight for Akt1 (~20% reduction in glucose uptake) relative to Akt2 (~50% reduction). Thus, they concluded that both Akt1 and Akt2 played a role in glucose transport as when both isoforms were ablated, glucose uptake was reduced by ~80%. They also stated that these findings explained why the Akt2-/- mice in Cho's study (2001a) were mildly insulin resistant—Akt1 could compensate for the missing isoform. Moreover, Katome et al., (2003) confirmed the results of Jiang's study above and found that both Akt1 and Akt2 had a role in glucose metabolism; however, Akt2 was the predominant isoform involved in uptake and transport. Still, the results of these studies indicate that the isoforms exhibit functional specificity under normal physiological conditions.

Similar to the observations made in the Akt2 knockout mice, Bae et al. (2003) using MEF (murine embryonic fibroblasts) and adipocytes showed that Akt2-knockout cells displayed reduced glucose uptake and Glut4 translocation. Contrasting findings to those reported by Jiang et al. (2003) and Katome et al. (2003) were reported, however. In this

particular study, it was found that Akt1 could not compensate for the functions relegated by Akt2—only re-expression of Akt2 into the Akt2-depleted cells could restore the observed defects in insulin signaling (Bae et al., 2003). It should also be noted that the knockout of Akt2 did not eliminate *all* glucose uptake in these cells—only a portion of it, which suggests that there are additional cellular mechanisms in place to ensure adequate glucose regulation and transport within the cells.

Furthermore, it was found that the Akt1-knockout cells in this study were unable to differentiate into adipocytes, while the Akt2 knockout cells were (Bae et al., 2003). The results of this study indicated that Akt1 regulates fibroblast differentiation into adipocytes (adipogenesis), while Akt2 primarily regulates glucose transport and uptake. Peng et al., (2003) also found reduced adipogenesis in their Akt1/Akt2 double knockout mouse. Thus, the results obtained in Bae's (2003) study further explain the results obtained in Peng's study and assist in the explanation of the double knockout phenotype.

In conclusion, although the regulation of Akt1 and Akt2 may share some functional overlap in glucose transport and uptake, it appears that this only occurs when the homeostatic balance of the biological system is threatened. Thus, Akt1 and Akt2 show preferential specificity for their individual functions, however, when a loss-of-function occurs, ultimately the other isoform will ensure survival.

1.3.4 Akt isoform regulation in cancer

Analysis of the Akt isoforms in cancer usually falls into one of the following categories: amplification or mutation analyses, and/or overexpression and downregulation studies. Mende et al. (2001) noted that overexpression of any of the Akt isoforms is

sufficient to cause transformation and promote tumour progression. Nonetheless, the results of isoform-specific regulation in cancer are discussed below.

1.3.4.1 Akt1

Mutations or deletions: Discerning the exact functions of the Akt1 isoform in cancer is difficult given that the majority of published studies that examine 'Akt' may actually be Akt1, although this requires a careful and thorough analysis of the literature to separate those studies which examine pan-Akt, and those that specifically study Akt1. While deletions or mutations in the PI3K axis have been found, either in *PI3KCA,* the gene encoding the p110α subunit (Shayesteh et al., 1999), or in PTEN (reviewed in LoPiccolo et al., 2008), very few deletions or mutations in Akt1 have been reported. One of the earliest published studies found amplification of Akt1 in a human gastric adenocarcinoma (Staal, 1987). Recently, Carpten et al. (2007) reported a mutation from glutamatic acid to lysine (E> K, referred to as E17K) in Akt1 that occurred in human breast, ovarian, and colon cancers. They found that this mutation caused constitutive activation of Akt1 in cancers by docking the kinase to the plasma membrane, thereby causing uncontrolled Akt signaling. Further, it was concluded that this mutation was oncogenic given that it caused transformation of cells in culture. This E17K mutation was found to be specific to Akt1 and was not found in Akt2 or Akt3 in the same samples. However, a study published shortly after this landmark study indicated that the same activating mutation in Akt3 was found in melanoma (Davies et al., 2008).

Akt1-specific activation and upregulation: Other studies have reported a role for the Akt1 isoform in the regulation of proliferation and metastases. Overexpression studies

and endogenous upregulation of Akt1 protein were associated with higher Her2 expression in breast cancer (Ahmad et al., 1999). Liu et al. (2001) found that inhibition of Akt1 using Akt1-targeted antisense RNA reduced cell growth in soft agar and induced apoptosis in different types of cancer cells (MiaPaCa-2, H460, HCT-15, HT1080). Increased Akt1 activation was also found in breast, prostate, and ovarian cancers (Sun et al., 2001a). Similar to Liu's findings reported above, Sun et al. (2001a) reported that Akt1 overexpression promoted the proliferation of cancer cells in soft agar assays. Further, Akt1 overexpression in this study caused tumour formation when injected into nude mice (Sun et al., 2001a). Collectively, the results of these studies indicated that activation or overexpression of the Akt1 isoform is oncogenic and provides a rationale for Akt1-targeted treatment in cancer therapy.

1.3.4.2 Akt2

Amplification and upregulation: Frequently, amplification and upregulation of Akt2 has been reported in various kinds of cancer; in both *in vitro* cell lines and in analyses of primary tumour samples. One early and frequently cited study reported the amplification and subsequent overexpression of Akt2 in breast and ovarian carcinomas, with incidences occurring at 2.1% and 12.1% for breast and ovarian cancer, respectively (Bellacosa et al., 1995). The discovery of Akt2 amplification in both pancreatic cancer cell lines and primary tumour samples followed shortly thereafter (Altomare et al., 2002; Cheng et al., 1996; Ruggeri et al., 1998; Yamamoto et al., 2004), as well as additional studies providing further evidence for Akt2 amplification in ovarian and breast cancer (Sun et al., 2001b; Yuan et al, 2000). One study also reported amplification of the Akt2 gene (30%) in squamous cell

carcinoma from primary tumour samples excised from head and neck cancers (Pedrero et al., 2005).

Positive correlational analyses between expression levels of Akt2 and Her2/neu have been reported (Bacus et al., 2002), as well as associations between Akt2 and the estrogen receptor α (ERα) (Sun et al., 2001b). In this particular report, Sun et al. (2001b) also demonstrated that Akt2 may regulate estrogen signaling, as ERα was phosphorylated by Akt2 at S167. The Akt2 regulation of ERα as a substrate could potentially regulate the transcriptional activities of the receptor. To date, this is the only report detailing such regulation, other than studies that have indicated that Akt2 is activated by growth factors (Liu et al., 1998; Okano et al., 2000). However, the authors noted that this association may be contributing factor in cancer therapy failure (Sun et al., 2001b).

An analysis of both Akt1 and Akt2 expression in hepatocellular carcinoma indicated that Akt2 expression was associated with the prognosis of hepatocellular carcinoma. In contrast, low to moderate expression levels were observed for Akt1 in these samples (Xu et al., 2004). One study also reported the occurrence of somatic mutations in Akt2 in the kinase domain of both stomach and lung cancer using single strand conformation polymorphism assays. While the incidence rates of the mutation were low (2.0-2.5%) the authors concluded that this mutation could contribute to cancer progression (Soung et al., 2006).

Analysis of Akt2-specific functions in cancer: Overexpression studies examining the regulation of Akt2 have shown that upregulation of this isoform can increase both cancer progression and severity by regulating the processes of invasion and metastases. A study conducted by Arboleda et al. (2003) found that the overexpression of Akt2 in both breast and ovarian cancer cells was associated with increased metastases and invasion measured via

attachment to collagen I, IV and laminin. Further analysis indicated that the Akt2-overexpressing cells displayed upregulated protein levels of β1-integrins. Perhaps more importantly, the injection of MDA-MB435 breast cells transfected with or without Akt2 into nude mice revealed that Akt2 overexpression was associated with increased tumour formation and metastases (many nodules). In contrast, the MDA-MB435 control (without Akt2 overexpression) showed the development of a single tumour (Arboleda et al., 2003). Thus, the implications of this study are that increased expression of Akt2 may enhance the aggressiveness of metastatic breast cancer.

A study conducted by Jin and Woodgett (2005) found that a myristolated or membrane-targeted Akt2 construct promoted morphological changes in Hek293 (human epithelial kidney) cells which may contribute to the transformation process. Among the noted changes, were increased cell growth and cell size, as well as increased multinucleation and cell fusion. The authors concluded that the morphological changes observed in these Akt2 cells induced by prolonged Akt2 activation may promote increased tumorigenesis via increased 'genetic instability and autophagy', the features commonly associated with cancer (Jin & Woodgett, 2005).

Since Akt2 upregulation has been associated with cancer progression, it is logical that the downregulation of the isoform would have the opposite effect. Results of one study indicated that knockdown of Akt2 with siRNA and pharmacological inhibition of PI3K, with LY294002 caused reduced cell proliferation in ovarian cancer cells (Noske et al, 2005). Further, lung adenocarcinoma cells treated with siRNA targeted to all three isoforms showed that siRNA-ablation of Akt2 reduced both cell migration and invasion, whereas Akt1 siRNA had no discernable effects on lung cancer cells. Interestingly, cell migration and invasion

were partially inhibited by Akt3 siRNA treatment, but not to the same extent as Akt2 siRNA (Sithanandam et al., 2005).

1.3.4.3 Akt3

Akt3 regulation of melanoma: Akt3 is the least studied of the three isoforms, and as a result, a clear understanding of its function in both normal and cancer cells has yet to be determined. To date, Akt3 appears to play an important role in melanoma cancer. Published studies have reported elevations of the isoform in a cDNA microarray in melanoma (Bloethner et al., 2005). As well, the same E17K mutation found in Akt1 (cited above) was also found in Akt3 in melanoma cells (Davies et al., 2008).

Interesting results from one published study found elevations in Akt3 activity or kinase activation in melanoma cells and correlated the highest kinase activity with the most advanced and aggressive form of the cancer (Stahl et al., 2004). Ablation of Akt3 in melanoma cells by treatment with siRNA was effective in reducing the increased Akt activity observed in these cells, while siRNA against Akt1 and Akt2 had no effect (Stahl et al., 2004). Further, the increased activation of Akt3 in malignant melanoma, in this study, was associated with both increased copy numbers of Akt3 or deletions or mutations in PTEN (Stahl et al., 2004). Additional studies from Robertson's lab (Cheung et al., 2008; Tran et al., 2008) have since linked Akt3 with melanoma progression via Akt3-dependent phosphorylation of B-Raf, further contributing to a growing body of evidence that this isoform may play an important role in the regulation of a very serious form of skin cancer.

Akt3 regulation in other types of cancer: Deregulation of Akt3 activity has been reported in other types of cancer, such as ovarian and breast, in addition to the findings discussed in melanoma above. Cristiano et al. (2006) reported upregulation of Akt3 in 20%

of ovarian tumours. In addition, Akt3 was associated with cell cycle control in this study as the ablation of Akt3 using shRNA reduced proliferation in ovarian cancer cells through inhibition of G2/M progression (Cristiano et al., 2006).

Focused studies on breast cancer have shown that constitutively active Akt3 expressed in MCF-7 cells (which is an estrogen-dependent cell line) promoted estrogen-independent-tumour formation in nude mice (Faridi et al., 2003). Further, the overexpression of Akt3 in these cells caused resistance to tamoxifen treatment, most likely attributable to the fact that they were rendered estrogen-independent by the upregulation of Akt3. Thus, tamoxifen treatment would only further stimulate tumour growth (Faridi et al., 2003; Glaros et al., 2006). Akt3 activity was also linked with increased aggressiveness in breast and prostate cancer in another study. In this particular study, an association was found between breast cancer cell lines that were estrogen receptor-negative and prostate cancer cell lines that were androgen receptor-positive, an effect not noted for either Akt1 or Akt2 when the remaining isoforms were examined in this study (Nakatani et al., 1999b). The authors concluded that this association may be a contributing factor in the progression to the more aggressive types of breast and prostate cancers that are typically resistant to conventional treatment regimens (Nakatani et al., 1999b).

Collectively, the results from the studies above indicate that upregulation of any Akt isoform (via overexpression systems or *in vivo* amplification) can increase proliferation, metastasis and invasion—processes all associated with tumorigenesis and aggressive forms of cancer. Out of all the isoforms, Akt2 has been the most studied isoform in cancer, overlooking the limitations that are present in studying Akt1. The results of these studies have implicated Akt2 to be most important in the regulation of increased invasion and transformation. Indeed, Akt2 activity is dramatically increased upon stimulation with a

variety of growth factors such as EGF, IGF-I, and PDGF (Liu et al., 1998). However, the exact mechanism as to how Akt2—or any of the isoforms—contribute to cancer progression has not yet been determined. Moreover, the mechanisms involved in the isoform-specific contribution to tumorigenesis are most likely multifactorial.

1.3.5 The Akt isoforms and isoform-specific cancer treatment

The well-documented use of PI3K/Akt inhibitors such as LY294002 and wortmannin is an effective treatment strategy for cancer. However, to date, treatment with PI3K/Akt inhibitors have had limited success in clinical trials; further the broad specificity of some of the inhibitors have rendered them highly toxic (LoPiccolo et al., 2008). However, accumulating lines of evidence citing the differential regulation of the Akt isoforms in various types of cancer (such as Akt3 in melanoma, for instance) raise the question as to whether or not isoform-targeted treatment therapy might be a viable option. Certainly, targeting one isoform would alleviate the observed toxicities seen when all of the isoforms are inhibited.

Strategic inhibition of the Akt pathway would likely target the upstream players involved in Akt activation, or prevent the activation of downstream substrates (Hennessy et al., 2005). To date, however, there have been significant problems regarding inhibition of Akt in cancer treatment: First, the broad specificity of many inhibitors produces potential toxicities. As proof of this, Triciribine, also known as API-2, specifically inhibits Akt. However in early clinical trials, the drug showed little effect and was found to be highly toxic—the most significant symptoms appear related to the known functions of Akt2 such as hyperglycemia (reviewed in LoPiccolo et al., 2008). According to LoPiccolo et al. (2008)

API-2 has recently been re-examined for use in patients but employing lower doses and screening patients whose cancers show high Akt activation (LoPiccolo et al., 2008).

Downstream inhibition of the Akt pathway by using inhibitors of mTOR like rapamycin, have their own caveats. The discovery of a feedback loop from p70S6K that signals back to the insulin-receptor (IRS) causes Akt activation and further promotes tumour progression (reviewed in Harrington et al., 2005; O'Reilly et al., 2006). Perhaps the combination of either rapamycin or a rapamycin derivative together in combination with an Akt inhibitor is a valid strategy that remains to be tested (Hennessy et al., 2005).

Treatment with certain types of inhibitors may even promote resistance via unintentional upregulation of the Akt pathway. Bruzek et al., (2005) chronically exposed a colorectal cancer cell line (HCT 116) to increasing concentrations of FTIs (farnesyl protein transferase inhibitors (SCH6636) in order to select a FTI-resistant drug cell line. The authors of the study did not find any differences in drug uptake mechanisms that would render the cells resistant (almost 100-fold) to the FTIs. Examination of the Akt pathway revealed that the resistant cells had upregulated endogenous levels of Akt1 and Akt2, as well as the downstream substrates mTOR and p70S6K (Bruzek et al., 2005). Treatment of this cell line with rapamycin was able to restore drug sensitivity.

Thus, selective targeting of any of the isoforms could potentially alleviate toxic side effects caused when all of the functions of Akt are inhibited. Further, careful therapeutic monitoring could assess whether treatment of a tumour with an isoform-specific inhibitor would be effective. Clouding this issue, however, is the fact that the isoforms may function differentially in different systems—i.e., Akt2 may not behave the same way in lung cancer as it does in breast cancer, and further intensive studies are required to sort these issues out. Moreover, Akt-isoform-specific signaling needs to be examined in detail: it is assumed that

the isoforms signal to the same downstream substrates as pan-Akt, and very few studies have shown if any of the isoforms exhibit preferential substrate specificity. This tenet is particularly important if selective Akt isoform inhibition promotes the activation of feedback loops and networks from downstream substrates (Hennessy et al., 2005). Further, effective treatments that selectively target the isoforms would require the development of highly sensitive prognostic markers that would clearly identify the isoform involved.

Despite the advantages gained by hypothetically targeting the individual isoform implicated in the cancer system being treated, the reality is that targeted-specificity of the Akt isoforms via pharmacological inhibitors in cancer treatment remains elusive due to the shared homology between the isoforms. Recently published findings from a research group at Merck screened compounds and analyzed their effect on Akt inhibition (Barnett et al., 2005). Out of 270,000 chemicals, 2 were found to be isoform specific: 1 compound inhibited Akt1 (Akt-I-1), while the other compound was able to inhibit both Akt1 and Akt2, but not very efficiently (Akt-I-1,2). Neither compound showed any activity towards Akt3 (Barnett et al., 2005). Both of these inhibitors blocked access of PDK1, the upstream kinase that phosphorylates Akt at the required activation site at T308, suggesting that the inhibitors bind to the PH domain. Treatment of LNCaP prostate cancer cells with the AktI-1,2 inhibitor and analysis of downstream Akt substrates revealed that both Akt1 and Akt2 inhibition caused an upregulation of both Bad and p27, and a downregulation of p21. More importantly, treatment with Akt-I-1, which inhibited only Akt1, did not affect these downstream pathways suggesting that preferential signaling from the Akt2 isoform was present (Barnett et al., 2005). Recently, Hartnett et al. (2008), also from Merck, published findings regarding the development of another Akt1/Akt2 inhibitor. This particular inhibitor showed more activity against Akt2 in enzyme assays but showed poor activation in cell-based assays. The structure

of the compound was then reformulated to correct this (Hartnett et al., 2008). Future development of isoform-specific inhibitors and careful analysis of signaling to downstream substrates—to determine both preferential substrate specificity as well as monitor aberrant activation of any component of the Akt pathway—will be a much needed area of focused research investigation in the near future.

1.4 SUMMARY

Analysis of the individual Akt isoform-specific contribution in cancer development, and progression has been difficult to ascertain. Technical constraints, such as the widespread use of cross-reactive antibodies for example, has led to generalized assumptions that regulation of the Akt isoforms is consistent with that observed for pan-Akt. Despite this, the development of genetically engineered knockout mice has provided evidence that the Akt isoforms regulate very specific functions. Further, the development of siRNA technology has led to advances in understanding the regulation of the isoforms in cancer. Future studies need to discern the intricate network of Akt regulation and signaling by assessing if the isoforms share the same specificity for substrate regulation, or if in fact, one isoform displays very specific preferences for certain signaling intermediates. The results obtained from these future studies will aid in the development of more finely-targeted and enhanced cancer therapy regimens in patients whose tumours show elevated activation of Akt. The knowledge that Akt3 is important in melanoma cancer and is implicated in its progression for example, can provide potential strategies for increased treatment efficacy, providing that the precise mechanisms involved can be determined. One issue that remains unaddressed, however, is to determine which isoform is the most important for cancer cell survival. An analysis of the

function and regulation of the mechanisms intrinsic to the isoforms needs to be investigated, beyond the finding that one type of cancer shows upregulation or amplification of a specific isoform.

An understanding of how the isoforms are similar or are different from the accepted theories about the regulation of Akt will profoundly affect the current knowledge surrounding Akt signaling. In consideration of the important role that Akt plays in both the initiation and progression of cancer, finding that one isoform is more important for cancer survival, or that the isoforms can compensate for the functions of each other, will have implications beyond what is currently known about Akt in tumorigenesis. Therefore, a thorough investigation and characterization of how the Akt isoforms function in cancer is essential.

Thus, the current need to challenge the accepted notions regarding Akt isoform regulation prompted the investigation outlined in the studies included within the thesis. A breast cancer cell line (MDA-MB231 cells) was chosen to examine the regulation of the isoforms in these studies. Collectively, the studies included and described within the thesis indicate that the Akt isoforms are regulated differentially within this clinically advanced breast cancer model. The first analysis that needed to be undertaken involved examining the subcellular localization of the isoforms to determine how their regulation compares to what is accepted for Akt function. Data obtained from this study suggested that specific differences in the localization of the isoforms can provide insight into the function and regulation of each Akt isoform (Chapter 3.0). The studies included in the next section (Chapter 4.0) examined which isoform was most important for breast cancer proliferation and survival. This chapter detailed how the function one of specific isoform (Akt2) was more important for survival, and outlined the mechanisms and cellular processes regulated by this

isoform in a breast cancer cell line. Further, these studies also detailed the mechanism by which the breast cancer cells die by examining the processes related to targeted deletion of Akt2. Collectively, the results and conclusion detailed in the studies included in this thesis challenge currently accepted views about Akt signaling, and provide evidence that the Akt isoforms are more intricately regulated than previously thought.

CHAPTER 2.0

MATERIALS AND METHODS

2.0 MATERIALS AND METHODS

The following section contains the general methods and routine protocols used in the experiments described in this thesis. Any additions or changes to these protocols are discussed in the relevant 'Materials and Methods' section within the specific studies outlined in each chapter.

2.1 Cell Culture

The MDA-MB231 breast cancer cell line purchased from ATCC (Manassas, VA), was grown in RPMI 1640 media (Hyclone), supplemented with 10% (v/v) fetal bovine serum (FBS), 2.05 mM L-glutamine, 100 μg/ml streptomycin and 100 units/ml penicillin (Hyclone). Cells were routinely cultured and maintained under standard culture conditions in a humidified atmosphere at 37°C, 5% $C0_2$, 95% air. MDA-MB231 cells are a breast cancer cell line (adenocarcinoma) and were derived from a breast metastasis (pleural effusion) (ATCC). They are both p53 negative and ER (estrogen receptor) negative, and exhibit no known alterations in the Akt pathway.

2.2 Protein Extraction and Quantification

Cells were plated in 10-cm plates (Sarstedt, Laval QB) the day prior to extraction and grown under standard culture conditions as indicated above. The culture media was removed and the plates were placed on ice prior to being washed three times with ice-cold PBS (137 mM NaCl, 2.7 mM KCl, 10 mM Na_2HPO_4, 2 mM KH_2PO_4).

Cell Lysis Buffer (20 mM Tris-HCl, pH 7.5, 150 mM NaCl, 1 mM EDTA, 1 mM EGTA, 1% (v/v) Triton X-100) supplemented with 1 mM PMSF, 1x protease inhibitor

cocktail tablets (Roche), 2 mM sodium orthovanadate (Na_3VO_4), and 10 mM sodium fluoride (NaF) was added to each of the plates and the adhered cells were scraped with a rubber policeman. Cells were then collected into pre-chilled 1.5-ml eppendorf tubes and sheared with a 21-gauge needle (20-30 times). The cell lysates were incubated on ice for 15-20 min and were then cleared by centrifugation. The proteins were quantified using a BCA Assay (Pierce) which measures the amount of protein in a sample relative to a standard curve against a known amount of BSA (25-2000 μg/ml). The samples were read at 540 nm using a Titertek Multiscan MCC/340 plate reader (Titertek, Huntsville, AL) and the unknown protein concentrations were analyzed against the values obtained from the standard curve and interpolated using a linear regression analysis (GraphPad Prism version 4.03).

2.3 SDS-PAGE

Protein extracts (20-40 μg) were diluted in 5x Laemmli sample buffer (0.1 M Tris-HCl, pH 6.8, 10% (w/v) SDS, 40% (v/v) glycerol, 2% (w/v) DTT, 10% (w/v) bromophenol blue) and loaded onto 8-15% polyacrylamide gels (acrylamide:N,N'-methylene bisacrylamide, 29:1). Proteins were resolved by electrophoresis using a Hoefer miniVE electrophoresis unit (GE Health Care) in running buffer (25 mM Tris, 192 mM Glycine, 0.1% (w/v) SDS, pH 8.3, Bio-Rad) at 90-150 volts for 1-2 h.

2.3.1 Immunoblotting (Western Blot Analysis)

Proteins were transferred onto PVDF membranes (GE Health Care) which were immersed prior in transfer buffer (48 mM Tris, 39 mM glycine, 20% (v/v) methanol, 0.037% (w/v) SDS, pH 9.2) using a semi-dry transfer apparatus at 12 volts for 1 h (Bio-Rad,

Burlington, ON). Membranes were incubated in blocking buffer for 1 h at room temperature in 0.1% TBST (50 mM Tris-HCl, pH 7.4, 150 mM NaCl, 0.1% (v/v) Tween-20) with 5% Carnation non-fat skim milk prior to overnight incubation with the primary antibody. The primary antibody was diluted in 0.1% TBST with 5% BSA on a rotating shaker at 4°C (see Table A1 in Appendix II for the antibody dilutions used in experiments). Membranes were washed three times with 0.1% TBST and incubated in the secondary antibody in 0.1% TBST supplemented with 5% non-fat skim milk for 1 h at room temperature. The blots were then washed four times; twice with 0.1% TBST, and twice with TBS prior to visualization using enhanced chemiluminescence (ECL) (GE Health Care). For analysis of phosphorylated proteins, the phosphorylated protein was probed first and then stripped, if necessary, in a stripping buffer (62.5 nM Tris-HCl, pH 6.7, 100 mM β-mercaptoethanol, 2% (w/v) SDS) prior to analysis with the endogenous or non-phosphorylated protein.

2.3.2 Densitometric Analysis

Intensity of the protein bands (scanned images) was determined by densitometry using AlphaEase Fluorochem (FC) 8900 version 4.0.1 software, which was supplied with an Alpha Innotech scanner (Fisher Scientific). Protein levels were expressed as a ratio [protein of interest/loading control] and graphed using Excel (Microsoft Office 2003, Microsoft). In general, γ-tubulin was used as a control for the experiments within this thesis.

2.4 Immunoprecipitation/Western Blot Analysis (IP/Western)

For the immunoprecipitation procedure, MDA-MB231 cells were plated on a 10-cm plate in RPMI media supplemented with 10% (v/v) FBS and antibiotics and allowed to

adhere overnight (see culture protocols, Section 2.1, in this chapter). The next day, the media was decanted, the plate was washed three times with ice cold PBS, and the residual PBS was removed from the plate using a pipette. Proteins were solubilized in 500 μl of Cell Lysis Buffer and quantified using a BCA Assay (Pierce) (see Section 2.2, above). The protein extract (200 μg) was added to 0.5-2.0 μg of isoform-specific primary antibodies against Akt1 (Cell Signaling Technology, Danvers, MA), Akt2 (Santa Cruz Biotechnology, Santa Cruz, CA), and Akt3 (Upstate Biotechnology, Lake Placid, NY). The required antibody concentration was initially determined via titration. The protein-antibody mixture was then incubated overnight at 4°C on a nutating shaker. Protein A/G sepharose beads (20 μl, Santa Cruz) were first cleared by washing three times in 500 μl of Cell Lysis Buffer prior to being added to the protein-antibody mixture. The antibody slurry was incubated for an additional 2 h at 4°C, with constant rotation, and the beads were collected by centrifugation. The supernatant was retained in order to assess the efficiency of the immunoprecipitation, and the beads were then washed three times in 500 μl of Cell Lysis Buffer. After the last wash, the beads were collected and resuspended in 3x Sample Buffer (20 μl), boiled for 5 min, and centrifuged again to allow collection of the immunoprecipitated fraction. The immunoprecipitate (15 μl) was then loaded onto 10% polyacrylamide gels alongside a whole cell extract control (30-35 μg) and the collected supernatant prior to analysis via western blotting (Chapter 2, Section 2.3.1).

2.5 RNA Extraction and Reverse Transcription (RT)

Total RNA was extracted using an RNeasy Kit (Qiagen) according to the manufacturers' instructions. Briefly, the cell culture medium was removed and the plate was

washed with PBS. Cells were lysed by addition of Buffer RLT (600 µl, supplemented with 10 µl β-mercaptoethanol/ml), scraped and aliquoted into an eppendorf tube. The cell sample was homogenized by shearing through a 21-guage needle (20-25 times) and mixed with 70% (v/v) ethanol. The lysates were placed on a column (supplied by Qiagen) and centrifuged (> 8000 x g). The RNA sample in the column was washed, and then eluted with RNase-free water. Total mRNA was quantified using a spectrophotometer (UV 1101 Biotech Photometer) taking standard $OD_{260/280}$ absorbance measurements. RNA integrity was analyzed using one of two methods: (1) The 28S/18S ratio was performed using a RNA 6000 Nano Assay LabChip Kit and analyzed with an Agilent 2100 Bioanalyzer or (2) The 28S/18S ratio was verified by native gel electrophoresis of RNA on 1% agarose gels. The RNA samples were then DNase I-treated, and 1 µg of total RNA was reverse transcribed with M-MLV, 10 mM dNTPs (ID Labs), and T_{20}-VN primers (20 ng/µl), in accordance with the protocol published by Hembruff et al., 2005.

2.6 Quantitative-PCR (Q-PCR)

Q-PCR was performed to analyze mRNA expression using an ABI Prism 7900 HT Sequence Detection System (SDS) (Applied Biosystems). The standard curve was generated using the cDNA from MDA-MB231 cells diluted 1/4 in water (PCR-grade, Invitrogen). This initial dilution was then further diluted incrementally (1/4, 1/8, 1/16, 1/32, 1/64) for analysis (Hembruff et al., 2005). The cDNA from each sample was diluted 1/8 and loaded in triplicate onto a plate with gene primers (300 nM) and SYBR Green I chemistry (from Applied Biosystems or Bio-Rad). The S28 ribosomal RNA was used as the control, and the mRNA levels were determined by the following formula: [mRNA level of Akt isoform/S28 mRNA

level]. The PCR conditions used were 95°C for 15 s, 55°C for 15 s, and 72°C for 30 s, for 40 cycles. Subsequently, the data was acquired and analyzed with ABI SDS software (version 2.1 from Applied Biosystems).

2.7 Small interfering RNA (siRNA)

siRNA transfections were performed in both 10-cm cell-culture dishes and in 6-well plates on glass coverslips, scaled according to the volumes required. Cells were plated 24 h prior to transfection with siRNA and the transfection procedure lasted for 24 h. For transfections in 10-cm plates, MDA-MB231 cells were trypsinized with 0.05% (w/v) Trypsin-EDTA (Gibco) and replated onto 10-cm plates (~30% confluency) in RPMI media supplemented with 10% (v/v) FBS (antibiotics were omitted for these experiments). The next day, cells were transfected using Opti-MEM I Reduced Serum Medium (which is serum free) (Gibco) and Lipofectamine 2000 (Invitrogen). The cell culture medium was removed, the plates were washed with sterile DPBS and 12 ml of Opti-MEM I medium was added to each plate to be transfected (1.5 ml in 6-well culture dishes). For transfection, 1.5 ml of Opti-MEM I medium was added to two wells in a 6-well culture dish. In one well, the isoform-specific siRNA oligo was diluted to the appropriate concentration and Lipofectamine 2000 (25 µl) was added to the second well. After 5 min, the siRNA and Lipofectamine were mixed (3 ml in total) and further incubated for an additional 20 min at room temperature. For transfections in 6-well plates siRNA was diluted in 250 µl Opti-MEM I and mixed with 5 µl Lipofectamine 2000 in 24-well plates. The mixture was slowly added to the plates and mixed by gentle rocking. The plates were incubated overnight, and the transfection media was removed the next morning (24 h post-transfection initiation) and replaced with RPMI 10%

(v/v) FBS. The plates were returned to the incubator and processed for downstream applications at the timepoints required (i.e., protein, mRNA, or immunostaining). A scrambled control (10 nm), or a reagent control (mock-transfected with Lipofectamine 2000 only) was included for the siRNA transfections.

All siRNA oligonucleotides, including the scrambled controls were purchased from Ambion (TX), and were determined to be isoform-specific (i.e., the siRNA for Akt1 did not knockdown Akt2 or Akt3, etc.). Two siRNA oligonucleotides per isoform were chosen to ensure that the experimental results obtained were due to ablation of the specific Akt protein, and not due to non-specific effects. Further, the choice to transfect one oligonucleotide per target at low concentrations minimized the off-target or non-specific effects often associated with pools of siRNA. The siRNA transfections were optimized for each oligonucleotide and evaluated for the lowest concentration that gave the maximum knockdown, as well as incubation time. The dose curves (see Appendix II, Fig. A3) indicated that all oligonucleotides included in the studies achieved an average knockdown of 70-85% (measured by protein densitometry), or even higher (84-95%) when mRNA was quantified by qPCR (Chapter 4, Section 4.3.5). The optimal time that full knockdown was achieved was 48 h post-transfection initiation. The siRNA concentrations tested ranged from 5 nm to 30 nm, and knockdown was achieved within this range (the nucleotide alignment of the siRNAs employed is also highlighted in Appendix I, Fig. A1). The siRNA sequences and final concentrations used in this study are as follows:

siRNA Set 1: Akt1 10 nm 5' GGCUCCCCUCAACAACUUC 3'
Akt2 10 nm 5' GGAUGAAGUCGCUCACACA 3'
Akt3 20 nm 5' GGACCGCACACGUUUCUAU 3'

siRNA Set 2: Akt1 30 nm 5' GCCCUCAGAACAAUCCGAU 3'
Akt2 5 nm 5'GGUCGACACAAGGUACUUC 3'
Akt3 10 nm 5' GGCCAAGAUACUUCCUUUU 3'

2.8 General Immunocytochemistry and Immunofluorescence Experiments

2.8.1 Single antibody staining

Cells were plated on 1.8-cm (0.13-0.17 mm thick) sterile glass coverslips (Fisher Scientific) that had been placed in a well of a 6-well clustered dish and allowed to attach overnight. At the indicated timepoints, the coverslips were removed from the media, washed in TBS, fixed in 4% paraformaldehyde for 10 min, and then permeabilized in 0.2% Triton X-100 for 5 min (both from Sigma). The coverslips were then treated in blocking solution (10% equine serum, 1% (w/v) BSA, 0.02% (w/v) NaN_3, PBS) for 1 h at room temperature and washed in TBS prior to antibody staining. The primary antibodies were diluted (for dilutions, please see Table A1, Appendix II) and incubated for 45 min. After washing in TBS, fluorescence-conjugated secondary antibodies were added to the coverslips and incubated for 30 min in the dark. Both primary and secondary antibodies were diluted in 1% BSA in TBS. All primary and secondary antibodies were titrated to determine the optimal concentrations for these experiments. The secondary antibodies were also evaluated to ensure that there was no bleedthrough or excessive background/noise (see Appendix II, Fig. A4, and Chapter 3.2.2, Fig. 3.4). All experiments also included primary omission controls to ensure this.

Next, the coverslips were mounted onto slides containing 5 µl of 90% glycerol/PBS prior to being viewed via confocal microscopy using a LSM 510 Meta laser scanning microscope (Carl Zeiss) with a 63x objective lens. Throughout all trials, a minimum of 10 fields/per coverslip/per trial were captured for each experiment, when possible.

2.8.2 Live MitoTracker Staining

MitoTracker Red CMXRos (Cambrex Biscience Walkersville Inc., Charles City, IA) was used for active/live labeling of the mitochondria in Chapters 3.0 and Chapter 4.0 of this thesis. MitoTracker use in these experiments was optimized according to the protocols suggested by the manufacturer. In order to label the mitochondria, 50 nM (final concentration) of MitoTracker was diluted in pre-warmed media, and added to each well of a 6-well clustered dish that contained cells that were plated on coverslips. The cells were further incubated at 37°C, 5% CO_2 for 45 min to allow the incorporation of the probe. Afterwards, the coverslips were removed from the media, washed in TBS and then fixed and permeabilized for further analysis with Akt2 immunostaining as outlined in Section 2.8.1, above.

The determination of the final concentration of MitoTracker that was employed was optimized via titration until it was determined that 50 nM of MitoTracker was the optimal dose for use in these experiments (the recommended concentration of MitoTracker labelling from the manufacturer for these experiments ranges from 25-500 nM). MitoTracker labelling using concentrations in the live-incorporation experiments above 50 nm (100-500 nm) were saturated when tested. Fig. A7 in Appendix III shows MitoTracker staining in MDA-MB231 cells, LNCaP cells and HeLa cells and demonstrates that no signal was present in the green channel during the course of the MitoTracker experiments at the concentrations employed.

2.8.3 Confocal Microscopy

All immunocytochemistry experiments were visualized by confocal microscopy using a Zeiss 510 Meta laser scanning microscope (Carl Zeiss) equipped with a 63x objective lens. Three lasers lines were utilized for excitation with the following band pass filter settings used for detection: Argon 488 nm (band pass 505-530), HeNe 543 nm (long pass

560) and 633 nm (long pass 650). During the initial optimization of the Akt isoform triple staining experiments, the long pass and band pass filter settings indicated above were chosen for stringency and to ensure that no signal was present in the other three detector channels (please see Appendix II, Figure A4). Once these settings were in place, they were employed in every experiment thereafter. All images were captured and analyzed (including co-localization statistics and analyses) using LSM 510 software included with the microscope (LSM Image Examiner, Carl Zeiss).

2.9 MTT Proliferation Assays

Cell proliferation was measured using MTT assays. In these experiments, cells were first transfected with siRNA specific to each Akt isoform in 10-cm plates (Sarstedt). At the 48 h timepoint, cells were washed, trypsinized, and counted. 3000 cells suspended in 100 µl culture media were plated per well of a 96-well clustered dish (16 replicates per transfection condition), and allowed to attach overnight. The plates were maintained under standard conditions until samples were taken at scheduled timepoints. A portion of the leftover cell sample at 48 h was used for Western blot analysis to confirm the efficiency of siRNA transfection. At each timepoint, 10 µl of MTT stock (5 mg/ml MTT in PBS) was added to each well and incubated for 4 h at 37°C, 5% $C0_2$. At the end of the incubation, the MTT-culture medium was gently removed from each well using a pipette. 200 µl of DMSO was then added to each well and mixed thoroughly. Plates were read on a SPECTRAmax 340 PC plate reader (Molecular Devices) at 570 nm and 650 nm (reference wavelength). All absorbance measurements were corrected to the reference wavelength (Corrected absorbance=570-650 nm). The optimal initial plating number for the cells was determined

by increasing the cell number in increments of 3000 (replicates of 4 wells per increment) and assessing the linear range of the assay. Please see Appendix II, Fig. A5 for these optimization curves.

2.10 Focus Formation Cell Survival Assay

Cells were first harvested by trypsinization at 48 h post-siRNA transfection, and then plated (1000 cells in a 10-cm dish). After 10-12 days of incubation, the culture medium was removed, and the plates were gently washed with PBS solution. Subsequently, cells were fixed and stained with 2% (w/v) methylene blue in 100% methanol for 10 min at room temperature. Colonies comprised of >50 cells were counted as positives.

2.11 Treatment with X-ray Irradiation

Cells were treated with X-ray irradiation and analyzed at the indicated timepoints in Chapter 3. MDA-MB231 cells were trypsinized, plated and allowed to adhere overnight (RPMI, 10% (v/v) FBS). The next day, the plates were treated with 5 Gy irradiation using a RS320 Irradiation System (Gulmay Medical Inc.) returned to the incubator, and processed at the indicated timepoints. The radiation dose (5 Gy) was chosen as previous studies within our lab indicated this was a mid- or medium level dose for MDA-MB231 cells. The plates of cells were placed on the second shelf within the X-ray machine on top of a Perspex plate to accommodate backscatter. The shelf position was chosen to minimize the time the cells were out of the incubator (positioning cells closer to the X-ray tube minimized the time of irradiation treatment.) Cells received a dose of 5 Gy (300 kV, 9 mA) in approximately 2.1 min. For a view of the setup of the X-ray machine, please refer to Appendix II, Fig. A6.

CHAPTER 3.0

The characterization and subcellular localization of the Akt isoforms

OVERVIEW OF THE STUDY

Akt/PKB (protein kinase B), a serine/threonine kinase involved in the regulation of many diverse cellular functions such as proliferation, metabolism and apoptosis, is comprised of three isoforms Akt1, Akt2 and Akt3. A recurrent and pervasive theme in the Akt literature is that the similarity and homology of the isoforms (~80% at the amino acid level) renders them functionally redundant in signal transduction pathways. The present study was undertaken to characterize the Akt isoforms in cancer cell lines by examining their subcellular localizations, protein and mRNA levels. Differential subcellular localizations were observed for the isoforms in the cancer cell lines, with Akt1, the most abundant isoform, displaying a ubiquitous cytoplasmic localization. Akt2 was also localized in the cytoplasm, while Akt3 was strictly localized to the nucleus and nuclear membrane. Akt2 was co-localized with the mitochondria in cancer cells as determined by confocal microscopy with subcellular markers. The subcellular localization of the Akt isoforms was independent of deletions in PTEN, the phosphatase that dephosphorylates $PI(3,4,5)P_3$ and regulates the activation of PI3K, or phosphorylated Akt. Ablation of one, or two of the isoforms by siRNA, serum starvation, or treatment with growth factors did not change their subcellular status. However, treatment with X-ray irradiation provoked the translocation of Akt2 from the cytoplasm to a more perinuclear localization 3 h after exposure to 5 Gy radiation. The results of the study shed new light on the potential interaction between the isoforms and provide evidence that the isoforms intricately regulate the function(s) of Akt signaling.

3.1 INTRODUCTION

Many previously published reports have made generalized conclusions regarding the isoform-specific regulation of Akt. There are many reasons for this: First, given the high

degree of similarity at both the nucleotide and amino acid level, many studies have concluded that the regulation of Akt1, Akt2 and Akt3 are functionally redundant. Lending further credence to this is the fact that all three kinases appear to be activated in the same manner: The conversion of $PI(4,5)P_2$ to $PI(3,4,5)P_3$ at the plasma membrane by PI3K promotes the subsequent phosphorylation and activation of Akt on two well-studied phosphorylation sites, threonine 308 (T308) in the regulatory domain and serine 473 (S473) in the kinase domain for Akt1, while T309/S474 and T305/S472 are the parallel activation sites for Akt2 and Akt3, respectively. Akt regulates many of its cellular functions via a series of downstream phosphorylations that either inhibits or activates substrates containing the 'phospho-Akt-substrate' or PAS motif (R-X-R-X-X-S/T; Manning & Cantley, 2008). Considering that the Akt isoforms are activated in the same manner, it may be logical to conclude that the three isoforms regulate and pass their signals to the same downstream substrates known for pan-Akt, or Akt1.

Second, the fact that the phosphorylation sites differ by the position of only one amino acid residue has made the examination of isoform specific differences in both activation and regulation difficult to examine. The proximity of these activation sites has also made antibody generation and the targeting of isoform-specific phosphorylated antibodies elusive. To circumvent this issue, differences in phosphorylation and kinase activation are usually determined by isoform-specific immunoprecipitation assays, followed by Western blot analysis using a 'pan' phosphorylated-Akt antibody that recognizes either all of the threonine or serine phosphorylation sites, assuming that the antibodies are both specific and efficient in an immunoprecipitation. Overexpression of an Akt isoform with a recombinant protein (i.e., HA-Akt1) has also been employed to facilitate the studies of isoform-specific function. Functional studies have also used constructs that have mutated the key activation

residues, such as Akt1 T308A/S473A, where the essential threonine and serine phosphorylation sites are converted to other amino acid residues (mostly alanine). According to Manning and Cantley (2007), these mutated constructs function more in a dominant negative manner in their experiments. They further noted that the functions that these constructs regulate are not well understood, despite their widespread use in the literature. They cited the example of the recently discovered S473 phosphorylation which is phosphorylated by mTOR and acts both up- and downstream of Akt in the signaling pathway which is regulated by mTOR. In light of these findings, it may be that the mutated constructs may have more consequences on downstream regulation than originally presumed (Manning and Cantley, 2007).

Thus, an understanding of isoform-specific functions in Akt has been difficult to ascertain. In the past, few studies have examined and compared the isoforms in consideration of the limitations listed above. Many of these published studies have examined pan-Akt or only one isoform, and in most cases, Akt1 has been the most investigated isoform. Moreover, the widespread use of antibodies that are cross-reactive to one or more of the isoforms has led to confusion regarding isoform-specific regulation. However, differences, when noted, have also been attributed to variations in tissue distribution and these tissue-specific representations have led to the study of the isoforms in specific systems. For instance, the regulation of Akt2 is often studied in insulin-responsive tissues or in cell systems such as skeletal muscle cells or adipocytes in consideration of the role that Akt2 plays in insulin signaling and glucose transport.

Further, the examination of protein and mRNA levels in different cell lines has produced some inconsistency between studies. In consideration of this, the cumulative results of carefully conducted isoform-specific research have emphasized one important

tenet: isoform-specific regulation is dependent upon the system being examined. For example, breast cancer may display differential isoform regulation compared to lung cancer, thereby making generalizations about isoform-specific function difficult.

It is also generally accepted that the regulation of the Akt isoforms is the same as that observed for pan-Akt. Due to what is currently understood about Akt activation, the localization of the Akt isoforms are all considered to be cytoplasmic and translocate to the plasma membrane once PI3K is activated. As proof of this, cytoplasmic localization of Akt2 has been reported for both tumour and normal cells (Cheng et al., 1997). More recent studies suggest that each isoform may regulate different cellular functions. With recent advances in genetic engineering and the development of siRNA technology, many studies are finding that the regulation of the Akt isoforms may not be redundant—in fact, they are more intricately networked than previously realized. Moreover, the commercial availability of Akt isoform-specific antibodies has now enabled the examination of isoform-specific functions.

The purpose of the present study was to gain an insight and understanding as to how the subcellular localization of the Akt isoforms may regulate Akt signaling. Protein, mRNA levels and siRNA knockdown studies were utilized to examine the function(s) of the Akt isoforms *in vitro*. The differential regulation of the Akt isoforms may promote further understanding of the role that Akt has in processes such as cellular proliferation and oncogenesis. Ultimately, these findings would challenge the current understanding of Akt regulation. The studies presented in this chapter report on the differential localization and characterization of the Akt isoforms in various cancer and non-tumorigenic cell lines. Furthermore, the subcellular localization is independent of Akt activation in cell lines with PTEN deletions or mutations. Studies conducted with targeted siRNA ablation to the three isoforms indicate that the isoforms function independently of one another. The data

presented here are consistent with a model that the individual isoforms intricately regulate the cellular function(s) of Akt.

3.2 MATERIALS AND METHODS

Many relevant *'Materials and Methods'* are outlined in Chapter 2.0 of the thesis. Modifications and additional protocols specific to the experiments within this section are described below.

3.2.1 Cell Culture

The following cell lines were used in these studies and, unless otherwise stated, were purchased from American Type Cell Culture (ATCC) (Manassas, VA): three breast cancer cell lines (MDA-MB231, MDA-MB468, MCF-7); one cervical carcinoma cell line (HeLa); one prostate cancer cell line (LNCaP) and one liver cancer cell line (HepG2). MCF-10A, a non-transformed epithelial breast cell line was included as a control. Hek293 (human embryonic kidney cell line) and the variant of this cell line, 293T, which contains the SV40 large T antigen were also employed. MDA-MB231, MDA-MB468 and LNCaP cells were maintained in RPMI 1640 growth medium, while MCF-7, HepG2, Hek293 and 293T cells were cultured in DMEM media (both from Hyclone). RPMI and DMEM media were supplemented with 10% (v/v) fetal bovine serum (FBS) and a penicillin-streptomycin antibiotic solution (100 units/ml penicillin, 100 μg/ml streptomycin) (Hyclone). MCF-10A cells (a gift from Dr. Carita Lanner) were cultured in DMEM F-12 media (Hyclone) supplemented with 10% (v/v) equine serum (Hyclone), 20 ng/ml rhEGF (Calbiochem, Gibbstown, NJ), 0.5 μg/ml hydrocortisone (Sigma), 10 μg/ml insulin (Sigma), 100 ng/ml

cholera toxin (Gibco) and a penicillin-streptomycin antibiotic solution (100 units/ml penicillin, 100 μg/ml streptomycin) (Hyclone). All cells were maintained in a humidified atmosphere at 37°C, 5% CO2, 95% air.

3.2.2 Antibodies, Chemicals and Reagents

Commercially available isoform specific antibodies against Akt1, Akt2 and Akt3 were purchased from three different companies: anti-Akt1 (D-17), Akt2 (F-7), and Akt3 (M-14 and C-14) along with their corresponding blocking peptides (Akt1 (D-17) sc-7126-P, Akt2 (F-7) sc-5270-P, and Akt3 (M-14) sc-11521-P) were from Santa Cruz Biotechnology (Santa Cruz, CA). Anti-Akt1 (2H10) (#2967), Akt2 (#2962), and Akt3 (#4059), were purchased from Cell Signaling Technology (Danvers, MA). The third set of Akt isoform specific antibodies (Akt1 (07-416), Akt2 (07-372), Akt3 (05-780 and 07-383)) and recombinant proteins specific for each of the Akt isoforms were purchased from Upstate Biotechnology (Lake Placid, NY). Antibodies against phosphorylated-Akt (p-Akt S473), pan-Akt, and PTEN were obtained from Cell Signaling Technology. For the co-localization experiments, antibodies against Lamin B1 (H-90), Calnexin (H-70), PDI (H-160), TGN38 (C-15), and VDAC1 were from Santa Cruz Biotechnology (Santa Cruz, CA), while anti-α-tubulin and -γ-tubulin antibodies were purchased from Sigma. For antibody dilutions in the experiments, please see Table A1 in Appendix II. MitoTracker Red CMXRos Mitochondrial Probe was from Cambrex Bioscience Walkersville, Inc. (Charles City, IA). Secondary peroxidase-conjugated antibodies (anti-mouse, -rabbit, and –goat antibodies) employed in the Western blot analysis were purchased from Sigma, Pierce, and Calbiochem, respectively. Fluorescein (FITC)-conjugated AffiniPure donkey anti-mouse IgG, AffiniPure Fab fragment

rabbit anti-goat (IgG) (H +L), and Cy5-conjugated AffiniPure donkey anti-rabbit IgG were purchased from Jackson Immunoresearch (West Grove, PA). Donkey anti-goat IgG FITC, goat anti-mouse IgG FITC, donkey anti-rabbit IgG-rhodamine, and rhodamine-conjugated donkey anti-goat IgG were obtained from Santa Cruz Biotechnology (Santa Cruz, CA). Lipofectamine 2000 transfection reagent, and Opti-MEM I reduced serum media utilized in the siRNA transfections was supplied by Invitrogen. DNase I and M-MLV were also from Invitrogen.

3.2.3 Immunocytochemistry

The Akt isoform localization experiments required protocols that incorporated single, double and triple antibody staining techniques followed by visualization and analysis using confocal microscopy as outlined in Chapter 2, Section 2.8.3.

3.2.3.1 Single Staining

All immunostaining experiments that employed single staining were performed according to the protocol outlined in Chapter 2, Section 2.8.1. All Akt isoform primary antibodies used in the immunofluorescence experiments were diluted 1:10 while the fluorescein-(FITC) conjugated IgG secondary antibody was diluted 1:100 (1% BSA in TBS) (please refer to Appendix II, Table A1 for more detailed information regarding the antibodies employed). Additional coverslips where the primary antibody incubation step was omitted were included as controls (primary-omission controls). The primary-omission controls were performed for each experiment to ensure specificity of the signals, and to evaluate non-specific background staining caused by the secondary antibody.

3.2.3.2 Co-localization Studies and Double Staining

Cells on a coverslip were washed in TBS, fixed in paraformaldehyde, and permeabilized in Triton X-100/PBS, as indicated in Chapter 2, Section 2.8.1 prior to proceeding with immunostaining. For double labeling with two antibodies, cells on coverslips were first processed according to the single staining procedure (i.e., cells were treated with blocking solution and then incubated with the primary and secondary antibodies). This process was then repeated for the second probe. The only notable exception to the procedure was that all coverslips had to be incubated in the dark for the duration of the experiment to avoid photobleaching of the signals. The Akt isoforms were stained first, followed with a FITC-conjugated IgG secondary antibody for detection. Fluorescent antibodies for the second probe were either rhodamine (1:100) or Cy5 (1:500) and were used for the detection of the following subcellular markers: Lamin B1 (nucleus), calnexin (smooth endoplasmic reticulum), PDI (rough endoplasmic reticulum), and TGN38 (Golgi apparatus). All concentrations of the subcellular markers were initially determined by titration via immunostaining with the single staining procedure and diluted 1:10 for the final experiments. Whenever possible, Lamin B1, a protein localized to the nucleus and nuclear membrane was used in place of DAPI staining to denote the location of the nucleus in the immunostaining experiments.

In order to examine the co-localization between Akt2 and the mitochondria, 50 nM of MitoTracker Red CMXRos was added to the media of each coverslip in a 6-well plate, and incubated for 45 min at 37°C, 5% CO_2. The cells on the coverslips were then removed from the media, washed in TBS, and followed by fixation and permeabilization prior to immunostaining with an anti-Akt2 antibody. Matched controls were included during all experiments, with the primary antibody omitted during the staining procedure (primary-omission condition).

3.2.3.3 Akt Isoform Triple Staining and Akt1-Akt3 Double Staining

When all three sources of the primary antibodies species were different (i.e., Akt1, Akt2, and Lamin B1 were raised in goat, mouse and rabbit, respectively), the coverslips containing cells were processed in the same manner as in double staining, but incorporated an additional third block and third antibody incubation to the procedure. Due to the fact that two of the isoform-specific antibodies used for immunofluorescence were raised in the same species (Akt1 and Akt3 were both raised in goat), alterations had to be made to the staining protocols for triple isoform staining, as well as Akt1-Akt3 double staining. First, BSA, which was added to the blocking buffer and solutions used to dilute the primary and secondary antibodies, had to be omitted due to the introduction of non-specific noise in the system. Second, all secondary antibodies used in the procedure had to be raised in the same species, in this case, donkey. After fixation and permeabilization, the cells on coverslips were blocked (10% (v/v) equine serum in PBS) for 1 h at room temperature and washed once in TBS. Anti-Akt1 antibody was diluted in TBS, incubated for 45 min and washed. An AffiniPure Fab Fragment rabbit anti-goat antibody (100 μg/ml diluted in PBS) was added to the coverslips (cells) to sterically flood the goat immunoglobulins, thereby allowing the first goat antibody to be 'seroconverted' to rabbit. This step lasted for 30 min and the coverslips were washed once in TBS. Next, donkey anti-rabbit Cy5 antibody was added to the coverslips for 30 min. To ensure that the Fab fragment incubation worked, an additional control was also stained with any donkey anti-goat fluorescent secondary antibody after the Fab incubation, mounted and visualized by confocal microscopy. If the signal from the primary antibody was visible on this control, then the immunoglobulins were not efficiently blocked during the process. The cells on the coverslip were washed and then blocked for a

second time, and incubated with anti-Akt2 and donkey anti-mouse FITC-conjugated antibodies. For Akt3, the same process was repeated, with a third blocking step; however, the secondary antibody was donkey anti-goat rhodamine-conjugated antibody. Double staining with Akt1 and Akt3 proceeded in the same manner. Primary-omission control coverslips were also incubated in addition to the Fab control for the double/triple staining procedure.

3.2.4 SDS-PAGE and Western Blot Analysis

Experimental procedures are outlined in Chapter 2, Section 2.3.

3.2.5 Subcellular Fractionation

MDA-MB231 cells in 10-cm plates (4-5 plates that were pooled to give approximately 2 x 10^7 cells) were plated the day prior to the experiments, and grown under standard culture conditions. Subcellular fractions were collected using the Mitochondrial Isolation Kit for Cultured Cells (Pierce Biotechnology) according to the directions specified by the manufacturer, with some modifications. Briefly, the cells on the plates were washed 3 times with ice-cold PBS, with the residual PBS removed by pipetting. The cells were scraped from the plates in PBS (800 µl-1.0 ml), transferred into a 2.0-ml eppendorf tube, and centrifuged at 850 x g for 2 min using a refrigerated Eppendorf centrifuge (Model 5415 D). The PBS was discarded and the cell pellet was resuspended in 800 µl of Reagent A (supplied) which was supplemented with inhibitors (1x Complete Protease Inhibitor Tablets (Roche), 1 mM PMSF, 2 mM Na_3VO_4, 10 mM NaF). The cells were gently vortexed for 5 s and incubated on ice for 2 min. Cells were then lysed with approximately 60-80 strokes using a Dounce homogenizer. To ensure complete cell lysis, 5 µl of this suspension was

spotted onto a slide and stained with trypan blue (Sigma). On average, 85-95% cell lysis was achieved. Next, 800 μl of Reagent C (supplied; also supplemented with inhibitors) was added to the cell suspension which was transferred to a pre-chilled 2.0-ml eppendorf tube. The contents of the tube were mixed by inversion and centrifuged at 700 x g at 4°C for 10 min in a table-top Eppendorf centrifuge. The supernatant was transferred into a new tube to be centrifuged further and the remaining pellet (nuclear fraction) was washed twice with 500 μl PBS and retained. The supernatant was then further centrifuged at 3000 x g at 4°C for 15 min to obtain the mitochondrial fraction. This resultant supernatant from this fraction (cytosol fraction) was decanted into a new eppendorf tube. The remaining pellet containing the mitochondrial fraction was resuspended in Reagent C (500 μl) and further centrifuged at 12000 x g for 5 min to wash the pellet. The supernatant was discarded and the pellet was resuspended in 50 μl of Cell Lysis Buffer. An aliquot of the nuclear fraction, cytosol fraction, and mitochondrial fraction were all diluted in 5x Sample Buffer and boiled for 5 min. The fractions were loaded onto a polyacrylamide gel (10%), resolved by electrophoresis, and the proteins were transferred onto PVDF membranes, as previously described. The protein fractions were analyzed via Western blot analysis using Akt isoform specific antibodies (Akt1 from Cell Signal, Akt2 from Santa Cruz, and Akt3 from Upstate) in the first round of Western blotting, and then probed for specific subcellular markers in the second round of blotting to evaluate the efficiency of fractionation and the localization of the Akt isoforms. The cytosolic fraction was probed with an antibody against α-tubulin; the nuclear fraction was analyzed with anti-Lamin B1, while the fractionation and localization of the mitochondrial fraction was assessed by the mitochondrial protein VDAC1.

3.2.6 Antibody Specificity Determination. To determine the specificity of each Akt isoform antibody, four techniques were employed: (1) peptide blocking/competition experiments, (2) targeted siRNA ablation to each Akt isoform, (3) Western blot analysis using isoform specific recombinant proteins, and (4) immunoprecipitation of each Akt isoform, followed by Western blot analysis (IP/Western).

3.2.6.1 Peptide Blocking Experiments

Antigen binding by antibodies was prevented by preincubating the antibody with a 5-fold excess (w/v) of blocking peptides. Akt1, Akt2, and Akt3 antibodies (2 μg) (Santa Cruz) were incubated with 10 μg of each blocking peptide in a 0.5 ml eppendorf tube with constant rotation on a nutating shaker for 2 h at room temperature. After the incubation period, TBS supplemented with 1% (w/v) BSA was added to the solution to obtain a final volume of 100 μl. The antibody-peptide solution was then used in place of the primary antibody incubation in the immunocytochemistry procedure for single staining (see Section 3.2.3.1, above). Blocking peptides were incubated with their respective corresponding antibody, as well as with the antibodies of the two remaining isoforms (i.e., Akt1 blocking peptide was incubated with Akt1, Akt2 and Akt3 antibodies) to discern if the peptides showed binding activity toward the other Akt isoform antibodies. The peptide-antibody solutions were then used during the primary antibody incubation step in the immunocytochemistry single staining procedure and the results were analyzed by confocal microscopy.

3.2.6.2 Targeted siRNA ablation to each Akt isoform

MDA-MB231 cells were plated onto sterile glass coverslips that were placed in one well of a 6-well clustered dish the day before transfection and allowed to adhere overnight. The following day, the cells on coverslips were transfected according to the protocol outlined

in Chapter 2, Section 2.7. All cells on coverslips were processed for immunostaining 48 h post-transfection with a single antibody stain as outlined in Chapter 2, Section 2.8.1. For these experiments, siRNA Set #1 was utilized.

3.2.6.2 Recombinant Protein Analysis

Isoform-specific recombinant proteins for Akt1, Akt2 and Akt3 (20 ng) were loaded onto 10% SDS-polyacrylamide gels, transferred onto PVDF membranes and then subjected to Western blot analysis with each Akt isoform-specific antibody in order to assess both the specificity and cross-reactivity of each antibody. Every lot of each isoform-specific antibody was tested in this manner to ensure that no cross-reactivity was present between the lots of antibodies purchased from the same vendor with the same catalogue number.

3.2.6.3 Immunoprecipitation/Western Blot Analysis (IP/Western)

For the immunoprecipitation procedure, please see Chapter 2, Section 2.4.

3.2.7 RNA Extraction, Reverse Transcription (RT) and Quantitative-PCR (Q-PCR)

Q-PCR was performed for each Akt isoform on each cell line using MDA-MB231 cells as the reference cell line for the standard curve, as protein analysis had indicated that MDA-MB231 cells expressed all three isoforms in a relatively similar degree (i.e, none of the isoforms were overexpressed in this cell line). For a more detailed protocol, please refer to Chapter 2, Sections 2.5 and 2.6. The following primers were used in the PCR reactions:

Akt1 Forward 5'-TGGGCCTGGCAAAACCT-3'
Akt1 Reverse 5'-CGGTCTGAATCTGGTTCATTCA-3'

Akt2 Forward 5'-CAAGGATGAAGTCGCTCACACA-3'
Akt2 Reverse 5'-GAACGGGTGCCTGGTGTTC-3'

Akt3 Forward 5'-GTCGAGAGAGCGGGTGTTCT-3'
Akt3 Reverse 5'-TGTAGATAGTCCAAGGCAGAGACAA-3'

S28 Forward 5'-TCCATCATCCGCAATGTAAAAG-3'
S28 Reverse 5'-GCTTCTCGCTCTGACTCCAAA-3'

3.2.8 Plasmid DNA Transfections

To verify the localization of Akt2, plasmid constructs were used for overexpression studies in MDA-MB231 cells. Akt2 cDNA in a pCR 2.1-TOPO vector (a kind gift from Dr. J.M. Woodgett, Department of Medical Biophysics and Ontario Cancer Institute) was digested with SpeI and EcoRV and the fragment containing an Akt2 ORF inserted into a pECFP-N1 vector at the BglII and KpnI site. The insert was confirmed by both restriction enzyme digestion analysis and nucleotide sequencing.

To overexpress Akt2 in MDA-MB231 cells, cells were plated onto 1.8-cm sterile glass coverslips placed in a 6-well dish and allowed to adhere overnight. Transfections were performed in the same manner as the siRNA transfections, with adjustments made for volume. Four micrograms (4 μg) of plasmid DNA was added to 250 μl of Opti-MEM I, and 10 μl Lipofectamine 2000 was added to 250 μl of Opti-MEM I medium. After 5 min incubation, the DNA and Lipofectamine solutions were mixed. The transfection mixture was incubated for 20 min, prior to being gently added to the well. The cells were incubated overnight, and the media was changed to regular growth medium the next day. The cells on the coverslips were co-stained with MitoTracker CMXRos or anti-Akt2 antibody according to the immunostaining protocols specified above (Section 3.2.3.1 and 3.2.3.2).

3.2.9 Treatment with Radiation and Epidermal Growth Factor (EGF)

3.2.9.1 Akt Isoform Localization Examined After Radiation Treatment

MDA-MB231 cells were plated onto sterile glass coverslips placed in 6-well dishes and allowed to adhere overnight (RPMI, 10% (v/v) FBS). The next day, cells were treated with 5 Gy (RS320 Irradiation System, Gulmay Medical Inc) processed for immunostaining (Section 3.2.3.1), and the localization of the Akt isoforms was examined 3 h-16 h post-irradiation treatment.

3.2.9.2 Akt2 Translocation and Statistical Analysis

Differences in the perinuclear morphology between control and radiated conditions were analyzed by counting cells in a minimum of 10 fields over the course of 3 independent experiments, with the exception of the 8 h timepoint which was performed 5 times. Cell counts were analyzed using a univariate 2-way ANOVA and Kruskal-Wallis' tests to ensure consistency between parametric and non-parametric analyses. All statistics were analyzed using SPSS for Windows v. 12.0

3.2.9.3 Akt Isoform Localization Examined After Radiation or EGF treatment in serum-starved cells

MDA-MB231 cells were plated onto glass coverslips as indicated above. The next day, the medium was removed and the cells were serum starved overnight (RPMI, 0.1% (v/v) FBS) prior to treatment with either 5 Gy radiation or EGF (100 ng/ml, Santa Cruz) and returned to the incubator for 1 h. At the end of the timepoint, the cells on the coverslips were fixed, permeabilized, and processed for immunostaining.

3.3 RESULTS

3.3.1 Antibody specificity

Rigorous antibody screening was performed to ensure that each antibody recognized each Akt isoform without displaying cross-reactivity. Four screening methods were

employed: (1) peptide-blocking competition assays were used in the immunofluorescence experiments; (2) targeted siRNA-ablation to each isoform followed by immunostaining; (3) isoform-specific antigen-recognition of recombinant Akt proteins by antibodies; and (4) immunoprecipitation of Akt proteins with isoform-specific antibodies, followed by Western blot analysis. In many cases, more than one antibody was required to effectively study isoform subcellular localization. For instance, the same antibody used in the immunofluorescence experiments may not have been efficient in the immunoprecipitation or Western blot analyses. Thus, in order to determine the subcellular localization of each Akt isoform, the additional screening methods had to be employed.

Due to the similarity in the amino acid sequence of the Akt isoforms, many commercially available isoform-specific antibodies are cross-reactive. Thus, to determine specificity in the immunocytochemistry applications, a panel of isoform-specific antibodies from Santa Cruz Biotechnology was used. In order to ensure that the antibodies showed specific binding activity towards their own antigen, the antibodies were incubated with their own blocking peptides and with the blocking peptides specific to the remaining isoforms, plated on coverslips containing fixed MDA-MB231 cells and analyzed via confocal microscopy. The results demonstrated that the Akt1 antibody from Santa Cruz recognized only Akt1, and prior incubation of the Akt1 antibody with the Akt1 neutralizing peptide effectively inhibited the binding of the antibody in the cells (Fig. 3.1a, ii). Further, the Akt1 antibody did not bind the blocking peptides specific to Akt2 or Akt3. Thus, these peptides had no inhibitory effect on the ability of the Akt1 antibody to bind to Akt1 protein in cells (Fig. 3.1a, iii-iv). Incubation of the Akt2 antibody with the Akt2 blocking peptide prevented the association of the Akt2 antibody with Akt2 protein (Fig. 3.1b, vii). Blocking peptides specific to the Akt1 or Akt3 antigen also showed no inhibition in Akt2 antigen-binding (Fig.

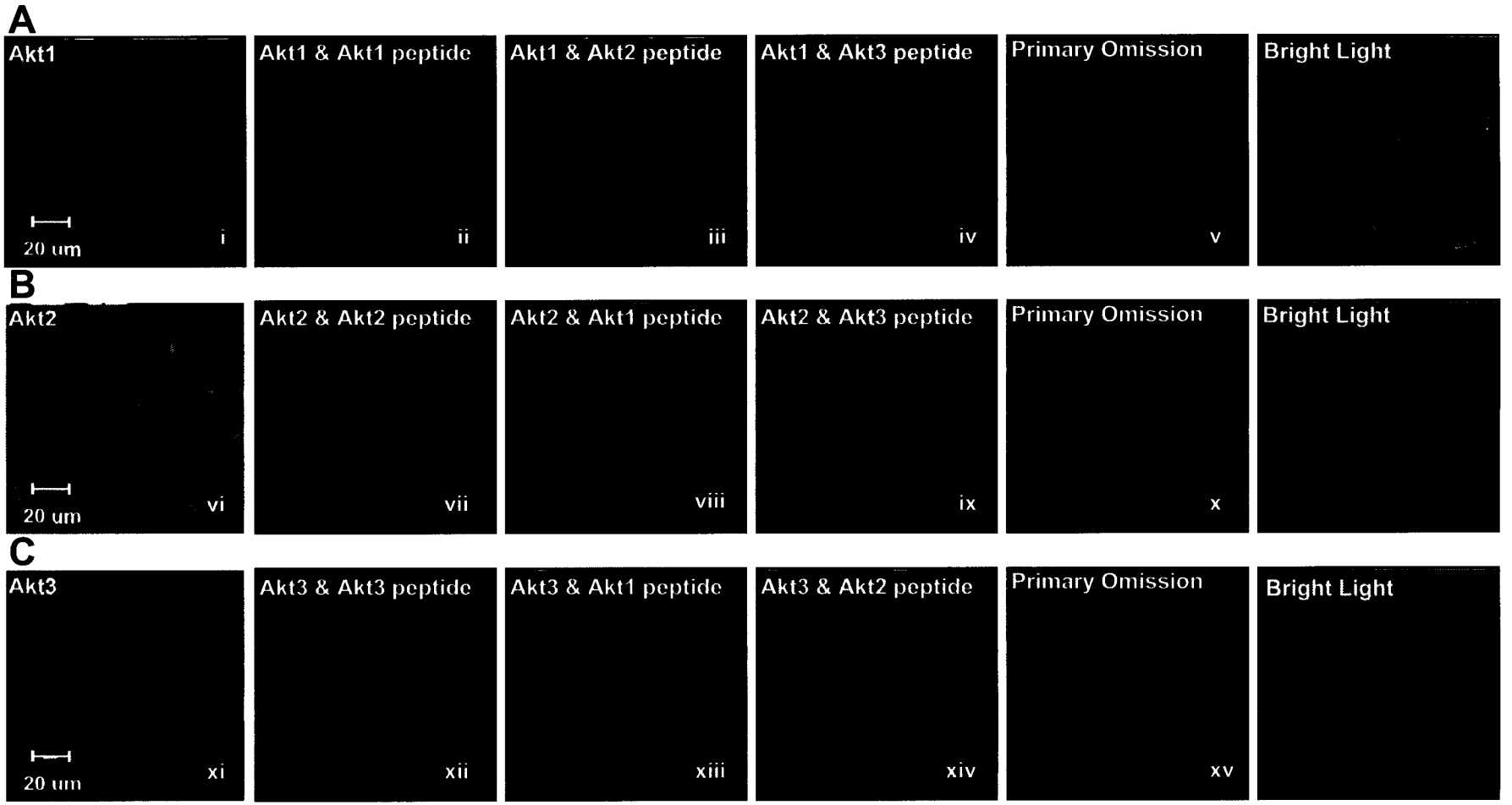
A
Akt1
20 um
i
Akt1 & Akt1 peptide
ii
Akt1 & Akt2 peptide
iii
Akt1 & Akt3 peptide
iv
Primary Omission
v
Bright Light
B
Akt2
20 um
vi
Akt2 & Akt2 peptide
vii
Akt2 & Akt1 peptide
viii
Akt2 & Akt3 peptide
ix
Primary Omission
x
Bright Light
C
Akt3
20 um
xi
Akt3 & Akt3 peptide
xii
Akt3 & Akt1 peptide
xiii
Akt3 & Akt2 peptide
xiv
Primary Omission
xv
Bright Light

3.1b, viii-ix). Similar results obtained for the Akt3 isoform demonstrated the specificity of the Akt3 antibody towards the Akt3 antigen (Fig. 3.1c, xi-xv). Primary-omission controls demonstrated that the immunostaining seen with each isoform was due to antibody-antigen recognition and not due to either autofluorescence or background staining from the secondary antibody (Fig. 3.1a-v; 3.1b, x; and 3.1c, xv).

To further confirm the specificity of the antibodies, each Akt isoform was knocked down using isoform-specific siRNA oligos. Each isoform was transfected into MDA-MB231 cells and knockdown of the proteins, as well as the specificity of the antibodies were examined at 48 h post-transfection. The results presented in Fig. 3.2 show that the antibodies recognize all three antigens. The most efficient knockdown was achieved with Akt2 siRNA (Fig. 3.2b) and Akt3 siRNA (Fig. 3.2c), while Akt1 (Fig. 3.2a) displayed the lowest efficiency in this trial (typically knockdown with this Akt1 siRNA exhibited the most variation and transfections ranged in efficiency from 30-92% over the course of many experiments with this siRNA, with an average knockdown of approximately 68%, as determined by protein densitometry).

The third method of antibody screening involved loading isoform-specific recombinant proteins onto SDS-PAGE gels and probing for specificity using Western blot analyses. Out of nine commercially available antibodies tested, two were found to be cross reactive with another isoform, and were not included in subsequent experiments (Fig. 3.3b, Akt2; and Fig. 3.3c, Akt1). Variation also existed between different antibody lots for the same catalogue number. For example, even when previous screening had shown the antibody to be isoform-specific, antibodies with other lot numbers sometimes showed cross-reactivity with other Akt isoforms. Thus, every lot of each antibody purchased had to be screened prior to use. In Fig. 3.3a, Akt1 Lot G0804 was only slightly cross-reactive with Akt3 in the

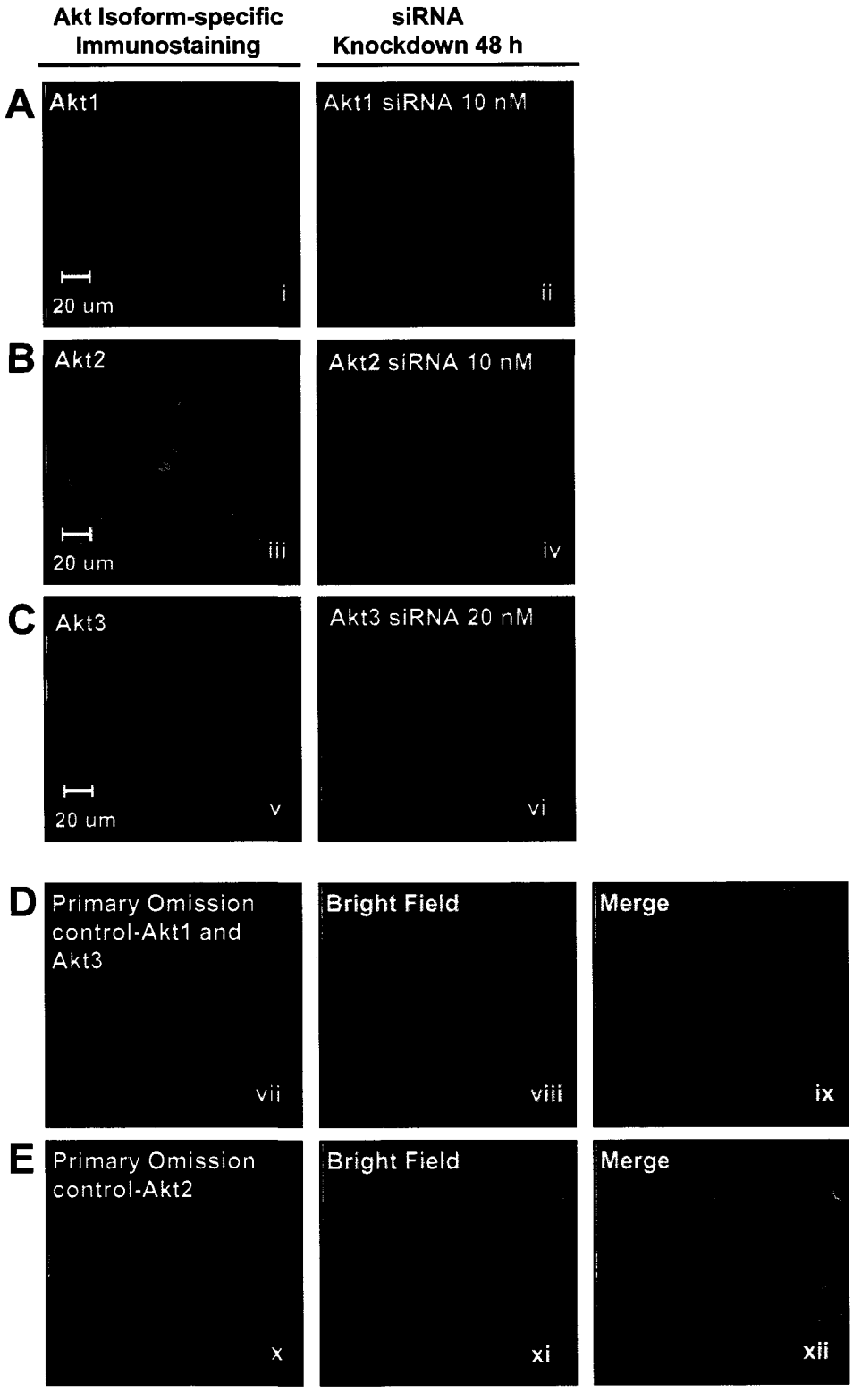
Akt Isoform-specific Immunostaining
siRNA Knockdown 48 h
A
Akt1
20 um
i
Akt1 siRNA 10 nM
ii
B
Akt2
20 um
iii
Akt2 siRNA 10 nM
iv
C
Akt3
20 um
v
Akt3 siRNA 20 nM
vi
D
Primary Omission control-Akt1 and Akt3
vii
Bright Field
viii
Merge
ix
E
Primary Omission control-Akt2
x
Bright Field
xi
Merge
xii

recombinant protein analysis; however, this lot efficiently pulled down both Akt1 and Akt3 isoforms during immunoprecipitation (data not shown). As a result, this antibody could only be used for the immunofluorescence experiments, since there were no discernible differences caused by the slight cross-reactivity in that particular application. A widely used pan-Akt antibody was also screened with the recombinant proteins and was found to effectively recognize all three isoforms with the greatest specificity exhibited towards Akt1 (Akt> Akt2> Akt3) (Fig. 3.3b). Based on the results obtained from the recombinant protein recognition analyses, the following isoform-specific antibodies were chosen for inclusion in the remaining experiments: Akt1 from Cell Signaling Technology (Cat. #2967), Akt2 from Santa Cruz Biotechnology (Cat. #sc-5270), and Akt3 from Upstate Biotechnology (Cat. # 05-780). Including the panel of antibodies from Santa Cruz used in the immunofluorescence applications; this allowed for the analysis of the subcellular localization of the Akt isoforms with two sets of isoform specific antibodies, with the exception of anti-Akt2 where only one antibody was found suitable.

In vitro immunoprecipitation of each isoform with these antibodies in MDA-MB231 cells followed by Western blotting was performed to ensure that the selected antibodies were able to pull down each isoform and exhibit no additional cross-reactivity. As shown in Fig. 3.3d, the Akt1 antibody from Cell Signaling Technology (Cat. #2967) was able to effectively pull down Akt1 and exhibited no cross-reactivity to immunoprecipitated Akt2 from Santa Cruz Biotechnology (Cat. #sc-5270) or anti-Akt3 from Upstate Biotechnology (Cat. #05-780). Similar results were obtained for both anti-Akt2 and anti-Akt3 (Fig. 3.3d), thus demonstrating the specificity of the antibodies used in this study.

3.3.2 Differential subcellular localization of the Akt Isoforms in MDA-MB231 cells

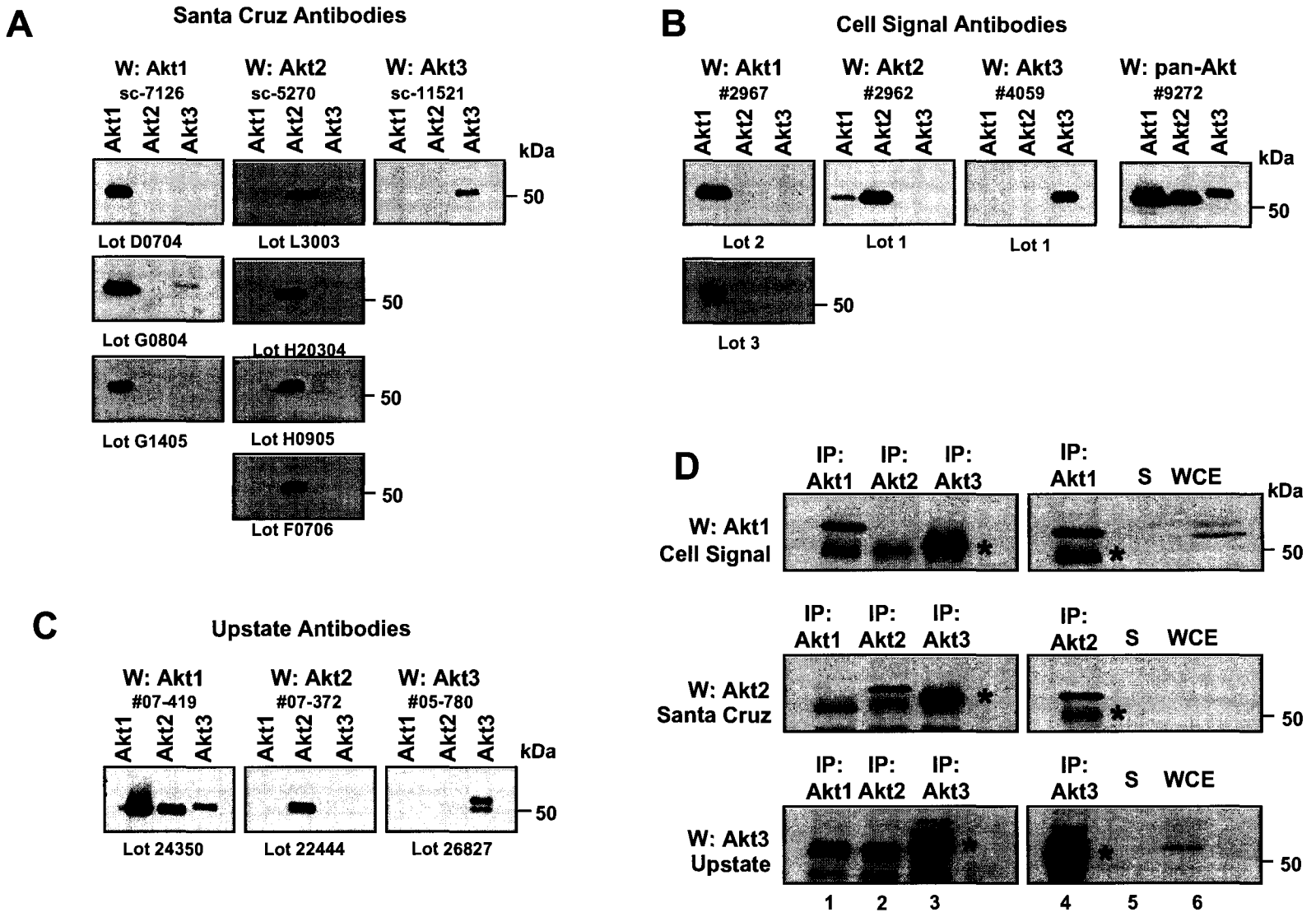
A
Santa Cruz Antibodies
W: Akt1
sc-7126
W: Akt2
sc-5270
W: Akt3
sc-11521
Akt1 Akt2 Akt3
kDa
50
Lot D0704
Lot L3003
Lot G0804
Lot H20304
Lot G1405
Lot H0905
Lot F0706
B
Cell Signal Antibodies
W: Akt1
#2967
W: Akt2
#2962
W: Akt3
#4059
W: pan-Akt
#9272
Lot 2
Lot 1
Lot 1
Lot 3
C
Upstate Antibodies
W: Akt1
#07-419
W: Akt2
#07-372
W: Akt3
#05-780
Lot 24350
Lot 22444
Lot 26827
D
IP: Akt1 IP: Akt2 IP: Akt3
IP: Akt1 S WCE
W: Akt1 Cell Signal
IP: Akt2 S WCE
W: Akt2 Santa Cruz
IP: Akt3 S WCE
W: Akt3 Upstate
1 2 3 4 5 6

One pervasive thought throughout the Akt literature is that the Akt isoforms are localized to the cytoplasm and therefore, may exhibit functional redundancy. Some of these conclusions may be erroneous as antibodies used in the past have been cross-reactive, or the degree of cross-reactivity was never evaluated (many early publications used the Akt1 antibody from Upstate, which recognizes all three isoforms in the recombinant protein analysis [Fig. 3.3c]). Further, many studies have examined the signaling properties of pan-Akt, as opposed to elucidating the contribution of each individual Akt isoform. The current model of Akt activation suggests that PI3K activation (the conversion of $PI(4,5)P_2$ to $PI(3,4,5)P_3$) promotes the translocation of Akt to the inner leaflet of the plasma membrane, where it is phosphorylated/activated. This widely accepted model assumes that all three isoforms behave similarly and are therefore present in the cytoplasm, however studies examining the subcellular localization of the isoforms together has not yet been examined. To gain an understanding of this aspect, MDA-MB231 cells were immunostained with isoform-specific antibodies and the subcellular localization of the isoforms was examined. Triple staining of Akt1, Akt2 and Akt3 demonstrates that each isoform has a unique subcellular localization pattern, at least in MDA-MB231 breast cancer cells. Akt1 localization was ubiquitous throughout the cytoplasm and exhibited some nuclear exclusion (Fig 3.4a, i; Fig. 3.4b, v; and Fig. 3.4c, ix). Akt2 was also localized throughout the cytosol, but displayed two distinct morphologies: a punctuate staining that was either within the cytoplasm, or localized to the perinuclear region (Fig. 3.4a, ii; Fig. 3.4b, vi; and Fig. 3.4d, xii). Akt3 was localized to the nucleus, including the nuclear membrane (Fig. 3.4a). The merged image indicates that the Akt isoforms occupy different subcellular locations in MDA-MB231 breast cancer cells (Fig. 3.4a, panel iv). Although experimental artifacts can often occur in immunocytochemistry experiments (i.e., sources of artifact can be introduced

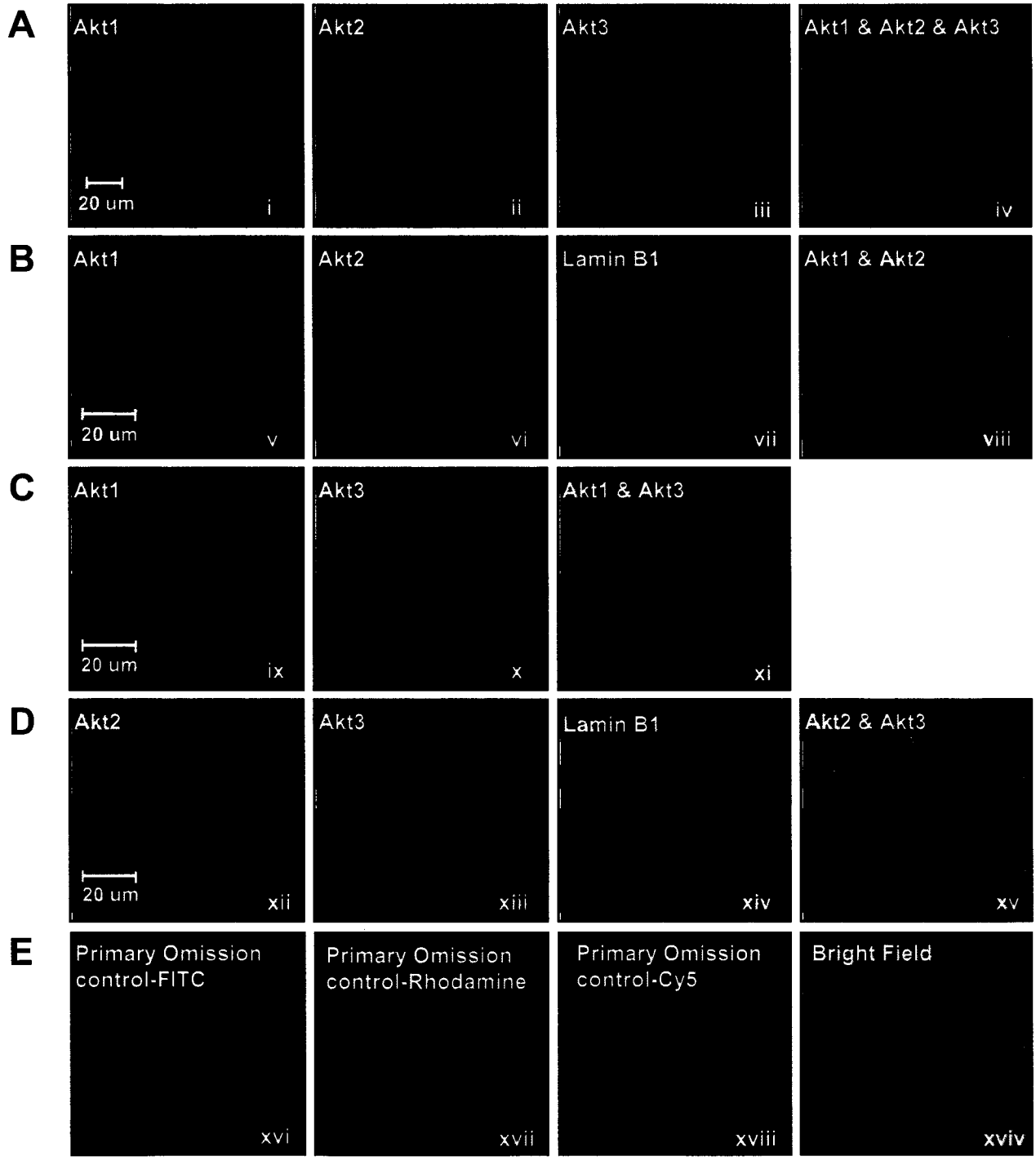
A
Akt1
20 um
i
Akt2
ii
Akt3
iii
Akt1 & Akt2 & Akt3
iv
B
Akt1
20 um
v
Akt2
vi
Lamin B1
vii
Akt1 & Akt2
viii
C
Akt1
20 um
ix
Akt3
x
Akt1 & Akt3
xi
D
Akt2
20 um
xii
Akt3
xiii
Lamin B1
xiv
Akt2 & Akt3
xv
E
Primary Omission control-FITC
xvi
Primary Omission control-Rhodamine
xvii
Primary Omission control-Cy5
xviii
Bright Field
xviv

during the fixation process, through elevated background noise due to non-specificity in both the primary and secondary antibodies, necrotic/damaged cells may uptake the probes differently from the viable cells in the same field or plane on the coverslip, photobleaching, etc.,), Fig. A4 in Appendix II demonstrates the specificity of the signals observed in these experiments, as no bleedthrough into other channels was present. As well, the primary omission controls (Fig. 3.4e) show that the amount of non-specific staining associated with the secondary antibodies was neglible.

Double and triple antibody staining was performed in different combinations to confirm the localization results observed in Fig 3.4a. Triple immunostaining of either Akt1-Akt2-Lamin B1 (Fig. 3.4b) or Akt2-Akt3-Lamin B1 (Fig 3.4d) further supported the original subcellular analysis performed with all three isoforms. Incorporation of Lamin B1 in combination with Akt3 staining revealed that Akt3 and Lamin B1 were co-localized in the nucleus and nuclear membrane (although the image in 3.4d, xiii shows that there is some cytoplasmic staining for Akt3 as well, this may be due to artifact in this particular image. An additional image from this same trial is shown in Appendix III, Fig. A8). Nevertheless, Akt3 showed neither co-localization with Akt1 (Fig. 3.4c, xi) nor with Akt2 (Fig. 3.4d). Thus, triple staining of the Akt isoforms, revealed that while some overlap occurs (both Akt1 and Akt2 have cytoplasmic representation), they also have a distinct subcellular localization in MDA-MB231 cells (Fig. 3.4).

3.3.3 The subcellular localization of the Akt Isoforms is not specific to MDA-MB231 cells

Previously published reports have determined the subcellular localization of the isoforms in adipocytes (3T3-L1 cells) in glucose signaling (Calera et al., 1998) or in widely

used non-transformed cell lines such as Hek293 cells (Andjelkovic et al., 1997; Meier et al., 1997). To determine if the subcellular localization of the isoforms observed in MDA-MB231 cells is a common feature of other cancer cells; immunostaining analysis with the isoforms was performed in two additional breast cancer cell lines, MDA-MB468 and MCF-7. A non-transformed breast epithelial cell line (MCF-10A) was also included as a control. To exclude the possibility that the localization of the isoforms was specific to breast cancer, a prostate cancer cell line (LNCaP), and a liver cancer cell line (HepG2) were also included in the analysis. Human embryonic kidney cells (Hek293) and the variant of this cell line, 293T, which contains the SV40 large T antigen were also included to extend the analyses to non-cancer cell lines and allow for comparison with previously published findings (Andjelkovic et al., 1997; Meier et al., 1997). Further, inclusion of Hek293 and 293T cells allowed an opportunity to examine if transformation by the SV40 large T antigen altered the localization of Akt. Indirect immunostaining analysis in Fig. 3.5 revealed that the subcellular localization of the Akt isoforms in MDA-MB468 and MCF-7 breast cancer cells was consistent with the previous findings observed for MDA-MB231 cells in Fig. 3.4 (Figs. 3.5a, b). Endogenous Akt1 was primarily localized to the cytoplasm, again exhibiting some nuclear inclusion, while Akt2 was found along the perinuclear region, also within the cytoplasm. Akt3 resided mainly in the nucleus with representation on the nuclear membrane and was also co-localized with Lamin B1 in both MDA-MB468 and MCF-7 breast cancer cells. There was no difference observed in the localization of the isoforms in MCF-10A cells, the non-transformed breast cell control, suggesting that the observed localization of the isoforms is intrinsic to breast cells, and not a result of oncogenic transformation (Fig. 3.5c). Further, the localization of the isoforms was similar in HeLa cervical cancer cells (Fig. 3.5d), LNCaP prostate cancer cells (Fig. 3.5e), and HepG2 hepatocytes (Fig. 3.5f), suggesting that the

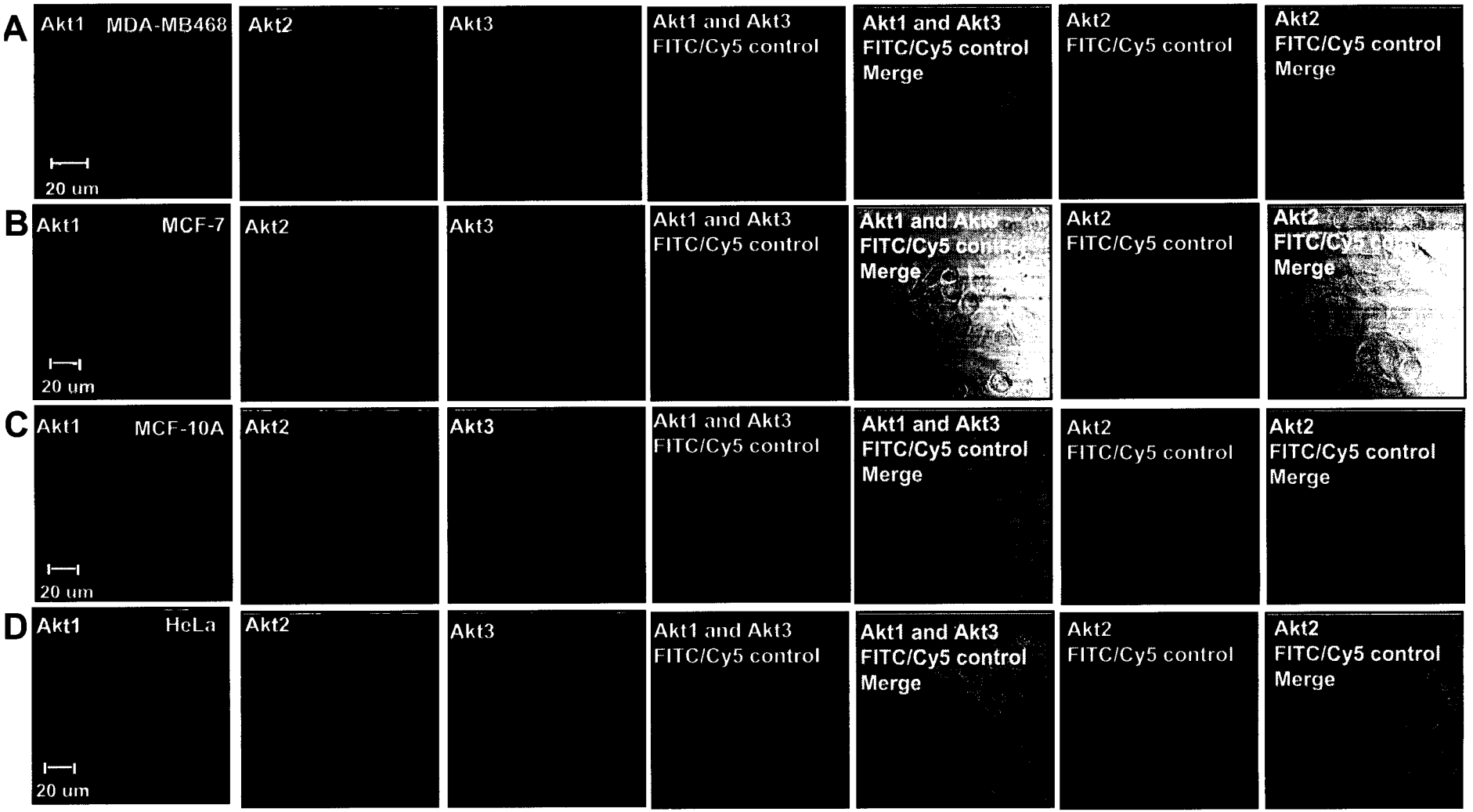
A
Akt1 MDA-MB468
20 um
Akt2
Akt3
Akt1 and Akt3 FITC/Cy5 control
Akt1 and Akt3 FITC/Cy5 control Merge
Akt2 FITC/Cy5 control
Akt2 FITC/Cy5 control Merge
B
Akt1 MCF-7
20 um
Akt2
Akt3
Akt1 and Akt3 FITC/Cy5 control
Akt1 and Akt3 FITC/Cy5 control Merge
Akt2 FITC/Cy5 control
Akt2 FITC/Cy5 control Merge
C
Akt1 MCF-10A
20 um
Akt2
Akt3
Akt1 and Akt3 FITC/Cy5 control
Akt1 and Akt3 FITC/Cy5 control Merge
Akt2 FITC/Cy5 control
Akt2 FITC/Cy5 control Merge
D
Akt1 HeLa
20 um
Akt2
Akt3
Akt1 and Akt3 FITC/Cy5 control
Akt1 and Akt3 FITC/Cy5 control Merge
Akt2 FITC/Cy5 control
Akt2 FITC/Cy5 control Merge

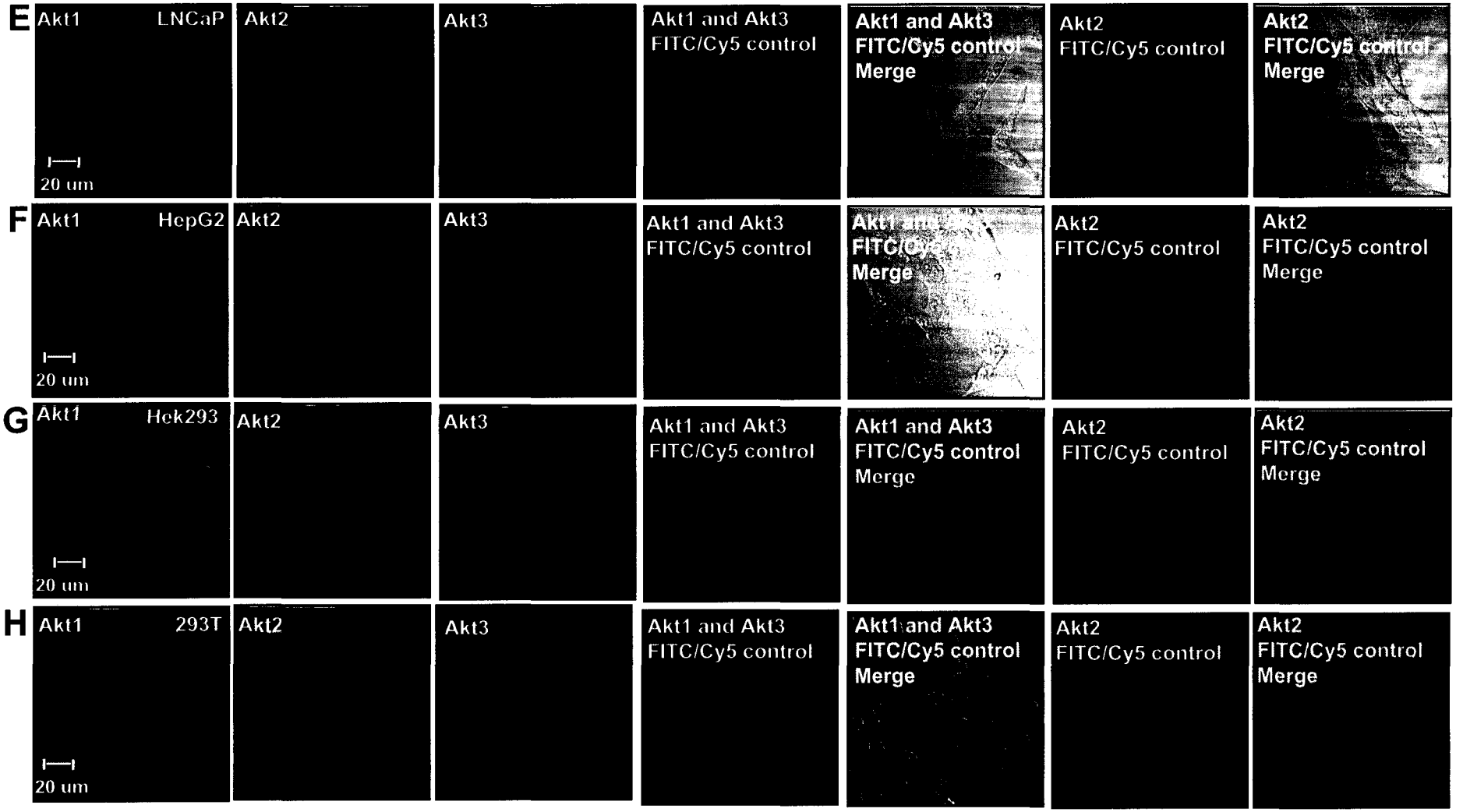
E
Akt1
LNCaP
20 um
Akt2
Akt3
Akt1 and Akt3
FITC/Cy5 control
Akt1 and Akt3
FITC/Cy5 control
Merge
Akt2
FITC/Cy5 control
Akt2
FITC/Cy5 control
Merge
F
Akt1
HepG2
20 um
Akt2
Akt3
Akt1 and Akt3
FITC/Cy5 control
Akt1 and Akt3
FITC/Cy5 control
Merge
Akt2
FITC/Cy5 control
Akt2
FITC/Cy5 control
Merge
G
Akt1
Hek293
20 um
Akt2
Akt3
Akt1 and Akt3
FITC/Cy5 control
Akt1 and Akt3
FITC/Cy5 control
Merge
Akt2
FITC/Cy5 control
Akt2
FITC/Cy5 control
Merge
H
Akt1
293T
20 um
Akt2
Akt3
Akt1 and Akt3
FITC/Cy5 control
Akt1 and Akt3
FITC/Cy5 control
Merge
Akt2
FITC/Cy5 control
Akt2
FITC/Cy5 control
Merge

subcellular localization of the Akt isoforms observed in MDA-MB231 cells is not specific to breast cells or breast cancer.

However, the subcellular localization of the Akt isoforms was quite different for Hek293 cells. Both Akt2 and Akt3 showed nuclear localization, while Akt1 was ubiquitously localized throughout the cell in both the cytoplasm and the nucleus, and did not display the nuclear exclusion evident in the Akt1 localization in the other cell lines (Fig. 3.5g). Consistent with the results observed for Hek293 cells, Akt2 and Akt3 were still primarily localized within the nucleus in 293T cells, the transformed analogue of Hek293 (Fig. 3.5h). Akt1, however, was primarily localized within the cytoplasm and displayed the nuclear exclusion evident of the staining shown in the other cell lines (Fig. 3.5h).

3.3.4 The mRNA and protein levels of the isoforms varies within the cell lines

Previously published studies reported overexpression in some of the Akt isoforms and correlated their protein/mRNA levels to the aggressiveness of some types of cancers. Since the subcellular localization of the isoforms did not differ among the cancer cell lines, the levels of both protein and mRNA were examined to discern if overexpression in any of the Akt isoforms was present. Protein levels for each of the cell lines examined by Western blot analysis revealed variations among the isoforms. The breast cell lines, MDA-MB231, MDA-MB468 and MCF-10A expressed all three isoforms to a similar degree (Fig 3.6a). MCF-7 cells, however, expressed very little Akt3 (see lane 3), even though the expression of Akt3 protein was evident in the immunostaining analysis (see Fig. 3.6b). The LNCaP and HepG2 cell lines expressed both Akt1 and Akt2, but like MCF-7 cells, showed a very low level of Akt3 protein (Fig. 3.6a, lanes 8 and 9). Interestingly, HeLa cells expressed a higher level of the Akt2 isoform, but showed little Akt1 or Akt3 protein expression (Fig. 3.6a, lane

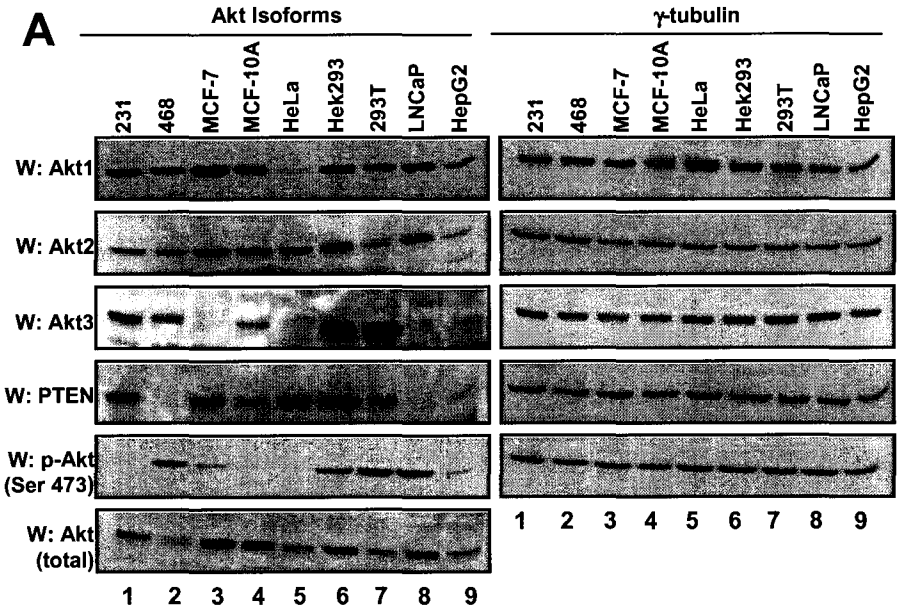
A
Akt Isoforms
γ-tubulin
231
468
MCF-7
MCF-10A
HeLa
Hek293
293T
LNCaP
HepG2
W: Akt1
W: Akt2
W: Akt3
W: PTEN
W: p-Akt (Ser 473)
W: Akt (total)
1 2 3 4 5 6 7 8 9

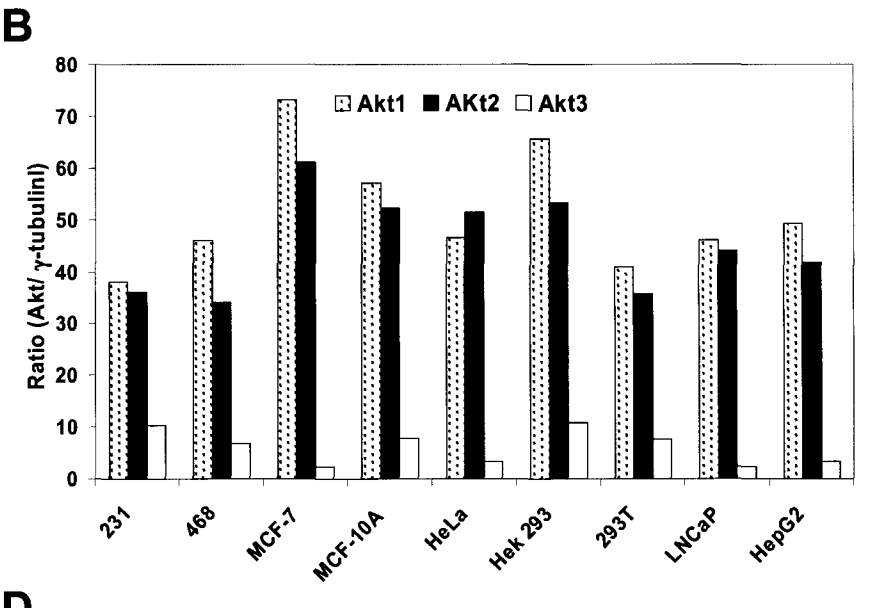
B
Akt1 AKt2 Akt3
Ratio (Akt/ γ-tubulinl)
0 10 20 30 40 50 60 70 80
231 468 MCF-7 MCF-10A HeLa Hek 293 293T LNCaP HepG2

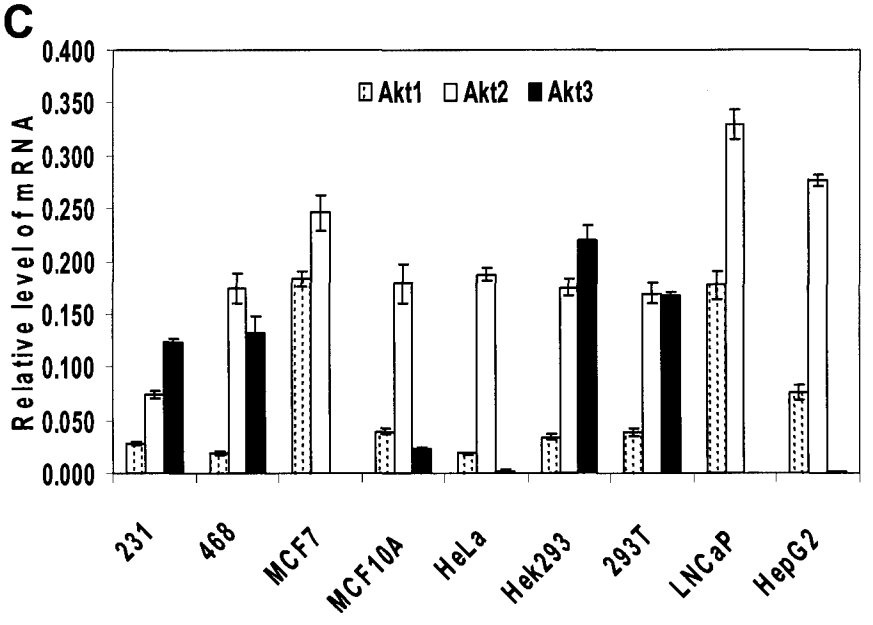
C
Akt1 Akt2 Akt3
Relative level of mRNA
0.000 0.050 0.100 0.150 0.200 0.250 0.300 0.350 0.400
231 468 MCF7 MCF10A HeLa Hek293 293T LNCaP HepG2

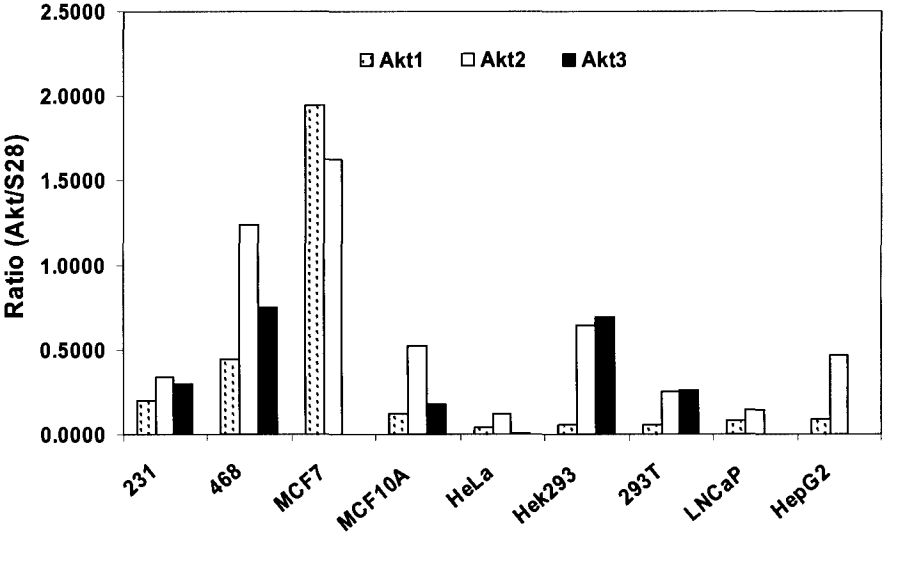
D
Akt1 Akt2 Akt3
Ratio (Akt/S28)
0.0000 0.5000 1.0000 1.5000 2.0000 2.5000
231 468 MCF7 MCF10A HeLa Hek293 293T LNCaP HepG2

5). Although Hek293 and 293T expressed all three isoforms, they showed the highest level of Akt3 protein. Taken together, the densitometric analysis revealed that Akt1 and Akt2 proteins were shown to be expressed in all of the cell lines to a similar degree (Fig. 3.6b). Akt3, however, displayed the lowest level of protein expression in all the cell lines examined (Fig. 3.6b).

Deletion or mutation in PTEN, the phosphatase which counteracts PI3K activity, causes uncontrolled Akt activation and can be observed through the constitutive phosphorylation of the serine 473 residue on Akt. Western blot analysis of PTEN demonstrated that MDA-MB468 and LNCaP cells did not express PTEN confirming previous reports that the PTEN gene is deleted in these cell lines (Howells et al., 2002; Sharrard and Maitland, 2007). Consistent with the PTEN deletion, these cells displayed high basal levels of Akt phosphorylation (Fig. 3.6a). Interestingly, although Hek293 and 293T cells did not display reduced protein levels of PTEN, these cell lines displayed the highest levels of p-Akt phosphorylation. Collectively, the analyses of the Akt isoforms and PTEN suggested that the subcellular localization of the Akt isoforms in the cell lines examined was independent of the PTEN status or phosphorylation of Akt (p-Akt) (Figs. 3.6a and 3.6b).

Next, the levels of Akt1, -2, and -3 mRNA were examined by quantitative-PCR (Q-PCR). Akt1 and Akt2 mRNA were highly expressed in the cell lines examined, compared to the mRNA levels for Akt3 (Figs. 3.6c and 3.6d). The mRNA levels of Akt3 were extremely low, or at the threshold of detection in HeLa, LNCaP, and HepG2 cells (Figs. 3.6c and 3.6d). In general, the mRNA expression of the isoforms followed the same trend observed with that of the protein analysis.

The low expression levels of both Akt3 protein and mRNA in some of the cell lines was disconcerting given that indirect immunostaining showed that these cells expressed Akt3

protein. There is discrepancy in the literature as to whether Akt3 is present in these cell lines at all. Some studies demonstrated that MCF-7 or LNCaP cells do not express Akt3, while others found it present (deFeo-Jones et al., 2005; Okano et al., 2000). The anti-Akt3 antibody used in the immunostaining assay was directed to the C-terminus of Akt3, while the antibody used in the Western blot analysis was targeted to the N-terminus. When a Western blot analysis employing the same C-terminal antibody used in the immunostaining was used in Western blotting an interesting result emerged: the Western blot showed two bands for Akt3. To clearly resolve the two bands, longer gel-running times were required (Fig. 3.7a). The bottom band corresponded to the Western blot obtained with the N-terminal antibody. This finding could potentially indicate two things: (1) the immunostaining seen in these cell lines that express low levels of Akt3 protein and mRNA is non-specific; or (2) the C-terminal Akt3 antibody could be recognizing both full-length Akt3 and the splice, Akt3-variant 1 (Brodbeck et al., 2001). However, communication with Santa Cruz indicated that the C-terminus antibody would recognize a full-length Akt3 (personal communication), suggesting that the first hypothesis is likely. To fully elucidate the nature of Akt3 protein expression in MCF-7, HeLa, HepG2 and LNCaP cells, two further experiments were performed. First, MDA-MB231 cells were transfected with a siRNA oligonucleotide specific to Akt3, and a Western blot analysis was performed with both the N- and C-terminus Akt3 antibodies. Results of the siRNA transfection and subsequent western blot analysis indicated that the bottom band was specific for full-length Akt3 (compare the N-terminus and C-terminus panels in Fig. 3.7b) indicating that the top band in the C-terminus Western was non-specific. For the second experiment, all the cell lines were processed for immunocytochemistry using both the N-terminus and C-terminus antibody. MDA-MB231 cells were also incorporated as a positive control. The results of the experiment indicated that regardless of whether the N-

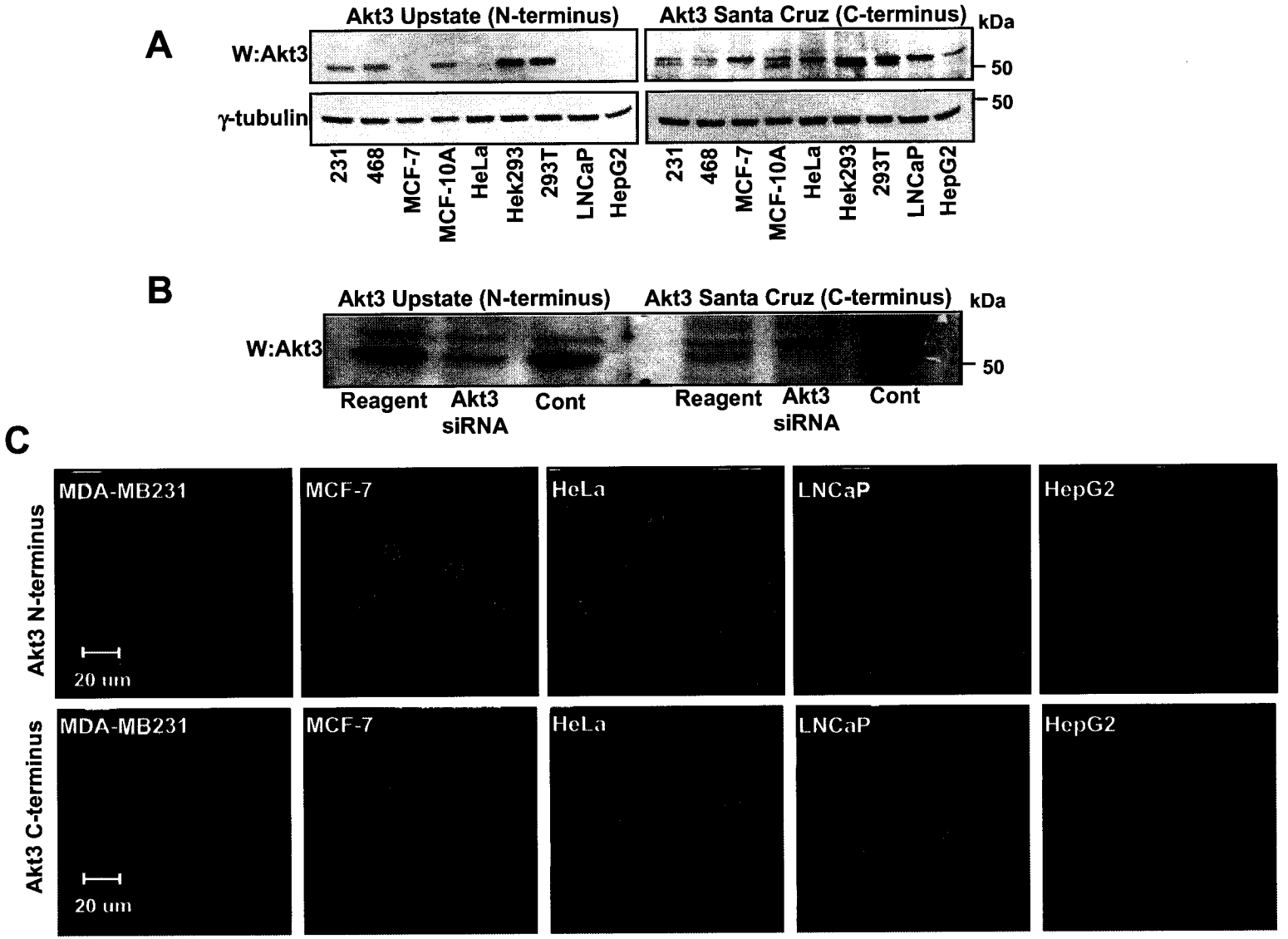
A
Akt3 Upstate (N-terminus)
Akt3 Santa Cruz (C-terminus)
kDa
W:Akt3
γ-tubulin
50
50
231
468
MCF-7
MCF-10A
HeLa
Hek293
293T
LNCaP
HepG2
B
Akt3 Upstate (N-terminus)
Akt3 Santa Cruz (C-terminus)
kDa
W:Akt3
50
Reagent
Akt3 siRNA
Cont
C
Akt3 N-terminus
Akt3 C-terminus
MDA-MB231
MCF-7
HeLa
LNCaP
HepG2
20 um

terminal antibody (Upstate) or C-terminal antibody (Santa Cruz) was chosen, Akt3 was present in these cell lines (Fig. 3.7c). Furthermore, the cell lines stained with the N-terminal antibody showed that Akt3 was localized in the nucleus and nuclear membrane further substantiating the results observed in Figs. 3.4 and 3.5 (above). Taken together, all the cell lines expressed the three Akt isoforms with some variation. Akt3 is present within these cells in a low level, perhaps below or at the threshold for detection by Western blotting or Q-PCR.

3.3.5 Akt2 is co-localized with the mitochondria

Akt2 was stained in tandem with other subcellular markers and the degree of co-localization was analyzed with software after visualization by confocal microscopy. MDA-MB231 cells were stained with Akt2 and with markers specific to the Golgi apparatus, the mitochondria, and the endoplasmic reticulum (both smooth and rough). The results indicated that Akt2 was not co-localized with the endoplasmic reticulum (Fig. 3.8b-c). Image analysis with software (equipped with the Carl Zeiss confocal microscope used) indicated that the R-correlational value (Pearson) between Akt2 and Calnexin (smooth ER), and between Akt2 and PDI (rough ER) was $R=0.11$ ($R^2=0.04$ and $R^2=0.03$ respectively). Statistically, there was some shared localization between Akt2 and trans-Golgi network 38 (TGN38), a marker for the Golgi apparatus ($R=0.30$, $R^2=0.10$). However, the immunostaining analysis in Fig. 3.8d, indicates that there were discernible differences between the staining pattern of Akt2 and that of TGN38. When MDA-MB231 cells were probed with MitoTracker Red and co-stained with anti-Akt2, the co-localization of Akt2 and the mitochondria was evident by visual inspection (Fig. 3.8e). Pearson correlational analysis also indicated that Akt2 and the mitochondria were co-localized; $R= 0.53$, $R^2= 0.30$. Since the total cellular area was assessed, as opposed to regions of interest where both the staining intensity of Akt2 and

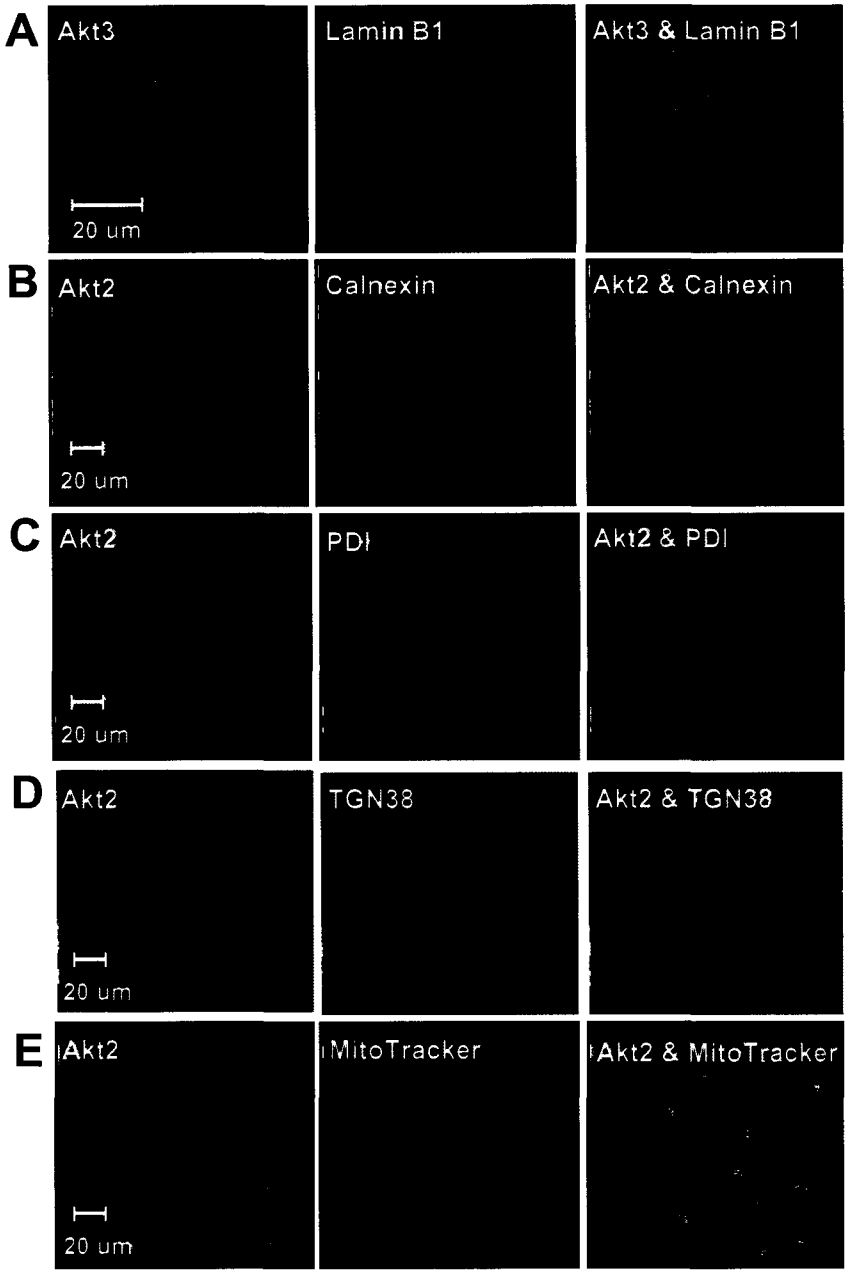
A
Akt3
20 um
Lamin B1
Akt3 & Lamin B1
B
Akt2
20 um
Calnexin
Akt2 & Calnexin
C
Akt2
20 um
PDI
Akt2 & PDI
D
Akt2
20 um
TGN38
Akt2 & TGN38
E
Akt2
20 um
MitoTracker
Akt2 & MitoTracker

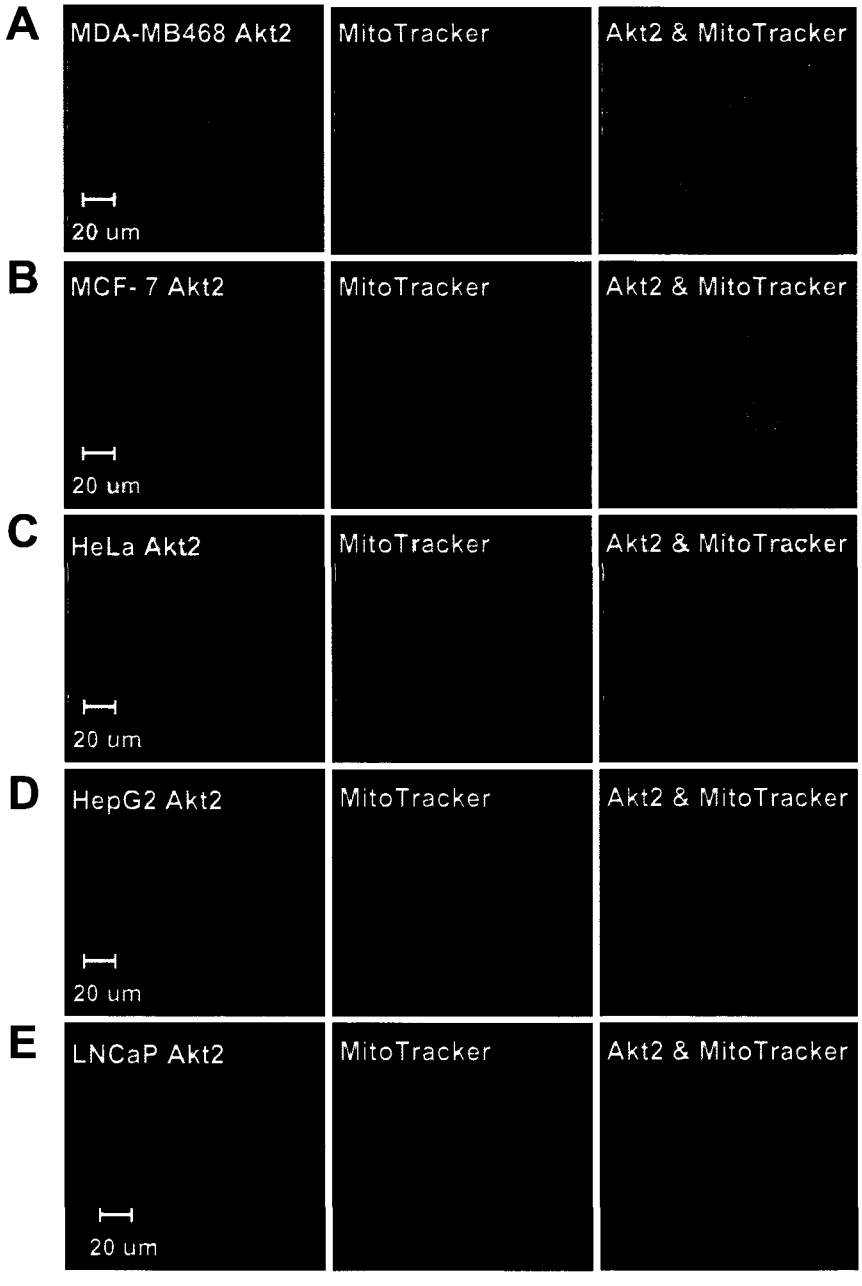
A
MDA-MB468 Akt2
MitoTracker
Akt2 & MitoTracker
20 um
B
MCF- 7 Akt2
MitoTracker
Akt2 & MitoTracker
20 um
C
HeLa Akt2
MitoTracker
Akt2 & MitoTracker
20 um
D
HepG2 Akt2
MitoTracker
Akt2 & MitoTracker
20 um
E
LNCaP Akt2
MitoTracker
Akt2 & MitoTracker
20 um

MitoTracker would be highest; this R-value is most likely conservative due to the fact that the lighter background staining of Akt2 is also incorporated into the calculations. Nonetheless, Akt2 was mostly co-localized with the mitochondria in MDA-MB231 cells. The Akt2-mitochondria association was also apparent when other cell lines were examined. Co-localization of Akt2 with the mitochondria was seen in MDA-MB468 (Fig. 3.9a), MCF-7 (Fig. 3.9b), HeLa (Fig. 3.9c), HepG2 (Fig. 3.9d), and LNCaP cells (Fig. 3.9e). The correlation was highest between Akt2 and the mitochondria in MDA-MB468 cells ($R=0.56$, $R^2=0.32$), and Pearson R-correlational values ranged from 0.29-0.38 in the other cell lines Fig A7 in III shows MDA-MB231 cells, LNCaP cells and HeLa cells stained in tandem with either MitoTracker, Akt2 antibody or both Akt2 and MitoTracker further demonstrating the co-localization of Akt2 and the mitchondria.

The nuclear localization of Akt3 and mitochondrial co-localization of Akt2 were novel findings. Thus, the protein sequences of Akt2 and Akt3 were further analyzed for mitochondrial targeting sequences and nuclear localization signals using software from the Expert Protein Analysis System (EXPASY, http://ca.expasy.org). Analysis of Akt2 by MitoProt II, v1.101 (Claros and Vicens., 1996) indicated that Akt2 did not have a mitochondrial targeting sequence and the probability of export to the mitochondria was evaluated at 0.092. Similarly, Akt3 did not contain a classical nuclear localization sequence as determined by analysis of two different software servers, PredictNLS (Cokol et al., 2000) and NucPred (Brameier et al., 2007, both cited in Emanuelsson et al., 2007).

In order to confirm the results observed in the subcellular localization studies (Fig. 3.4) subcellular fractionation of the Akt isoforms was performed. This allowed confirmation of the findings using a second set of isoform-specific antibodies for Western blotting analysis. Differential centrifugation of MDA-MB231 cells showed that Akt1 was primarily

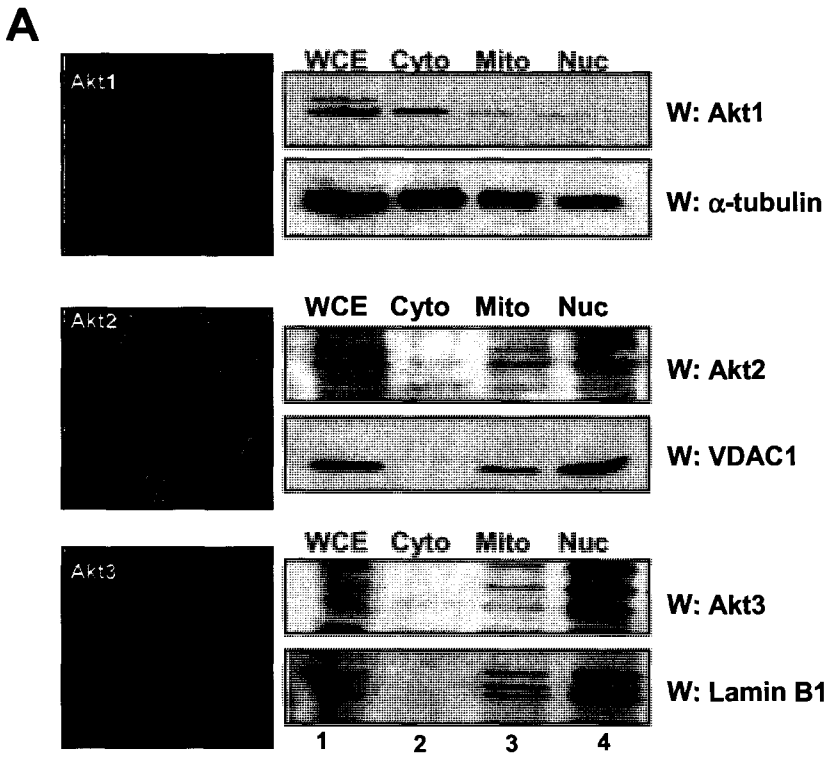
A
Akt1
WCE Cyto Mito Nuc
W: Akt1
W: α-tubulin
Akt2
WCE Cyto Mito Nuc
W: Akt2
W: VDAC1
Akt3
WCE Cyto Mito Nuc
W: Akt3
W: Lamin B1
1 2 3 4
B
Akt2-ECFP
MitoTracker
Akt2-ECFP & MitoTracker
20 um
Akt2-ECFP
Akt2 antibody
Akt2-ECFP & Akt2
20 um

localized in the cytoplasm (Fig. 3.10a, lane 2). Western blot analysis of the fractionated samples showed that Akt2 was found in both the mitochondrial and the nuclear fractions (Fig. 3.10a, lane 3). The localization of Akt2 in the nuclear fraction is most likely due to contamination of the nuclear fraction with mitochondria since Western blotting for VDAC1 (a mitochondrial protein) was also detected in the nuclear fraction. In addition, Akt3 and Lamin B1 (nuclear fraction) were also found to contaminate the mitochondrial fraction. The degree of contamination could have been decreased using a different protocol (i.e., higher centrifugal forces, use of a sucrose gradient, etc). Nevertheless, the subcellular localization of the Akt isoforms determined by indirect immunostaining shown in Fig. 3.4 were confirmed by subcellular fractionation of MDA-MB231 cells and Western blotting with a second set of isoform-specific antibodies.

Since only one commercially available Akt2 antibody was found suitable for these applications and the co-localization of Akt2 to the mitochondria was a novel finding, further analysis of Akt2 was required. MDA-MB231 cells were transiently transfected with Akt2-ECFP and the co-localization between the endogenous and overexpression construct was examined in conjunction with mitochondrial staining. The data shown in Fig. 3.10b suggest that Akt2-ECFP was co-localized with MitoTracker (top panel). Further, Akt2-ECFP was co-localized with endogenous Akt2. Collectively, the results presented in Figure 3.10 further confirm the differential subcellular localization of the Akt isoforms.

3.3.6 The subcellular localization of the Akt isoforms did not change in response to siRNA ablation, or treatment with X-ray irradiation or growth factors

The finding that the three Akt isoforms displayed differential subcellular localizations prompted the examination of their functional relationship to one another. In order to

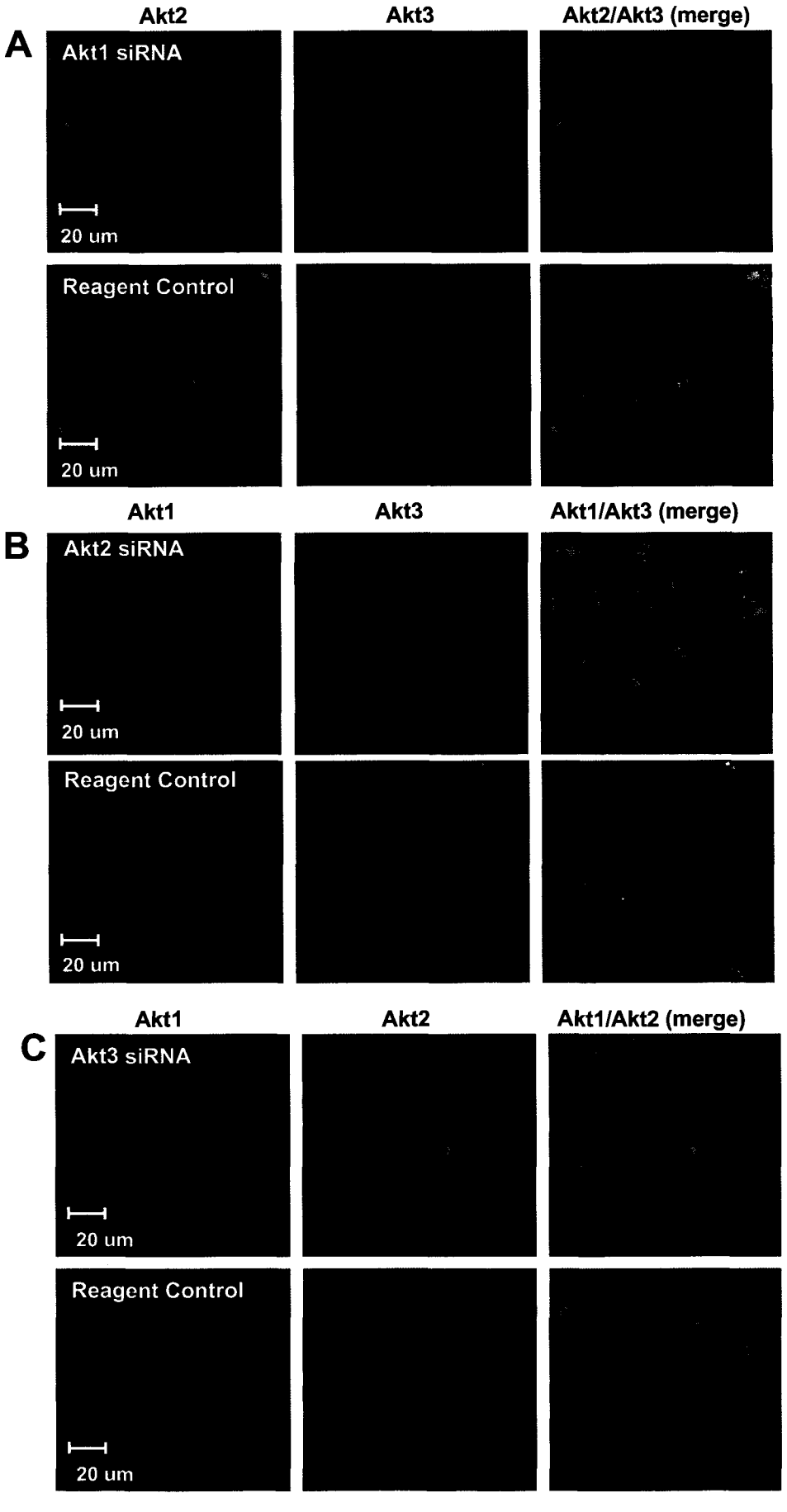
A
Akt2
Akt3
Akt2/Akt3 (merge)
Akt1 siRNA
20 um
Reagent Control
20 um
B
Akt1
Akt3
Akt1/Akt3 (merge)
Akt2 siRNA
20 um
Reagent Control
20 um
C
Akt1
Akt2
Akt1/Akt2 (merge)
Akt3 siRNA
20 um
Reagent Control
20 um

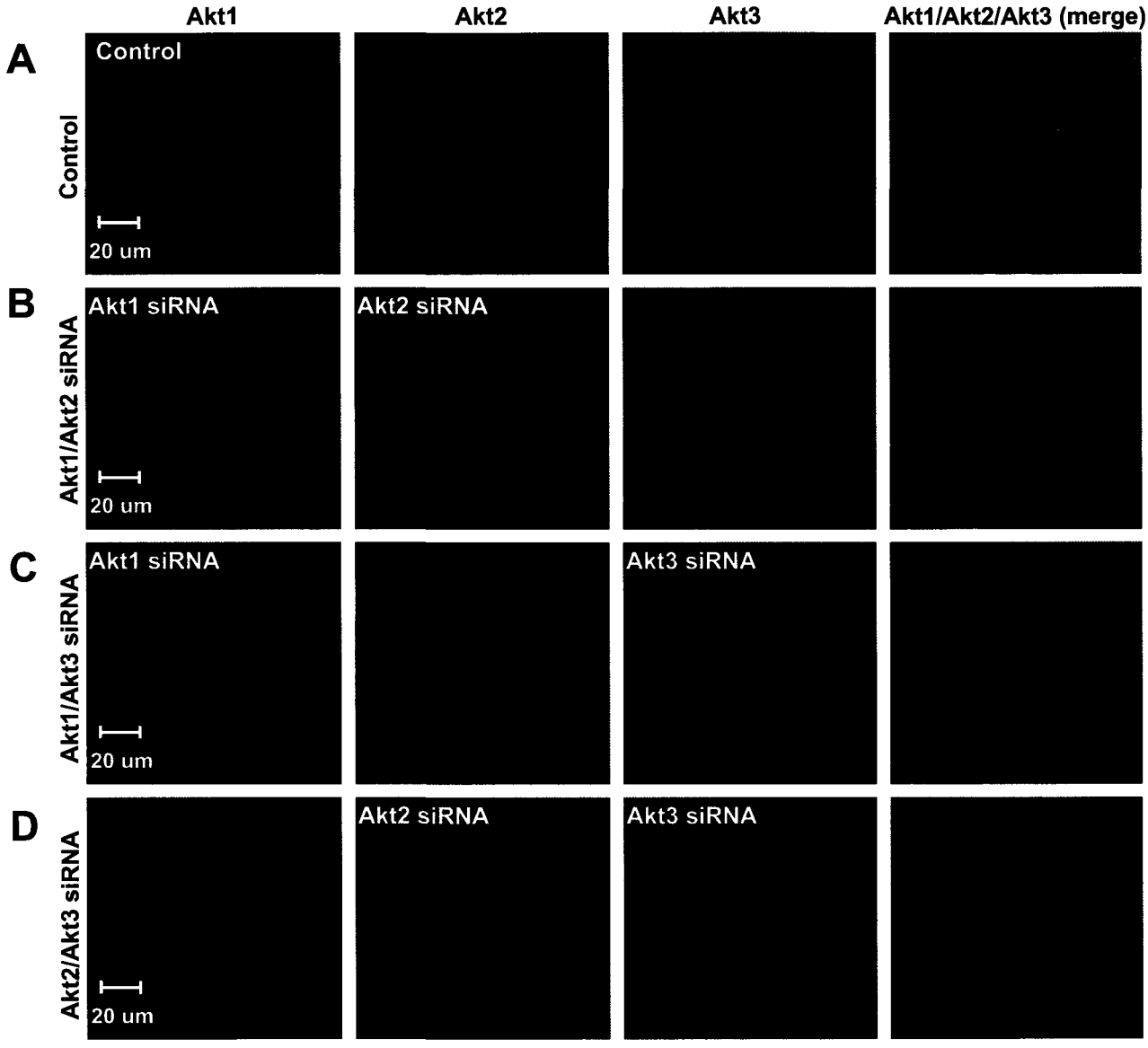
Akt1
Akt2
Akt3
Akt1/Akt2/Akt3 (merge)
A
Control
Control
20 um
B
Akt1 siRNA
Akt2 siRNA
Akt1/Akt2 siRNA
20 um
C
Akt1 siRNA
Akt3 siRNA
Akt1/Akt3 siRNA
20 um
D
Akt2 siRNA
Akt3 siRNA
Akt2/Akt3 siRNA
20 um

determine if the localization of one isoform was crucial; or alternatively, if one isoform would alter its subcellular location to compensate for the other, small interfering RNA technology was employed. These experiments were conducted in two ways. First, one isoform was ablated, and the subcellular localization of the remaining two isoforms was determined. Second, two isoforms were targeted with isoform-specific siRNA and then the subcellular location of the remaining isoform was examined. Single Akt isoform knockdown did not alter the localization of the remaining two Akt isoforms in MDA-MB231 cells (Fig. 3.11a-c). Similarly, double-knockdown of the isoforms in different combination did not alter the localization of the one remaining isoform (Fig. 3.12a-d). The expression of the Akt isoforms by siRNA was knocked down by at least 68% (determined by protein densitometry). While it could be argued that this level of residual isoform could maintain the normal isoform localization, the knockdown of the Akt isoforms does not alter Akt localization in these experiments. These results suggest that the localization of the Akt isoforms is not affected by the presence or absence of the other Akt isoforms at 48 h post-siRNA transfection.

To further examine the localization of the isoforms *in vitro*, MDA-MB231 cells were exposed to two types of cellular stresses known to activate the Akt pathway. To determine if the isoforms would alter their localization in response to a cellular insult, cells on coverslips were first serum starved (0.1% (v/v) FBS) overnight, and then were treated with either 5 Gy X-ray irradiation, or stimulation with growth factors (100 ng/ml EGF) the next day. The localization of the isoforms was then examined 1 h post-treatment. The results indicated that the localization of the isoforms did not change in response to the serum starvation, or to the two different types of treatment (radiation or EGF) when examined 1 h later (Fig. 3.13). Any differences observed in the isoforms were subtle. For instance, treatment with 5 Gy showed

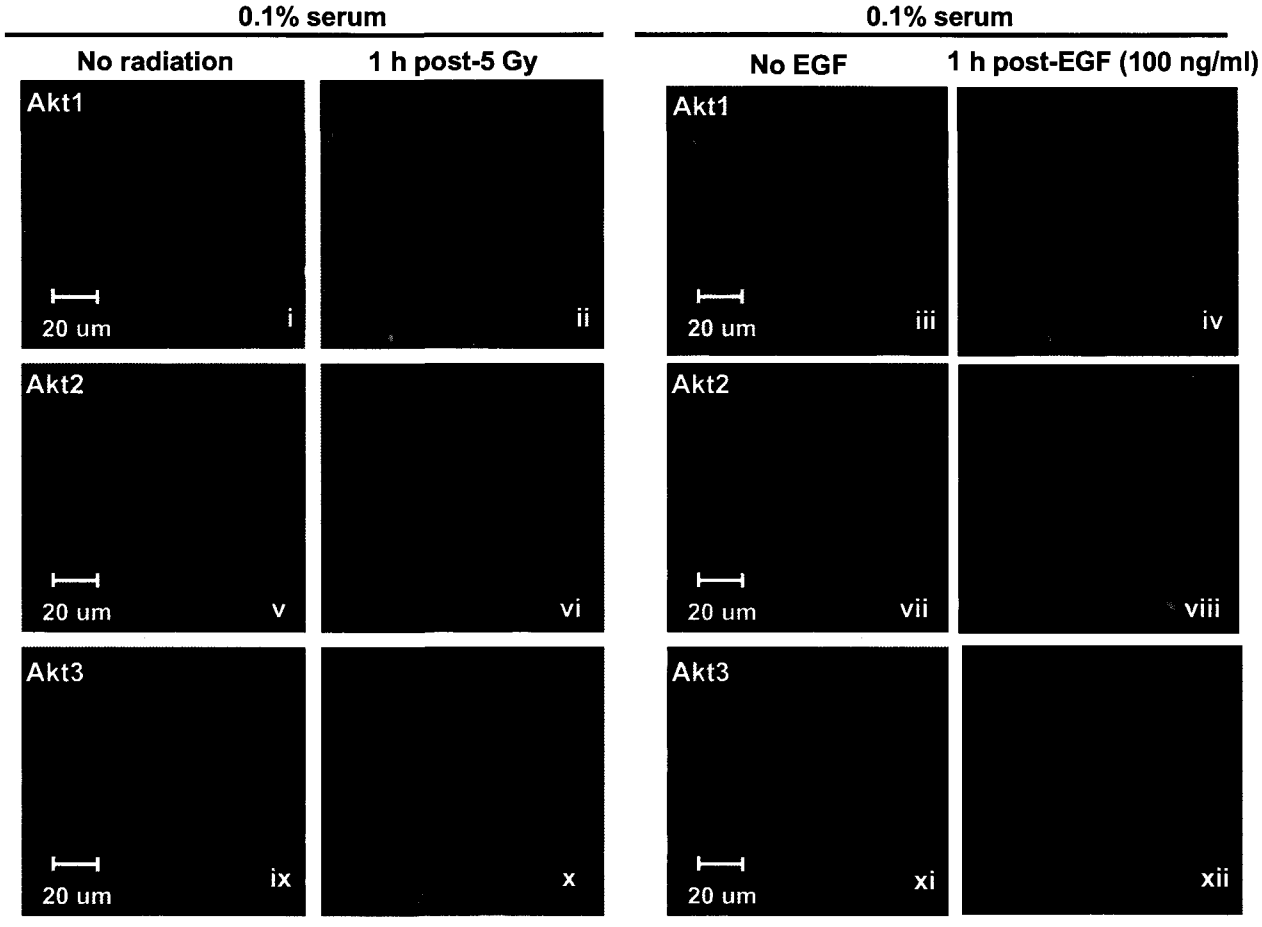
0.1% serum
No radiation
1 h post-5 Gy
0.1% serum
No EGF
1 h post-EGF (100 ng/ml)
Akt1
20 um
i
ii
iii
iv
Akt2
20 um
v
vi
vii
viii
Akt3
20 um
ix
x
xi
xii

less nuclear exclusion than the serum starved control in Akt1 (Fig. 3.13, i and ii). Similarly, Akt3 displayed a slight amount of cytoplasmic staining in the serum starved controls (Fig. 3.13, ix and xi). However, despite these subtle differences, the localization of Akt3 still remains in the nucleus. Thus, regardless of whether one isoform was ablated by siRNA, serum-starved, or treated with radiation or growth factors, the subcellular localization of the Akt isoforms remained unchanged at 1 h post-treatment.

3.3.7 Akt2 translocates to the perinuclear region after radiation treatment

Next, MDA-MB231 cells were treated with irradiation (5 Gy) and the subcellular localization of the isoforms was examined over a prolonged timecourse (3-16 h) as opposed to the 1 h timepoint examined above. After 3 h post-5 Gy, changes in the Akt2 staining pattern were observed (Fig. 3.14). In the control, Akt2 was either slightly perinuclear, or a rounded punctuate aggregate within the cytoplasm (Fig. 3.14a, ii). However, after 5 Gy irradiation, Akt2 was almost exclusively localized to the perinuclear region (Fig. 3.14a, v). Furthermore, this localization pattern was maintained up to the 12- and 16 h timepoint, when the Akt2 morphology, while still mainly perinuclear, became visibly larger and more cytoplasmic (Fig. 3.14a, xi and xiv).

Both Akt1 and Akt3 exhibited slight differences in localization. The localization of Akt1 is cytoplasmic and showed nuclear exclusion in the controls (Fig. 3.14a, i). Treatment with 5 Gy showed an increase in Akt1 nuclear localization, which is consistent with data reported prior by others (Borgatti et al., 2000; Li et al., 2005) and also seen in these experiments (Fig. 3.13). Similarly, Akt3 remained in the nucleus and nuclear membrane. However at 8 h post-irradiation, Akt3 showed slightly more cytoplasmic localization (Fig. 3.14a, ix) (Note that Fig. 3.14 is also included in Appendix III, Fig. A9 with all primary

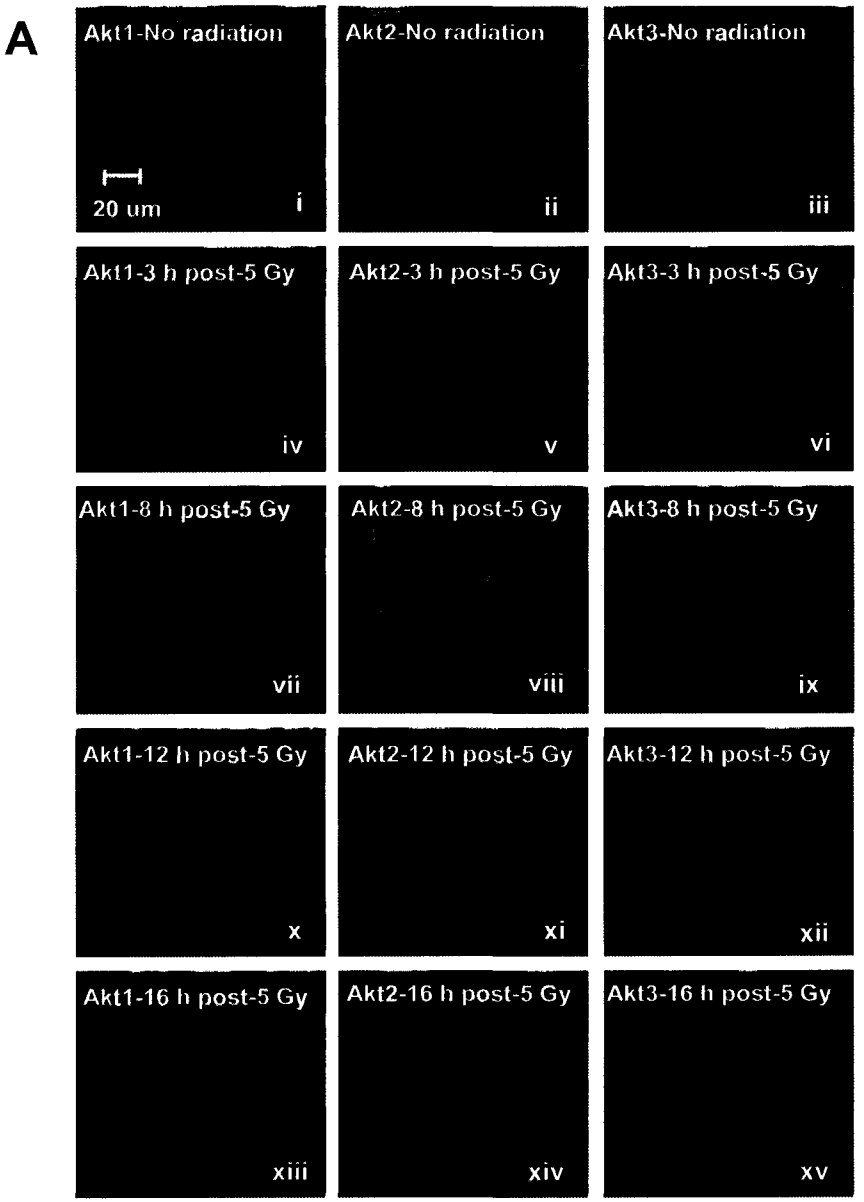
A
Akt1-No radiation
20 um
i
Akt2-No radiation
ii
Akt3-No radiation
iii
Akt1-3 h post-5 Gy
iv
Akt2-3 h post-5 Gy
v
Akt3-3 h post-5 Gy
vi
Akt1-8 h post-5 Gy
vii
Akt2-8 h post-5 Gy
viii
Akt3-8 h post-5 Gy
ix
Akt1-12 h post-5 Gy
x
Akt2-12 h post-5 Gy
xi
Akt3-12 h post-5 Gy
xii
Akt1-16 h post-5 Gy
xiii
Akt2-16 h post-5 Gy
xiv
Akt3-16 h post-5 Gy
xv

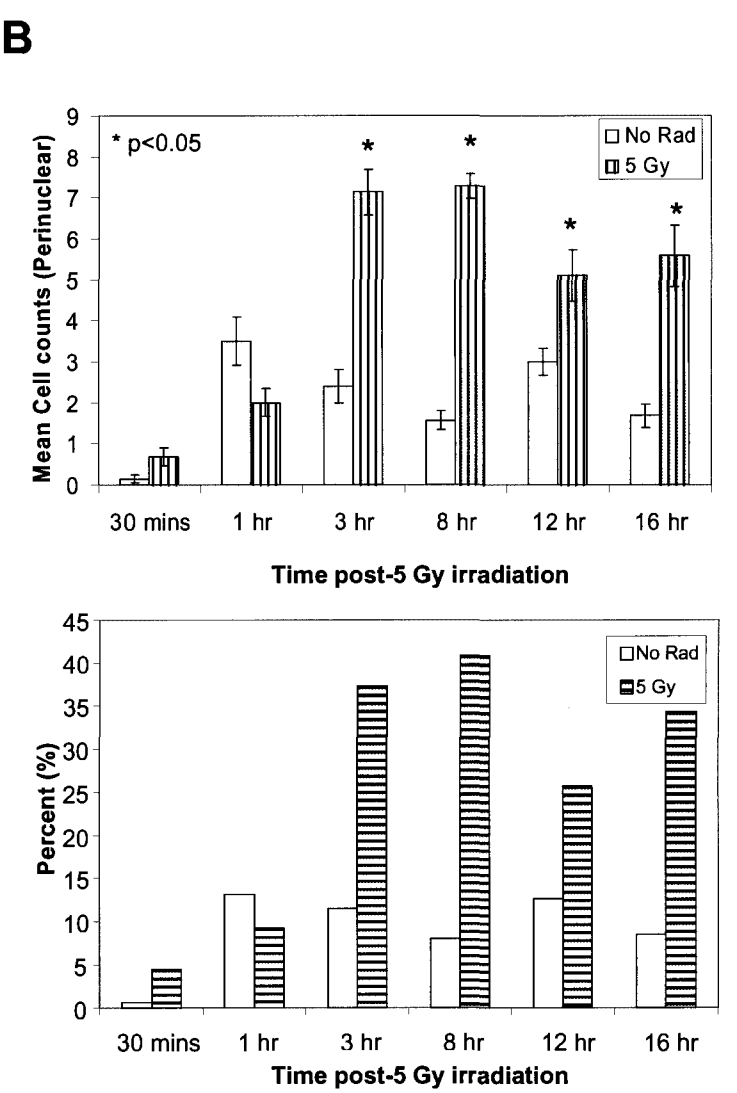
B
* p<0.05
No Rad
5 Gy
Mean Cell counts (Perinuclear)
0
1
2
3
4
5
6
7
8
9
30 mins
1 hr
3 hr
8 hr
12 hr
16 hr
Time post-5 Gy irradiation
No Rad
5 Gy
Percent (%)
0
5
10
15
20
25
30
35
40
45
30 mins
1 hr
3 hr
8 hr
12 hr
16 hr
Time post-5 Gy irradiation

omission controls present for each timepoint of the experiment). To ensure that the change in the morphology and localization of Akt2 was due to the radiation treatment, the perinuclear morphology was evaluated across 3 independent trials, where a minimum of 10 independent fields per trial were assessed. When the perinuclear morphology of Akt2 was compared to the controls and examined across the timecourse, dramatic increases in the perinuclear localization were apparent, with peaks observed at the 3 h and 8 h timepoint in the irradiation conditions, consistent with the initial observations. A 2-way analysis of variance (ANOVA) determined that the relative amount of perinuclear localization was significantly different from the controls from 3 h through to the 16 h timepoint [$p<0.05$, effect size $eta^2=20\%$] (Fig. 3.14b).

Next, Akt2 localization was analyzed in conjunction with the mitochondria to determine if the radiation treatment had any effect on their co-localization. The results presented in Fig. 3.15a clearly demonstrate that Akt2 and the mitochondria remained associated with one another during and after the 5 Gy radiation treatment up to 16 h post-radiation treatment. Further, the differences in Akt2 morphology observed were also consistently observed in the mitochondria, particularly at 8 and 16 h after treatment (Fig. 3.15a). Analysis of Akt2 and MitoTracker staining in MDA-MB468 and MCF-7 breast cancer cells also showed co-localization of Akt2 and the mitochondria during the radiation treatment. Slight differences in both Akt2 and mitochondrial morphology were noted in MDA-MB468 cells at 3 h post-irradiation, and more noticeable differences in mitochondrial morphology were observed in MCF-7 cells. Taken together, the data shown in Figs. 3.14 and Fig. 3.15 suggest that both Akt2 and the mitochondria were enlarged in size and altered in morphology in response to 5 Gy. Further, these results may be general phenomena as they are not specific to MDA-MB231 cells.

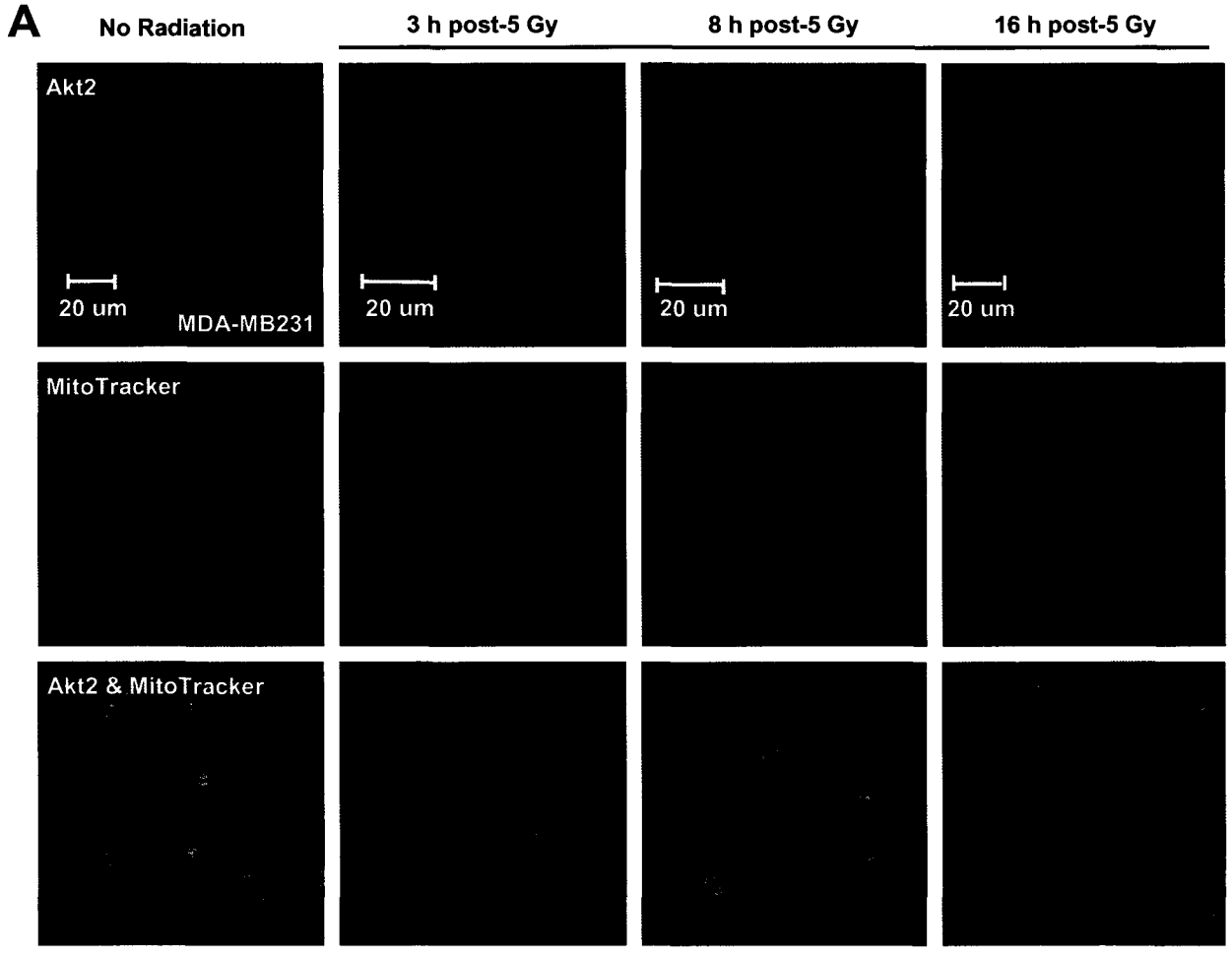
A
No Radiation
3 h post-5 Gy
8 h post-5 Gy
16 h post-5 Gy
Akt2
20 um
MDA-MB231
20 um
20 um
20 um
MitoTracker
Akt2 & MitoTracker
B
No Radiation
3 h post-5 Gy
Akt2 & MitoTracker
20 um
MDA-MB468
Akt2
MitoTracker
Akt2 & MitoTracker
Akt2 & MitoTracker
20 um
MCF-7
Akt2
MitoTracker
Akt2 & MitoTracker

3.4 DISCUSSION

3.4.1 The differential subcellular localization of Akt1, Akt2, and Akt3

The differential subcellular localization of the Akt isoforms represents novel findings and sheds new light on the regulation of Akt signaling. The localization of the isoforms in cancer cells in these *in vitro* studies may provide further insight into the regulation of Akt function, in light of the fact that aberrant Akt activation is associated with oncogenesis and tumour progression. The major finding of this study—Akt2 localization to the mitochondria in cancer cells and the nuclear localization of Akt3 in both tumour and non-cancerous cell lines, is fascinating considering that neither kinase contained a targeting sequence for those subcellular organelles. This suggests that the localization is based on other factors such as protein-protein interactions. Further, these differences in subcellular localization were maintained during radiation or growth factor stimulation, as well as during genetic ablation using siRNA-mediated knockdown technology. The fact that none of the isoforms altered their subcellular localization in lieu of one or two ablated isoforms suggests a mechanistic function for their localization. In addition, it demonstrated that a compensatory mechanism between the endogenous localization of the isoforms may not exist. Akt kinases are activated via two key phosphorylation residues, S473 and T308. Compensation between the isoforms may occur at the level of activation measured via phosphorylation. However, the phosphorylation residues differ by one amino acid for each of the isoforms (S473/S474/S472 for Akt1, -2 and -3, respectively) rendering isoform-specific detection and measurement via confocal microscopy difficult. Nevertheless, the results of this study show that the knockdown of one isoform does not produce a shift in the subcellular localization of the remaining isoforms.

3.4.2 Akt2 co-localization with the mitochondria

Although the co-localization of isoform-specific Akt2 and the mitochondria is a novel finding, previous publications have reported the presence of pan-Akt in the mitochondria. Bijur and Jope (2003) found basal levels of Akt detected by anti-pan Akt antibodies in the mitochondrial matrix as well as in the inner/outer mitochondrial membranes in Hek293 and SH-SY5 neuroblastoma cells. In their study, treatment with insulin-like growth factor-1 (IGF-1) augmented the levels of phosphorylated or activated Akt at the mitochondria. The authors speculated that a selective uptake of Akt into the mitochondria occurred, although the mechanisms of transport of Akt into the mitochondria are largely unknown. Further, this mitochondrially-localized Akt was found to phosphorylate GSK-3β and ATP synthase (β-subunit). In support of their findings, a recent study by others also indicated that insulin-stimulated p-Akt2 translocated to the inner mitochondrial membrane and facilitated the phosphorylation of nNOS (Finocchietto et al., 2008). Akt was also found to localize to the Golgi apparatus as well as to the mitochondria in a study that used a recombinant Akt-fluorescent construct (Sasaki et al., 2003). The authors hypothesized that Akt localization to these compartments may be a more efficient method of phosphorylating target substrates located in these cellular domains. Since endogenous Akt2 localized to the mitochondria in this study, differences in the mitochondrial levels of phosphorylated Akt2 were not assessed. However, the findings presented here suggest that Akt2 is physically associated with the mitochondria considering that Akt2 and the mitochondria co-fractionated with one another. The results presented herein demonstrate the isoform-specific localization of endogenous Akt2 to the mitochondria in cancer cells.

Earlier studies that examined the subcellular localization of Akt1 and Akt2 were usually performed in isolated rat adipocytes or 3T3-L1 adipocytes and assessed for their role in the regulation of glucose metabolism. Published data showed that Akt2 associated with Glut4 transporters in the heavy microsome fraction (Calera et al., 1998; Kupriyanova and Kandror, 1999). The fractionation results in that study found Akt2 in almost all areas of the cell, including the mitochondria/nuclear fraction. However, the strongest Akt2 signal was associated with microsomes, which further supported the role of Akt2 in the intracellular transport of glucose. Consistent with the findings presented here, Akt1 fractions were mainly cytoplasmic (Calera et al., 1998). Kupriyanova and Kandror (1999) reported that only 5-7% of Akt2 co-localizes with Glut4, while the predominant amount of Akt2 remains in the cytoplasm. One inherent problem with fractionation studies is obtaining a pure fractionated sample, without contamination from other cellular compartments. In point of this, an early study conducted on the regulation of glucose transport indicated that the microsomal portions of adipocytes used in their study may not be pure and may contain peroxisomes or the Golgi apparatus (Cushman and Wardzala, 1980; Kupriyanova et al., 1999). Based on the findings from the above studies, it seems logical to conclude that there may be evidence for Glut4 localization to the mitochondria which would connect the pathways between Akt2 localization and glucose transport. Although, there is some evidence that at least one glucose transporter (Glut1) may localize to the mitochondria, there is no evidence to date that Glut4 does as well. One study determined that Glut1 possessed a mitochondrial targeting sequence, and then subsequently confirmed its mitochondrial localization. The sequences for Glut2, Glut3, Glut4, Glut5 and Glut7 were all assessed in this study for target localization sequences. The Glut4 sequence, however, did not contain the target residues that would direct it to the mitochondria (KC et al., 2005). Furthermore, Calera et al., (1998) did not

observe Glut4 in the mitochondria/nuclear fraction in their experiments. However, it was very recently published that Glut4 exhibits a perinuclear distribution in myoblast cells (Dugani et al., 2008). Considering the role that Akt2 plays in glucose transport and the localization to the mitochondria in cancer cells, the mechanism of Akt2 regulation in glucose transport is an important issue that warrants further study.

A question that remains is, why would Akt2 be localized to the mitochondria? Although the potential reasons are most likely complex and multifaceted, the two main reasons could be the involvement of Akt regulation that impinge on the mitochondria mainly, cell survival and cellular metabolism. With regards to Akt and cell survival, Akt functions in anti-apoptotic signaling via a series of downstream phosphorylations to substrates including NF-κb, Bad/Bcl-2, and the FoxO family. At least in the case of Bad/Bcl-2, this signaling would converge on the mitochondria. In support of this idea, a number of published reports indicate that Akt may play a role in the 'functional integrity' of the mitochondria (Gottlob et al., 2001; Majewski et al., 2004a; Majewski et al., 2004b). Thus, phosphorylated Akt may protect the mitochondria to prevent apoptosis thereby, maintaining mitochondrial integrity and promoting cell survival. However, the ability of Akt to perform this function would require glucose and ATP (Gottlob et al, 2001). It is known that Akt is associated with hexokinases in the mitochondria (Gottlob et al., 2001; Majewski et al., 2004b). Hexokinases are important in glucose metabolism as they regulate the first step in glycolysis; the coversion of glucose to glucose-6-phosphate (reviewed in Mathupala et al., 2006). Hexokinases also bind VDAC which regulates its conformation. Glucose transporters (Gluts) deliver glucose to hexokinase II that is bound to VDAC (Mathupala et al., 2006). This association of Akt with hexokinases would effectively couple the role of Akt to both glucose

metabolism in the mitochondria as well as the regulation of apoptosis. Thus, the localization of Akt2 in the mitochondria would be advantageous by being placed in close proximity to function as a glucose transporter. In terms of energy requirements for the cancer cell which requires a constant source of glucose, the localization of Akt2 to both Glut4 (from previous studies) and the mitochondria (from this study) place Akt2 in a most ideal position.

3.4.3 Akt3 is localized in the nucleus

The nuclear localization of Akt3 was surprising considering that Akt3 did not possess a classical nuclear localization signal or nuclear export sequence. Akt3 is the only isoform to have a known splice variant, where the C-terminal portion of the protein is truncated (Akt3-variant 1 lacks the C-terminal S472 phosphorylation site) (Brodbeck et al., 2001). The function of Akt3 and the splice variant warrants further investigation, as few reports have ever investigated the regulation of the Akt3-v1 (Brodbeck et al., 2001; Taniyama et al., 2005). Presently, there are approximately 129 articles in PubMed on Akt3, and only one that confirmed the nuclear localization by indirect immunofluorescence in NPA cells (human papillary thyroid carcinoma) (Saji et al., 2005). The authors noted that both Akt2 and Akt3 were localized to the nucleus in their cells, however, their study focused on examining a nuclear export sequence in Akt1 and did not further investigate the subcellular localization of Akt3. Akt3 is the most under-represented isoform in the literature, and its exact function is not known. The nuclear localization of Akt3 raises many questions regarding its possible functions. The significance of the nuclear localization is not yet understood and future studies are required to determine its precise role.

The term 'nuclear Akt' is often used in the literature. Nuclear Akt has been classified as either pan-Akt that has translocated, or phosphorylated-Akt (on both phosphorylation

residues) (Andjelkovic et al., 1997; Borgatti et al, 2000; Borgatti et al., 2003; Das et al., 2007; Xuan Nguyen et al., 2006). Given that the commercially available anti-pan-Akt antibodies and phosphorylated antibodies recognize all phosphorylated isoforms, it would be of interest to discern if nuclear Akt is indeed Akt3, or translocated Akt1. The results in Figs. 3.13 and 3.14 suggest that after stimulation by either EGF treatment or irradiation, a minor population of Akt1 was found in the nucleus. The localization of Akt3 remained entirely nuclear in the absence or presence of stimulation. Thus, unless future studies carefully distinguish between the Akt isoforms, immunoprecipitation or fractionation analysis of 'nuclear Akt' could conceivably represent both Akt1 and Akt3 in their endogenous and phosphorylated forms.

The Akt3 isoform had the lowest representation in both the levels of protein and mRNA among the three Akt isoforms in the cell lines examined. This could potentially be explained by tissue-specific differences, as Akt3 has been found to be most highly expressed in heart, placenta, and brain tissue (Nakatani, 1999a). The levels of both Akt3 protein and mRNA were below the levels of detection by Western blotting or Q-PCR. The detection of Akt3 by Q-PCR could have been improved in this study by incorporating an Akt3-gene-specific primer during the RT, as opposed to the T_{20} primers used. In fact, Okano et al. (2000) used RT-PCR to detect endogenous Akt3 in their study because a commercially available antibody to Akt3 was not available at that time. They also found a lack of Akt3 in their HepG2 and MCF-7 cell line, and noted that Akt3 varied the most among the three isoforms in terms of tissue distribution. However, they found Akt3 expression in both MCF-7 and HepG2 cells when they performed a Southern blot analysis using a P^{32}-labelled Akt3 probe to increase sensitivity. Similarly, Brognard et al. (2001) also found that the levels of Akt2 and Akt3 were very low in certain non-small cell lung cancer cell lines. However, RT-

PCR analysis of the isoforms in their study showed the presence of transcripts for all three isoforms. Thus, Okano's and Brognard's findings, in addition to the results presented in Figs. 3.5 to 3.7, substantiate the results observed in the present study that HepG2, MCF-7, HeLa and LNCaP cells have endogenous Akt3, that is localized to the nucleus. These findings also underscore the importance of having more than one method of confirmation in these experiments, since it was primarily the immunofluorescence results which indicated that these cells expressed the Akt3 protein. Thus, the low expression level of Akt3 in certain cell lines is an issue of detection, and does not imply the absence of the Akt3 isoform. This finding is important in that many studies utilizing the routine methods of protein detection may draw erroneous conclusions that Akt3 is absent in their cell lines. Some studies have employed LNCaP or MCF-7 cells due to the very fact that Akt3 is either absent or present at very low levels. This is based on the assumption that the 'absence' of Akt3 lends a better interpretation of the Akt1/Akt2 regulation in these cells. Conversely, other studies have upregulated Akt3 kinase in an attempt to better understand its regulation in cells based on the observed low levels of the Akt3 isoform in certain cell lines (Barnett et al., 2005, de Feo-Jones et al, 2005; Faridi et al., 2003).

3.4.4 Akt isoform subcellular localization in different cell lines

When the subcellular location of the isoforms is analyzed from previously published reports, a few important facts begin to emerge. First, the majority of the studies examined the differences between Akt1 and Akt2 during cellular differentiation. For example, isoform differences have been examined between fibroblasts and their differentiated counterparts, adipocytes; or between myoblasts and myocytes. Second, most of these studies used non-transformed proliferating cell lines such as Hek293 cells. Differences in the literature may be

attributable to the different cell lines employed, overlooking the fact that some of these studies may have included the use of cross-reactive antibodies. For the most part, Akt2 protein levels increased during differentiation (Calera and Pilch, 1998; Hill et al., 1999; Vandromme et al., 2001). In addition, some studies observed the translocation of Akt2 into the nucleus (Meier et al., 1997). Differences in the localization of the isoforms have also been observed during differentiation. For instance, after treatment with IGF, Akt1 was translocated to the nucleus from the cytoplasm in C2.7 myoblasts, whereas the localization of Akt2 did not change from the nucleus in response to IGF treatment (Heron-Milhavet et al., 2006). One study reported that both Akt1 and Akt2 exhibited a cyto-nuclear distribution prior to differentiation. Afterwards, Akt1 was cytoplasmic whereas Akt2 displayed a nuclear localization (Vandromme et al., 2001).

The subcellular localization of the Akt isoforms was consistent in the different cancer cell lines examined in this study, suggesting that tissue specific differences were not present between breast, prostate, cervical and liver cancer. One surprising finding, however, was the differential localization of the Akt isoforms in Hek293 and 293T cells (Fig. 3.5). In the cancer cell lines, Akt1 was mainly cytoplasmic, displaying some nuclear exclusion in the basal state. However, Akt1 was nuclear in Hek293 cells, while the immunostaining of Akt1 in 293T cells was reminiscent of the cancer cells. It is interesting, but speculative to hypothesize that transformation by the SV40 large T antigen may alter the localization of Akt1.

The cytoplasmic localization of the isoforms in cancer cells has been attributed to processes such as proliferation and metastasis. Cheng et al. (1997) found Akt2 was localized to the cytoplasm in both cancer and non-cancerous cell lines. Further, Akt2 protein expression was highest in mitotic cells, suggesting an association between the level of Akt2

protein and cell cycle progression. Differences in the subcellular localization of recombinant Akt1 and Akt2 proteins were reported in MDA-MB435 cells overexpressing Her2 analyzed on different collagen substrates (Arboleda et al., 2003). Although the overexpression of Her2 would constitutively activate PI3K signaling in these cells, these findings, nonetheless, suggest that differences in Akt1 and Akt2 subcellular localization were observed when plated onto collagen IV matrices.

The subcellular location of the endogenous Akt proteins in MDA-MB231 did not significantly alter in response to EGF, or 5 Gy radiation 1 h post-treatment. Although subtle changes in Akt1 and Akt3 were observed (i.e., less nuclear exclusion, and less cytoplasmic staining), the subcellular localization of the isoforms remained more or less the same at this timepoint (Fig.3.13). However, Akt2 did translocate in response to radiation treatment beginning at 3 h post-radiation (Fig. 3.14). The subcellular translocation and differences in the morphology of Akt2 in response to radiation in these experiments is novel and very interesting. There have been no reports on either the co-localization of Akt2 with the mitochondria, or alterations in its morphology and subcellular translocation in response to radiation.

Changes in mitochondrial morphology have been reported after photoirradiation (Peng and Jou, 2004). These authors found that mitochondrial swelling coincided with generated increases in reactive oxygen species (ROS) when rat brain astrocytes were exposed to photoirradiation. The swelling and increase in ROS was associated with the opening of the mitochondrial permeability transition pore (MPTP). Further, the enlarged mitochondria were all localized to the perinuclear region after photoirradiation (Peng and Jou, 2004). Membrane potential of the mitochondria and reactive oxygen species generation were not analyzed in this study, and remain to be examined further. While this could

potentially explain the morphological differences observed in the mitochondria after radiation, what is still puzzling, however, is the change in the morphology of Akt2 in conjunction with the mitochondria.

Upon radiation treatment and other stimuli that activate cellular stress, Akt can regulate cell survival through a multitude of signaling pathways which involve the mitochondria. For instance, Akt signaling to the mitochondria is controlled through phosphorylation of Bad (at S136). Pro-apoptotic Bad is complexed to anti-apoptotic Bcl-2. Upon phosphorylation by Akt, Bad is released from Bcl-2 and binds to 14-3-3 in the cytoplasm, where its proapoptotic activities are ultimately inhibited (reviewed in Zhan and Han, 2004). Through a mechanism that is not well understood, Akt can phosphorylate and prevent the activation of caspase-9. Further, Mcl-1 has recently been found to be a downstream inhibitory target of GSK-3 (Manning and Cantley, 2007). For the most part, none of these pathways have been examined to determine if any of them exhibit isoform-specific substrate preference. Thus, the isoform-specific regulation of downstream targets, particularly the ones associated with the mitochondria need to be analyzed further.

The results of the present study underscore the absolute importance of using isoform-specific antibodies to properly measure Akt isoform regulation. The differential subcellular localization of Akt2 and Akt3 found by these studies further represents novel findings, although arguably the most important finding is the co-localization of Akt2 and the mitochondria in cancer cells. In light of the differences observed in the subcellular localization of the Akt isoforms, the contribution of each isoform to breast cancer cell survival is currently being investigated (Chapter 4).

CHAPTER 4.0

The ablation of Akt2 induces autophagy of the mitochondria through upregulation of p27 and downregulation of p70S6K, Cdk2 and cyclin D

4.1 OVERVIEW OF THE STUDY

The present study was initially undertaken to examine the specific roles of each Akt isoform in breast cancer using the MDA-MB231 cell line. In Chapter 3.0, it was demonstrated that each Akt isoform exhibited a specific subcellular localization, which may ultimately underlie the regulation of isoform-specific functions. Thus, it was hypothesized that one of the Akt isoforms may be more important for cell survival and cell cycle progression in breast cancer based upon the data observed from their characterization.

In order to test this hypothesis, the isoforms (singularly or in combination) were ablated by selective targeting using isoform-specific siRNA-mediated interference. Cell survival, cell proliferation, and cell cycle markers over a prolonged timecourse (24-144 h post-transfection) were examined. Further, the downstream signaling substrates known to be regulated by Akt were also examined to determine if isoform-specific substrate recognition occurs.

The data obtained from this study demonstrated a specific role for Akt2 in cell proliferation and cell cycle progression. The targeted ablation of Akt2 caused the downregulation of Cdk2, and cyclin D, and a concurrent upregulation of p27, which caused cell cycle arrest in G0/G1. This is one of the first reports to show transcriptional Akt regulation of p27 in an isoform specific manner. The analysis of the downstream Akt pathways suggested that Akt2 specifically regulated the phosphorylation of p70S6K, a downstream target of mTOR. Furthermore, Akt2 did not regulate the phosphorylation of FoxO1 and Erk1/2 in this system.

Given the important role of mTOR in the regulation of cell metabolism and Akt2 in glucose transport, the upstream activation of AMPKα was examined to discern if siRNA-

mediated ablation of Akt2 caused fluctuations in the AMP/ADP ratio within the cells. While no initial activation of AMPKα was observed in the Akt2-knockdowns, the knockdown of Akt2 resulted in the enlargement of the mitochondria, and increase in the transcriptional coactivator PGC-1α, a regulator of mitochondrial biogenesis. Inhibition of the mTOR pathway caused by Akt2-ablation was associated with increased autophagy. Further, an analysis of the Akt2-knockdown conditions during the late experimental timepoints revealed that the Akt2-transfectants were targeted for autophagic degradation, specifically mitophagy, based on the co-localization of the mitochondria in autophagolysosomes. The data presented here point to a novel Akt2-mediated homeostatic regulation of mitochondrial function, and show that Akt2 is the most important isoform for breast cancer cell survival.

4.2 MATERIALS AND METHODS

Materials and Methods specific for these experiments and not included in Chapter 2.0 are outlined below. Alterations to the protocols outlined in Chapter 2.0 are also noted in the applicable sections.

4.2.1 Cell Culture

The MDA-MB231 breast cancer cell line purchased from ATCC (Manassas, VA) was the main cell line used for the experiments in these studies. Cells were maintained and cultured regularly as described in Chapter 2.1.

4.2.2 Antibodies, Chemicals and Reagents

Antibodies against the following proteins were purchased from Cell Signaling Technology (Danvers, MA): Akt1 (2H10), p-FoxO1 (S256), FoxO1, p-GSK-3α/β (S9/21), GSK-3β, p-p70S6K, p70S6K, p-4E-BP1, 4E-BP1, p-AMPKα (T172), AMPKα, Skp2 and LC3B. Antibodies against the following proteins were purchased from Santa Cruz Biotechnology (Santa Cruz, CA): Akt2 (F7), cyclin A, cyclin D, cyclin E, p-Cdc2 (Y15), p-ERK1/2 (p42/44), p21, p-p27 (T187), p27, PGC-1α and VDAC1. Phosphorylated p27 antibodies (p-p27) specific for the Akt-mediated phosphorylation residues at T157 and T198 were supplied by R&D Systems (Minneapolis, MN). Anti-Cdk2 was purchased from Lab Vision Inc (Fremont, CA) and anti-Akt3 was obtained from Upstate Biotechnology (Lake Placid, NY). Anti-mouse, -rabbit and -goat peroxidase-conjugated secondary antibodies were obtained from Sigma, Pierce and Calbiochem, respectively. The fluorescein (FITC)-conjugated AffiniPure donkey anti-mouse IgG secondary antibody used in the immunofluorescence experiments was from Jackson Immunoresearch (West Grove, PA). Anti-γ-tubulin antibodies, propidium iodide (PI), thiazolyl blue tetrazolium bromide (MTT), dimethyl sulfoxide (DMSO), acridine orange and monodansylcadaverine (MDC) were purchased from Sigma. Lipofectamine 2000 transfection reagent, Opti-MEM I transfection medium, DNAse I, and M-MLV were from Invitrogen. MitoTracker Red CMXRos Mitochondrial Probe was from Cambrex Bioscience Walkersville, Inc. (Charles City, IA). Methylene blue was purchased from Acros Organics (Fisher Scientific). For antibody dilutions, please refer to Table A1 in Appendix II.

4.2.3 Small interfering RNA (siRNA) Transfections

All siRNA transfections were performed as outlined in Chapter 2, Section 2.7. The 24 h timepoint in these experiments is defined as 24 h post-transfection initiation. Accordingly, the 48 h timepoint is 48 h post-transfection initiation, etc. Two isoform-specific siRNA oligonucleotides were used to knockdown each Akt isoform in these experiments to ensure specific knockdown of the target isoform.

4.2.4 Cell Proliferation Assays and Cell Survival Assays:

4.2.4.1 MTT Assay: Cell proliferation was measured using both MTT and BrdU incorporation assays. For the MTT Assay, timepoints were taken from 72-144 h post-transfection initiation. A detailed protocol is described in Chapter 2, Section 2.9.

4.2.4.2 BrdU (5-Bromo-2'-deoxy-uridine) Incorporation Assays: 5-Bromo-2'-deoxy-uridine incorporation was performed according to the manufacturer's protocol (Roche). Briefly, MDA-MB231 cells were plated on 1.8 cm sterile glass coverslips (Fisher) and placed in a 6-well plate 24 h prior to transfection (Sarstedt). Cells on the coverslips were transfected with Akt2 siRNA or scrambled siRNA and analyzed for BrdU incorporation 24, 48 and 72 h post-transfection initiation. BrdU pulse-labelling was carried out during the last 45 min of each sampling timepoint. A minimum of 10 fields per coverslip/per trial were captured using a LSM 510 Meta laser scanning confocal microscope (Zeiss), using a 488 nm laser (band pass 505-530 nm). Cells in each field were counted and analyzed for BrdU incorporation.

4.2.4.3 Focus Formation Cell Survival Assay: Please refer to Chapter 2.10 for the full procedure.

4.2.5 FACS Analysis

MDA-MB231 cells transfected with siRNA in 10-cm plates were washed with PBS and trypsinized at each timepoint (24-144 h post-transfection initiation). Floating cells were collected first, and 2-3 plates of cells were trypsinized and pooled for each sample. All cells were then transferred into a 15-ml conical tube (Sarstedt) and collected by centrifugation. Cell pellets were resuspended in 500 μl of PBS, followed by fixation with 6 ml of 75% cold ethanol overnight at -20°C. Cells were then centrifuged, the fixation solution decanted, and the pellet resuspended in propidium iodide staining solution (0.1% sodium citrate, 0.3% Nonidet P-40, 100 μg/ml RNase A, 100 μg/ml propidium iodide) for 1 h prior to being analyzed by flow cytometry using an Epics Elite Flow Cytometer (Beckman Coulter).

4.2.6 Quantitative Real-Time PCR (Q-PCR)

Quantitative real-time PCR was performed as previously described in Chapter 2.5 and 2.6. The cDNA from the 96-h Reagent Control was used to calibrate the standard curve and S28 ribosomal protein was used as a quantification control. The mRNA expression levels were calculated by the ratio of [Akt2/S28 RNA] and [p27/S28 RNA]. The following primers (below) were used in the PCR reactions (300 nM), and data was acquired using an ABI Prism 7900 HT Sequence Detection System (SDS) and analyzed with ABI SDS software (version 2.1) (Applied Biosystems).

Akt2: Forward 5'-CAAGGATGAAGTCGCTCACACA-3'
Reverse 5'-GAACGGGTGCCTGGTGTTC-3'

p27: Forward 5'-CGGTGGACCACGAAGAGTTAA-3'
Reverse 5'-GGCTCGCCTCTTCCATGTC-3'.

S28: Forward 5'-TCCATCATCCGCAATGTAAAAG-3'
Reverse 5'-GCTTCTCGCTCTGACTCCAAA-3'.

4.2.7 Detection of Autophagy

MDA-MB231 cells were plated onto sterile 1.8-cm glass coverslips and transfected with Akt2 siRNA and scrambled siRNA prior to being evaluated for autophagy/mitophagy at 120 h and 144 h post-transfection initiation. Cells on coverslips were first incubated in a humidified cell culture incubator at 37°C with 50 nM MitoTracker Red CMXRos probe in cell culture medium for 30 min, prior to the addition of acridine orange and monodansylcadaverine (a specific marker for autophagolysosome formation) as described previously (Kim et al., 2007; Kuo et al., 2006; Munafo and Colombo, 2001; Takeuchi et al., 2005). Monodansylcadaverine (0.05 mM) and acridine orange (1 μg/mL) were simultaneously added to each well and incubated for an additional 10 min at 37°C. The cells on coverslips were then rinsed with PBS and mounted on glass slides for visualization by microscopy. The cells were stained individually with each label (AO, MDC and MitoTracker) in addition to the triple staining condition to verify the specificity of the staining. This also ensured that all channels viewed in the triple staining condition were separate and showed no bleedthrough. Fluorescent images were captured using a LSM 510 Meta confocal microscope (Zeiss) with the 63x objective, and processed using LSM 510 Meta analysis software as described in Chapter 2.8.3).

To determine the process of autophagy, the induction of LC3B was examined in cells transfected with Akt2 or scrambled siRNA, as previously outlined (Chapter 4.2.4), and at 96 h post-transfection, plated onto sterile glass coverslips. At the indicated timepoints (120 h and 144 h post-transfection initiation), cells were washed in PBS, fixed in 4% paraformaldehyde, and permeabilized with 100% (v/v) ice-cold methanol for 10 min at -20°C. The cells on coverslips were then treated with blocking solution for 1 h at room

temperature. The primary antibody (LC3B) was diluted in 1% (w/v) BSA in TBS, added to the cells and incubated overnight at 4°C. The next day, the cells on coverslips were washed and incubated with the secondary antibody in the dark. Cells were rinsed and counterstained with DRAQ5 (10 μm) for 30 min at room temperature (Biostatus Ltd., Shepshed, Leicestershire, UK) prior to visualization by confocal microscopy.

4.2.8 Densitometric Analysis

Intensity of the protein bands (scanned images) was determined via densitometry using AlphaEase Fluorochem (FC) 8900 version 4.0.1 software, which was supplied with the Alpha Innotech scanner (Fisher Scientific). Protein levels were expressed as a ratio [protein/loading control] and graphed using Excel (Microsoft Office 2003, Microsoft). All Western blots shown are representative of 3-4 independent trials. The densitometry is a compiled average of the ratios for 2 or more of these trials. Because most of the proteins were examined over a prolonged timecourse, it was determined that the average ratios would better represent the protein expression observed in these experiments, Thus, each timepoint was analyzed accordingly with the scrambled control at the same timepoint and the average was compiled for these experiments.

4.2.9 Statistical Analyses

A univariate 2-way ANOVA, with subsequent post-hoc analyses for significance testing (Tukey $p<0.05$) was used to determine differences in cellular proliferation and BrdU incorporation of the Akt siRNA conditions over time, as well as in the analyses of mitochondrial area. Univariate analysis of variance (Oneway ANOVA) was performed on

the focus formation assay data to analyze differences in clonogenic survival among the Akt-transfected conditions. All statistics were performed using SPSS v.12.0 for Windows.

4.3 RESULTS

4.3.1 Akt2 siRNA downregulated DNA replication and cell proliferation

To gain insight into the unique role of each Akt isoform, siRNA oligonucleotides were transfected into MDA-MB231 cells. The isoform specificity of the oligonucleotides was confirmed by Western blotting in these experiments and no cross-reactivity was observed (i.e., knockdown of Akt1 did not knockdown Akt2, or Akt3) (Fig. 4.1c). Quantification of the scanned gel images by densitometry (Fig. 4.1d and e) showed that the downregulation of each Akt isoform was routinely achieved in the range of ~40-70% of the trial shown here (Akt1 30.0%, Akt2 64.4% and Akt3 68.1%), which was consistent with the transfection efficiency obtained with the second set of Akt isoform-specific siRNA (~40%-70.3% knockdown). Morphological changes in the Akt2-transfected cells were apparent near the last timepoints of the experiment (120-144 h post-transfection initiation), with these cells appearing more elongated and granular with larger cytoplasmic extensions (please refer to Fig. A10 in Appendix IV to view phase contrast pictures of MDA-MB231 cells after siRNA transfection).

Akt has been established as a critical regulator of the cell cycle and cell cycle progression (reviewed in Liang & Slingerland, 2003). However, published data regarding the involvement of the Akt isoforms in cell cycle regulation have resulted in conflicting reports. Several groups have reported a role for either Akt1 (Heron-Milhavet et al., 2006; Meng et al., 2006), Akt2 (Cheng et al., 1997; Noske et al., 2007; Sithanandam et al., 2005) or Akt3 (Cristiano et al., 2006) in cell proliferation. To examine the role of each Akt isoform on

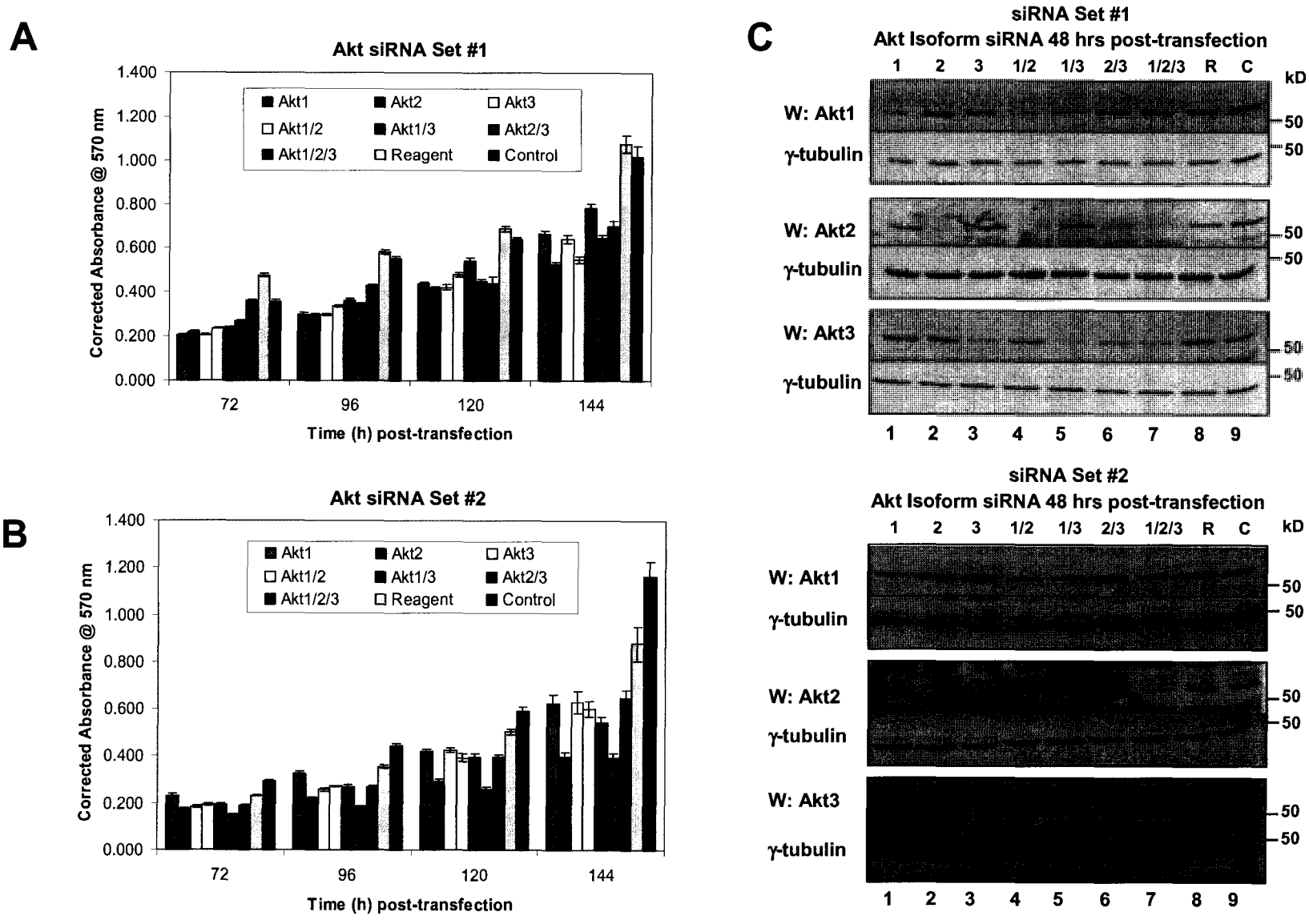
A
Akt siRNA Set #1
Akt1
Akt2
Akt3
Akt1/2
Akt1/3
Akt2/3
Akt1/2/3
Reagent
Control
Corrected Absorbance @ 570 nm
1.400
1.200
1.000
0.800
0.600
0.400
0.200
0.000
72
96
120
144
Time (h) post-transfection
B
Akt siRNA Set #2
Akt1
Akt2
Akt3
Akt1/2
Akt1/3
Akt2/3
Akt1/2/3
Reagent
Control
Corrected Absorbance @ 570 nm
1.400
1.200
1.000
0.800
0.600
0.400
0.200
0.000
72
96
120
144
Time (h) post-transfection
C
siRNA Set #1
Akt Isoform siRNA 48 hrs post-transfection
1 2 3 1/2 1/3 2/3 1/2/3 R C
kD
W: Akt1
γ-tubulin
W: Akt2
γ-tubulin
W: Akt3
γ-tubulin
50
50
50
50
50
50
1 2 3 4 5 6 7 8 9
siRNA Set #2
Akt Isoform siRNA 48 hrs post-transfection
1 2 3 1/2 1/3 2/3 1/2/3 R C
kD
W: Akt1
γ-tubulin
W: Akt2
γ-tubulin
W: Akt3
γ-tubulin
50
50
50
50
50
50
1 2 3 4 5 6 7 8 9

D

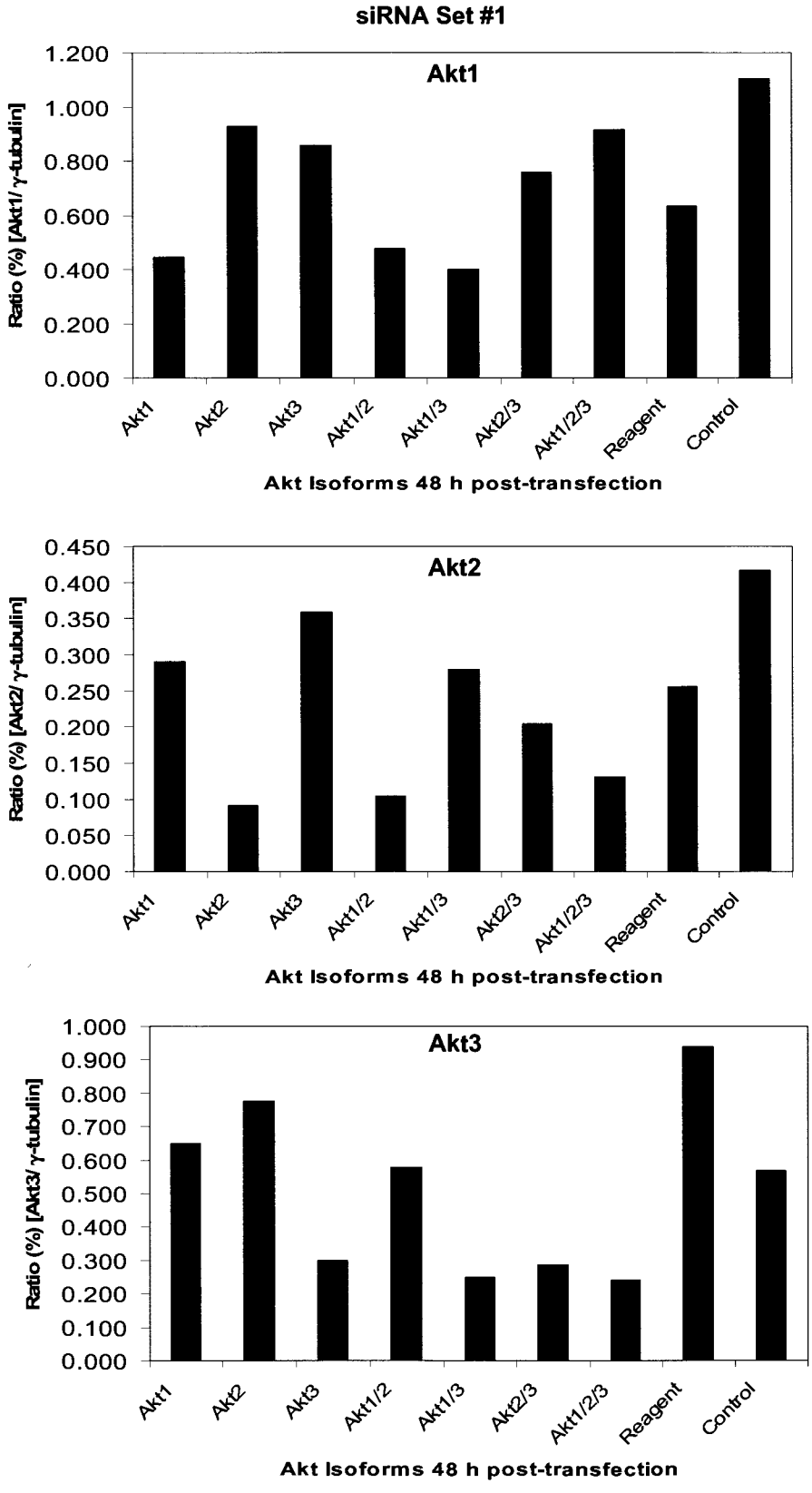
siRNA Set #1
Akt1
Ratio (%) [Akt1/ γ-tubulin]
1.200
1.000
0.800
0.600
0.400
0.200
0.000
Akt1
Akt2
Akt3
Akt1/2
Akt1/3
Akt2/3
Akt1/2/3
Reagent
Control
Akt Isoforms 48 h post-transfection
Akt2
Ratio (%) [Akt2/ γ-tubulin]
0.450
0.400
0.350
0.300
0.250
0.200
0.150
0.100
0.050
0.000
Akt Isoforms 48 h post-transfection
Akt3
Ratio (%) [Akt3/ γ-tubulin]
1.000
0.900
0.800
0.700
0.600
0.500
0.400
0.300
0.200
0.100
0.000
Akt Isoforms 48 h post-transfection

E

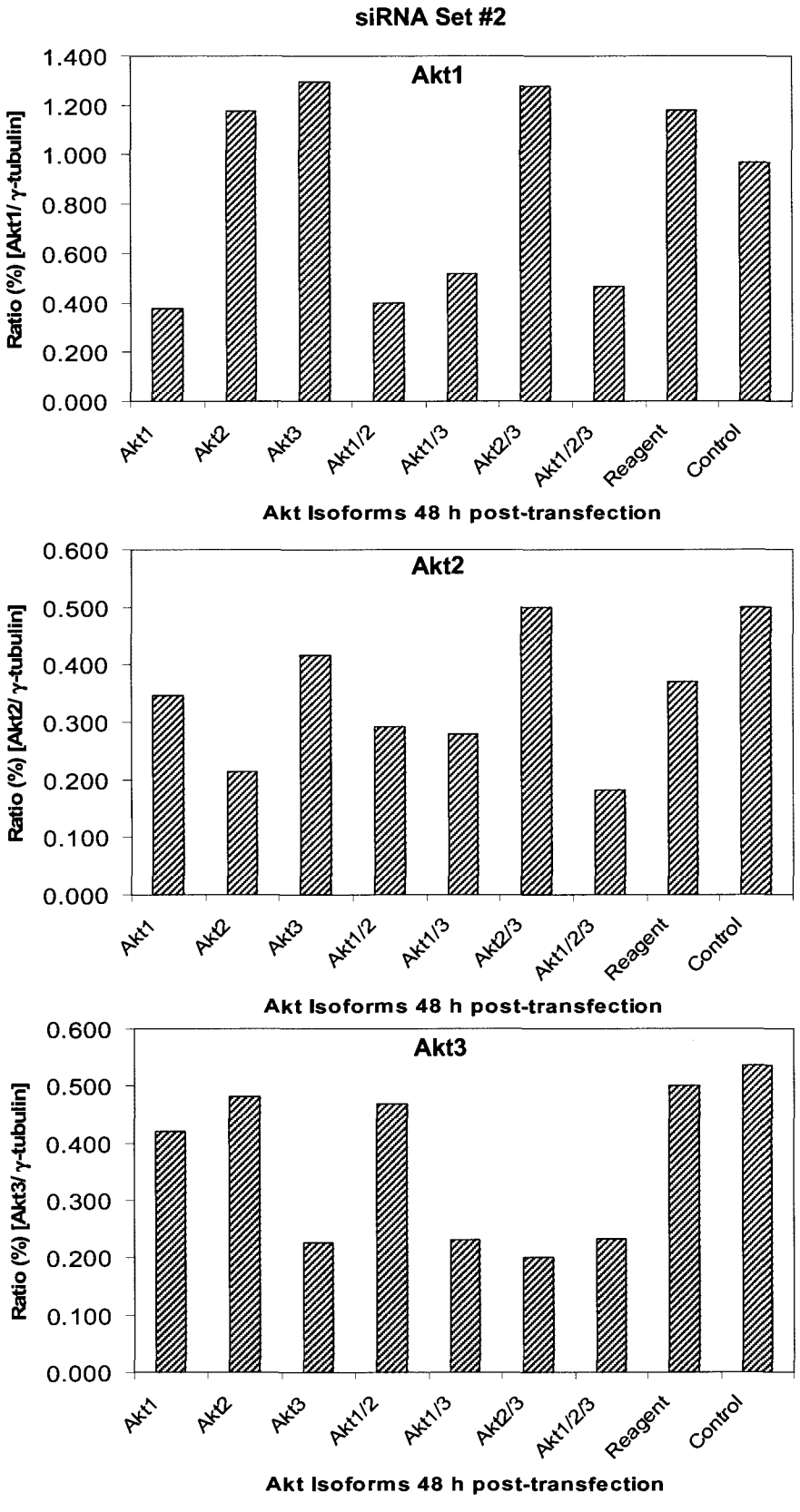
siRNA Set #2
Akt1
Ratio (%) [Akt1/ γ-tubulin]
1.400
1.200
1.000
0.800
0.600
0.400
0.200
0.000
Akt1
Akt2
Akt3
Akt1/2
Akt1/3
Akt2/3
Akt1/2/3
Reagent
Control
Akt Isoforms 48 h post-transfection
Akt2
Ratio (%) [Akt2/ γ-tubulin]
0.600
0.500
0.400
0.300
0.200
0.100
0.000
Akt Isoforms 48 h post-transfection
Akt3
Ratio (%) [Akt3/ γ-tubulin]
0.600
0.500
0.400
0.300
0.200
0.100
0.000
Akt Isoforms 48 h post-transfection

cell proliferation, MTT assays were carried out with cells transfected with isoform-specific siRNA oligos 72-144 h post-transfection. The results of the experiment indicated that by 144 h post-transfection initiation, knockdown of any Akt isoform resulted in a decrease in cell proliferation (Fig. 4.1a-b). However, the decrease was most pronounced with cells transfected with Akt2 siRNA ($p<0.05$) (Fig. 4.1a-b). The results obtained from the second set of isoform-specific siRNA oligos were also consistent with these findings (Fig. 4-1b). Further, reduced cellular proliferation was also observed in the double knockdown conditions when Akt2 was one of the isoforms involved in the knockdown (i.e., Akt1/2 and/or Akt2/3). Interestingly, the double knockdown did not show synergistic effects and compared to cells transfected with Akt1, Akt2, or Akt3 single siRNA (Fig. 4-1a-b).

To further confirm the results of the MTT assay, DNA replication activities were examined by analyzing the incorporation of BrdU in MDA-MB231 cells transfected with Akt2 siRNA and scrambled siRNA. As shown in Fig. 4.2a-b, the incorporation of BrdU into DNA was dramatically decreased in the cells transfected with Akt2 siRNA ($p<0.001$). At 24 h, when samples were incubated in serum-free medium during the transfection procedure, cell proliferation was reduced in all transfection conditions. However, when the cells were in full serum at 48-72 h, BrdU-positive staining was seen only in the control cells and was not evident in the Akt2-siRNA treatment confirming that these cells were not proliferating ($p < 0.001$). Further, this effect was independent of serum-withdrawal. This result was observed with both Akt2-targeted siRNA oligos (Akt2 siRNA #1 and siRNA #2).

Next, clonogenic cell survival was measured to examine if long-term Akt2 ablation also caused reduced colony formation and cell survival. MDA-MB231 cells were transfected with both sets of isoform-specific siRNA(s), and colony formation was examined 12-14 days post-transfection initiation. Consistent with the data shown in 4.1, Akt2 knockdown caused

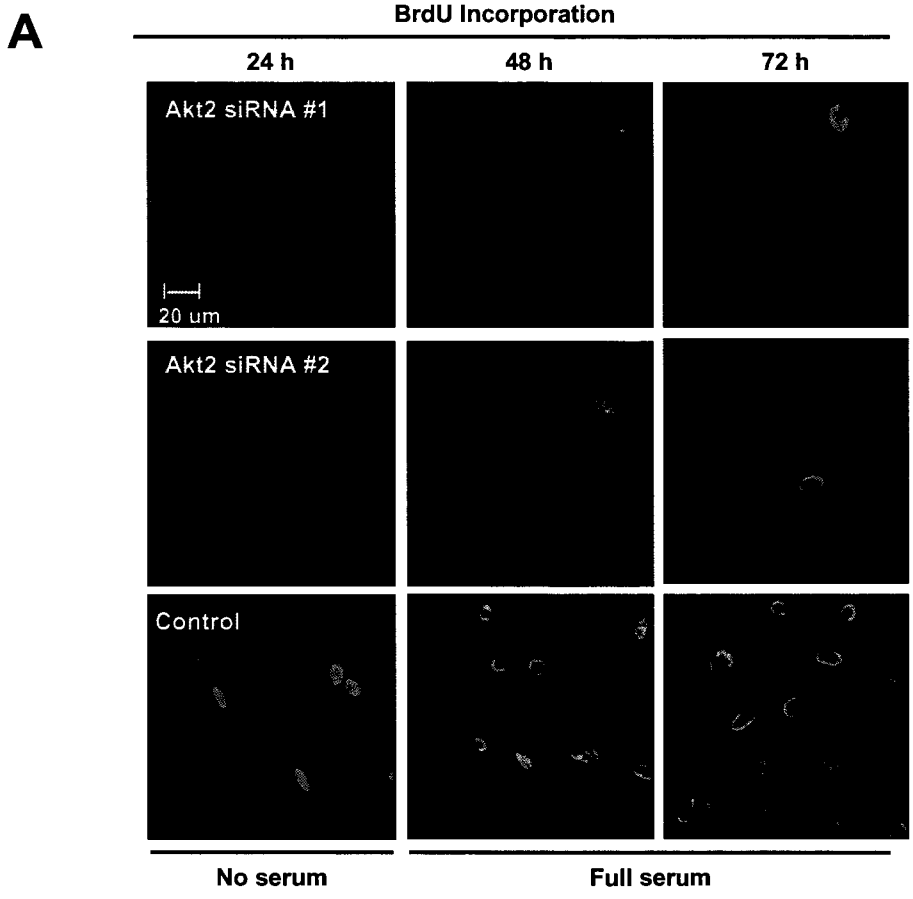
A
BrdU Incorporation
24 h
48 h
72 h
Akt2 siRNA #1
20 um
Akt2 siRNA #2
Control
No serum
Full serum

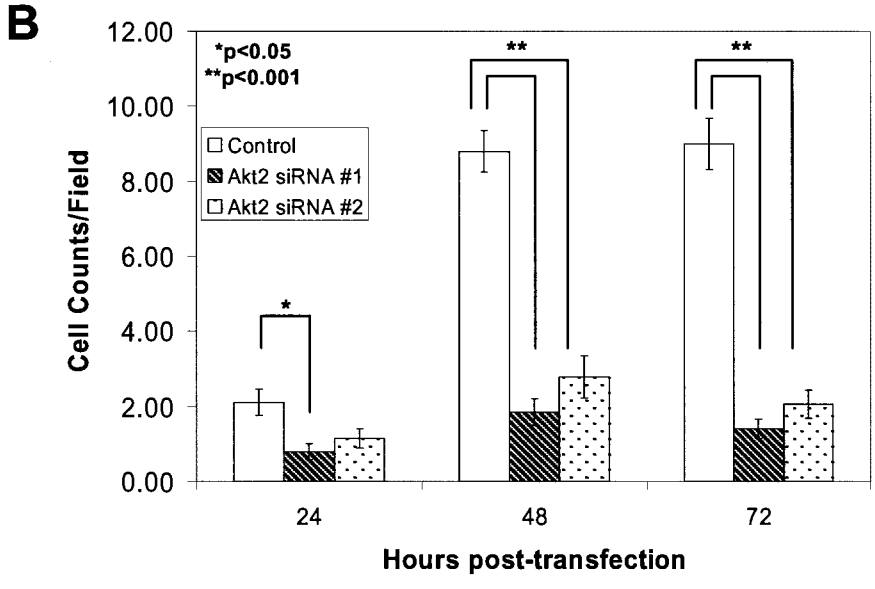
B
*p<0.05
**p<0.001
Control
Akt2 siRNA #1
Akt2 siRNA #2
Cell Counts/Field
12.00
10.00
8.00
6.00
4.00
2.00
0.00
*
**
**
24
48
72
Hours post-transfection

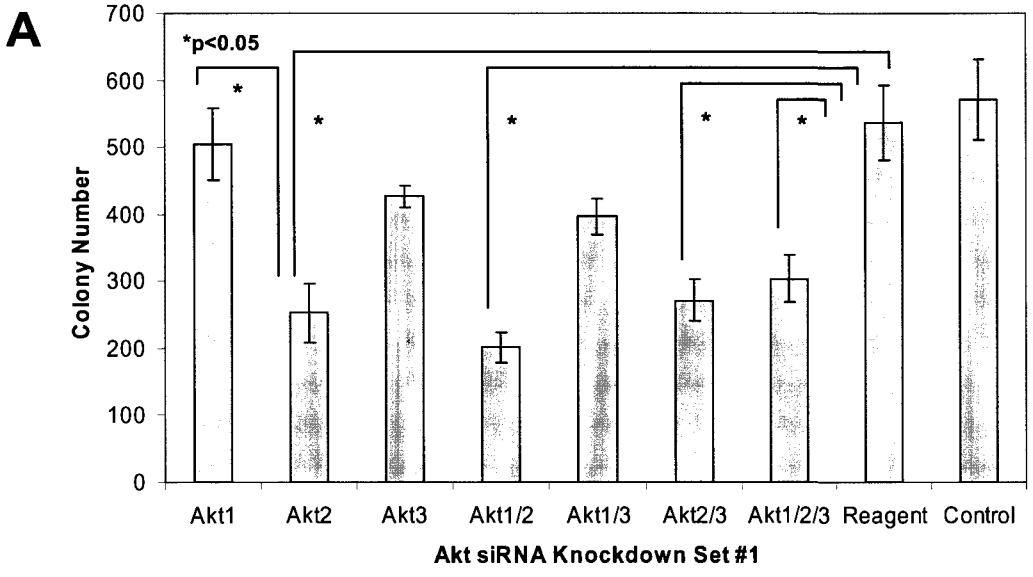
A
*p<0.05
Colony Number
700
600
500
400
300
200
100
0
Akt1
Akt2
Akt3
Akt1/2
Akt1/3
Akt2/3
Akt1/2/3
Reagent
Control
Akt siRNA Knockdown Set #1

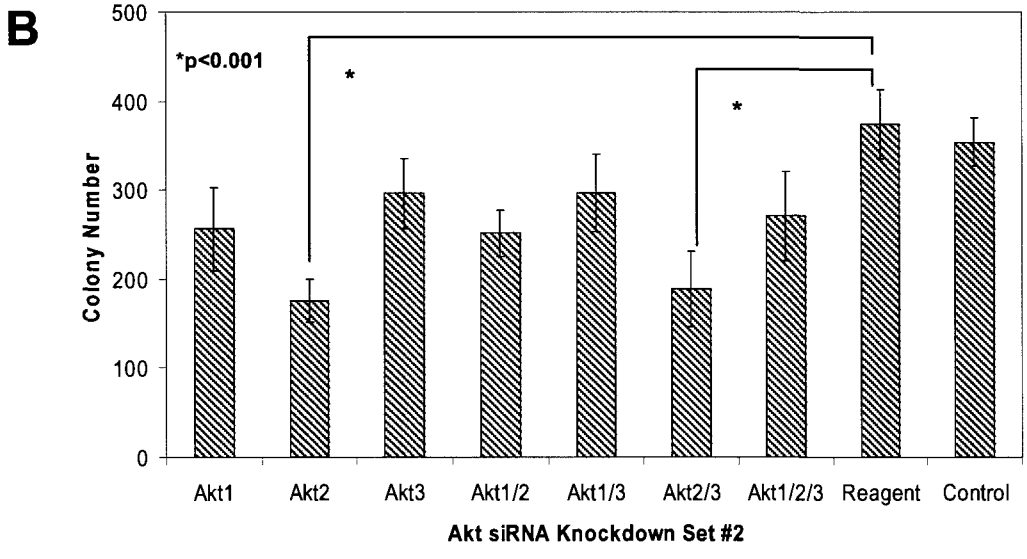
B
*p<0.001
Colony Number
500
400
300
200
100
0
Akt1
Akt2
Akt3
Akt1/2
Akt1/3
Akt2/3
Akt1/2/3
Reagent
Control
Akt siRNA Knockdown Set #2

the most significant decrease in the colony forming ability among the three Akt isoforms ($p < 0.001$) (Fig. 4.3). Colony-forming assays performed with the second set of siRNA oligos confirmed the same trend although the effect was more pronounced for siRNA Set #1 (compare Fig. 4.3a with Fig. 4.2b). Taken together, the data presented in Fig(s). 4.1-4.2 suggests that Akt2 is most relevant for both cell proliferation and survival among the three isoforms.

4.3.2 The knockdown of Akt2 induced cell cycle arrest

Since both cellular proliferation and DNA replication were downregulated in the Akt2-ablated cells (Figs. 4.1 to 4.3), analysis of cell cycle progression was performed next using flow cytometry. Cells were transfected with Akt2 siRNA in serum-free medium for 24 h. At the end of 24 h, cells were maintained in normal growth medium containing 10% FBS for 48-144 h post-transfection initiation (thus, only the 24 h timepoint is in serum-free conditions). At the 24 h timepoint, the cell cycle profiles for the controls and Akt2 siRNA-treated conditions were similar, and were consistent with cell profiles that are synchronized with reduced serum medium (serum-starved cells are usually synchronized in G0/G1) (see Fig. 4.4, 24 h timepoint). However, after the medium was replaced with complete medium at 24 h, the FACS profile indicated that both the negative and mock-transfected reagent controls progress into the cell cycle with the majority of cells accumulating at the S and G2/M phase at 48 h (see Fig. 4.4, 48 h timepoint). In contrast, Akt2-siRNA-treated cells did not progress into the cell cycle and the medium change at 24 h to complete medium did not change the flow profile compared to the controls (see Akt2 siRNA condition, Fig. 4.4, 48 h). However, at the later timepoints (i.e., 120-144 h post-transfection), some cells treated with Akt2-siRNA progress slowly into S-phase (see Fig. 4.4, 120 h in the Akt2-transfected cells).

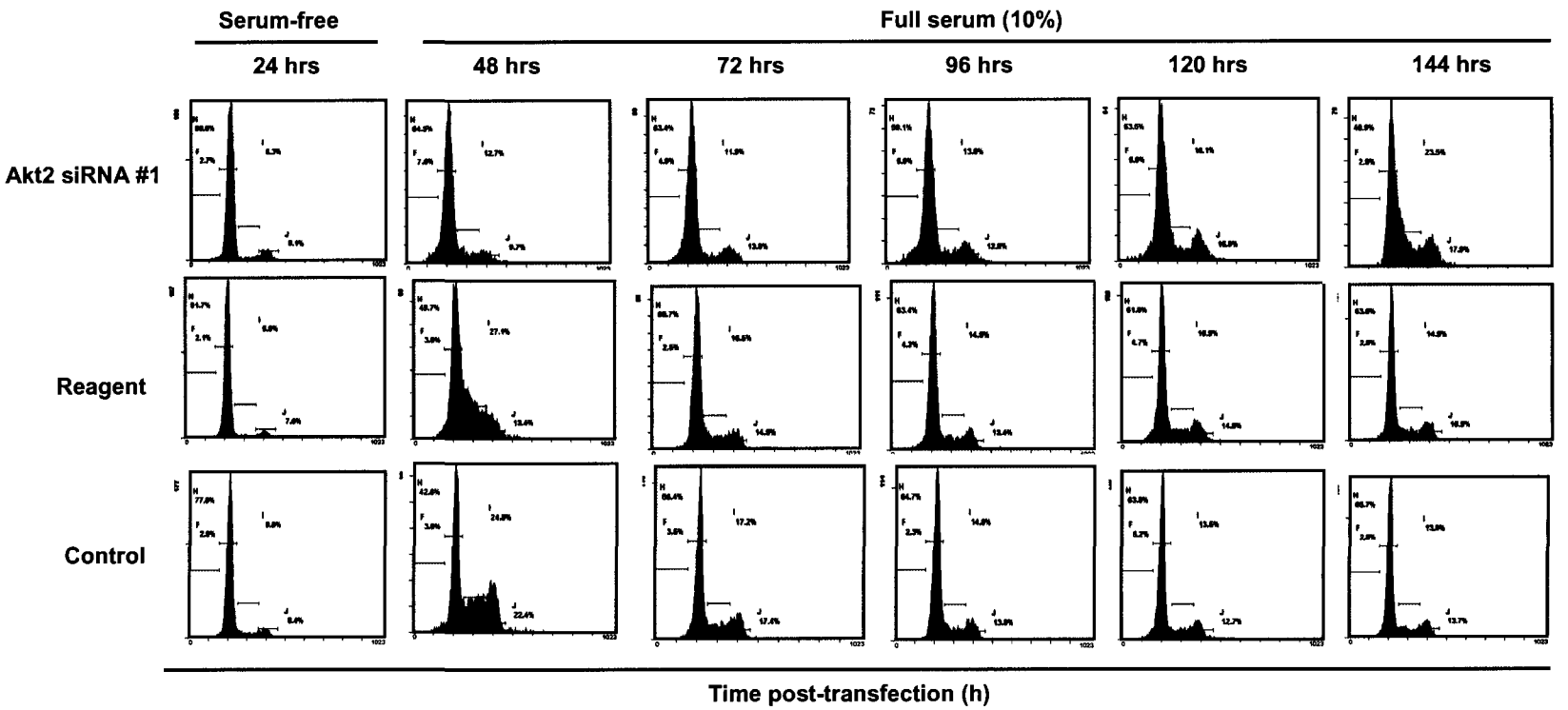
Serum-free
Full serum (10%)
24 hrs
48 hrs
72 hrs
96 hrs
120 hrs
144 hrs
Akt2 siRNA #1
Reagent
Control
Time post-transfection (h)

Given that the average transfection efficiency of Akt2 in these experiments is approximately 70-85% (protein expression determined by densitometry and mRNA determined by Q-PCR, respectively), it is likely that these cycling cells are the untransfected sub-population. Given the essential role that Akt plays in cell survival, both floating and adhered cells were collected for the FACS analysis in these experiments. Surprisingly, there was no observed sub-G1 population in the Akt2-transfected cells, suggesting that the reduced cell number observed in both the MTT proliferation assays and the clonogenic assays was not likely due to increased apoptotic cell death (Fig. 4.4).

4.3.3 Akt2-ablated cells downregulated Cdk2 protein

To further investigate the mechanism of the cell cycle block mediated by Akt2-ablation, proteins involved in cell cycle control were examined next. Protein expression of Cdk2 was chosen as a preliminary candidate as previously published reports have indicated Akt involvement and some isoform specificity in its regulation (Bacqueville et al., 1998; Skeen et al., 2006). All siRNA transfection conditions were included in this experiment to simultaneously examine Akt1 and Akt3 at the same timepoint (48 h post-transfection initiation). Data obtained from a Western blot assay showed that the level of Cdk2 was downregulated in the cells transfected with Akt2 siRNA, but not with Akt1 or Akt3 siRNA by 48 h post-transfection initiation (Fig. 4.5a and b). The downregulation of Cdk2 in the Akt2-ablated cells was further confirmed by indirect immunostaining of the Akt2-siRNA-transfected cells with an anti-Cdk2 antibody at 48 and 72 h post-transfection. Note that both Akt2 siRNA oligos showed the downregulation of Cdk2 compared to the control in Fig. 4.5c. The downregulation of Cdk2 at 48 h post-siRNA transfection prompted a more thorough analysis of Cdk2 across the timecourse. Fig 4.5d shows that Cdk2 is downregulated in the

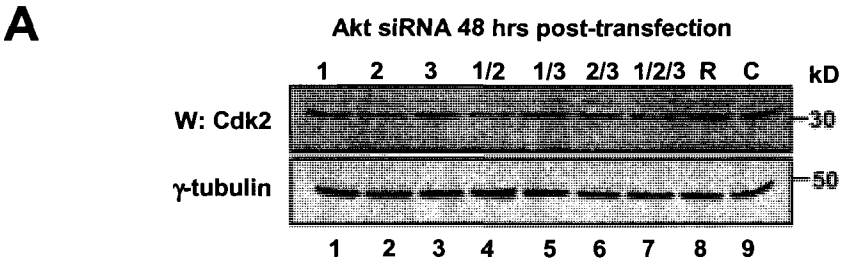
A
Akt siRNA 48 hrs post-transfection
1 2 3 1/2 1/3 2/3 1/2/3 R C kD
W: Cdk2
γ-tubulin
30
50
1 2 3 4 5 6 7 8 9

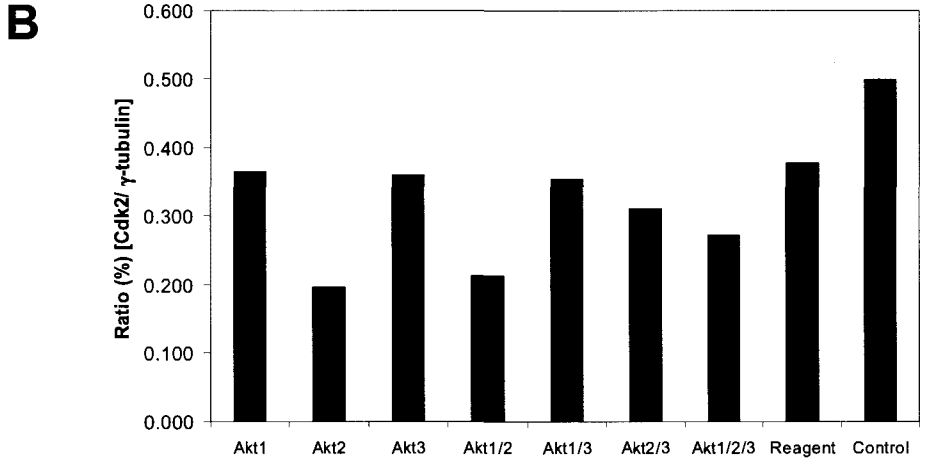
B
0.600
0.500
0.400
0.300
0.200
0.100
0.000
Ratio (%) [Cdk2/ γ-tubulin]
Akt1
Akt2
Akt3
Akt1/2
Akt1/3
Akt2/3
Akt1/2/3
Reagent
Control

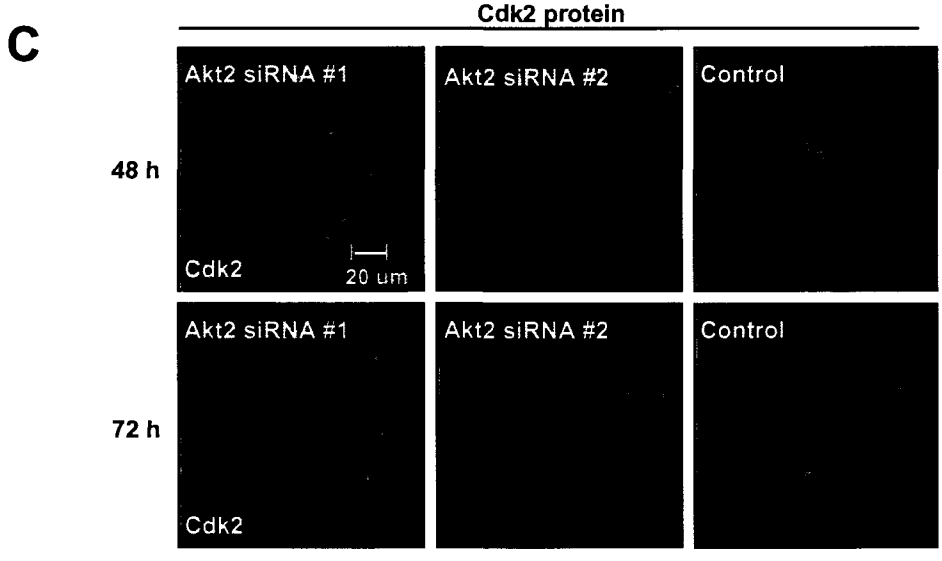
C
Cdk2 protein
Akt2 siRNA #1
Akt2 siRNA #2
Control
48 h
Cdk2
20 um
Akt2 siRNA #1
Akt2 siRNA #2
Control
72 h
Cdk2

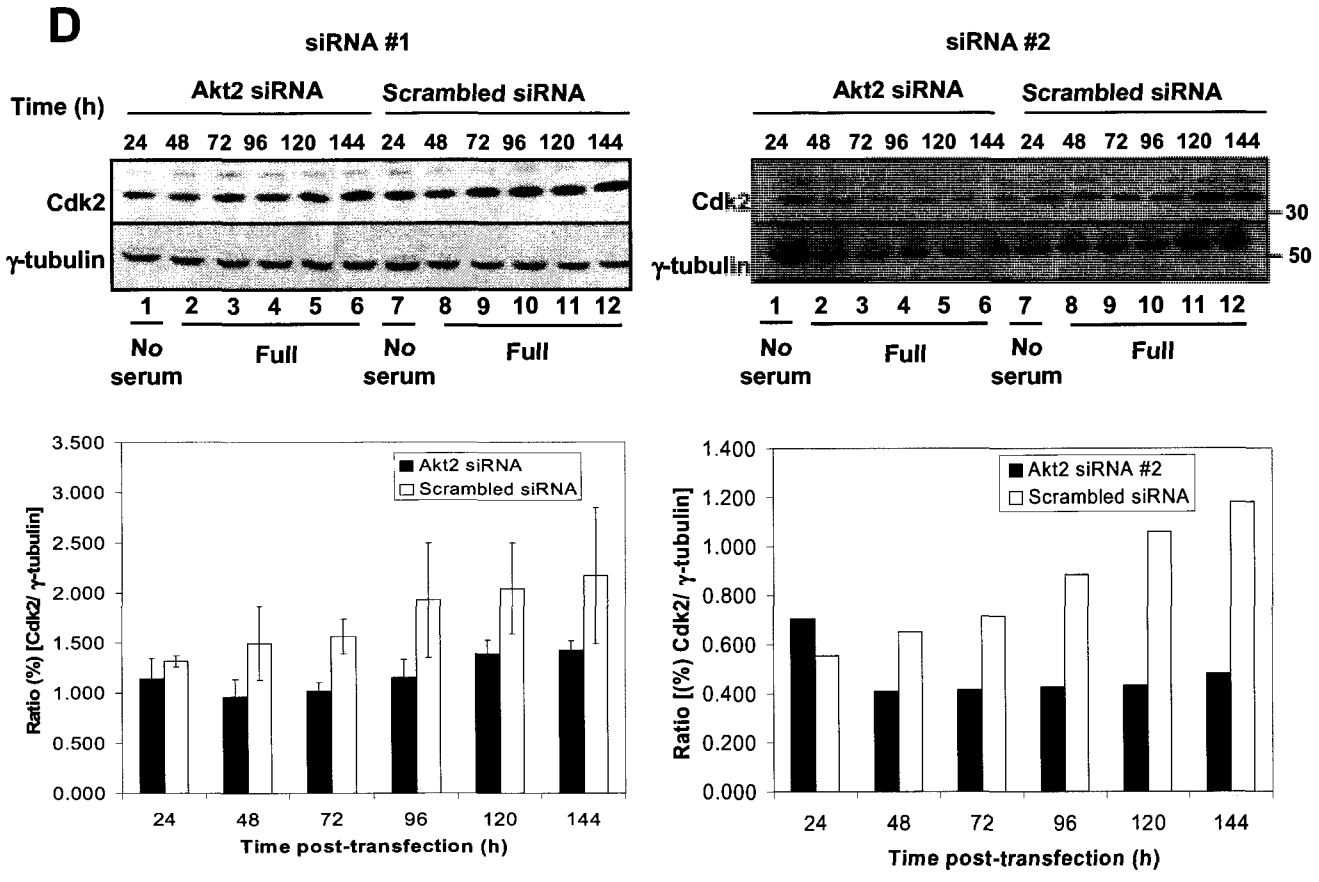
D
siRNA #1
siRNA #2
Time (h)
Akt2 siRNA
Scrambled siRNA
24 48 72 96 120 144 24 48 72 96 120 144
Cdk2
γ-tubulin
30
50
1 2 3 4 5 6 7 8 9 10 11 12
No serum
Full
No serum
Full
Ratio (%) [Cdk2/ γ-tubulin]
Akt2 siRNA
Scrambled siRNA
Time post-transfection (h)
Ratio [(%) Cdk2/ γ-tubulin]
Akt2 siRNA #2
Scrambled siRNA
Time post-transfection (h)

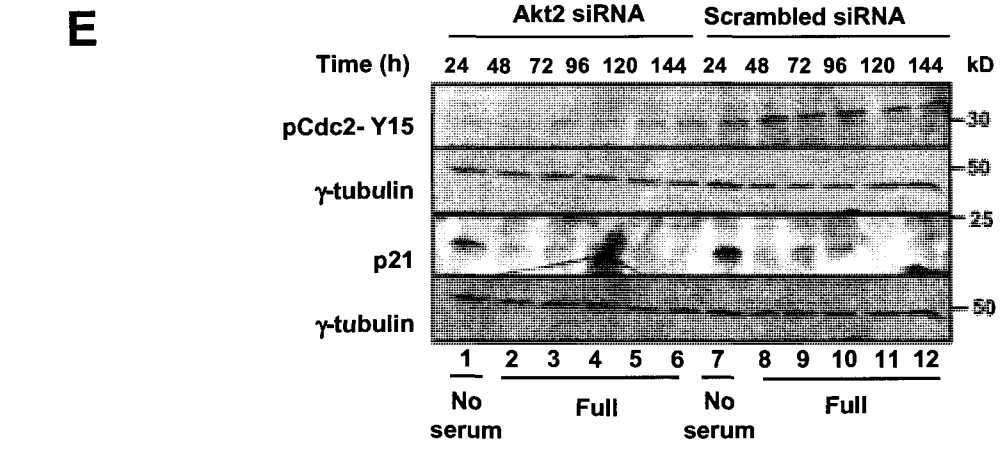
E
Akt2 siRNA
Scrambled siRNA
Time (h)
24 48 72 96 120 144 24 48 72 96 120 144
kD
pCdc2- Y15
γ-tubulin
p21
γ-tubulin
30
50
25
50
1 2 3 4 5 6 7 8 9 10 11 12
No serum
Full
No serum
Full

Akt2-transfected condition at all timepoints compared to the scrambled controls (Western blot and densitometry). This result was observed with both Akt2 siRNAs (Akt2 siRNA #1 and #2) (Fig. 4.5d).

The involvement of other key cell cycle regulators was also examined. Levels of p21 protein were upregulated only during the 24 h timepoint in both the Akt2-siRNA cells and scrambled controls, corresponding to the incubation time in serum-free conditions during transfection (Fig 4.5e) and G1/G0 arrest. Once cells were released into complete medium after transfection, protein expression levels of p21 were downregulated and there was no appreciable difference between the Akt2 siRNA or scrambled siRNA conditions at any other timepoint. Phosphorylated-Cdk1 (pCdc2 Y15), which occurs in G2/M of the cell cycle, was completely downregulated in the Akt2-ablated cells, suggesting that the cells were not entering G2/M phase. This finding is consistent with the results of the MTT and BrdU incorporation assays (Fig. 4.5e). Thus, this data supports the hypothesis that the cell-cycle arrest of Akt2-ablated cells, was, at least in part, mediated by the downregulation of Cdk2.

Next, levels of cyclin A, D, and E proteins were measured in the Akt2-siRNA transfected cells and the scrambled controls 24-144 h post-transfection initiation (Fig. 4.6a). Cyclin D was markedly downregulated in cells transfected with Akt2-specific siRNA and this result is consistent with the cell cycle arrest in G0/G1 (Fig. 4.6a and c). Levels of cyclin E were upregulated in the Akt2-siRNA transfected cells (Fig. 4.6a and d). Cyclin E is degraded by the ubiquitin pathway through SCF-Fbw7-ubiquitin ligase, and subsequent binding to Skp1 (reviewed in Hwang & Clurman, 2005). Turnover or degradation of cyclin E is prevented by when Cdk2-cyclin E complexes are inhibited by p27, a Cdk inhibitor (data in presented in the next figure will clarify this point). Thus, Cdk2-p27 binding inhibits the

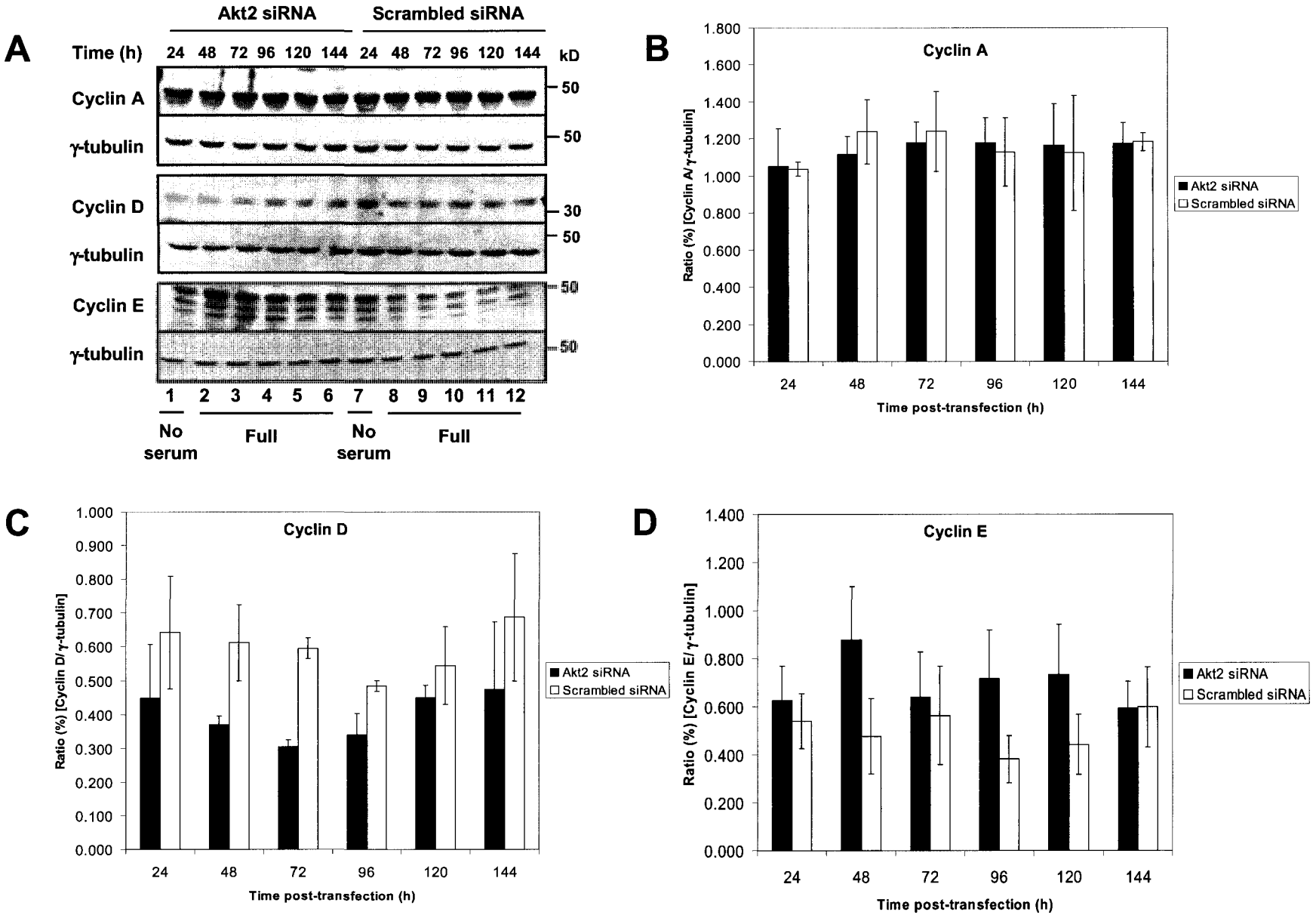
A
Akt2 siRNA
Scrambled siRNA
Time (h)
24 48 72 96 120 144 24 48 72 96 120 144
kD
Cyclin A
γ-tubulin
Cyclin D
γ-tubulin
Cyclin E
γ-tubulin
50
50
30
50
50
50
1 2 3 4 5 6 7 8 9 10 11 12
No serum
Full
No serum
Full
B
Cyclin A
Ratio (%) [Cyclin A/ γ-tubulin]
1.800
1.600
1.400
1.200
1.000
0.800
0.600
0.400
0.200
0.000
24 48 72 96 120 144
Time post-transfection (h)
Akt2 siRNA
Scrambled siRNA
C
Cyclin D
Ratio (%) [Cyclin D/ γ-tubulin]
1.000
0.900
0.800
0.700
0.600
0.500
0.400
0.300
0.200
0.100
0.000
24 48 72 96 120 144
Time post-transfection (h)
Akt2 siRNA
Scrambled siRNA
D
Cyclin E
Ratio (%) [Cyclin E/ γ-tubulin]
1.400
1.200
1.000
0.800
0.600
0.400
0.200
0.000
24 48 72 96 120 144
Time post-transfection (h)
Akt2 siRNA
Scrambled siRNA

turnover of cyclin E. In contrast, no changes in the levels of cyclin A were observed between the Akt2-knockdown and scrambled conditions (Fig. 4.6a and b).

4.3.4 p27 is upregulated and is localized in the nucleus in the Akt2-knockdowns

The finding that Akt2-ablated cells arrest in G0/G1 prompted an examination of p27 regulation. The p27 cyclin-dependent kinase inhibitor is a key mediator in G0/G1 cell cycle arrest, and is involved in mediating cell cycle progression at G1/S-phase. p27 is regulated either transcriptionally or post-translationally (reviewed in Caldon et al., 2006). When levels of p27 are upregulated, cells are arrested in G0/G1. Cancer cells, which are constantly cycling, usually have extremely low levels of p27 protein.

When p27 is active, it is bound in a complex with Cdk2-cyclin D in the nucleus to inhibit progression of the cell cycle. p27 is a known target of the PI3K/Akt pathway and regulation can occur indirectly via downstream signaling to substrates such as the FOXO transcription factors (Medema et al., 2000) and mTOR (Nourse et al., 1994); and also directly through phosphorylation of p27 by Akt itself on 2 threonine residues, T157 (Liang et al., 2002; Shin et al., 2002; Viglietto et al., 2002) and T198 (Kossatz et al., 2006). The Akt-mediated phosphorylation of p27 is inhibitory and promotes the translocation of p27 from the nucleus to the cytoplasm. Cytoplasmic retention of phosphorylated p27 results in ubiquitin-mediated proteasomal degradation by Skp2, which is required for cell cycle progression to occur (reviewed in Caldon et al., 2006). p27 is also phosphorylated by Cdk2-cyclin E at T187 during S-phase which also targets it for Skp2-mediated degradation (Caldon et al., 2006). Furthermore, inhibition of PI3K/Akt by LY294002 and wortmannin (Bacqueville et al., 1998; Gao et al., 2004), as well as by rapamycin (Nourse et al., 1994; Shapira et al.,

2006), has been found to upregulate protein levels of p27 and promote a G0/G1 cell cycle arrest.

To determine the regulation of p27 in the Akt2 knockdown, the subcellular localization and phosphorylation status of the relevant threonine residues on p27 were examined. It was hypothesized that p27 would be localized in the nucleus in the Akt2-siRNA-transfected cells, thereby mediating the observed inhibition of the cell cycle. Analysis of the subcellular distribution of p27 by immunostaining revealed that p27 was localized in the nucleus of Akt2-ablated cells 24-72 h post-transfection, while a cytoplasmic-nuclear localization of p27 was observed in the controls 48-72 h post transfection. Note that the 24 timepoint would be serum-starved, which would experimentally induce a G0/G1 arrest. Release into the cell cycle at 24 h post-transfection by the addition of full serum only caused a change in the localization of p27 at 48 h and 72 h in the controls (see Fig. 4.7a). This result indicated that cell cycle progression was indeed inhibited in the Akt2-siRNA transfected cells through the regulation of p27 (Fig. 4.7a). Further, this result was observed with both siRNA oligos (Akt2 siRNA #1 and siRNA #2) at all timepoints examined (Fig. 4.7a). Thus, the nuclear localization of p27 in the Akt2-ablated cells coincides with the cell cycle arrest in G0/G1.

If the nuclear localization of p27 was mediated through phosphorylation by Akt, then levels of p-p27, particularly on the T157 residue would be downregulated relative to the scrambled controls. Surprisingly, both Akt-mediated phosphorylation sites (T157 and T198) were not significantly altered by the Akt2-ablation (Fig. 4.7c and d). Further, an additional phosphorylation site, T187 was found upregulated in the Akt2-siRNA transfected cells compared to the scrambled controls (Fig. 4.7e). Since this phosphorylation site targets

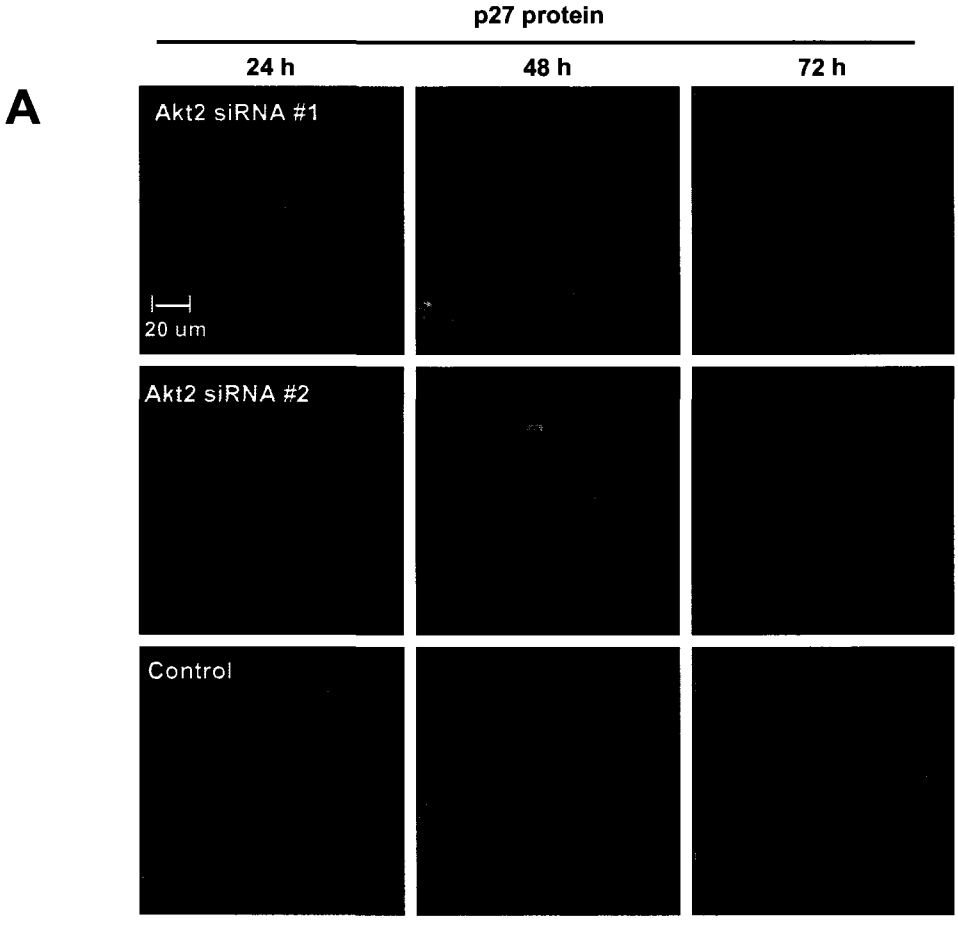
p27 protein
24 h
48 h
72 h
A
Akt2 siRNA #1
20 um
Akt2 siRNA #2
Control

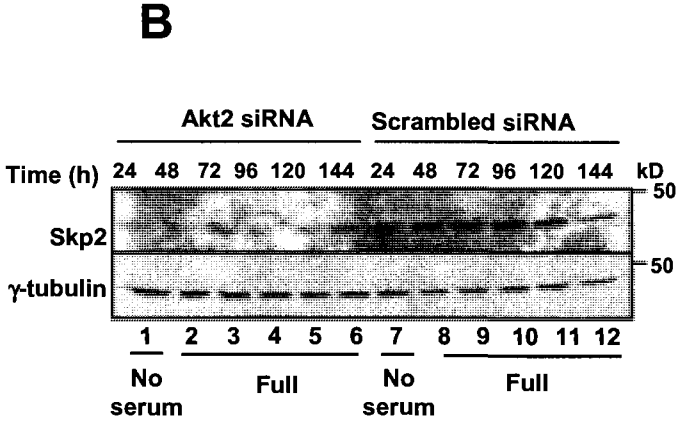
B
Akt2 siRNA
Scrambled siRNA
Time (h) 24 48 72 96 120 144 24 48 72 96 120 144 kD
Skp2
γ-tubulin
50
50
1 2 3 4 5 6 7 8 9 10 11 12
No serum
Full
No serum
Full

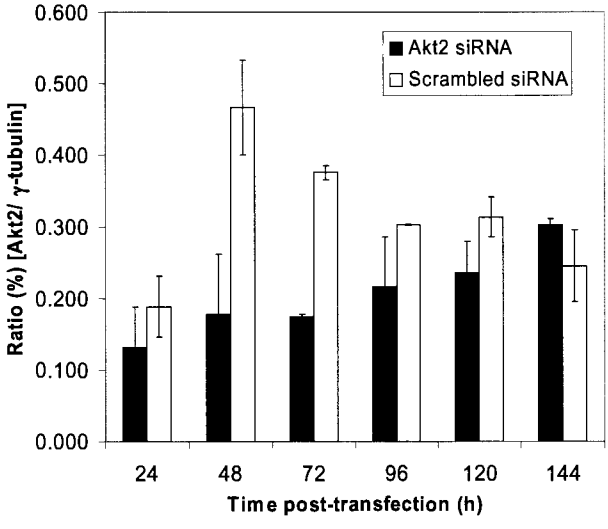
Akt2 siRNA
Scrambled siRNA
Ratio (%) [Akt2/ γ-tubulin]
0.600
0.500
0.400
0.300
0.200
0.100
0.000
24
48
72
96
120
144
Time post-transfection (h)

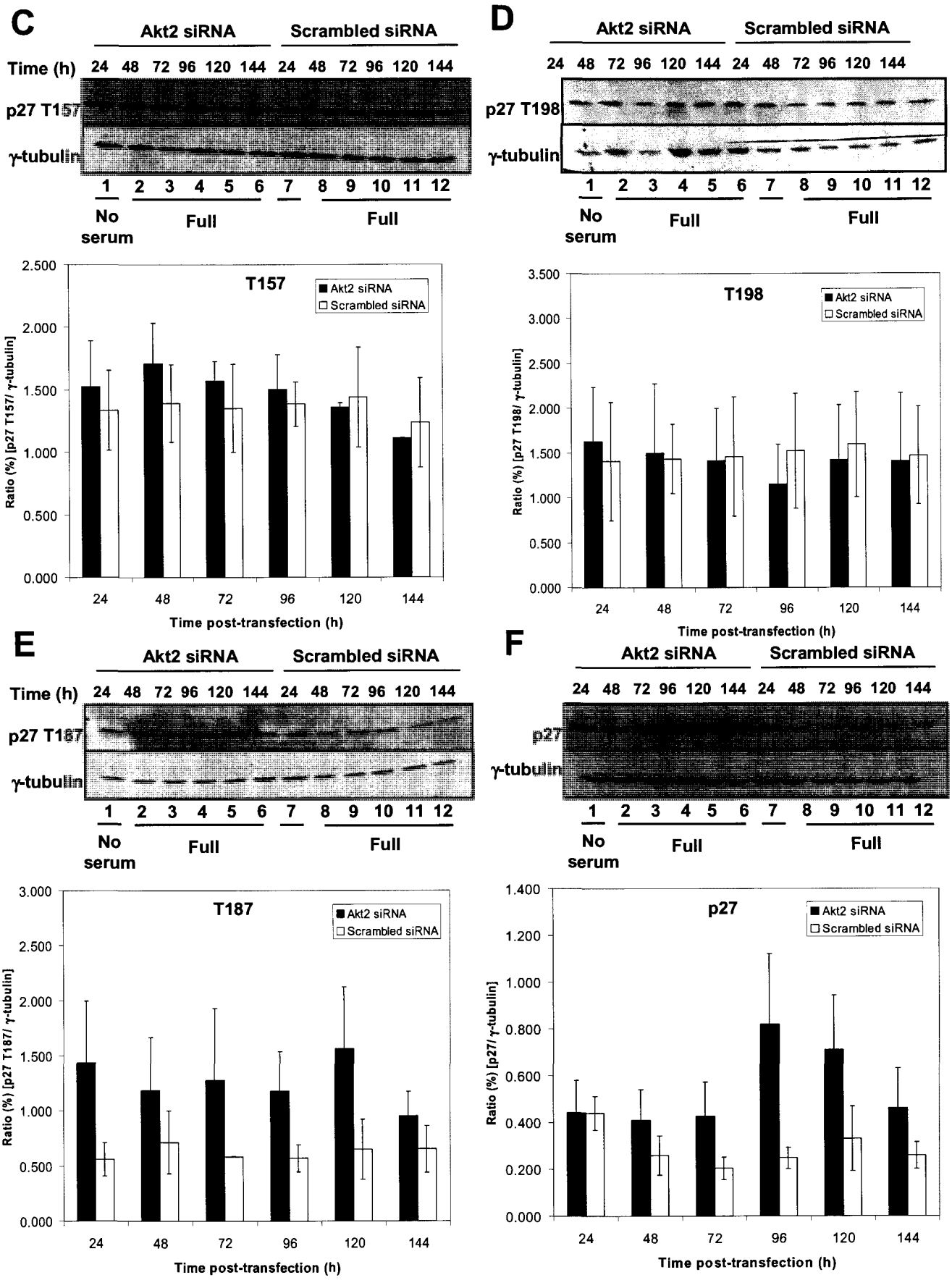
C
Akt2 siRNA
Scrambled siRNA
Time (h) 24 48 72 96 120 144 24 48 72 96 120 144
p27 T157
γ-tubulin
1 2 3 4 5 6 7 8 9 10 11 12
No serum
Full
Full
T157
Akt2 siRNA
Scrambled siRNA
Ratio (%) [p27 T157/ γ-tubulin]
Time post-transfection (h)
D
Akt2 siRNA
Scrambled siRNA
24 48 72 96 120 144 24 48 72 96 120 144
p27 T198
γ-tubulin
1 2 3 4 5 6 7 8 9 10 11 12
No serum
Full
Full
T198
Akt2 siRNA
Scrambled siRNA
Ratio (%) [p27 T198/ γ-tubulin]
Time post-transfection (h)
E
Akt2 siRNA
Scrambled siRNA
Time (h) 24 48 72 96 120 144 24 48 72 96 120 144
p27 T187
γ-tubulin
1 2 3 4 5 6 7 8 9 10 11 12
No serum
Full
Full
T187
Akt2 siRNA
Scrambled siRNA
Ratio (%) [p27 T187/ γ-tubulin]
Time post-transfection (h)
F
Akt2 siRNA
Scrambled siRNA
24 48 72 96 120 144 24 48 72 96 120 144
p27
γ-tubulin
1 2 3 4 5 6 7 8 9 10 11 12
No serum
Full
Full
p27
Akt2 siRNA
Scrambled siRNA
Ratio (%) [p27/ γ-tubulin]
Time post-transfection (h)

p27 for ubiquitin-mediated proteasomal degradation by Skp2, the results observed from the above analyses of p27 in the Akt2-siRNA cells suggested that the rate of protein degradation of p27 may also be affected by the Akt2 knockdown, since cytoplasmic localization of p27 is necessary for degradation by Skp2. Analysis of Skp2 by immunoblotting analysis determined that Skp2 was completely downregulated in the Akt2 siRNA-transfected cells, across the timepoints examined, with the exception of 144 h (Fig. 4.7b). Further, Skp2 expression was downregulated in the scrambled controls only during the 24 h timepoint, coincident with the nuclear localization of p27 in serum-free conditions at this time (Fig. 4.7b, lane 7). Expression levels of Skp2 increased with the return to full serum incubation in the scrambled controls (48-144 h post-transfection initiation) (Fig. 4.7b, lanes 8-12). Thus, nuclear localized p27 was in part mediating the cell cycle arrest in the Akt2-knockdown, along with the observed downregulation of Cdk2. Downregulated levels of Skp2 and the concurrent upregulation of p27 would affect the turnover of p27 as well as levels of cyclin E (from Fig 4.6a and d). As expected, the levels of p27 protein were upregulated in the Ak2-transfected cells compared to the scrambled controls, particularly at 72 h and 96 h post-transfection initiation (Fig. 4.7f). Thus, p27 was both localized to the nucleus, and upregulated in the Akt2-transfected cells (Fig. 4.7a and f).

Since the regulation of p27 in the Akt2-transfectants was not mediated by the T157 and T198 Akt-mediated phosphorylation sites, the mRNA regulation of p27 and Akt2 was examined next across all timepoints using quantitative real-time PCR (Q-PCR). Cells that were maintained in serum-free medium for 24 h (i.e., the duration of the entire siRNA transfection) contained a high level of p27 mRNA, regardless of the Akt2 status (Fig. 4.8a, 24 h timepoint). This result is consistent with the FACS profile, which showed that most of the cells (both Akt2 siRNA control conditions) maintained in the serum-free medium were at

A

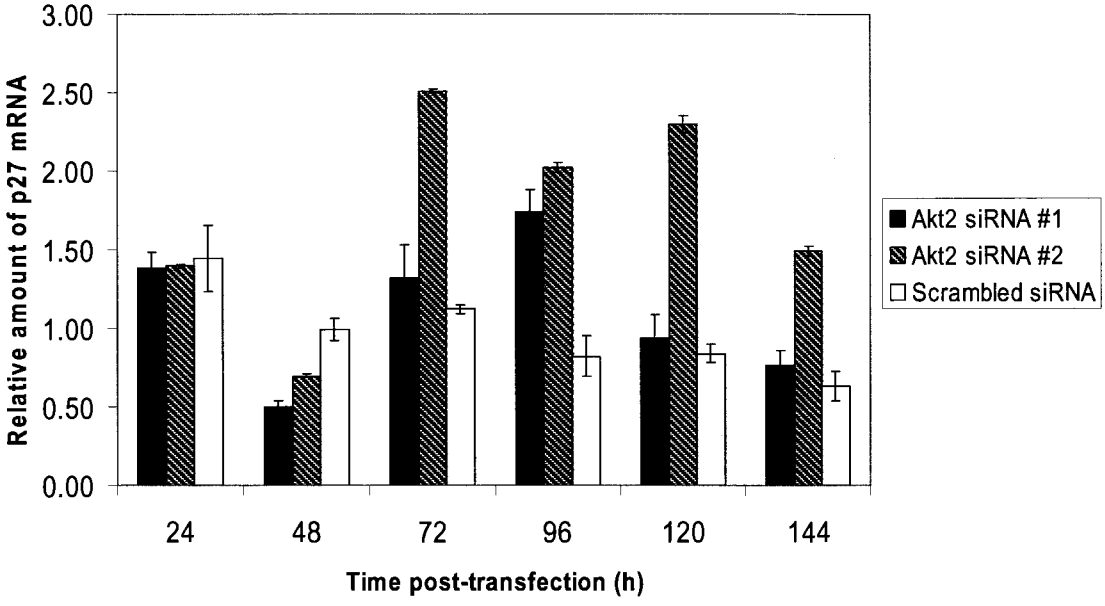
3.00
2.50
2.00
1.50
1.00
0.50
0.00
Relative amount of p27 mRNA
24
48
72
96
120
144
Time post-transfection (h)
Akt2 siRNA #1
Akt2 siRNA #2
Scrambled siRNA

B

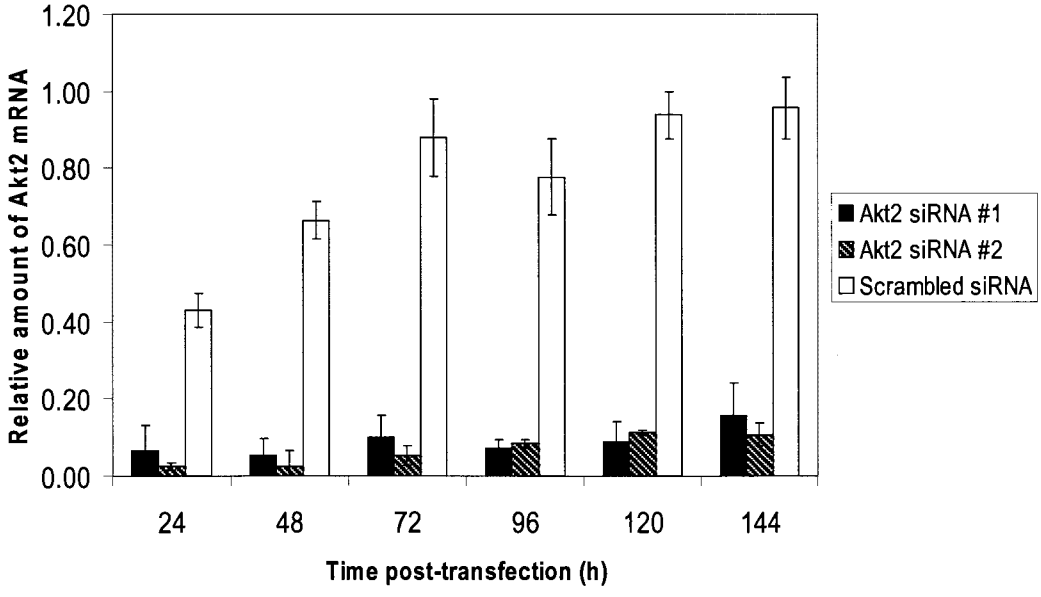
1.20
1.00
0.80
0.60
0.40
0.20
0.00
Relative amount of Akt2 mRNA
24
48
72
96
120
144
Time post-transfection (h)
Akt2 siRNA #1
Akt2 siRNA #2
Scrambled siRNA

G0/G1 at this time (Fig. 4.4). However, once cells were released into complete medium after transfection, the 48 h timepoint showed that the level of p27 mRNA was lower in the Akt2-ablated cells than the control at 48 h post-transfection initiation (Fig. 4.7a, 48 h). This result was surprising since the p27 Western blot indicated that the protein level was higher in the Akt2-ablated cells than in the controls at the same timepoint (compare lanes 2 and 8, Fig. 4.7f). This result, although surprising at first, suggests that p27 protein was more stable upon release into complete medium, and this could potentially be the result of the downregulation of Skp2 (Fig. 4.7b). However, after 48 h, the mRNA levels of p27 are upregulated in Akt2-siRNA conditions at 72-96 h post-transfection (Fig. 4.8a from 72-120 h). Further, the upregulated p27 mRNA levels were observed for both Akt2 siRNA oligos (Akt2 siRNA #1 and Akt2 siRNA #2). Thus, the mRNA upregulation of p27 in the Akt2-ablated cells was consistent with a G0/G1 arrest, thereby further confirming the data obtained by flow cytometry and the nuclear localization of p27 in the Akt2-knockdown samples.

The analysis of Akt2 mRNA expression (Fig. 4.8b) indicated that the siRNA transfection efficiency ranges from 83.7-96.1% at the mRNA level for these experiments (Akt2 siRNA #1: 83.7-91.8%; Akt2 siRNA #2: 89.2-96.1%) as determined by Q-PCR when the remaining levels of Akt2 were quantified in relation to their scrambled control at each timepoint.

4.3.6 The ablation of Akt2 markedly downregulated the phosphorylation of p70S6K at Thr 389

Akt has been shown to regulate the cell cycle through a series of activating or inactivating phosphorylations on multiple downstream substrates. Regulation can occur through the phosphorylation and inhibition of GSK-3β (reviewed in Caldon et al., 2006) and

the phosphorylation and inactivation of the Forkhead (FoxO) transcription factors (Medema et al., 2000). Further, mTOR and TSC2 (tuberin, an upstream regulator of mTOR) also regulate the cell cycle by the upregulation and stabilization of p27 (Liang & Slingerland, 2003; Nourse, 1994; Rosner et al., 2006), in addition to regulating protein synthesis and translation through p70S6K and 4E-BP1. Thus, the downstream Akt signaling substrates involved in the Akt2-knockdown were examined next.

Data obtained from Western blotting showed that the phosphorylation at S256 of FoxO1 was not altered by Akt2 ablation (Fig. 4.9b), although the levels of non-phosphorylated FoxO1 were downregulated in the Akt2-ablated cells from 72-144 h post-transfection (Fig. 4.9b). Previously published reports have indicated that overexpression of FoxO factors (FoxO1, FoxO3a, and FoxO4) can result in increased p27 (reviewed in Burgering & Kops, 2002; Liang & Slingerland, 2003). Since the levels of FoxO1 were downregulated in this study, this may suggest that the upregulation of p27 transcription was independent of FoxO1 in this system. Western blot analysis also showed little difference between the Akt2-siRNA conditions and the scrambled controls in the levels of p-GSK-3α/β (S21/S9), and GSK-3β protein (Fig. 4.9c). To ensure that the reduction in cell proliferation was not due to the downregulation of the MAPK pathway, protein levels of p-ERK1/2 (p42/44) were also examined. The phosphorylation pattern of ERK1/2 (p42/44) did not substantially differ between cells transfected with Akt2 siRNA or scrambled siRNA (Fig. 4.9). Thus, the inhibition of cell proliferation and subsequent G0/G1 arrest in these experiments was not being mediated through ERK, GSK-3, or FoxO1 signaling (Fig. 4.9a through d). The knockdown of Akt2 across all experimental timepoints is also shown (Fig. 4.9a).

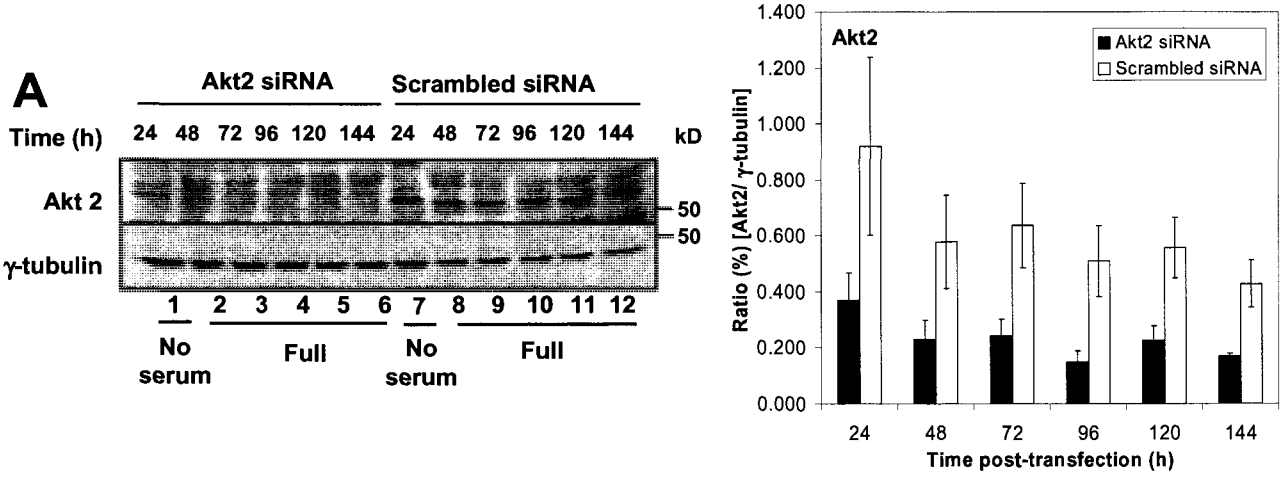
A
Akt2 siRNA
Scrambled siRNA
Time (h)
24 48 72 96 120 144 24 48 72 96 120 144
kD
Akt 2
γ-tubulin
50
50
1 2 3 4 5 6 7 8 9 10 11 12
No serum
Full
No serum
Full
Akt2
Akt2 siRNA
Scrambled siRNA
Ratio (%) [Akt2/ γ-tubulin]
1.400
1.200
1.000
0.800
0.600
0.400
0.200
0.000
24 48 72 96 120 144
Time post-transfection (h)

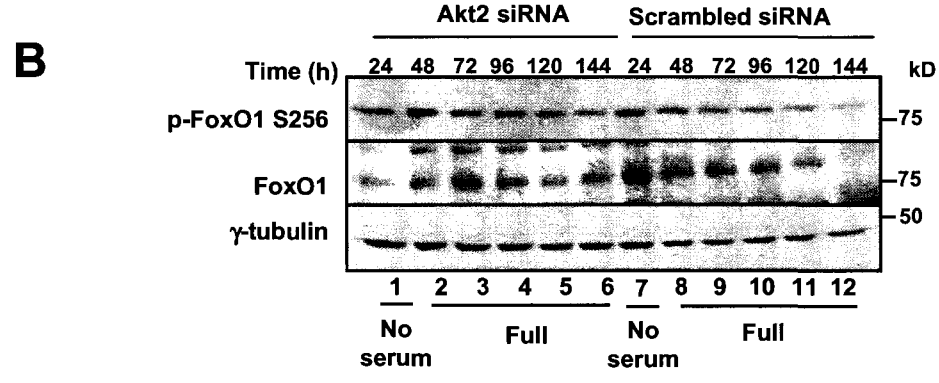
B
Akt2 siRNA
Scrambled siRNA
Time (h)
24 48 72 96 120 144 24 48 72 96 120 144
kD
p-FoxO1 S256
FoxO1
γ-tubulin
75
75
50
1 2 3 4 5 6 7 8 9 10 11 12
No serum
Full
No serum
Full

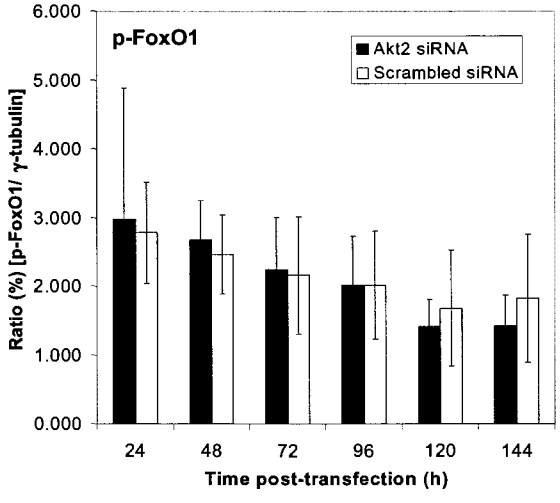
p-FoxO1
Akt2 siRNA
Scrambled siRNA
Ratio (%) [p-FoxO1/ γ-tubulin]
6.000
5.000
4.000
3.000
2.000
1.000
0.000
24 48 72 96 120 144
Time post-transfection (h)

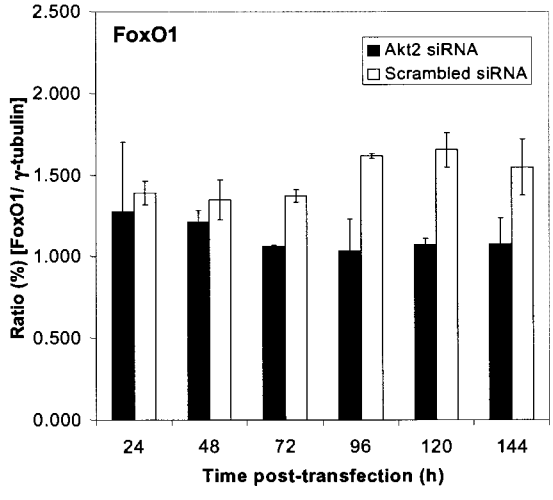
FoxO1
Akt2 siRNA
Scrambled siRNA
Ratio (%) [FoxO1/ γ-tubulin]
2.500
2.000
1.500
1.000
0.500
0.000
24 48 72 96 120 144
Time post-transfection (h)

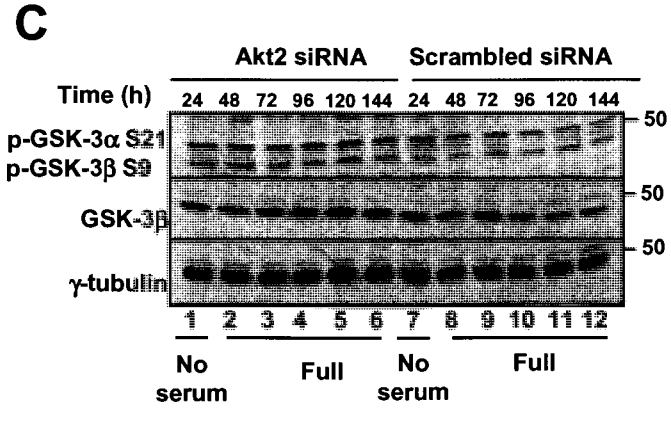
C
Akt2 siRNA
Scrambled siRNA
Time (h)
24 48 72 96 120 144 24 48 72 96 120 144
p-GSK-3α S21
p-GSK-3β S9
GSK-3β
γ-tubulin
50
50
50
1 2 3 4 5 6 7 8 9 10 11 12
No serum
Full
No serum
Full

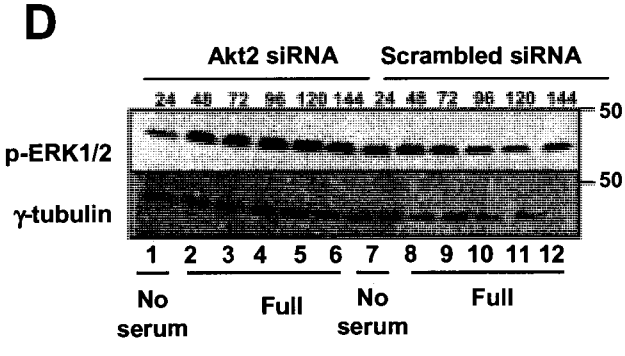
D
Akt2 siRNA
Scrambled siRNA
p-ERK1/2
γ-tubulin
50
50
1 2 3 4 5 6 7 8 9 10 11 12
No serum
Full
No serum
Full

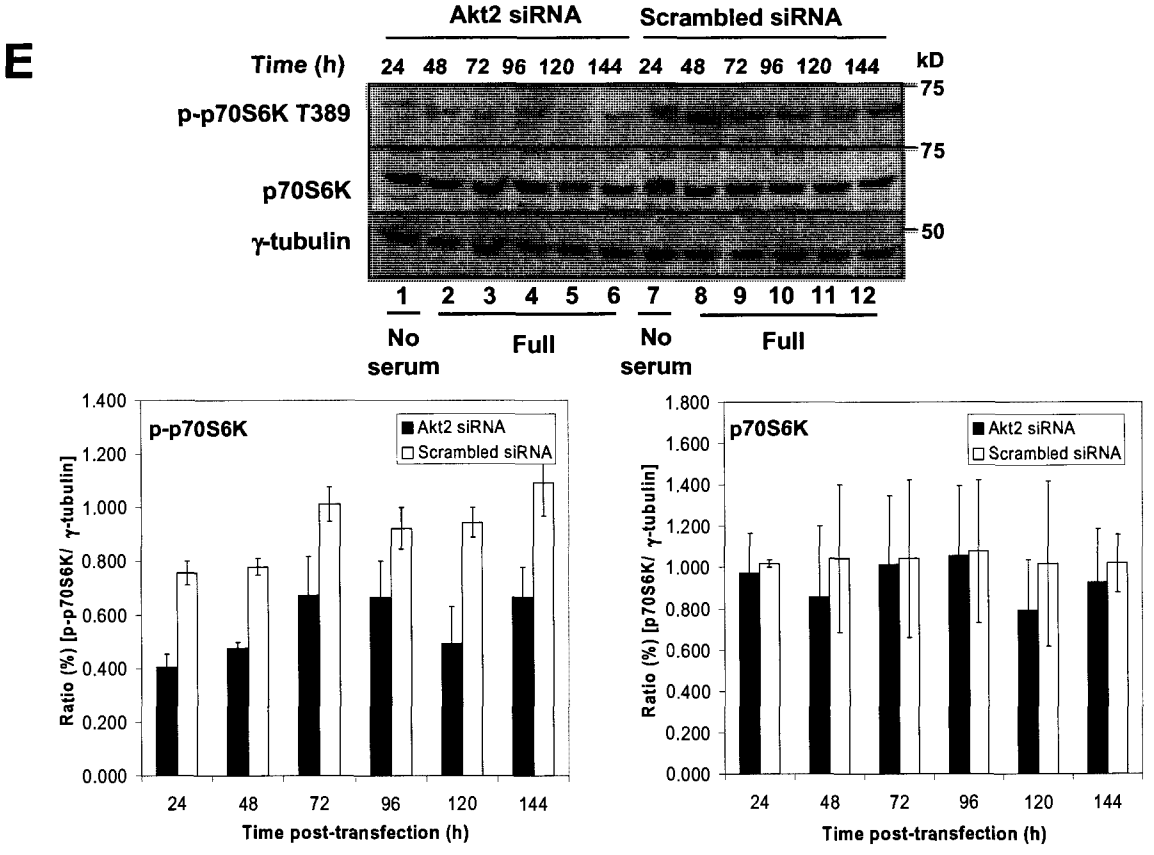
E
Akt2 siRNA
Scrambled siRNA
Time (h)
24 48 72 96 120 144 24 48 72 96 120 144
kD
p-p70S6K T389
p70S6K
γ-tubulin
75
75
50
1 2 3 4 5 6 7 8 9 10 11 12
No serum
Full
No serum
Full
p-p70S6K
Akt2 siRNA
Scrambled siRNA
Ratio (%) [p-p70S6K/ γ-tubulin]
Time post-transfection (h)
p70S6K
Akt2 siRNA
Scrambled siRNA
Ratio (%) [p70S6K/ γ-tubulin]
Time post-transfection (h)

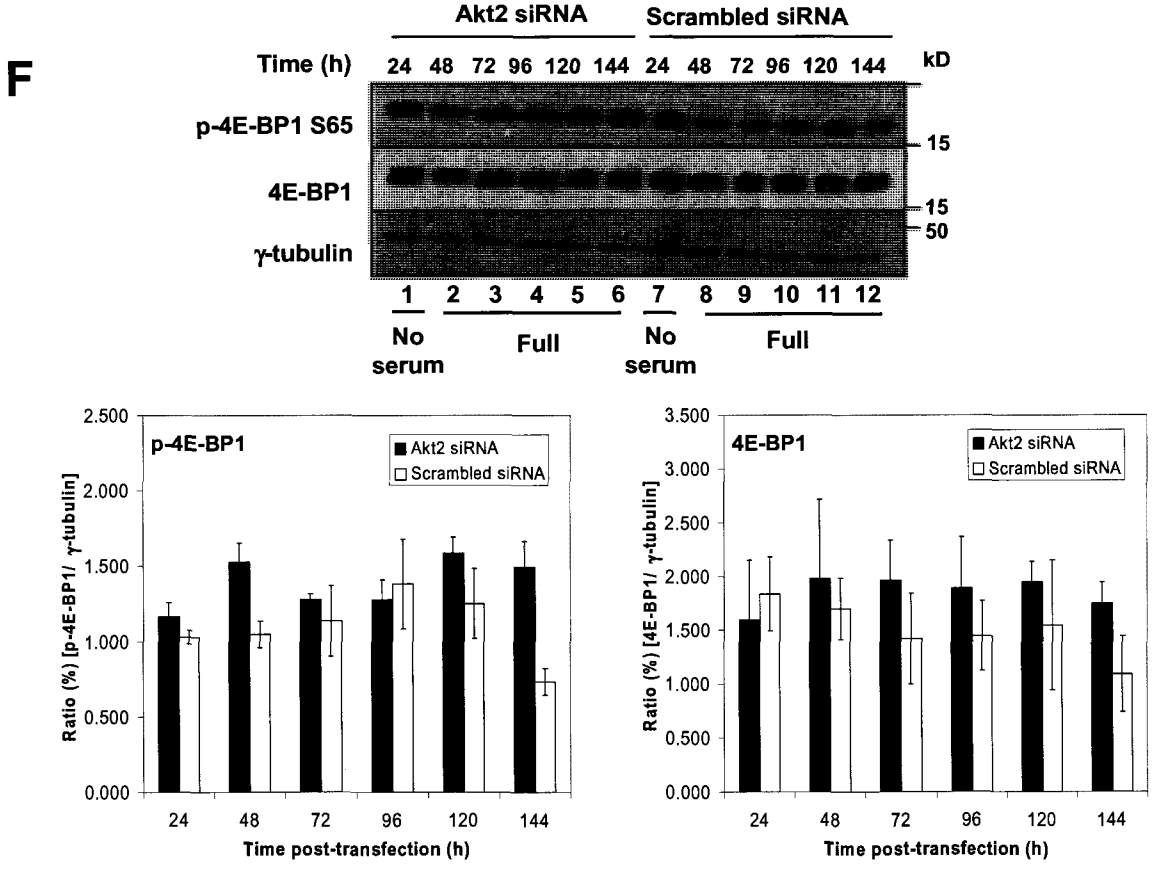
F
Akt2 siRNA
Scrambled siRNA
Time (h)
24 48 72 96 120 144 24 48 72 96 120 144
kD
p-4E-BP1 S65
4E-BP1
γ-tubulin
15
15
50
1 2 3 4 5 6 7 8 9 10 11 12
No serum
Full
No serum
Full
p-4E-BP1
Akt2 siRNA
Scrambled siRNA
Ratio (%) [p-4E-BP1/ γ-tubulin]
Time post-transfection (h)
4E-BP1
Akt2 siRNA
Scrambled siRNA
Ratio (%) [4E-BP1/ γ-tubulin]
Time post-transfection (h)

Since Akt can also regulate cell cycle progression through the mTOR signaling pathway, the activities of the two branches of the mTOR pathway, p70S6K and 4E-BP1 (eukaryotic initiation factor 4E-binding protein 1) were examined. Knockdown of Akt2 resulted in a complete downregulation of phosphorylated-p70S6K, across all timepoints examined, while there were no significant differences in the amount of total endogenous p70S6K between the Akt2-treated cells and the scrambled controls (Fig. 4.9e). This suggested that the activation and regulation of the mTOR pathway was mediated by Akt2. Conversely, no differences in p-4E-BP1 were observed compared to the scrambled controls, except at the 48 h timepoint, which is the first timepoint measured after serum repletion (Fig. 4.9f). Collectively, these results demonstrate that Akt2 was the specific Akt isoform involved in the regulation of cell proliferation and protein synthesis through signaling via mTOR-p70S6K in MDA-MB231 cells.

Hahn-Windgassen et al., (2005) have recently placed Akt upstream of AMPKα. AMPKα is a regulator of cellular energy and is activated when cells experience an energy crisis, or shifts in the ATP/ADP ratio within the cells. AMPKα can phosphorylate and regulate TSC2 thereby constraining mTOR activity (Um et al., 2006). Akt signaling can further regulate mTOR through Akt-mediated inhibition of AMPKα. (Please refer to Fig. 4.10 for a schematic illustration of Akt signaling through AMPK, FoxO and p27). Since it has been established that knockout of Akt2 in either cells or knockout mice is known to impart defects in glucose uptake and promote an insulin-resistant phenotype which is implicated in the pathogenesis of Type 2 diabetes (Bae et al., 2003; Cho et al., 2001a; Dummler et al., 2006; Jiang et al., 2003; Katome et al., 2003), it was essential to assess whether the downregulation of mTOR through Akt2-ablation was mediated by activation of

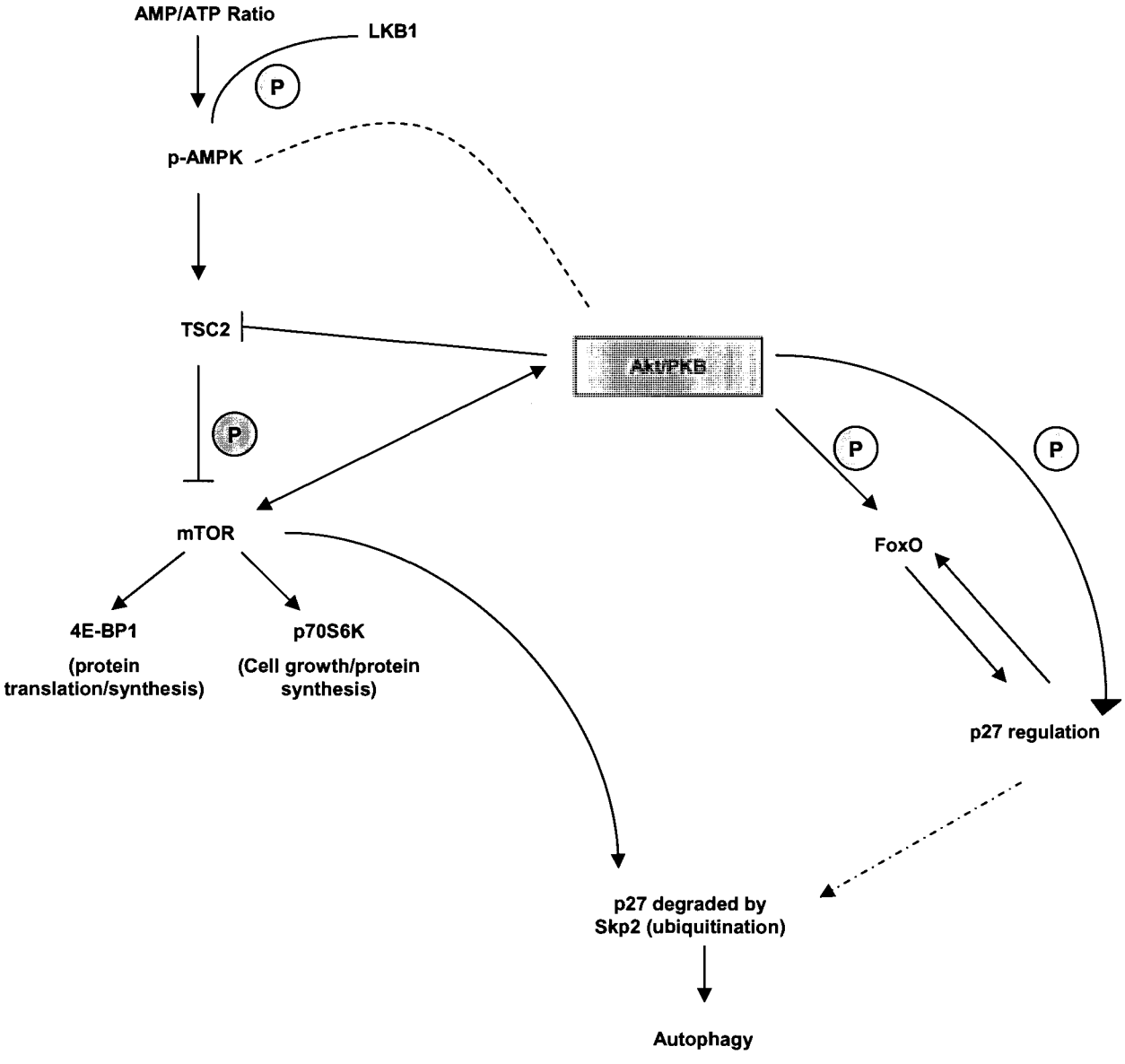
AMP/ATP Ratio
LKB1
P
p-AMPK
TSC2
Akt/PKB
P
P
P
mTOR
FoxO
4E-BP1
(protein translation/synthesis)
p70S6K
(Cell growth/protein synthesis)
p27 regulation
p27 degraded by Skp2 (ubiquitination)
Autophagy

AMPKα. Western blot analysis of phosphorylated AMPKα (p-AMPKα) indicated that p-AMPKα was downregulated in the Akt2-siRNA treated cells. Levels of p-AMPKα protein were lowest at 24 h and 48 h post-transfection initiation and increased at the last timepoints of the experiment (120 h and 144 h). If decreases in nutrients and growth factors were responsible for the mTOR downregulation in this system, then AMPKα would be activated and high levels of T172 phosphorylation would be apparent throughout the entire timecourse studied, as evident in the scrambled control at the serum-starved 24 h (Fig. 4.11a-note the increased level of p-AMPKα at 24 h in the scrambled controls). Levels of non-phosphorylated AMPKα in the Akt2-transfected cells showed no difference from the controls at 24 h and 48h, and then decrease at 72-144 h post-transfection initiation (Fig. 4.11b). A level of complication in this analysis, however, is the fact that MDA-MB231 cells are null for LKB1, the kinase responsible for phosphorylating AMPKα (Shen et al., 2002; Dowling et al., 2007). However, other kinases have been identified that phosphorylate the T172 residue such as CaMKKs (Hurley, et al., 2005). The fact that activation of AMPKα was seen in response to incubation in serum-free medium (in the scrambled controls) indicated that signaling through AMPKα can occur in LKB1-null MDA-MB231 cells. Furthermore, AMPKα activation was not mitigating the regulation of mTOR in this system. It was therefore concluded that the regulation of the cell cycle and p27 in the Akt2-siRNA treated cells was mediated through regulation of the mTOR pathway and was independent of GSK3, FoxO, ERK1/2, and AMPKα.

4.3.7 The mitochondrial volume was increased in Akt2-ablated cells

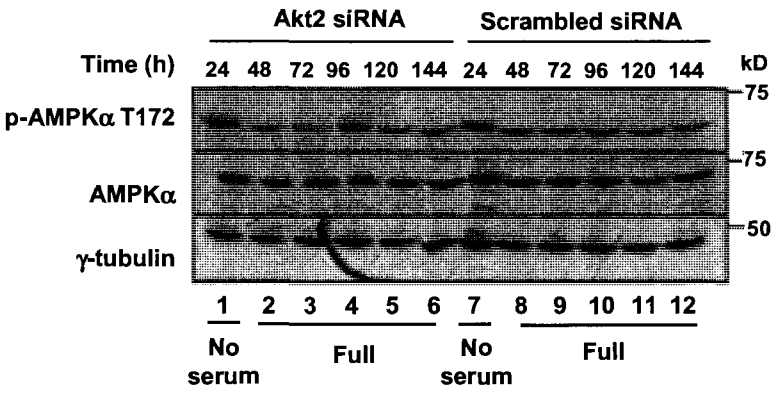
Akt2 siRNA
Scrambled siRNA
Time (h)
24 48 72 96 120 144 24 48 72 96 120 144
kD
p-AMPKα T172
AMPKα
γ-tubulin
75
75
50
1 2 3 4 5 6 7 8 9 10 11 12
No serum
Full
No serum
Full

A

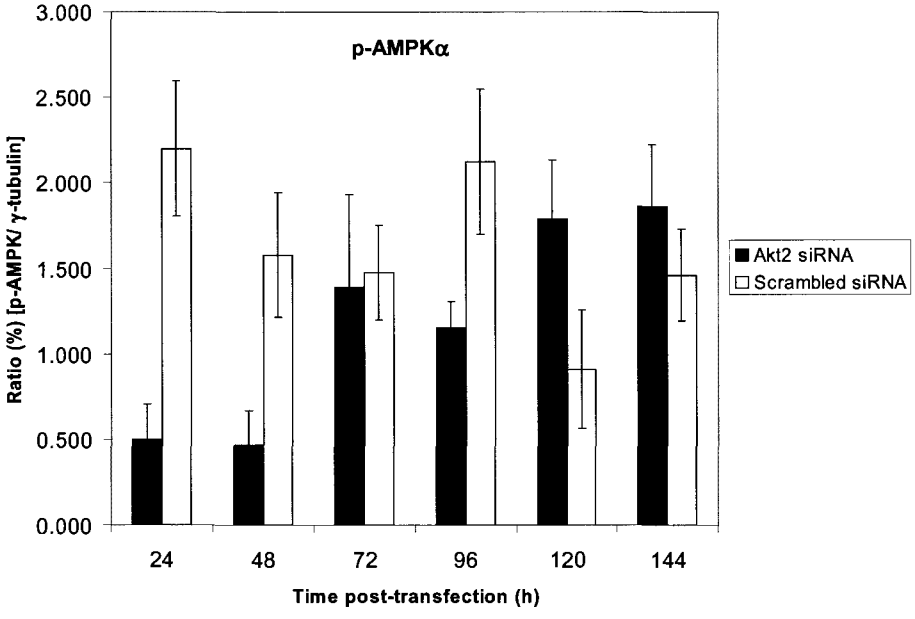
p-AMPKα
Ratio (%) [p-AMPK/ γ-tubulin]
3.000
2.500
2.000
1.500
1.000
0.500
0.000
24 48 72 96 120 144
Time post-transfection (h)
Akt2 siRNA
Scrambled siRNA

B

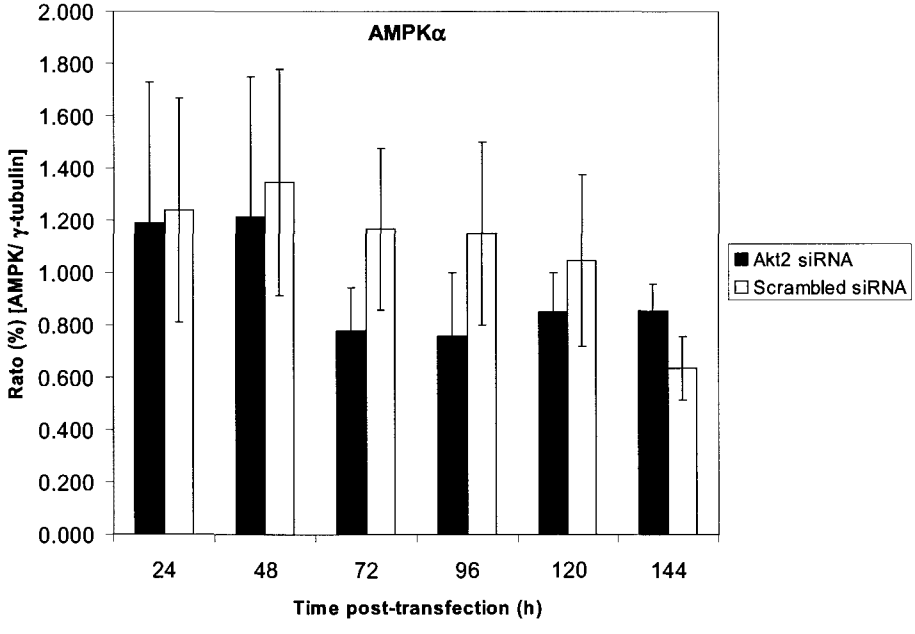
AMPKα
Rato (%) [AMPK/ γ-tubulin]
2.000
1.800
1.600
1.400
1.200
1.000
0.800
0.600
0.400
0.200
0.000
24 48 72 96 120 144
Time post-transfection (h)
Akt2 siRNA
Scrambled siRNA

It was previously demonstrated that Akt2 is co-localized and subfractionated with the mitochondrial portion of cell extracts in a variety of different cancer cells lines, including MDA-MB231 cells, suggesting that there was a physical association between Akt2 and the mitochondria (Chapter 3.0). If this is true, then Akt2 may be involved in the regulation of mitochondrial function. To gain insight into this aspect, the mitochondrial status of the Akt2-ablated cells was examined in conjunction with MitoTracker Red CMXRos, a membrane potential-dependent dye that is incorporated only into actively respiring cells, to discern if the knockdown of Akt2 caused any alternations to the mitochondria. Surprisingly, there was a very different mitochondrial size and morphology between the Akt2-siRNA transfected cells and the scrambled controls examined between 24-72 h post-transfection initiation (Fig. 4.12a). First, MitoTracker Red and Akt2 immunostaining were co-localized in the scrambled controls, a finding which is consistent with the previous observations (Chapter 3.0). Second, the mitochondria in the control cells usually exhibited one of two morphologies: a rounded, punctuate cellular localization or perinuclear localization (Fig.4.12a, xv and xviii), also consistent with previous observations. In contrast, mitochondria in the Akt2-ablated cells were substantially larger and spread throughout the cells beginning at 24 h (Fig. 4.12a, iii) and increasing to 72 h post-transfection initiation (Fig.4.12a, ix). A computer-assisted analysis of the mitochondrial surface area indicated that the mitochondria in the Akt2-siRNA cells occupied a larger cellular surface area, approximately double than that of the controls ($p<0.001$) (Fig. 4.12b). Further, the total cell area remained relatively constant suggesting that the observed phenomenon was not due to an increase in overall cell size at these times measured (Fig. 4.12c). (For the confocal microscopy pictures of Fig. 4.12a with Akt2 siRNA #2, please see Appendix IV, Fig. A11).

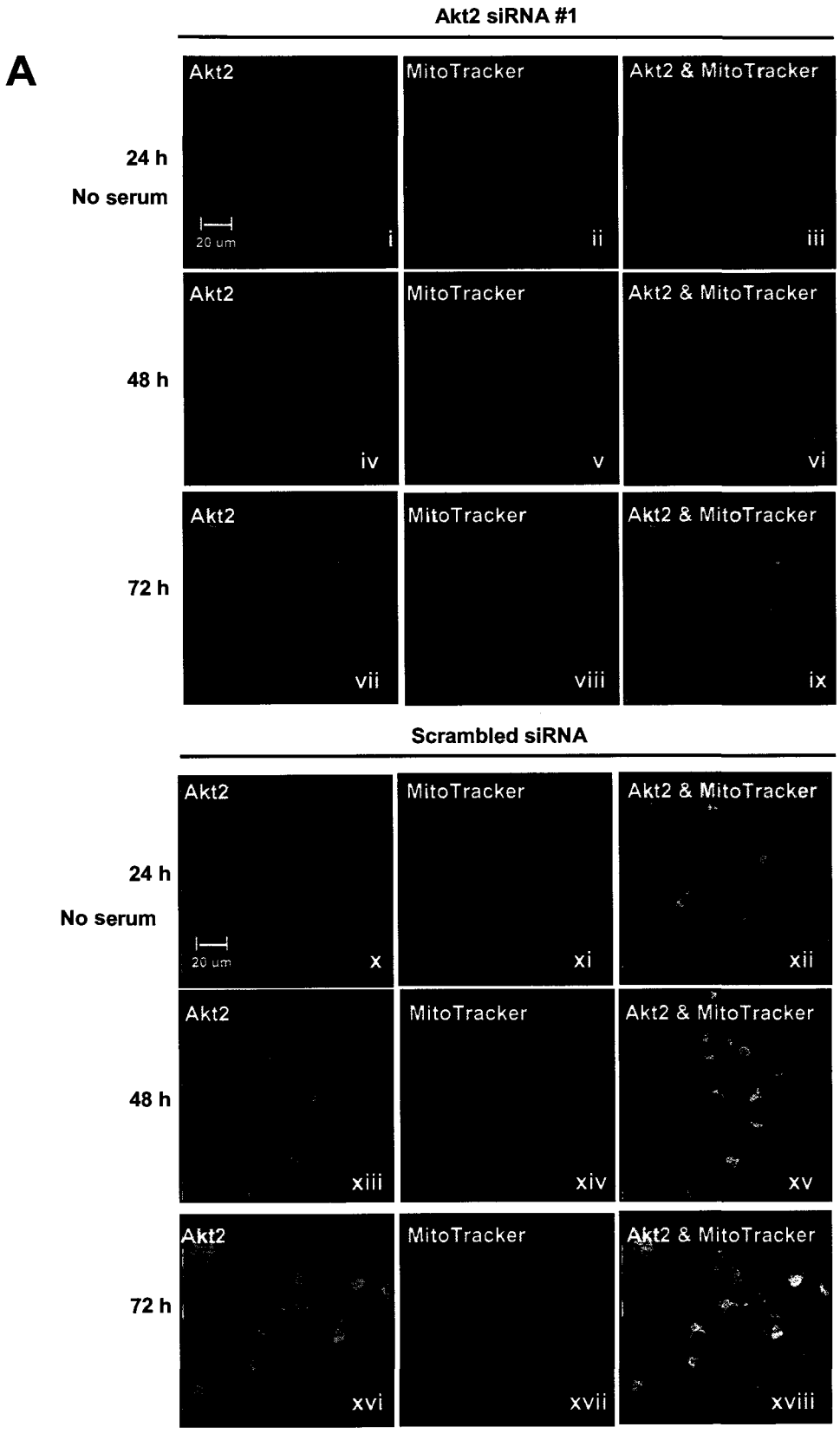
A
Akt2 siRNA #1
Akt2
MitoTracker
Akt2 & MitoTracker
24 h
No serum
20 um
i
ii
iii
48 h
iv
v
vi
72 h
vii
viii
ix
Scrambled siRNA
x
xi
xii
xiii
xiv
xv
xvi
xvii
xviii

B

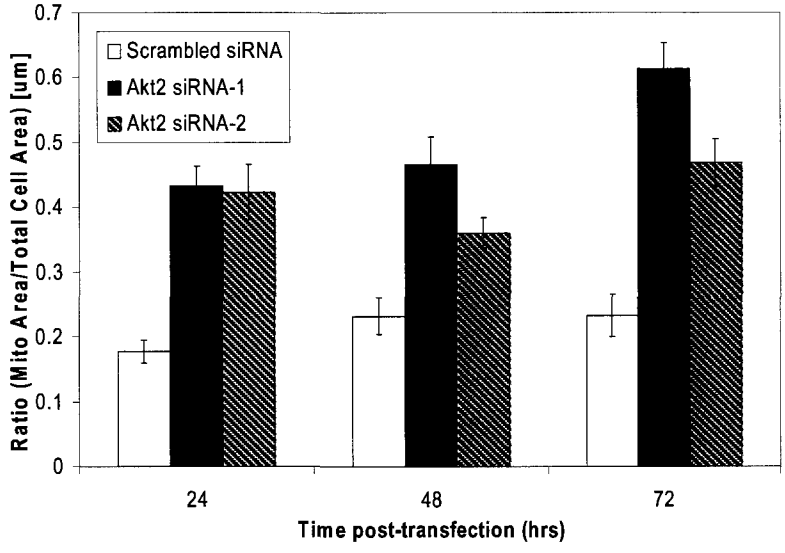
Scrambled siRNA
Akt2 siRNA-1
Akt2 siRNA-2
Ratio (Mito Area/Total Cell Area) [um]
0.7
0.6
0.5
0.4
0.3
0.2
0.1
0
24
48
72
Time post-transfection (hrs)

C

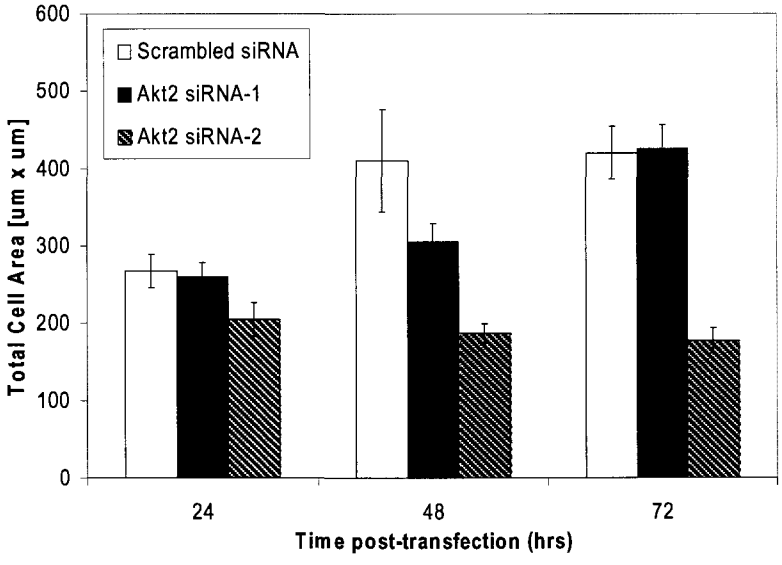
Scrambled siRNA
Akt2 siRNA-1
Akt2 siRNA-2
Total Cell Area [um x um]
600
500
400
300
200
100
0
24
48
72
Time post-transfection (hrs)

To determine if the increase in the mitochondrial volume in Akt2-ablated cells, affected the levels of a mitochondrial protein, VDAC1, a major component of the permeability transition pore on the outer mitochondrial membrane, was examined. As previously discussed in Chapter 3.3.2, hexokinases bind VDAC1, and pan-Akt is associated with mitochondrial hexokinases (Gottlob et al., 2001; Majewski et al., 2004b; Mathupala et al., 2006). Western blot analysis of VDAC1 indicated that the there was no difference in the level of VDAC1 protein in the Akt2-ablated cells relative to the controls, suggesting that the increase in mitochondrial volume did not cause an upregulation in the protein levels of VDAC1 (Fig. 4.13a).

Mitochondria are the site of energy metabolism within cells. It was hypothesized that because of the increased size of the mitochondria, and the role that Akt2 plays in regulating glucose metabolism, the increased mitochondria in the system may be due to increased mitochondrial biogenesis. Mitochondrial biogenesis has been shown to be regulated by components of the AMPK pathway (Zong et al., 2002), FoxO pathway (Puigerserver et al., 2003) and by levels of nitric oxide (NO) (reviewed in Reznick & Shulman, 2006). The mTOR pathway has also been demonstrated to regulate mitochondrial biogenesis through upstream AMPK signaling to mTOR, as well as mTOR itself (Aguilar et al., 2007; Cunningham et al., 2007). Experimental manipulation of any of these pathways results in the inhibition/activation of PGC-1α (peroxisome proliferator-activated receptor-coactivator 1α), a transcriptional co-activator involved in mitochondrial biogenesis, and the transcription of genes involved in gluconeogenesis, such as glucose-6-phosphatase, and PEPCK (phosphoenolpyruvate carboxykinase) (reviewed in Liang & Ward, 2006).

A

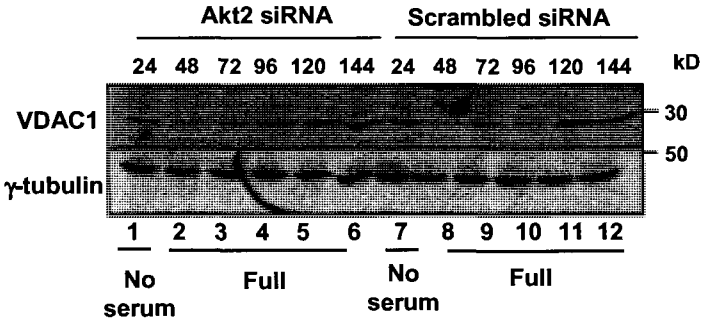
Akt2 siRNA
Scrambled siRNA
24 48 72 96 120 144 24 48 72 96 120 144
kD
VDAC1
γ-tubulin
30
50
1 2 3 4 5 6 7 8 9 10 11 12
No serum
Full
No serum
Full

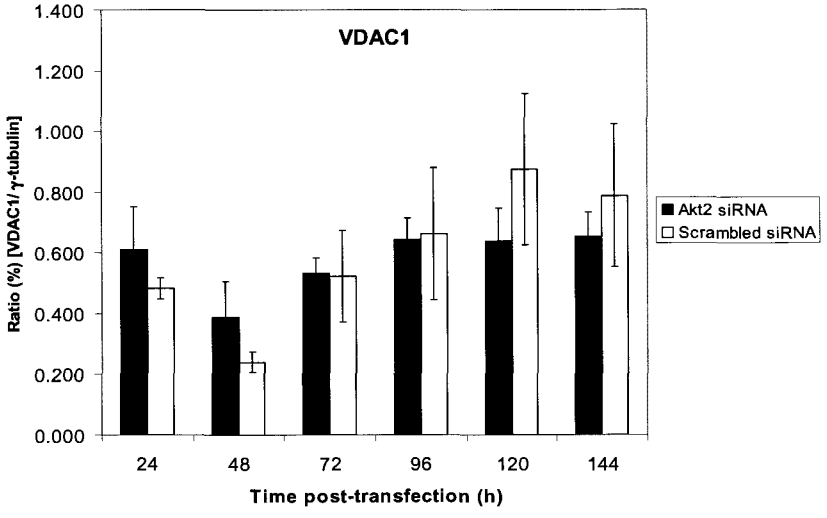
VDAC1
Ratio (%) [VDAC1/γ-tubulin]
1.400
1.200
1.000
0.800
0.600
0.400
0.200
0.000
24 48 72 96 120 144
Time post-transfection (h)
Akt2 siRNA
Scrambled siRNA

B

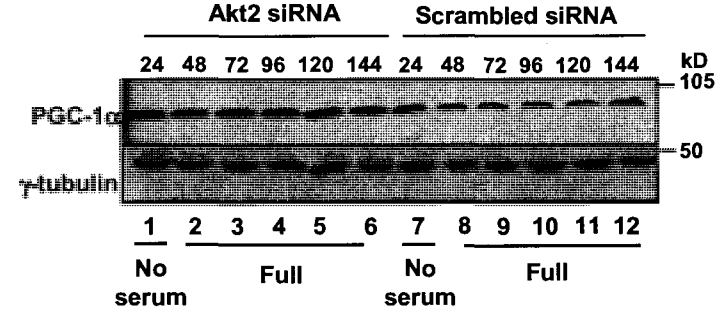
Akt2 siRNA
Scrambled siRNA
24 48 72 96 120 144 24 48 72 96 120 144
kD
PGC-1α
γ-tubulin
105
50
1 2 3 4 5 6 7 8 9 10 11 12
No serum
Full
No serum
Full

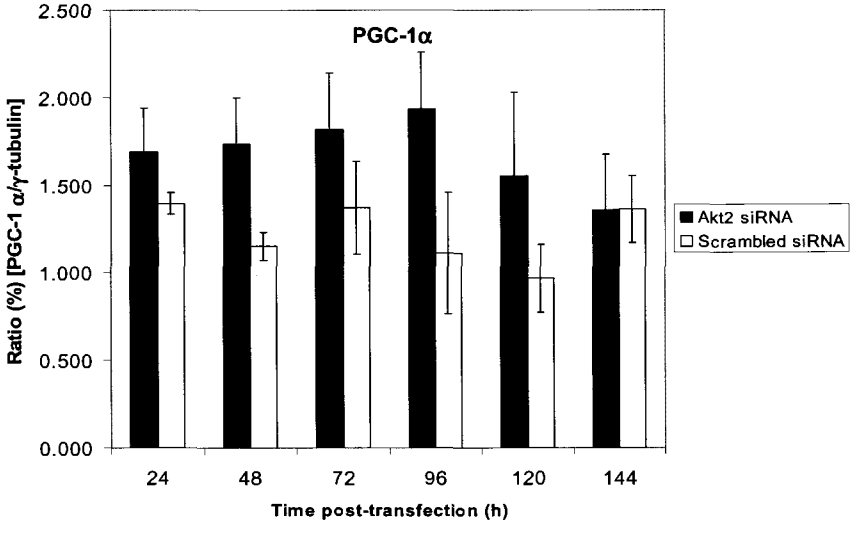
PGC-1α
Ratio (%) [PGC-1 α/γ-tubulin]
2.500
2.000
1.500
1.000
0.500
0.000
24 48 72 96 120 144
Time post-transfection (h)
Akt2 siRNA
Scrambled siRNA

There were two particular signaling pathways regulating mitochondrial biogenesis that were of interest in the Akt2-knockdown system. First, it is known that insulin suppresses FoxO1 transcription in an Akt phosphorylation-dependent mechanism, preventing the binding of FoxO1 to PGC-1α, and thus inhibiting the transcription of gluconeogenic genes (Puigserver, et al., 2003). Since there were no observed differences in the phosphorylation status of S256 on FoxO1 in the Akt2-ablated cells, this was unlikely the mechanism. Second, it was recently demonstrated that Akt2 can phosphorylate PGC-1α at Ser 570, and inhibit the transcription of genes involved in gluconeogenesis in a manner independent of FoxO1 in hepatocytes (Li et al., 2007). Thus, it was hypothesized that if this was occurring in this system, then the knockdown of Akt2 would be unable to phosphorylate and inhibit PGC-1α. Therefore, the regulator of mitochondrial biogenesis, PGC-1α was examined next to determine if Akt2-ablation was responsible for its induction. Since an antibody specific for the Ser570 site was not commercially available, the protein levels of PGC-1α were examined as an alternative. Protein levels of PGC-1α analyzed across the timepoints revealed that PGC-1α was upregulated in the Akt2-siRNA-treated cells (Fig. 4.13b). There were no changes in the protein expression levels of PGC-1α in the scrambled controls at any of the timepoints examined. Thus, it was concluded that increased levels of mitochondrial biogenesis were occurring in the Akt2-knockdowns, contributing to the observed increase in mitochondrial volume.

4.3.8 MDA-MB231 cells transfected with Akt2 siRNA underwent autophagic cell death

A cell may activate autophagy when the mTOR pathway is blocked; the upregulation of p27 persists; or the downregulation of Cdk2 is prolonged (Fujiwara et al., 2007, Liang et al., 2007b). All of these abnormalities were observed in Akt-ablated MDA-MB231 cells

(Fig(s). 4.1-4.7). In addition, the colony-forming ability was markedly downregulated suggesting that a high rate of cell death occurs in Akt2-ablated cells (Fig. 4.3). However, the data from flow cytometry analysis suggested that the mode of cell death was neither apoptosis nor necrosis, as there was no sub-genomic DNA fraction (Fig. 4.4). All of these observations suggested that the Akt2-ablated cells may undergo autophagy. Induction of autophagy was determined by analysis of LC3B, a known marker for autophagic cell death. During the activation of autophagy, LC3B-I is converted to LC3B-II, and becomes associated with newly formed autophagosomes (Kim et al., 2007).

As anticipated, Western blot analysis of the entire timecourse showed that during the 24 h serum-free timepoint, both the Akt2 siRNA-treated cells and the scrambled controls showed increased amounts of LC3-II conversion coincident with increased autophagy observed during conditions of serum starvation (Fig. 4.14a, 24 h timepoint, lanes 1 and 7). However, at 48 hours post-transfection, there was no increase in the conversion of LC3B-I to LC3B-II in the scrambled controls, indicating that other than at the 24 hour timepoint, the scrambled controls were not undergoing autophagy. In contrast, LC3B-II protein levels in the Akt2-treated cells were increased at every timepoint, indicating that the inhibition of the mTOR pathway through Akt2 caused increased autophagy (Fig 4.14a).

To further confirm the activation of autophagy in Akt2-ablated cells, LC3B immunostaining at 120 and 144 h post-transfection initiation was examined. Cells were also concurrently stained with MitoTracker Red CMXRos to examine the subcellular localization of autophagosomes and the mitochondria in the Akt2 siRNA-transfected cells. Results presented in Fig 4.14b, suggest that the mitochondria were co-localized with autophagosomes in cells transfected with Akt2, but not in the control cells (Fig. 4.14b, compare iv and viii with xii and xvi). Further, the immunostaining analysis of LC3B

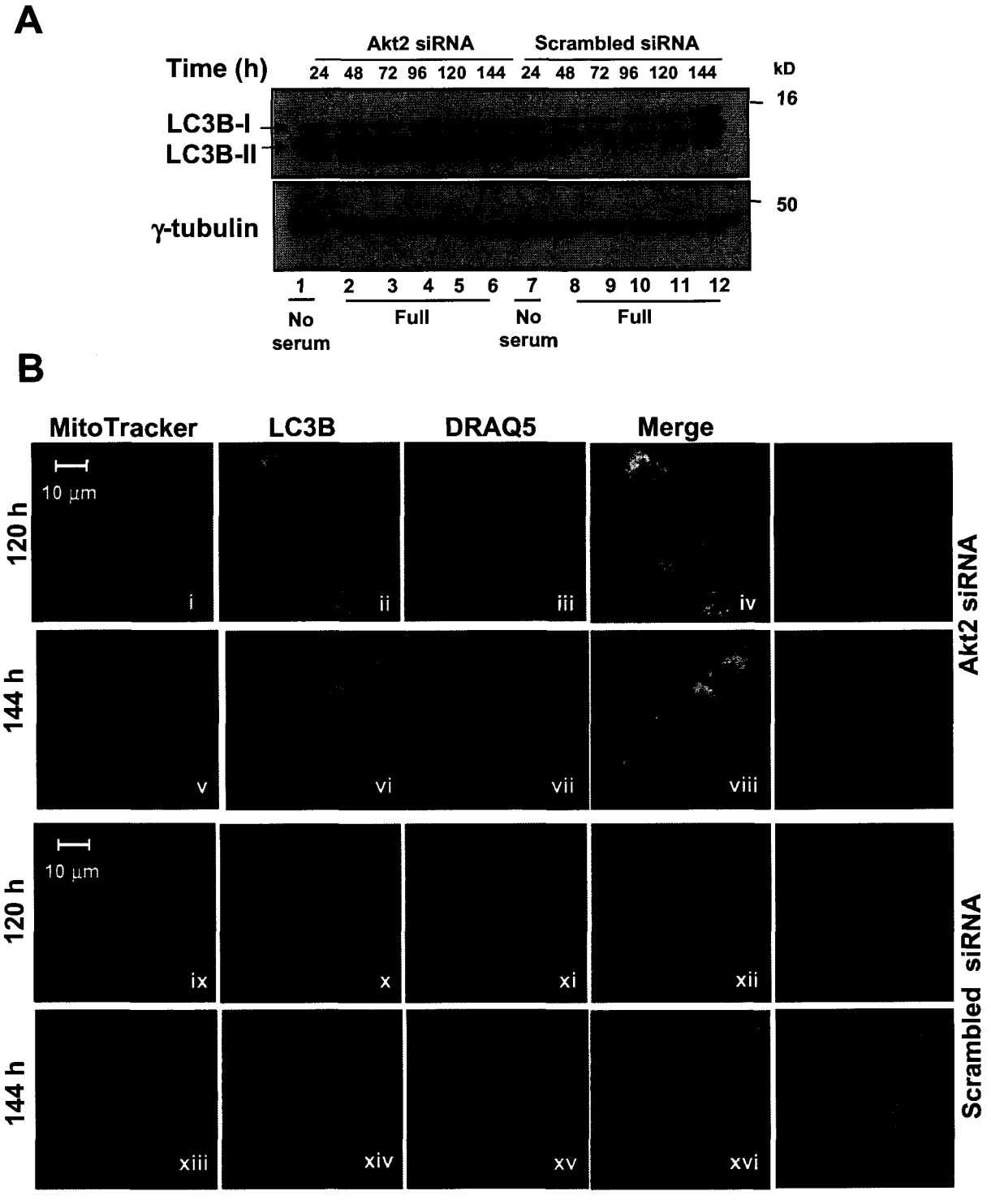
A
Akt2 siRNA
Scrambled siRNA
Time (h)
24 48 72 96 120 144 24 48 72 96 120 144
kD
16
LC3B-I
LC3B-II
50
γ-tubulin
1 2 3 4 5 6 7 8 9 10 11 12
No serum
Full
No serum
Full
B
MitoTracker
LC3B
DRAQ5
Merge
10 μm
120 h
144 h
i ii iii iv
v vi vii viii
ix x xi xii
xiii xiv xv xvi
Akt2 siRNA
Scrambled siRNA

determined the presence of LC3B in the Akt2 siRNA-transfected cells, while no observable amounts of LC3B staining were observed in the scrambled controls (Fig. 4-14b, compare iv and viii with xii and xvi).

In order to examine this further, the uptake of monodansylcadaverine (MDC), an autofluorescent drug shown to be incorporated into autophagolysosomes (Munafo et al., 2001) was examined. Cells were concurrently stained with acridine orange (AO) to identify the overall cell morphology and staining of acidic vesicular organelles (Takeuchi et al., 2005) and MitoTracker Red (CMXRos) to label the mitochondria. The results of the experiment demonstrated that the mitochondria were visibly enlarged (see top panel, Fig. 4.15) and co-localized with MDC, indicating that the mitochondria in the Akt2 siRNA-treated cells were selectively targeted for autophagic degradation, or mitophagy, at the later timepoints of the experiment. Acridine orange staining indicated an increase in the amount of acidic vesicles relative to the controls. However, the mitochondria were largely collapsed by 144 h post-transfection initiation (Fig. 4.15). Together, this data suggests that the mitochondria were selectively targeted for autophagic degradation in the MDA-MB231 cells transfected with Akt2 siRNA. Thus, Akt2-ablated cells activated autophagy of the mitochondria, perhaps by dysregulation of mitochondrial biogenesis. (For the fluorescent microscopy pictures of Fig. 4.15 with Akt2 siRNA #2, please see Appendix IV, Fig. A12).

4.4 DISCUSSION

In the current study, it was demonstrated that the knockdown of Akt2 resulted in devastating cellular and metabolic effects for MDA-MB231 cells compared to the knockdown of any other Akt isoform in this *in vitro* model of breast cancer. The data

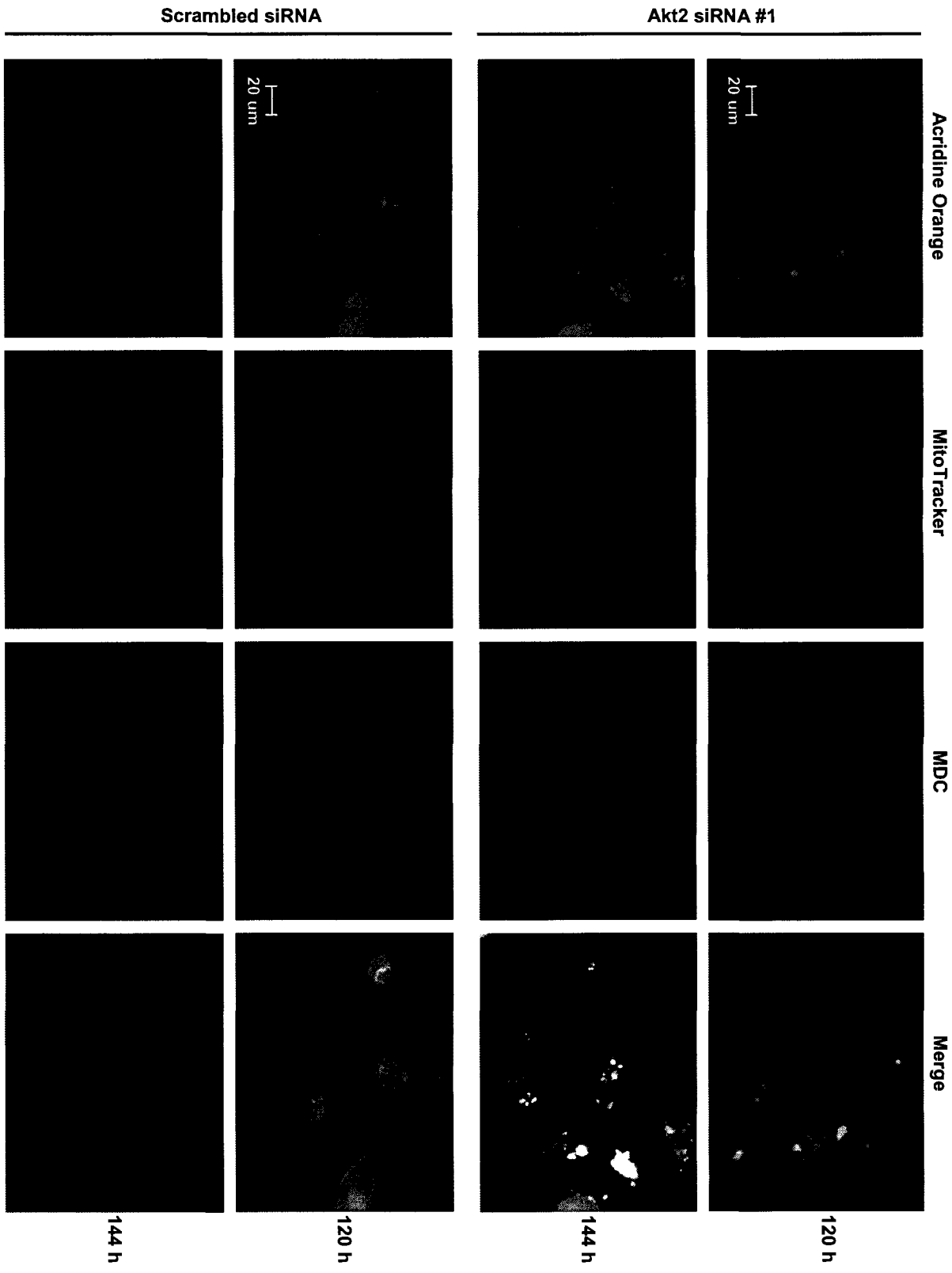
Scrambled siRNA
Akt2 siRNA #1
Acridine Orange
MitoTracker
MDC
Merge
20 um
20 um
144 h
120 h
144 h
120 h

obtained from these experiments indicates that Akt2 was the most critical isoform regulating both cell proliferation and cell survival compared to the other isoforms. Furthermore, ablation of Akt2 promoted a G0/G1-arrest through downregulation of Cdk2, mTOR activity, and subsequent transcriptional upregulation of p27. Akt2 was not involved in the regulation of known pan-Akt downstream substrates such as FoxO1, p21, GSK-3α/β, and ERK1/2 in MDA-MB231 cells in this system. The downregulation of Akt2 produced alterations in mitochondrial function, initially shown by an induction of mitochondrial biogenesis, and then in the later stages, mitochondrial-targeted autophagic degradation, or mitophagy. For a summary and proposed model of regulation from the results of this study, please see Fig. 4.16.

4.4.1 The role of Akt2 in the regulation of cell cycle progression and cell proliferation

In the current study, the targeted knockdown of Akt2 with siRNA reduced cellular proliferation through the downregulation of Cdk2 and cyclin D and the upregulation of p27, causing a G0/G1 cell cycle arrest. Studies in which the Akt isoforms have been targeted by siRNA-mediated interference and the regulation of their downstream signaling pathways evaluated have produced conflicting findings. With regard to Akt1, Meng et al. (2006) showed reduced proliferation in ovarian cancer cells with siRNA-targeted interference to Akt1. Ablation of Akt1 was associated with reduced proliferation, invasion, and phosphorylation of p-p70S6K1, but these findings were similar to those induced by siRNA targeted to p110α, the catalytic subunit of PI3K. Furthermore, Akt1 was the only Akt isoform targeted in this study.

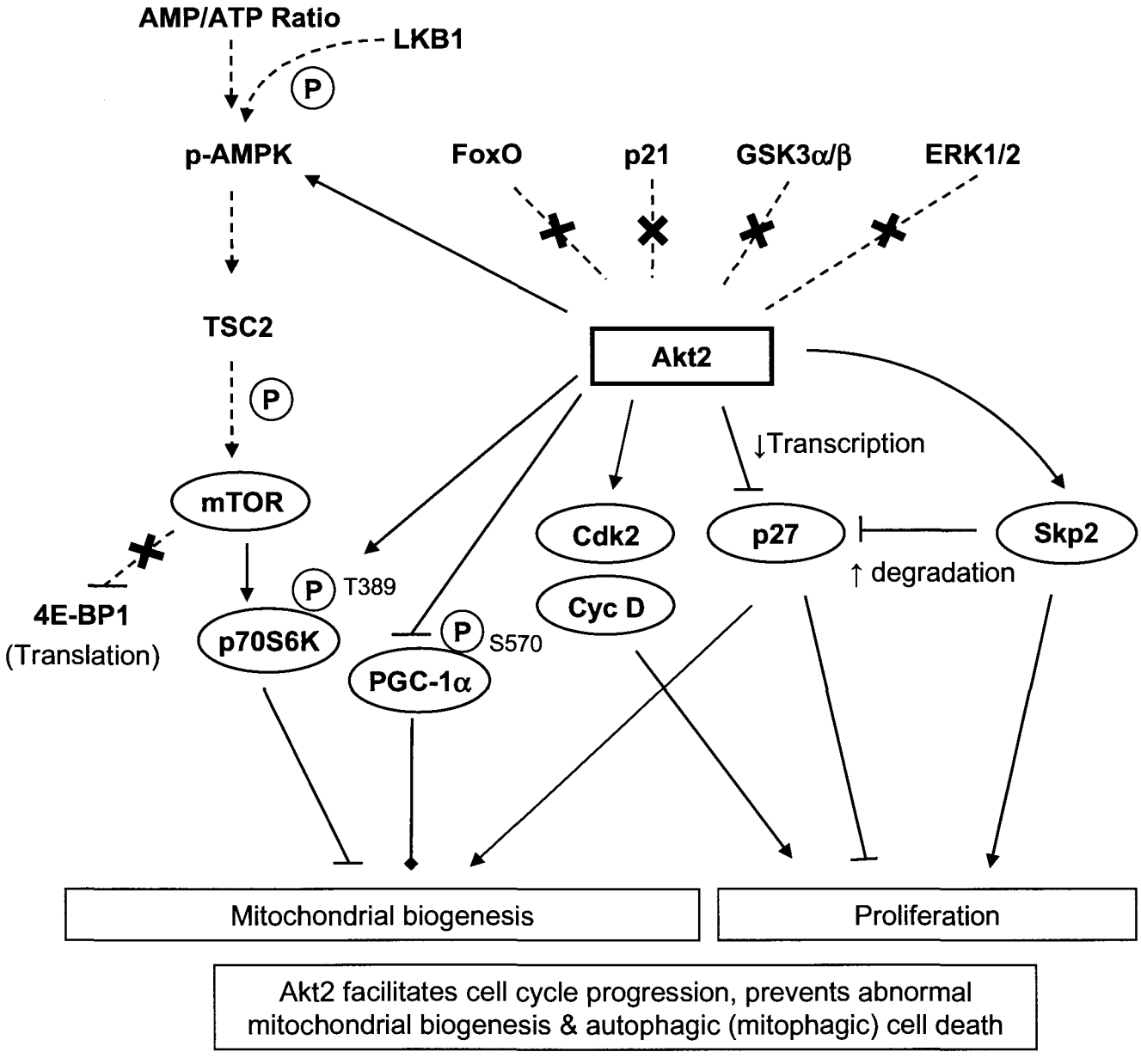
AMP/ATP Ratio
LKB1
P
p-AMPK
FoxO
p21
GSK3α/β
ERK1/2
TSC2
Akt2
P
↓Transcription
mTOR
Cdk2
p27
Skp2
↑ degradation
4E-BP1
(Translation)
P T389
p70S6K
Cyc D
P S570
PGC-1α
Mitochondrial biogenesis
Proliferation
Akt2 facilitates cell cycle progression, prevents abnormal mitochondrial biogenesis & autophagic (mitophagic) cell death

Similar to the results presented here, Noske et al. (2007) found reduced proliferation associated with Akt2-siRNA knockdown in ovarian cancer, while Sithanandam et al. (2005) found that ablation of Akt2 suppressed invasion and migration, compared to Akt1 and Akt3 in lung adenocarcinoma. Conversely, the overexpression of Akt2 was reported to show increased invasion and metastasis in both breast and ovarian cancer (Arboleda et al., 2003), coincident with increased β1-integrin expression. Further, activated Akt2 was associated with distinct changes in cell morphology (multinucleation) (Jin & Woodgett, 2005). Currently, there is only one report for Akt3 isoform-specific cell cycle regulation: Cristiano et al. (2006) reported siRNA-mediated interference of Akt3 regulated G2/M progression in ovarian cancer cells, although the cell lines utilized in this particular study did not express Akt2.

The data presented here indicate that over a prolonged timecourse, beginning at 24 h post-transfection and followed 6 days later to 144 h post-transfection, decreases in cell proliferation were seen only in the Akt2-transfectants. While there is some reduced proliferation in both Akt1 and Akt3-siRNA transfected cells compared to the controls, proliferation levels of Akt2 siRNA transfectants consistently fell below that of Akt1 and Akt3 at 144 hours post-transfection, and furthermore, proliferation in Akt2-siRNA cells did not increase significantly across the timecourse studied. Knockdown of the Akt isoforms in combination (double knockdown condition) did not potentiate a synergistic effect on either cell proliferation or survival, lending further support to the growing amount of evidence in the literature that the Akt isoforms regulate specific functions and may not be functionally redundant. However, differential representation of the isoforms among different cell lines

and cell types, as well isoform-specific regulation of biological and physiological functions adds another level of increased complexity to the Akt pathway.

The downregulation of Cdk2 has been observed prior in studies that have examined the PI3K/Akt signaling axis, but isoform-specific regulation has not yet been implicated. Previously published reports showed a downregulation of Cdk2 and a subsequent upregulation of p27 protein expression upon inhibition of PI3K in vascular smooth muscle cells (VSMCs) (Bacqueville et al., 1998). Downregulation of cyclin D1 and p21 during an LY294002-induced G1-arrest in ovarian cancer cells was also reported (Gao et al., 2004). Further, this study also demonstrated inhibition of p-p70S6K, with no alterations in Erk1/2, a finding similar to the results reported here. The decreased expression of cyclin D1 and p21 observed in Gao's study, and not observed here, may be explained by the fact that LY294002 inhibits upstream of Akt, and thus inhibits all Akt activity; whereas it is assumed that downstream Akt1- and Akt3-regulated processes and signaling would still be intact following the selective inhibition of Akt2 in the present study. Moreover, the downregulation of Cdk2 in the present study is of interest given that Nourse et al. (1994) found no alterations in Cdk2 expression or activity in cells treated with rapamycin concurrent with their noted upregulation of p27. Medema et al. (2000) reported no decreases in protein levels of cyclin E and Cdk2 when p27 was upregulated in their Forkhead transfectants, findings which are in contrast to those reported here.

Heron-Milhavet et al. (2006) recently published that cell proliferation was regulated by Akt1 and cell cycle exit was under the domain of Akt2 in nontransformed cells. Their results differ from this study in many ways. First, Akt1 inhibition by siRNA reduced cyclin A expression and showed reduced BrdU incorporation, while Akt2 inhibition was found to increase proliferation in undifferentiated myoblasts. Second, Akt2 was shown to be bound to

p21 and associated with p21 in co-precipitation experiments. However, in the present study, knockdown of Akt2 produced no difference in p21 protein levels with the exception of the serum-free conditions, and the only differences observed in the analysis of cyclins was the downregulation of cyclin D (although cyclin E was also upregulated it is most likely due to the decreased levels of protein degradation in this system). The binding status of p21, p27 or Cdk2 to each of the isoforms was not assessed in the present study, although there were some preliminary observations that Akt2 protein co-precipitated with Cdk2 and not p27 in MDA-MB231 cells (please see Fig. A13, Appendix IV). This would suggest that Akt2 could potentially regulate Cdk2 in MDA-MB231 cells. Consistent with this hypothesis, Maddika et al. (2008) recently showed that pan-Akt could phosphorylate Cdk2 at T39. Although their study did not examine the Akt isoforms, it could be possible that this phosphorylation is mediated by Akt2. Despite the preliminary evidence in the appendix, this is still speculative, and further investigation is required to determine the mechanism of how Akt2 and Cdk2 interact. Nonetheless, the differences between this study and Heron-Milhavet's could simply be due to the fact that cell cycle regulation in cancer cells is regulated by the Akt isoforms in a manner that is different from nontransformed cells. Hill et al. (1999) found differential regulation and expression levels of Akt1 and Akt2 in 3T3-L1 fibroblasts cells prior to being differentiated into adipocytes, indicating that isoform specificity exists between undifferentiated and differentiated cells. Bouzakri et al. (2006) also noted differences in Akt2 expression between undifferentiated myoblasts and differentiated myotubes. Further, MDA-MB231 cells are highly metatstatic, estrogen receptor negative, and p53 negative, all factors which could ultimately influence proliferation.

The results of the present study then demonstrated that cell cycle progression, at least in MDA-MB231 cells occured in an Akt2-dependent manner through the regulation of Cdk2,

mTOR and p27, showing an intricate level of isoform specificity. Since a prolonged timecourse was examined in this study, it is difficult to know which is causative or which occurred first, since the effects of Cdk2, p27 and mTOR were all observed at the 24 h timepoint (i.e., did the downregulation of Cdk2, cause the upregulation of p27, or vice versa). Conversely, is the observed upregulation of p27 either mTOR- or Akt2-dependent since reports indicate that rapamycin inhibition of mTOR upregulates p27 (Nourse et al., 1994; Martin et al., 2004)? Future studies discerning this will be of great interest.

With respect to the regulation of p27 by Akt, the data presented here found that the upregulation of p27 in Akt2-ablated cells was mainly due to the increase in mRNA. However, the upregulation of p27 during the first 24 h after Akt2-ablation (i.e., 48 h post-transfection initiation) was due to an increase in protein stability. Since the Skp2 subunit of the ubiquitin complex was substantially downregulated in Akt2-ablated cells, this might have resulted in the stabilization of p27 protein. These data are consistent with published data that the p27 protein level is regulated by both transcription and protein stability (Fujita et al., 2002; Medema et al., 2000; Liang et al., 2002). However, the finding that Akt2 siRNA knockdown regulated p27 transcriptionally was an unprecedented finding, and denotes a novel level of signaling associated with this isoform. Thus, in consideration that p27 can prevent autophagy and regulate cell cycle progression, signaling through p27 represents the central tenet of Akt2-regulated signaling in MDA-MB231 cells. Please see Fig 4.16 for a schematic of the findings from the present study and the proposed model of regulation via p27.

4.4.2 Akt2 regulates p70S6K

The finding that Akt2 signaled exclusively through mTOR to regulate cell cycle progression and cell proliferation was surprising in that no other branches of Akt signaling pathways examined in the present study such as FoxO1 were regulated in the same manner. Early studies examining the Akt isoforms often speculated that all downstream signaling substrates were redundant, a finding not supported here. However, the involvement of the mTOR pathway through downstream signaling to p70S6K, is not surprising considering that it regulates protein synthesis, while Akt2 regulates glucose transport and gluconeogenesis; ultimately, both are controllers of cellular energy and metabolism. Many published reports have demonstrated the link between energy metabolism (AMPK) and mTOR via TSC2 signaling. However, prior to Hahn-Windgassen's (2005) study, the regulation of TSC2 by Akt was considered to be independent of AMPK-signaling.

In order to rule out the possibility that p-p70S6K downregulation in the Akt2-siRNA transfected cells was not regulated by AMPKα, or by an alteration in the cellular ratio of ATP/ADP due to altered signaling through the insulin pathway, the activation of AMPKα in the Akt2-transfected cells was assessed, and phosphorylation was found only in the scrambled controls during the serum-free timepoints. However, p-AMPKα was upregulated in the Akt2-transfected condition during the later timepoints of the study that coincide with autophagy/mitophagy. Levels of non-phosphorylated AMPK were not different between the Akt2-ablated cells and scrambled controls in the early timepoints. However, the Akt2-ablated cells displayed lower levels of AMPK in the later timepoints (72-120 h, Fig. 4.11b). It is speculative, but the slight downregulation of AMPKα may be due to the fact that knockdown of Akt2 is associated with an insulin-resistant phenotype. Activation of AMPKα is often seen in studies where cells are serum-starved or deprived of nutrients as evidenced under the

serum-free conditions here at 24 h in the scrambled controls (Fig. 4.11a). It could very well be possible that even though the Akt2 knockdown is associated with defects in glucose uptake, there are reports that indicate that some of the functions of insulin signaling may be redundant and can be mediated through Akt1 in the absence of Akt2 (Jiang et al, 2003). Thus, in this system, if some of the energy requirements are being met through signaling via Akt1 or Akt3, then AMPKα would not be activated.

Prior reports have indicated that cells deficient in LKB1, the kinase responsible for activating AMPKα often do not respond to stimuli that would normally activate AMPKα (Corradetti et al., 2004), although there are other additional kinases that can regulate the phosphorylation of AMPKα (Hurley et al., 2005). It could be argued that the lack of AMPKα activation in the Akt2-cells was due to the LKB1-null status of MDA-MB231 cells. However, AMPKα activation was evidenced in the 24 h serum-free timepoints in the controls, which was abolished by the repletion of full serum, suggesting that the LKB1-null status of MDA-MB231 cells is not a factor here.

Thus, the link between Akt2 and the mitochondria and the regulation of p70S6K through mTOR was suggestive regarding the metabolism in MDA-MB231 cancer cells. Typically, cancer cells are dependent on glycolysis for their increased glucose consumption (Mathupala et al., 2006). The co-localization of Akt2 with the mitochondria, the regulation of mTOR, and the association of Akt and hexokinases places Akt2 in position to be the master regulator of cell metabolism, beyond glucose transport.

4.4.3 Akt2-siRNA transfected cells initially undergo mitochondrial biogenesis, but are ultimately targeted for mitophagy

One of the most exciting discoveries in the present study is the observation that the ablation of Akt2 had severe effects on the mitochondria of MDA-MB231 cells. The subcellular localization results of the previous studies within this thesis (Chapter 3.0) detailing the co-localization of Akt2 and the mitochondria provided the rationale to examine the mitochondria during the timecourse of the Akt2 knockdown. Surprisingly, increased mitochondrial size and surface area were upregulated in the Akt2 siRNA-treated cells, suggesting that the Akt2-ablated cells had increased their mitochondrial content. Complicating the analysis further is the fact that mitochondrial biogenesis can be regulated by mTOR (Cunningham et al., 2007), by FoxO in an Akt-dependent manner (Li et al., 2007; Puigserver et al., 2003), and by AMPK through an mTOR regulated pathway (Aguilar et al., 2007). It was previously shown that insulin treatment suppresses FoxO1-mediated transcription of PGC-1α, a transcription coactivator required for mitochondrial biogenesis, through Akt-mediated phosphorylation of FoxO1 at S256 (Puigserver et al., 2003). There were no notable differences in the levels of FoxO1 phosphorylation between the Akt2-siRNA and scrambled conditions, suggesting that these effects may not be mediated through the Forkhead pathway. However, the subcellular status of FoxO1, or the binding of FoxO1 to PGC-1α was not examined in the present study.

It was recently shown by Li et al., (2007) that signaling to PGC-1α can occur in a FoxO1-independent manner, regulated by Akt2 signaling. At present, this is the only published report to suggest that this level of regulation can occur. These authors demonstrated that after insulin treatment, Akt2 phosphorylates S570 of PGC-1α, thereby inhibiting the activation of PGC-1α and preventing the transcription of genes involved in gluconeogenesis. Certainly then, the reverse should be true; and downregulation of Akt2

would likely increase the activation of PGC-1α, because the mechanism to constrain mitochondrial biogenesis would be absent. In support of this hypothesis, the increased mitochondrial volume in the Akt2-siRNA treated cells was consistent with the upregulated protein expression of PGC-1α. Thus, the findings of the present study further validate the findings by Li et al. (2007), and extend the analysis to incorporate the deregulation of the mechanism after prolonged Akt2 inhibition. Unfortunately, examination of the S570 phosphorylation residue directly was not possible, due to the lack of a commercially available antibody. The data reported here suggest that the apparent increase in the mitochondria in this system was independent of FoxO signaling and rendered by Akt2 regulation. There is accumulating evidence that mitochondrial dysfunction underlies the pathogenesis of diabetes (reviewed in Reznick & Shulman, 2006) and since mitochondrial biogenesis is regulated by insulin signaling pathways it will be very interesting to see what the results of future studies conclude. However, at this time, the role of isoform-specific Akt2 regulation in this process is novel.

Levels of PGC-1α were upregulated in the Akt2 siRNA-treated cells relative to the scrambled controls. However, other mechanisms in addition to the upregulation of PGC-1α may be responsible for the morphological changes observed in the mitochondria of the Akt2-siRNA treatment. Liang et al., (2007) showed that while increases in mitochondrial biogenesis in their study were attributable to their 2-fold upregulation of PGC-1α in their transfected cells, reduced rates of mitochondrial protein degradation, and not *de novo* protein synthesis were also a contributing factor. Even though the half-life of mitochondrial protein degradation was not measured in the present study, downregulated Skp2 in the Akt2 siRNA-treated cells was shown, indicating that protein degradation was compromised in the Akt2-

ablated cells. Since protein synthesis is not occurring, as evidenced by the downregulation of p-p70S6K in this system, this hypothesis may indeed be valid.

While this thesis was in preparation, Finocchietto et al., (2008) published a study demonstrating that insulin signaling in muscle mitochondria is regulated by activated Akt2 and mtNOS (mitochondrial nitric oxide synthase). The results of their study showed that insulin caused the translocation of phosphorylated-Akt2 to the mitochondria thereby regulating mtNOS, and other metabolic parameters, providing evidence of the role of Akt2-regulation of the mitochondria in insulin signaling. According to their model, Akt2-ablation would decrease NOS activity and would lead to increased glucose and oxygen uptake in the mitochondria. In support of this theory, short term inhibition of eNOS in bovine aortic endothelial cells (BAEC) and HUVEC cells caused an initial short-term increase in PGC-1α (24 hours) (Borniquel et al., 2006). It is uncertain whether or not this level of regulation by Akt2 was occurring in the present study and remains to be elucidated. Furthermore, parameters of mitochondrial function such as rates of oxidative phosphorylation, cellular ATP levels and alterations in mitochondrial membrane potential, were not investigated. However, these studies will shed further insight into the physiological significance of the co-localization of Akt2 and the mitochondria and further delineate the potential role of Akt2-mediated mitochondrial regulation.

Mitochondria within cells constantly undergo fusion and fission to ensure that their relative number remains constant. Alterations in either one of these energy states can produce mitochondrial dysfunction (reviewed in Alirol & Martinou, 2006). Recently published findings (Navratil et al., 2008), indicated that inhibition of Class III PI3-Ks by using 3-methyladenine (3-MA), a classical tool used to inhibit autophagy in cells, promoted

the formation of giant mitochondria that could not fuse with one another. It is convenient to speculate that knockdown of Akt2 promotes the formation of giant mitochondria through an imbalance of degradation and increased fusion compared to fission. However, these conditions are favorable only when autophagy is inhibited.

During the process of autophagy, cells sequester organelles into compartments targeted for degradation. Inhibition of mTOR is a well-known regulator of autophagy. Liang et al., (2007) found that the upregulation of p27 alone could also mitigate the decision to enter autophagy. It is still uncertain whether the targeted degradation of the mitochondria promotes cell death through autophagy, or removes or recycles damaged organelles (reviewed in Kim et al., 2007). Regardless, the data included in this thesis are the first to show 1) co-localization of Akt2 to the mitochondria, and 2) knockdown of Akt2 downregulated mTOR activity and promoted mitochondrial degradation by autophagy, or mitophagy. One interesting finding from this study is that the early timepoints examined were associated with mitochondrial biogenesis from 24-72 hours, while at 120-144 hours large accumulations of MDC incorporation in autophagolysosomes were observed. Further, MitoTracker Red staining co-localized with MDC labeling, suggesting that the mitochondria were specifically targeted for autophagy.

The issue of how the uncontrolled increase in mitochondrial volume leads to mitophagy still remains unaddressed, however. Since Akt2 is co-localized with the mitochondria, ablation of Akt2 leads to increased mitochondrial volume. Akt2 is also linked to mTOR through p70S6K and ablation of Akt2 downregulates protein synthesis. The mechanism of Akt2 regulation in this system is thus summarized as follows: In the early timepoints, the mTOR-p70S6K pathway is downregulated and new protein synthesis is limited in Akt2-ablated cells. Under these conditions the usage of proteins would have to be

closely monitored. The uncontrolled mitochondrial biogenesis caused by the inactivation of Akt2-mediated inhibition would use large amounts of proteins. Since uncontrolled growth occurs while protein synthesis is limited, the newly synthesized mitochondria may not have a normal function or structure (Kim et al., 2007). A low level of autophagy may occur in the early stages to eliminate dysfunctional mitochondria. Ultimately, the cells respond in this manner for a short period of time before the system is overwhelmed. If the removal becomes excessive, then pathological mitophagy may occur.

In terms of cancer therapy, selective inhibitors for Akt isoforms have been developed but have not yet reached clinical trials (reviewed in LoPiccolo et al., 2008 and discussed in Chapter 1.3.5). Clinical trials with rapamycin have been shown to effective in some, but not all cancers. Although the sample size was small, O'Reilly et al., (2006) showed that treatment with current rapamycin analogues can activate Akt during treatment due to the negative regulation of p70S6K through IRS. The results of the present study provide evidence that selective inhibition of Akt2, either singularly or in combination with other treatments, may be a viable route for the treatment of breast cancer.

CHAPTER 5.0

GENERAL DISCUSSION

5.0 GENERAL DISCUSSION

5.1 Summary and conclusions

The main objective of the present study was to characterize the Akt isoforms and determine which isoform(s) was the most critical for breast cancer survival. Previously, it was assumed that the Akt isoforms were functionally redundant based on their amino acid sequence similarity, and a propensity for early studies to examine or inhibit all Akt activity. However, in light of recently published studies which have shown that the Akt isoforms may display functional specificity, the studies included within the thesis asked an important question: was one isoform predominantly important for breast cancer survival and progression?

The data obtained from these studies systematically demonstrated that Akt2 was the most important isoform for cell proliferation and survival in the MDA-MB231 breast cancer cell line. A combination of different approaches which analyzed cell survival, cellular proliferation and selective isoform inhibition by siRNA showed that Akt2 is necessary for cancer cell survival. In addition, the data from these studies challenge the previously accepted notions for Akt isoform regulation, by demonstrating differences in preferential substrate specificity (Akt2 to mTOR), survival (Akt2), as well as subcellular localization. These data also suggest that the cellular processes regulated by the Akt isoforms are far more intricate than previously thought.

5.2 Significant findings from the studies and suggestions for future work:

1. The Akt isoforms display differential subcellular localization

The data from the experiments described in Chapter 3.0 demonstrated that Akt1, Akt2 and Akt3 occupy distinct subcellular locations. The localization of Akt1 was mainly

cytoplasmic, while Akt3 was entirely nuclear. Akt2 was localized to the cytoplasm in one of two distinct morphologies: one was perinuclear and the other was a punctate aggregate localized within the cytoplasm. Further analysis demonstrated that Akt2 was co-localized with the mitochondria. Previous studies have shown that pan-Akt may have various functions associated with the mitochondria, including the regulation of apoptosis, and an association with mitochondrial hexokinases. However, this is the first study to show the co-localization of Akt2 to the mitochondria and also demonstrate that it is isoform-specific. Furthermore, the data presented in Chapter 3.0 demonstrate that Akt2 and the mitochondria co-localize in many different types of cancer cells, and that this mitochondrial localization is not specific to breast cancer or MDA-MB231 cells. The fact that Akt2 co-fractionated with the mitochondria suggested that they may be physically associated. Thus, the data shown in Chapters 3.0 and 4.0 together demonstrate that Akt2 regulates some of the functions associated with the mitochondria, including the regulation of mitochondrial biogenesis. Further, the targeted ablation of Akt2 leads to mitochondrial autophagy or mitophagy.

The nuclear localization of Akt3 was reported previously, although the study was carried out using only one cell line and focused on the nuclear import/export properties of Akt1 (Saji et al., 2005). The data presented in this thesis confirm the initial report by Saji et al. (2005), and extend their findings further to other cell lines. Further, the results of these studies also confirm that the localization of Akt3 is not due to translocation from the cytoplasm: Akt3 resides in the nucleus. In fact, this was one of the more interesting findings from these studies. Why is Akt3 localized to the nucleus? Little is known about the regulation and function of Akt3, because, at least in part, Akt3-specific antibodies were not commercially available until very recently. Barnett et al. (2005) made isoform-specific compounds that inhibited both Akt1 and Akt2 by blocking activation or phosphorylation of

these two by inhibiting PDK1. However, neither of these inhibitors was able to inhibit Akt3. Thus, it is possible that Akt3 doesn't function in the same manner as Akt1 and Akt2. The data presented in this thesis suggest that the different subcellular localization of Akt3 may be an important factor in the regulation of Akt3, and suggest that Akt3 may be regulated in a different manner. However, future studies need to examine the mechanisms of Akt3 functioning. The data reported herein suggest that Akt3 may not be a factor in cell proliferation or cell survival in MDA-MB231 cells, which prompts further questions about the function of Akt3. It should be noted that others have reported a negligible role for Akt3 in glucose regulation (Easton et al., 2005). Ultimately the role and regulation of Akt3 and it's localization in the nucleus needs to be examined further.

One surprising result from the studies described in Chapter 3.0 was the observation that the isoforms were steadfast in their subcellular localization. Analysis of changes in the subcellular localization of the Akt isoforms suggested that a compensatory mechanism was not present even when one or more of the isoforms were ablated with isoform-specific siRNA. This conclusion was derived from the observation that the isoforms did not change their location to compensate for the function of the missing isoform. However, changes in the levels of kinase activities or phosphorylation may have occurred, but these were not examined in the current study. It is difficult to discern isoform-specific differences in phosphorylation status as the activation residues are only one amino acid apart in the three Akt isoforms.

When $PI(4,5)P_2$ is converted to $PI(3,4,5)P_3$ by PI3K, Akt translocates from the cytoplasm to the plasma membrane where it is phosphorylated and subsequently activated (see Fig. 1.2, Chapter 1.0 for a schematic of the proposed model of Akt activation and regulation). Given that all three isoforms share the same activating residues (T308/S473 for

Akt1, T309/S474 for Akt2 and T305/S472 for Akt3), this model is widely accepted as the functional model for the different Akt isoforms. However, this model is only applicable if all three isoforms are localized within the cytoplasm. The data in this thesis show that Akt1 is localized within cytoplasm. In contrast, Akt2 was co-localized with the mitochondria, while Akt3 was primarily localized within the nucleus. The different localizations of both Akt2 and Akt3 suggest that the widely accepted model of Akt regulation is most likely that of Akt1. The localization of both Akt2 and Akt3 question whether these isoforms are phosphorylated and activated at the plasma membrane, according to what is known for pan-Akt, or Akt1.

The finding that neither Akt2, nor Akt3 shared a classical targeting sequence (to the mitochondria and nucleus respectively) requires further investigation, but suggests that the localization may be due to protein-protein interactions. Future studies using mass spectrometry to identify protein interactions may assist in uncovering binding proteins that may either anchor or localize Akt2 to the mitochondria and Akt3 within the nucleus. In addition, sequence mapping using various deletion constructs for both Akt2 and Akt3 may define the region(s) involved in the targeting of the unique localization observed for these isoforms.

Ultimately, functional studies assessing the activation of both Akt2 and Akt3 need to be conducted in order to determine if (1) they are activated in accordance with the widely accepted model of activation, or (2) if they are activated primarily within the mitochondria and nucleus for Akt2 and Akt3, respectively. Bijur and Jope (2003) found pan-Akt within the mitochondria (inner and outer mitochondrial membranes) was activated when treated with IGF-1. The authors hypothesized that selective uptake of Akt into the mitochondria occurred; however the mechanisms as to how this was regulated were not investigated. Saji et al., (2005) identified a leucine-rich region within Akt1 that could act as a nuclear export

sequence (NES). When the sequence within this region was altered using mutation constructs, Akt1 showed reduced interactions with CRM-1, a nuclear export protein, and thus, Akt1 remained localized within the nucleus. However, a rebuttal publication by Wang and Brattain (2006), found that Akt did not have a nuclear export sequence. Further, more than one region/segment of Akt was required for translocation into the nucleus. The authors concluded that the observed translocation of pan-Akt into the nucleus ultimately resided in protein-protein interactions, or alternatively, was determined by the conformation of Akt (Wang and Brattain, 2006). Further, these authors noted a nuclear localization of Akt in the cell lines used in their study (the Akt antibody used in their study however, B1 from Santa Cruz, was cross-reactive with all three isoforms). After treatment of cells with IGF-1, they found activated Akt within their nuclear extracts, suggesting that Akt was activated within the nucleus, and not translocated from the cytoplasm. The finding that Akt could be activated within the nucleus, suggests that the proposed regulation of Akt needs further investigation. If the results of their study are extended and interpolated with the results obtained in Chapter 3.0 of this thesis, it suggests that Akt3, which was found primarily localized within the nucleus and nuclear membrane can be phosphorylated and activated there.

The data shown in this study suggest that ultimately the structure and location of the isoforms must play a role in dictating their function; so much so that the other isoforms do not move in response to forced downregulation using targeted siRNA, treatment with X-rays or stimulation with growth factors. Although stimulation with growth factors or X-ray irradiation may have produced more changes in the levels of activated Akt, this is the first study to show that the isoforms do not alter their localization in response to this stimulation. Nevertheless, small changes were observed. For example, higher levels of Akt1 were found in the nucleus after both treatments which is consistent with previous reports that

phosphorylated Akt translocates into the nucleus, suggesting that the observed translocation is isoform-specific (Andjelkovic et al., 1997; Borgatti et al., 2000; Borgatti et al., 2003; Das et al., 2007; Xuan Nguyen et al., 2006). However, this also adds another level of complexity in the regulation of Akt signaling.

This is the first systematic study to examine the subcellular localization status of the Akt isoforms. Further, these results have been verified by in vitro experimentation (i.e., the immunofluorescence experiments both supported and confirmed the fractionation experiments).

2. Akt2 regulates cell proliferation and cell survival.

The data shown in Chapter 3.0 were critical for the rest of the experiments described in the thesis. The data from those experiments led to the establishment of methods to effectively evaluate the isoforms. More importantly, the results from those experiments provided the initial impetus to examine both Akt2 and the mitochondria in the studies described in Chapter 4.0. Thus, once the differential localization of the isoforms was determined and the methods to be able to evaluate the isoforms were established, the functional analysis of the isoforms was possible. In the first part of Chapter 4.0, the isoforms were examined after targeted ablation using siRNA to determine if one or more of the isoforms regulated both cell proliferation and/or cell survival. The results of the study revealed that Akt2 was critical for cell proliferation. More surprising was the fact that the combined ablation of two isoforms was not more effective in cell killing than the ablation of Akt2 alone. Examining both proliferation and cell survival in this study was critical: the results from both studies implicated Akt2 as the most relevant cancer target to focus on. Performing the survival assays alone would have led to the conclusion that Akt2 was most

relevant for cell survival; however it would not have been able to elucidate the mechanism, or the manner of cell death. It should be noted that targeted ablation using siRNA reduced cell proliferation in all three Akt isoforms, although not to the extent observed with Akt2 ablation. This finding alone is extremely important since the data clearly shows that Akt2 is the most important Akt isoform for cell survival in MDA-MB231 breast cancer cells. Not only did this finding demonstrate isoform-specificity and regulation, but it provides further evidence for the development of more specific Akt-targeted cancer treatments.

3. Targeted ablation of Akt2 induces autophagy of the mitochondria through the upregulation of p27 and downregulation of p70S6K, Cdk2 and cyclin D.

The initial results from the analysis of cell survival and proliferation in the Akt2-siRNA treated cells led to the elucidation of the cellular mechanisms regulated by Akt2. That is, Akt2 ablation resulted in the inhibition of cell proliferation by upregulating p27 and downregulating both Cdk2 and cyclin D. The combined effects of this strategically arrested the cells in G0/G1. Previous studies had demonstrated that Akt could regulate p27 on many levels: 1) p27 could be post-translationally regulated by Akt via phosphorylation on two Akt-specific residues, T157 and T198. Akt could also transcriptionally regulate the level of p27 through alteration in the phosphorylation status of FoxO1, or overexpression of non-phosphorylated FoxOs. Further, mTOR could also upregulate p27. The results from this study are the first to elucidate an isoform-specific role for Akt regulation in this process i.e., that the targeted downregulation of Akt2 and not Akt1 or Akt3, leads to the transcriptional upregulation of p27 in breast cancer cells. This result was initially surprising, as most documented Akt regulation of p27 occurred via phosphorylation and second, that the mechanism was isoform-specific.

It was found that Akt2 preferentially regulated mTOR signaling as demonstrated by the downregulation of phosphorylated p70S6K in the Akt2 ablated cells. This finding raises the possibility that each isoform may function on unique downstream targets. Thus, having the PAS motif (phospho-Akt motif, RXRXX(S/T) does not confer definitive regulation by all Akt isoforms. The fact that well-known Akt targets such as GSK-3 and FoxO were unaltered after the Akt2 ablation, further strengthens this argument.

With respect to cancer treatment, however, the data presented in this thesis provide support for targeting the mTOR pathway, particularly in aggressive breast cancers. Currently, rapamycin-like derivatives (or rapalogues) are in clinical trials. One caveat to inhibiting this pathway, however, is the presence of the feedback loop from p70S6K to the insulin receptor, which constitutively activates Akt signaling, thereby, making the cancers more resistant to therapy (O'Reilly et al., 2006). Thus, if Akt2 signaling is the preferential upstream substrate to mTOR treatment, the results from this study provide further support for the continued pursuance of the mTOR pathway as targeted treatment. However, if efficient and specific Akt2 inhibitors were used, thereby, targeting the proliferating cancer cells by acting on mTOR activity, the feedback loop may potentially be circumvented.

4. Prolonged downregulation of Akt2 induced autophagy of the mitochondria.

The co-localization of Akt2 and the mitochondria in this thesis was a novel finding. This finding is very significant, since it implies that Akt2 is associated with the regulation of the mitochondria. However, it has also opened the door to many new questions. Akt can regulate many of the same functions as the mitochondria—mainly, aspects of cell survival and metabolism, and as indicated in the study can also regulate mitochondrial biogenesis. Akt-mediated mitochondrial biogenesis has previously been shown to be regulated through

insulin signaling downstream to FoxO1. However, another level of regulation was recently shown, where Akt2 could phosphorylate and inhibit mitochondrial biogenesis via a phosphorylation site at S570 on PGC-1α, the master regulator of mitochondrial biogenesis (Li et al., 2007). Therefore, the downregulation of Akt2 would lead to deregulation of this pathway. Thus, the results of this study confirm those of Li et al., (2007) and extend it further by determining what happens if this process is uncontrolled in cancer cells.

The process of mitophagy is still not well understood and various models have been proposed to explain why it occurs. It is known that it exists to remove dysfunctional or damaged mitochondria (Kim et al., 2007). Further, mitophagy is known to occur under conditions of severe nutrient deprivation. Thus, the regulation of Akt2, its subcellular localization, and the functional role that Akt2 plays in glucose transport are functionally linked with the mitochondria. Without a doubt, the significance of the mitochondria-Akt2 interaction is multifactorial and needs further investigation. Furthermore, the specific mechanism of Akt2 in cancer cell metabolism needs to be further clarified. The results of this study are significant in that it is the first to show that Akt2 is localized to the mitochondria. Further, Akt2-ablation deregulates mitochondrial metabolism by inhibiting mitochondrial biogenesis, which extends the results of a previous study. Lastly, this is the first study to show that Akt2 ablation resulted in the loss of mitochondrial homeostasis, leading to the autophagy of the mitochondria.

The fact that Akt2 is associated with the mitochondria and regulates certain aspects of its functions is novel. However, much work needs to be continued to determine the exact mechanisms at play. The data presented in this thesis may also shed new light on the regulation of glucose metabolism in diabetes via Akt2-specific signaling. However, the

question remains: if loss of Akt2 in knockout mice causes insulin resistance then how can this be beneficial in terms of cancer treatment? Both LoPiccolo et al. (2007) and Bayascas et al. (2008) speculate that the side effects acquired by Akt2 inhibition (insulin resistance) may be treatable during a cancer treatment, providing that the inhibition is not long-term. While this is purely speculative, it is a worthwhile point to consider: if the *in vitro* studies on insulin regulation showed that Akt1 could compensate for some of the glucose regulation, then the targeted inhibition of Akt2 may not be as problematic as what has been seen in treatment for Akt inhibitors that inhibit all Akt function and activity. Nonetheless, much knowledge needs to be learned regarding Akt2 function.

5.3 Summary

An ideal cancer therapeutic treatment would exhibit specificity towards cancer cells while having little impact on normal cell function. The data shown in the thesis were designed to specifically examine Akt isoform regulation in breast cancer. However, the results of these studies need to be extended further to normal cells to determine if targeted inhibition of Akt2, exhibits preferential specificity towards constantly proliferating cancer cells. The data from these studies have provided insight that Akt2 is most important to target in breast cancer. Further, the results from these studies have also shown the mechanisms through which Akt2 regulates cancer proliferation, as well as the mode of cell death when inhibited. The current challenge is to develop effective and efficient therapeutics that would target Akt2 and minimize the off-target effects observed with pan-Akt inhibition.

6.0 REFERENCES

Ackah, E., Yu, J., Zoellner, S., Iwakiri, Y., Skurk, C., Shibata, R., Ouchi N., Easton, R.M., Galasso, G., Birnbaum, M.J., Walsh, K., and Sessa, W.C. (2005). Akt1/protein kinase Bα is critical for ischemic and VEGF-mediated angiogenesis. J Clin. Invest *115*, 2119-2127.

Aguilar, V., Alliouachene, S., Sotiropoulos, A., Sobering, A., Athea, Y., Djouadi, F., Miraux, S., Thiaudiere, E., Foretz, M., Viollet, B., Diolez, P., Bastin, J., Benit, P., Rustin, P, Carling, D., Sandri, M., Ventura-Clapier, R., and Pende, M. (2007). S6 kinase deletion suppresses muscle growth adaptations to nutrient availability by activating AMP kinase. Cell Metab *5*, 476-487.

Ahmad, S., Singh, N., and Glazer, R.I. (1999). Role of AKT1 in 17β-estradiol and insulin-like growth factor I (IGF-I)-dependent proliferation and prevention of apoptosis in MCF-7 breast carcinoma cells. Biochem Pharmacol. *58*, 425-430.

Alessi D.R., Andjelkovic, M., Caudwell, B., Cron, P., Morrice, N., Cohen, P., and Hemmings, B.A. (1996). Mechanism of activation of protein kinase B by insulin and IGF-1. EMBO J. *15*, 6541-6551.

Alirol, E., and Martinou, J.C. (2006). Mitochondria and cancer: is there a morphological connection? Oncogene 25, 4706-4716.

Altomare, D.A., Lyons, G.E., Mitsuuchi, Y., Cheng, J.Q., and Testa, J.R. (1998). Akt2 mRNA is highly expressed in embryonic brown fat and the Akt2 kinase is activated by insulin. Oncogene *16*, 2407-2411.

Altomare, D.A., Tanno, S., De Rienzo, A., Klein-Szanto, A.J., Tanno, S., Skele, K.L., Hoffman, J.P., and Testa, J.R. (2002). Frequent activation of Akt2 kinase in human pancreatic carcinomas. J Cell Biochem *87*, 470-476.

Andjelkovic, M., Alessi, D.R., Meier, R., Fernandez, A., Lamb, N.J.C., Frech, M., Cron, P., Cohen, P., Lucocq, J.M., and Hemmings, B.A. (1997). Role of translocation in the activation and function of protein kinase B. J Biol Chem *272*, 31515-31524.

Arboleda M.J., Lyons, J.F., Kabbinavar, F.F., Bray, M.R., Snow, B.E., Ayala, R., Danino, M., Karlan, B.Y., and Slamon, D.J. (2003). Overexpression of Akt2/Protein kinase Bβ leads to up-regulation of β1 integrins, increased invasion, and metastasis of human breast and ovarian cancer cells. Cancer Res. *63*, 196-206.

Bacqueville, D., Casagrande, F., Perret, B., Chap, H., Darbon, J.M., and Breton-Douillon, M. (1998). Phosphatidylinositol 3-kinase inhibitors block aortic smooth muscle cell proliferation in mid-late G1 phase: effect on cyclin-dependent kinase 2 and the inhibitory protein p27KIP1. Biochem Biophys Res Commun *244*, 630-636.

Bacus, S.S., Altomare, D.A., Lyass, L., Chin, D.M., Farrell, M.P., Gurova, K., Gudkov, A., and Testa, J.R. (2002). Akt2 is frequently upregulated in Her-2/neu-positive breast cancers and may contribute to tumor aggressiveness by enhancing cell survival. Oncogene *21*, 3532-3540.

Bae, S.S., Cho, H., Mu, J., and Birnbaum, M.J. (2003). Isoform-specific regulation of insulin-dependent glucose uptake by Akt/Protein kinase B. J Biol Chem *278*, 49530-49536.

Balendran, A., Casamayor, A., Deak, M., Paterson, A., Gaffney, P., Currie, R., Downes, C.P., and Alessi, D.R. (1999). PDK1 acquires PDK2 activity in the presence of a synthetic peptide derived from the carboxyl terminus of PDK1. Curr Biol *9*, 393-404.

Barnett, S.F., deFeo-Jones, D., Fu., S., Hancock, P.J., Haskell, K.M., Jones, R.E., Kahana, J.A., Kral, A.M., Leander, K., Lee, L.L., Malinowski, J., McAvoy, E.M., Nahas, D.D., Robinson, R.G., and Huber, H.E. (2005). Identification and characterization of pleckstrin-homology-domain-dependent and isoenzyme-specific Akt inhibitors. Biochem J *385*, 399-408.

Bellacosa, A., De Feo, D., Godwin, A.K., Bell, D.W., Cheng, J.Q., Altomare, D.A., Wan, M., Dubeau, L., Scambia, G., Masciullo, V., Ferrandina, G., Benedetti Panici, P., Mancuso, S., Neri, G., and Testa, J.R. (1995). Molecular alterations of the AKT2 oncogene in ovarian and breast carcinoma. Int J Cancer *64*, 280-285.

Bellacosa, A., Testa, J.R., Moore, R., and Larue, L. (2004). A portrait of AKT kinases: human cancer and animal models depict a family with strong individualities. Cancer Biol Ther *3*, 268-275.

Bellacosa, A., Kumar, C.C., Di Cristofano, A., and Testa, J.R. (2005). Activation of AKT kinases in cancer: implications for therapeutic targeting. Adv Cancer Res *94*, 29-86.

Burgering, B.M.T., and Kops, G.J.P.L. (2002). Cell cycle and death control: long live Forkheads. Trends in Biochem Sciences *27*(7), 352-360.

Bijur, G.N., and Jope, R.S. (2003). Rapid accumulation of Akt in mitochondria following phosphatidylinositol 3-kinase activation. J Neurochem *87*, 1427-1435.

Bloethner, S., Chen, B., Hemminki, K., Muller-Berghaus, J., Ugurel, S., Schadendorf, D., and Kumar, R. (2005). Effect of common B-RAF and N-RAS mutations on global gene expression in melanoma cell lines. Carcniogenesis *26*, 1224-1232.

Borgatti, P., Martelli, A.M., Bellacosa, A., Casto, R., Massari, L., Capitani, S., and Neri, L.M. (2000). Translocation of Akt/PKB to the nucleus of osteoblast-like MC3T3-E1 cells exposed to proliferative growth factors. FEBS Lett *477*, 27-32.

Borgatti P., Martelli, A.M., Tabellini, G., Bellacosa, A., Capitani, S., and Neri, L.M. (2003). Threonine 308 phosphorylated form of Akt translocates to the nucleus of PC12 cells under

nerve growth factor stimulation and associates with the nuclear matrix protein nucleolin. J Cell Physiol *196*, 79-88.

Borniquel, S., Valle, I., Cadenas, S., Lamas, S., and Monsalve, M. (2006). Nitric oxide regulates mitochondrial oxidative stress protection via the transcriptional coactivator PGC-1α. FASEB J *20*, 1889-1891.

Bouzakri, K., Zachrisson, A., A-Khalili, L., Zhang, B.B., Koistinen, H.A., Krook, A., and Zierath, J.R. (2006). siRNA-based gene silencing reveals specialized roles of IRS-1/Akt2 and IRS-2/Akt1 in glucose and lipid metabolism in human skeletal muscle. Cell Metab *4*, 89-96.

Brameier, M., Krings, A., Maccallum, R.M. (2007). NucPred—predicting nuclear localization of proteins. Bioinfomatics *23*, 1159-1160.

Brodbeck, D, Cron, P., and Hemmings, B.A. (1999). A human protein kinase Bγ with regulatory phosphorylation sites in the activation loop and in the C-terminal hydrophobic domain. J Biol Chem, *274*, 9133-9136.

Brodbeck, D., Hill, M.M., and Hemmings, B.A. (2001). Two splice variants of protein kinase Bγ have different regulatory capacity depending on the presence or absence of the regulatory phosphorylation site serine 472 in the carboxyl-terminal hydrophobic domain. J Biol Chem *276*, 29550-29558.

Brognard, J., Sierecki, E., Gao, T., and Newton, A.C. (2007). PHLPP and a second isoform, PHLPP2, differentially attenuate the amplitude of Akt signaling by regulating distinct Akt isoforms. Mol Cell *25*, 917-931.

Bruzek, L.M., Poynter, J.N., Kaufmann, S.H., and Adjei, A.A. (2005). Characterization of a human carcinoma cell line selected for resistance to the farnesyl transferase inhibitor 4-(2-(4-(8-chloro-3,10-dibromo-6,11-dihydro-5*H*-benzo-(5,6)-cyclohepta(1,2-*b*)-pyridin-11(*R*)-yl)-1-piperidinyl)-2-oxo-ethyl)-1-piperidinecarboxamide (SCH66336). Mol Pharmacol 68, 477-486.

Caldon, C.E., Daly, R.J., Sutherland, R.L., and Musgrove, E.A. (2006). Cell cycle control in breast cancer cells. J Cell Biochem *97*, 261-274.

Calera, M.R., Martinez, C., Liu, H., El Jack, A.K., Birnbaum, M.J., and Pilch, P.F. (1998). Insulin increases the association of Akt-2 with Glut4-containing vesicles. J Biol Chem *273*, 7201-7204.

Calera, M.R., and Pilch, P.F. (1998). Induction of Akt-2 correlates with differentiation in Sol8 muscle cells. Biochem Biophys Res Commun *251*, 835-841.

Carpten, J.D., Faber, A.L., Horn, C., Donoho, G.P., Briggs, S.L., Robbins, C.M., Hostetter, G., Boguslawski, S., Moses, T.Y., Savage, S., Uhlik, M., Lin, A., Du, J., Qian, Y.W., Zeckner, D.J., Tucker-Kellogg, G., Touchman, J., Patel, K., Mousses, S., Bittner, M.,

Schevitz, R., Lai, M.H.T., Blanchard, K.L., and Thomas, J.E. (2007). A transforming mutation in the pleckstrin homology domain of Akt1 in cancer. Nature 448, 439-444.

Chen, W.S., Xu, P.Z., Gottlob, K., Chen, M.L., Sokol, K., Shiyanova, T., Roninson, I., Wang, W., Suzuki, R., Tobe, K., Kadowaki, T., and Hay, N. (2001). Growth retardation and increased apoptosis in mice with homozygous disruption of the *akt1* gene. Genes Dev *15*, 2203-2208.

Cheng, J.Q., Godwin, A.K., Bellacosa, A., Taguchi, T., Franke, T.F., Hamilton, T.C., Tsichlis, P.N., and Testa, J.R. (1992). AKT2, a putative oncogene encoding a member of a subfamily of protein-serine/threonine kinases, is amplified in human ovarian carcinomas. Proc Natl Acad Sci USA *89*, 9367-9271.

Cheng, J.Q., Ruggeri, B., Klein, W.M., Sonoda, G., Altomare, D.A., Watson, D.K., and Testa, J.R. (1996). Amplification of AKT2 in human pancreatic cancer cells and inhibition of AKT2 expression and tumorigenicity by antisense RNA. Proc Natl Sci USA *93*, 3636-3641.

Cheng, J.Q., Altomare, D.A., Klein, M.A., Lee, W.C. Kruh, G.D., Lissy, N.A., and Testa, J.R. (1997). Transforming activity and mitosis-related expression of the Akt2 oncogene: evidence suggesting a link between cell cycle regulation and oncogenesis. Oncogene *14*, 2793-2801.

Cheung, M., Sharma, A., Madhunapantula, S.V., and Robertson, G.P. (2008). Akt3 and mutant ^{V600EB}-Raf cooperate to promote early melanoma development. Cancer Res *68*, 3429-3439.

Cho, H., Mu, J., Kim, J.K., Thorvaldsen, J.L., Chu, Q., Crenshaw, E. B., Kaestner, K.H., Bartolomei, M.S., Shulman, G.I., and Birnbaum, M.J. (2001a). Insulin resistance and a diabetes mellitus-like syndrome in mice lacking the protein kinase Akt2 (PKBβ). Science *292*, 1728-1731.

Cho, H., Thorvaldsen, J.K., Chu, Q., Feng, F., and Birnbaum, M.J. (2001b). Akt/PKBα is required for normal growth but dispensable for maintenance of glucose homeostasis in mice. J Biol Chem *276*, 38349-38352.

Claros, M.G., and Vicens, P. (1996). Computational method to predict mitochondrially imported proteins and their targeting sequences. Eur J Biochem *241*, 770-786.

Coffer P.J., and Woodgett, J.R. (1991). Molecular cloning and characterization of a novel putative protein-serine kinase related to the cAMP-dependent and protein kinase C families. Eur J Biochem *201*:475-481

Coffer, P.J., Jin, J., and Woodgett, J.R. (1998). Protein kinase B (c-Akt): a multifunctional mediator of phosphatidylinositol 3-kinase activation. Biochem J *335*, 1-13.

Cokol, M., Nair, R., and Rost, B. (2000). Finding nuclear localization signals. EMBO Reports 1:411-415.

Corradetti, M.N., Inoki, K., Bardeesy, N., DePinho, R.A., and Guan, K.L. (2004). Regulation of the TSC pathway by LKB1: evidence of a molecular link between tuberous sclerosis complex and Peutz-Jeghers syndrome. Genes Dev *18*, 1533-1538.

Cristiano B.E., Chan, J.C., Hannan, K.M., Lundie, N.A., Marmy-Conus, N.J., Campbell, I.G., Phillips, W.A., Robbie, M., Hannan, R.D., and Pearson, R.B. (2006). A specific role for AKT3 in the genesis of ovarian cancer through modulation of G_2-M phase transition. Cancer Res *66*, 11718-25.

Cunningham, J.T., Rodgers, J.T., ARlow, D.H., Vazquez, F., Mootha, V.K., and Puigserver, P. (2007). mTOR controls mitochondrial oxidative function through a YY1-PGC-1α transcriptional complex. Nature 29, 736-740.

Cushman, S.W., and Wardzala, L.J. (1980). Potential mechanism of insulin action on glucose transport in the isolated rat adipose cell. J Biol Chem *255*, 4758-4762.

Das, F., Mahimainathan, L., Ghoush-Choudhury, N, Venkatesan, B., Kasinath, B.S., Abboud, H.E., Ghosh Choudhury G. (2007). TGFβ intercepts nuclear glycogen synthase kinase-3β to inhibit PDGF-induced DNA synthesis in mesangial cells. FEBS Lett *581*, 5259-5267.

Davies, M.A., Stemke-Hale, K., Tellez, C., Calderone, T.L., Deng, W., Prieto, V.G., Lazar, A.J.F., Gershenwald, J.E., and Mills, G.B. (2008). A novel AKT3 mutation in melanoma tumours and cell lines. Br J Cancer *99*, 1265-1268.

deFeo-Jones, D., Barnett, S.F., Fu, S., Hancock, P.J., Haskell, K.M., Leander, K.R., McAvoy, E., Robinson, R.G., Duggan, M.E., Lindsley, C.W., Zhao,Z., Huber, H.E., and Jones, R.E. (2005). Tumor cell sensitization to apoptotic stimuli by selective inhibition of specific Akt/PKB family members. Mol Cancer Ther 4, 271-279.

Dowling, R.J., Zakikhani, M., Fantus, I.G., Pollak, M., and Sonenberg, N. (2007). Metformin inhibits mammalian target of rapamycin-dependent translation initiation in breast cancer cells. Cancer Res *67*, 10804-10812.

Dugani, C.B., Randhawa, V.K., Cheng, A.W.P., Patel, N., and Klip, A. (2008). Selective regulation of the perinuclear distribution of glucose transporter 4 (GLUT4) by insulin signals in muscle cells. Eur J Cell Biol *87*, 337-351.

Dummler, B., Tschopp, O., Hynx, D., Yang, Z.Z., Dirnhofer, S., and Hemmings, B.A. (2006). Life with a single isoform of Akt: Mice lacking Akt2 and Akt3 are viable but display impaired glucose homeostasis and growth deficiencies. Mol Cell Biol *26*, 8042-8051.

Easton, R.M., Cho, H., Roovers, K., Shineman, D.W., Mizrahi, M., Forman, M.S., Lee, V.M.Y., Szabolcs, M., de Jong, R., Oltersdorf, T., Ludwig, T., Efstratiadis, A., and Birbaum, M.J. (2005). Role for Akt3/Protein kinase Bγ in attainment of normal brain size. Mol Cell Biol *25*, 1869-1878.

Emanuelsson, O., Brunek, S., von Heijne, G., and Nielson, H. (2007). Locating proteins in the cell using TargetP, SignalP and related tools. Nature Protocols *2*, 953-971.

Eto, I. (2006). Nutritional and chemopreventive anti-cancer agents up-regulate expression of p27Kip1, a cyclin-dependent kinase inhibitor, in mouse JB6 epidermal and human MCF7, MDA-MB-321 and AU565 breast cancer cells. Cancer Cell Int *9*, 6-20.

Faridi, J., Wang, L., Endemann, G., and Roth, R.A. (2003a). Expression of constitutively active Akt-3 in MCF-7 breast cancer cells reverses the estrogen and tamoxifen responsivity of these cells i*n vivo*. Clin Cancer Res *9*, 2933-2939.

Feng, J., Park, J., Cron, P., Hess, D., and Hemmings, B.A. (2004). Identification of a PKB/Akt hydrophobic motif Ser-473 kinase as DNA-dependent protein kinase. J Biol Chem *279*, 41189-41196.

Finocchietto, P., Barreyro, F., Holod, S., Peralta, J., Franco, M.C., Mendez, C., Converso, D.P., Estevez, A., Carreras, M.C., and Poderoso, J.J. (2008). Control of muscle mitochondria by insulin entails activation of Akt2-mtNOS pathway: Implications for the metabolic syndrome. PLoS One 3, e1749-e1749.

Fujita, N., Sato, S., Katayama, K., Tsuruo, T. (2002). Akt-dependent phosphorylation of p27Kip1 promotes binding to 14-3-3 and cytoplasmic localization. J Biol Chem *277*, 28706-28713.

Fujiwara, K., Iwado, E., Mills, G.B., Sawaya, R., Kondo, S., Kondo, Y. (2007). Akt inhibitor shows anticancer and radiosensitizing effects on malignant glioma cells by inducing autophagy. Int J Oncol *31*, 753-760.

Gao, N., Flynn, D.C., Zhang, Z., Zhong, X.S., Walker, V., Liu, K.J., Shi, X., and Jiang, B.H. (2004). G1 cell cycle progression and the expression of G1 cyclins are regulated by PI3K/Akt/mTOR/p70S6K1 signaling in human ovarian cancer cells. Am J Physiol Cell Physiol *287*, C281-C291.

Garofalo, R.S., Orena, S.J., Rafidi, K., Torchia, A.J., Stock, J.L., Hildebrandt, A.L., Coskran, T., Black, S.C., Brees, D.J., Wicks, J.R., McNeish, J.D., and Coleman, K.G. (2003). Severe diabetes, age-dependent loss of adipose tissue, and mild growth deficiency in mice lacking Akt2/PKBβ. J Clin Invest *112*, 197-208.

Glaros, S., Atanaskova, N., Zhao, C., Skafar, D.F., and Reddy, K.B. (2006). Activation fuction-1 domain of estrogen receptor regulates the agonisitic and antagonistic actions of tamoxifen. Mol Endocrinol *20*:996-1008.

Gottlob, K., Majewski, N., Kennedy, S., Kandel, E., Robey, R.B., and Hay, N. (2001). Inhibition of early apoptotic events by Akt/PKB is dependent on the first committed step of glycolysis and mitochondrial hexokinase. Genes Dev 15, 1406-1418.

Hahn-Windgassen, A., Nogueira, V., Chen, C.C., Skeen, J.E., Sonenberg, N., and Hay, N. (2005). Akt activates the mammalian target of rapamycin by regulating cellular ATP level and AMPK activity. J Biol Chem *280* 32081-32089.

Harrington, L.S., Findlay, G.M., and Lamb, R.F. (2005). Restraining PI3K: mTOR signaling goes back to the membrane. Trends Biochem Sci *30*, 35-42.

Hartnett, J.C., Barnett, S.F., Bilodeau, M.T., Defeo-Jones, D., Hartman, G.D., Huber, H.E., Jones, R.E., Kral, A.M., Robinson, R.G., and Wu, Z. (2008). Optimization of 2,3,5-trisubstituted pyridine derivatives as potent allosteric Akt1 and Akt2 inhibitors. Bioorg Med Chem Lett. *18*, 2194-2197.

Hembruff, S.L., Villeneuve, D.J., and Parissenti, A.M. (2005). The optimization of quantitative reverse transcription PCR for verification of cDNA microarray data. Anal Biochem *345*, 237-249.

Hennessy, B.T., Smith, D.L., Ram, P.T., Lu, Y., and Mills, G.B. (2005). Exploiting the PI3K/Akt pathway for cancer drug discovery. Nat Rev Drug Discov *4*, 988-1004.

Heron-Milhavet, L., Franckhauser, C., Rana, V., Berthenet, C., Fisher D., Hemmings, B.A., Fernandez, A., and Lamb, N.J. (2006). Only Akt1 is required for proliferation while Akt2 promotes cell cycle exit through p21 binding. Mol Cell Biol *26,* 8267-8280.

Hill, M.M., Clark, S.F., Tucker, D.F., Birnbaum, M.J., James, D.E., and Macaulay, S.L. (1999). A role for protein kinase Bβ/Akt2 in insulin-stimulated GLUT4 translocation in adipocytes. Mol Cell Biol 19, 7771-7781

Howells, LM., Gallacher-Horely, B., Houghton C.E., Manson, M.M., and Hudson, E.A. (2002). Indole-3-carbinol inhibits protein kinase B/Akt and induces apoptosis in the human breast tumour cell line MDA-MB468 but not in the nontumorigenic HBL100 line. Mol Cancer Ther *1(13)*, 1161-72

Hresko, R.C., and Mueckler, M. (2005). mTOR-Rictor is the Ser^{473} kinase for Akt/Protein kinase B in 3T3-L1 adipocytes. J Biol Chem *280*, 40406-40416.

Huang, X., Begley, M., Morgenstern, K.A., Gu, Y., Rose, P., Zhao, H., and Zhu, X. (2003). Crystal structure of an inactive Akt2 kinase domain. Structure *11*, 21-30.

Hurley, R.L., Anderson, K.A., Franzone, J.M., Kemp, B.E., Means, A.R., and Witters, L.A. (2005). The Ca^{2+}/Calmodulin-dependent protein kinase kinases are AMP-activated protein kinase kinases. J Biol Chem *280*, 29060-29066.

Hwang, H.C. and Clurman, B.E. (2005). Cyclin E in normal and neoplastic cells. Oncogene *24*, 2776-2786.

Jiang, Z.Y., Zhou, Q.L., Coleman, K.A., Chouinard, M, Boese, Q., and Czech, M.P. (2003). Insulin signaling through Akt/protein kinase B analyzed by small interfering RNA-mediated gene silencing. PNAS *100*, 7569-7574.

Jin, J., and Woodgett, J.R. (2005). Chronic activation of protein kinase Bβ/Akt2 leads to multinucleation and cell fusion in human epithelial cells: events associated with tumorigenesis. Oncogene *24*, 5459-5470.

Jones, P.F., Jakubowicz T., Pitossi F.J., Maurer F., and Hemmings, B.A. (1991). Molecular cloning and identification of a serine/threonine protein kinase of the second-messenger subfamily. Proc Natl Acad Sci USA *88*, 4171-4175.

Katome, T., Obata, T., Matsushima, R., Masuyama, N., Cantley, L.C., Gotoh, Y., Kishi, K., Shiota, H., and Ebina, Y. (2003). Use of RNA interference-mediated gene silencing and adenoviral overexpression to elucidate the roles of Akt/Protein kinase B isoforms in insulin actions. J Biol Chem *278*, 28312-28323.

KC, S., Carcamo, J.M., and Golde, D.W. (2005). Vitamin C enters mitochondria via facilitative gluocose transporter 1 (Glut1) and confers mitochondrial protection against oxidative injury. FASEB *19*, 1657-1667.

Kim E.H., Sohn, S., Kwon, H.J., Kim, S.U., Kim, M., Lee, S., and Choi, K.S. (2007). Sodium-selenite induces superoxide-mediated mitochondrial damage and subsequent autophagic cell death in malignant glioma cells. Cancer Res *67*, 6314-6324.

Kim, I., Rodriguez-Enriquez, S., and Lemasters, J.J. (2007). Selective degradation of mitochondria by mitophagy. Arch Biochem Biophys *462*, 245-253.

Kossatz, U., Vervoorts, J., Nickeleit, I., Sundberg, H.A., Arthur, J.S.C., Manns, M.P., and Malek, N.P. (2006). C-terminal phosphorylation controls the stability and function of p27Kip1. EMBO J *25*, 5159-5170.

Kumar, C.C., and Madison, V. (2005). AKT crystal structure and AKT-specific inhibitors. Oncogene *24*, 7493-7501.

Kuo, P., Hsu, Y., and Cho, C. (2006). Plumbagin induces G_2-M arrest and autophagy by inhibiting the AKT/mammalian target of rapamycin pathway in breast cancer cells. Mol Cancer Ther *5*, 3209-3221.

Kupriyanova, T.A., and Kandror, K.V. (1999). Akt-2 binds to Glut4-containing vesicles and phosphorylates their component proteins in response to insulin. J Biol Chem *274*, 1458-1464.

Li., X., Monks, B., Ge, Q., and Birnbaum, M.J. (2007). Akt/PKB regulates hepatic metabolism by directly inhibiting PGC-1α transcription coactivator. Nature *447*, 1012-1016.

Li, X., Lu, Y., Liang, K., Liu, B., and Fan, Z. (2005). Differential responses to doxorubicin-induced phosphorylation and activation of Akt in human breast cancer cells. Breast Cancer Res *7*, R589-R597.

Liang, H., and Ward, W.F. (2006). PGC-1α: a key regulator of energy metabolism. Adv Physiol Educ 30, 145-151.

Liang, H., Bai, Y., Li, Y., Richardson, A., and Ward, W.F. (2007). PGC-1*a*-induced mitochondrial alterations in 3T3 fibroblast cells. Ann NY Acad Sci *1100*, 264-279.

Liang, J., Zubovitz, J., Petrocelli, T., Kotchetkov, R., Connor, M.K., Han, K., Lee, J.H., Ciarallo, S., Catzavelos, C., Beniston, R., Franssen, E., and Slingerland, J.M. (2002). PKB/Akt phosphorylates p27, impairs nuclear import of p27 and opposes p27-mediated G1 arrest. Nat Med *8*, 1153-1160.

Liang, J., and Slingerland, J.M. (2003). Muliple roles of the PI3K/PKB (Akt) pathway in cell cycle progression. Cell Cycle *2*, 339-345.

Liang, J., Shao, S.H., Xu, Z.X., Hennessy, B., Ding, Z., Larrea, M., Kondo, S., Dumont, D.J., Gutterman, J.U., Walker, C.L., Slingerland, J.M., and Mills, G.B. (2007). The energy sensing LKB1-AMPK pathway regulates p27*kip1* phosphorylation mediating the decision to enter autophagy or apoptosis. Nat Cell Biol *9*, 218-224.

Liu, A., Testa, J.R., Hamilton, T.C., Jove, R., Nicosia, S.V. and Cheng, J.Q. (1998). Akt2, a member of the protein kinase B family, is activated by growth factors, v-Ha-*ras*, and v-*src* through phosphatidylinositol 3-kinase in human ovarian epithelial cancer cells. Cancer Res *58*, 2973-2977.

Liu X., Shi, Y., Han, E.K-H, Chen, Z., Rosenberg, S.H., Giranda, V.L., Luo, Y., and Ng, S.C. (2001). Downregulation of Akt1 inhibits anchorage-independent cell growth and induces apoptosis in cancer cells. Neoplasia *3*, 278-286.

LoPiccolo, J., Granville, C.A., Gills, J.J., and Dennis, P.A. (2007). Targeting Akt in cancer therapy. Anti-Cancer Drugs *18*, 861-874

LoPiccolo, J., Blumenthal, G.M., Bernstein, W.B., Dennis, P.A. (2008). Targeting the PI3K/Akt/mTOR pathway: Effective combinations and clinical considerations. Drug Resist Updates *11*, 32-50.

Maddika, S., Ande, S.R., Wiechec, E., Hansen, L.L., Wesselborg, S., and Los, M. (2008). Akt-mediated phosphorylation of CDK2 regulates its dual role in cell cycle progression and apoptosis. J Cell Sci *121*, 979-988.

Majewski, N., Nogueira, V., Robey, R.B., and Hay, N. (2004a). Akt inhibits apoptosis downstream of BID cleavage via a glucose-dependent mechanism involving mitochondrial hexokinases. Mol Cell Biol *24*, 730-740.

Majewski, N., Nogueira, V., Bhaskar, P., Coy, P.E., Skeen, J.E., Gottlob, K., Chandel, N.S., Thompson, C.B., Robey, R.B., and Hay, N. (2004b). Hexokinase-mitochondria interaction mediated by Akt is required to inhibit apoptosis in the presence or absence of Bax and Bak. Mol Cell *16*, 819-830.

Manning, B.D., and Cantley, L.C. 2007. Akt/PKB signaling: Navigating downstream. Cell 129, 1261-1274.

Martin, K.A., Rzucidlo, E.M., Merenick, B.L., Fingar, D.C., Brown, D.J., Wagner, R.J., and Powell, R.J. (2004). The mTOR/p70 S6K1 pathway regulates vascular smooth muscle cell differentiation. Am J Physiol Cell Physiol *286*, C507-C517.

Masure, S., Haefner, B., Wesselink, J.J., Hoefnagel, E., Moriter, E., Verhasselt, P., Tuytelaars, A., Gordon, R., and Richardson, A. (1999). Molecular cloning, expression and characterization of the human serine/threonine kinase Akt-3. Eur J Biochem *265*, 353-360.

Mathupala, S.P., Ko, Y.H., and Pedersen, P.L. (2006). Hexokinase II: cancer's double-edged sword acting as both facilitator and gatekeeper of malignancy when bound to mitochondria. Oncogene *25*, 4777-4786.

Medema, R.H., Kops, G.J., Bos, J.L., and Burgering, B.M. (2000). AFX-like Forkhead transcription factors mediate cell-cycle regulation by Ras and PKB through p27kip1. Nature *404*, 782-787.

Meier, R., Alessi, D.R., Cron, P., Andjelkovic, M., and Hemmings, B.A. (1997). Mitogenic activation, phosphorylation, and nuclear translocation of protein kinase Bβ. J Biol Chem 272, 30491-30497.

Mende, I., Malstron S., Tsichlis, P.N., Vogt, P.K., and Aoki, M. (2001). Oncogenic transformation induced by membrane-targeted Akt2 and Akt3. Oncogene *20*, 4419-4423.

Meng, Q., Xia, C., Fang, J., Rojanasakul, Y., and Jiang, B.H. (2006). Role of PI3K and AKT specific isoforms in ovarian cancer cell migration, invasion and proliferation through the p70S6K1 pathway. Cell Signal 18, 2262-2271.

Mitsuuchi, Y., Johnson, S. W., Moonblatt, S., and Testa, J.R. (1998). Translocation and activation of Akt2 in response to stimulation by insulin. J Cell Biochem *70*, 433-441.

Munafo, D.B., and Colombo, M.I. (2001). A novel assay to study autophagy: regulation of autophagosome vacuole size by amino acid deprivation. J. Cell Sci *114*, 3619-3629.

Nakatani, K., Sakaue, H., Thompson, D.A., Weigel, R.J., and Roth, R.A. (1999a). Identification of a human Akt3 (Protein kinase Bγ) which contains the regulatory serine phosphorylation site.

Nakatani, K., Thompson, D.A., Barthel, A., Sakaue, H., Liu, W., Weigel, R.J., and Roth R.A.. (1999b). Up-regulation of Akt3 in estrogen receptor-deficient breast cancers and androgen-independent prostate cancer lines. J Biol Chem *274*, 21528-21532.

Navratil, M., Terman, A., and Arriaga, E.A. (2008). Giant mitochondria do not fuse and exchange their contents with normal mitochondria. Exp Cell Res *314*, 164-172.

Nicholson, K.M., and Anderson, N.G. (2002). The protein kinase B/Akt signalling pathway in human malignancy. Cellular Signal *14*, 381-395.

Noske, A., Kaszubiak, A., Weichert, W., Sers, C., Niesporek, S., Koch, I., Schaefer, B., Sehouli, J., Dietel, M., Lage, H., Denkert, C. (2007). Specific inhibition of Akt2 by RNA interference results in reduction of ovarian cancer cell proliferation: Increased expression of Akt in advanced ovarian cancer. Cancer Lett *246*, 190-200.

Nourse, J., Firpo, E., Flanagan, W.M., Coats, S., Polyak, K., Lee, M.H., Massague, J., Crabtree, G.R., and Roberts, J.M. (1994). Interleukin-2-mediated elimination of the p27Kip1 cyclin-dependent kinase inhibitor prevented by rapamycin. Nature 372, 570-573.

Okano, J., Gaslightwala, I., Birnbaum, M.J., Rustgi, A.K., and Nakagawa, H. (2000). Akt/Protein kinase B isoforms are differentially regulated by epidermal growth factor stimulation. J Biol Chem *275*, 30934-30942.

O'Reilly, K.E., Rojo, F., She, Q.B., Solit, D., Mills, G.B., Smith, D., Lane, H., Hofmann, F., Hicklin, D.J., Ludwig, D.L., Baselga, J., and Rosen, N. (2006). mTOR inhibition induces upstream receptor tyrosine kinas signaling and activates Akt. Cancer Res *66*, 1500-1508.

Pedrero, J.M.G., Carracedo, D.G., Pinto, C.M., Zapatero, A.H., Rodrigo, J.P., Nieto, C.S., and Gonzalez, M.V. (2005). Frequent genetic and biochemical alterations of the PI 3-K/Akt/PTEN pathway in head and neck squamous cell carcinoma. Int J Cancer *114*, 242-248.

Peng, X.D., Xu, P.Z., Chen, M.L., Hahn-Windgassen, Skeen, J., Jacobs, J., Sundararajan, D., Chen, W.S., Crawford, S.E., Coleman, K.G., and Hay, N. (2003). Dwarfism, impaired skin development, skeletal muscle atrophy, delayed bone development, and impeded adipogenesis in mice lacking Akt1 and Akt2. Genes Dev *17*:1352-1365.

Peng, T.I., and Jou, M.J. (2004). Mitochondrial swelling and generation of reactive oxygen species induced by photoirradiation are heterogeneously distributed. Ann N.Y. Acad Sci *1011*, 112-122.

Puigserver, P., Rhee, J., Donovan, J., Walkey C.J., Yoon, J.C., Oriente, F., Kitamura, Y., Altomonte, J., Dong, H., Accili, D., and Spiegelman, B.M. (2003). Insulin-regulated hepatic gluconeogenesis through FOXO1-PGC1α interaction. Nature *423*, 550-555.

Reznick, R.M., and Shulman, G.I. (2006). The role of AMP-activated protein kinase in mitochondrial biogenesis. J Physiol *574*, 33-39.

Rosner, M., Freilinger, A., and Hengstschlager, M. (2006). The tuberous sclerosis genes and regulation of the cyclin-dependent kinase inhibitor p27. Mutat Res *613*, 10-16.

Ruggeri, B.A., Huang, L., Wood, M., Cheng, J.Q., and Testa, J.R. (1998). Amplification and overexpression of the AKT2 oncogene in a subset of human pancreatic ductal adenocarcinomas. Mol Carcinog *21*, 81-86.

Saji, M., Vasko, V., Kada, F., Allbritton, E.H., Burman, K.D., and Ringel, M.D. (2005). Akt1 contains a functional leucine-rich nuclear export sequence. Biochem Biophys Res Commun *332*, 167-173.

Sarbassov, D.D., Guertin, D.A., Ali, S.M., and Sabatini, D.M. (2005). Phosphorylation and regulation of Akt/PKB by the Rictor-mTOR complex. Science *307*, 1098-1101.

Sasaki, K., Sato, M., and Umezawa, Y. (2003). Fluorescent indicators for Akt/Protein kinase B and dynamics of Akt activity visualized in living cells. J Biol Chem *278*, 30945-30951.

Shapira, M., Kakiashvili, E., Rosenberg, T., and Hershko, D.D. (2006). The mTOR inhibitor rapamycin down-regulates the expression of the ubiquitin ligase subunit Skp2 in breast cancer cells. Breast Cancer Res *8*, R46-R54.

Sharrard, R.M., and Maitland, N.J. (2007). Regulation of protein kinase B activity by PTEN and SHIP2 in human prostate-derived cell lines. Cell Signal *19(1)*, 129-138.

Shayesteh, L., Lu, Y., Kuo, W.L., Baldocchi, R., Godfrey, T., Collins, C., Pinkel, D., Powell, B., Mills, G.B., and Gray, J.W. (1999). *PI3KCA* is implicated as an oncogene in ovarian cancer. Nat Genet *21*, 99-102.

Schieke, S.M., and Finkel, T. (2006). Mitochondrial signaling, TOR and life span. Biol Chem *387*, 1357-1361.

Shen, Z., Wen, X.F., Lan, F., Shen, Z.Z., and Shao, Z.M. (2002). The tumor suppressor gene LKB1 is associated with prognosis in human breast carcinoma. Clin Cancer Res *8*, 2085-2090.

Shin, I., Yakes, F.M., Rojo, F., Shin. N.Y., Bakin, A.V., Baselga, J., and Arteaga, C.L. (2002). PKB/Akt mediates cell-cycle progression by phosphorylation of p27(Kip1) at threonine 157 and modulation of its cellular localization. Nat Med *8*, 1145-1152.

Sithanandam, G., Fornwald, L.W., Fields, J., and Anderson, L.M. (2005). Inactivation of ErbB3 by siRNA promotes apoptosis and attenuates growth and invasiveness of human lung adenocarcinoma cell line A549. Oncogene *24*, 1847-1859.

Skeen, J.E., Bhaskar, P.T., Chen, C.C., Chen, W.S., Peng, X.D., Nogueira, V., Hahn-Windgassen, A., Kiyokawa, H., and Hay, N. (2006). Akt deficiency impairs normal cell proliferation and suppresses oncogenesis in a p53-independent and mTORC1-dependent manner. Cancer Cell *10*, 269-280.

Soung, Y.H., Lee, J.W., Nam, S.W., Lee, J.Y., Yoo, N.J., and Lee, S.H. (2006). Mutational analysis of *AKT1*, *AKT2*, and *AKT3* genes in common human carcinomas. Oncology *70*, 285-289.

Staal, S.P., Hartley, J.W., and Rowe, W.P. (1977). Isolation of transforming murine leukemia viruses from mice with a high incidence of spontaneous lymphoma. Proc Natl Acad Sci USA *74*, 3065-3067.

Staal, S.P. (1987). Molecular cloning of the *akt* oncogene and its human homologues *AKT1* and *AKT2*: Amplification of *AKT1* in a primary human gastric adenocarcinoma. Proc Natl Acad Sci USA *84*, 5034-5037.

Stahl, J.M., Sharma, A., Cheung, M., Zimmerman, M., Cheng, J.Q., Bosenberg, M.W., Kester, M., Sandirasegarane, L., and Robertson, G.P. (2004). Deregulated Akt3 activity promotes development of malignant melanoma. Cancer Res *64*, 7002-7010.

Stambolic, V., and Woodgett, J.R. (2006). Functional distinctions of protein kinase B/Akt isoforms defined by their influence on cell migration. Trends Cell Biol *16*, 461-466.

Sun, M., Wang, G., Paciga J.E., Feldman, R.I., Yuan, Z.Q., Ma, X.L., Shelley, S.A., Jove, R., Tsichlis, P.N., Nicosia, S.V., and Cheng, J.Q. (2001a). AKT1/PKBα kinase is frequently elevated in human cancers and its constitutive activation is required for oncogenic transformation in NIH3T3 cells. Am J Pathol *159*, 431-437.

Sun, M., Paciga, J.E, Feldman, R.I., Yuan, Z.Q., Coppola, D., Lu, Y.Y., Shelley, S.A., Nicosia, S.V., and Cheng, J.Q. (2001b). Phosphatidylinositol-3-OH kinase (PI3K)/AKT2, activated in breast cancer, regulates and is induced by estrogen receptor a (ERα) via interaction between ERα and PI3K. Cancer Res *61*, 5985-5991.

Takeuchi, H., Kondo, Y., Fujiwara, K., Kanzawa, T., Aoki, H., Mills, G.B., and Kondo S. (2005). Synergistic augmentation of rapamycin-induced autophagy in malignant glioma cells by phosphatidylinositol 3-kinase/protein kinase B inhibitors. Cancer Res *65*, 3336-3346.

Taniyama, Y, Ito, M., Sato, K., Kuester, C., Veit, K., Tremp, G., Liao, R., Colucci, W.S., Ivashchenko, Y., Walsh, K., Shiojima, I. (2005). Akt3 overexpression in the heart results in progression from adaptive to maladaptive hypertrophy. J Mol Cell Cardiol *38*, 375-385.

Toker, A., and Newton, A.C. (2000). Akt/Protein kinase B is regulated by autophosphorylation at the hypothetical PDK-2 site. J Biol Chem *275*, 8271-8274.

Tran, M.A., Gowda, R., Sharma, A., Park, E.J., Adair, J., Kester, M., Smith, N.B., and Robertson, G.P. (2008). Targeting ^{V600E}B-Raf and Akt3 using nanoliposomal-small interfering RNA inhibits cutaneous melanocytic lesion development. Cancer Res 68, 7638-7649.

Troussard, A.A., Mawji, N.M., Ong, C., Mui, C., St.-Arnaud, R., and Dedhar, S. (2003). Conditional knock-out of integrin-linked kinase demonstrates an essential role in protein kinase B/Akt activation. J Biol Chem 278, 22374-22378.

Tschopp, O., Yang, Z.Z., Brodbeck, D., Dummler, B.A., Hemmings-Mieszczak, M., Watanabe, T., Michaelis, T., Frahm, J., and Hemmings, B.A. (2005). Essential role of protein kinase Bγ (PKBγ/Akt3) in postnatal brain development but not in glucose homeostasis. Development *132*, 2943-2954.

Um, S.H., D'Alessio, D., and Thomas, G. (2006). Nutrient overload, insulin resistance and ribosomal protein S6 kinase 1, S6K1. Cell Metab *3*, 393-402.

Vandromme, M, Rochat A., Meier, R., Carnac, G., Besser, D., Hemmings, B.A., Fernandez, A., and Lamb, N.J. (2001). Protein kinase Bβ/Akt2 plays a specific role in muscle differentiation. J Biol Chem *276*, 8173-8179.

Viglietto, G., Motti, M.L., Bruni, P., Melillo, R.M., D'Alessio, A., Califano, D., Vinci, F., Chiappetta, G., Tsichlis, P., Bellacosa, A, Fusco, A., and Santoro, M. (2002). Cytoplasmic relocalization and inhibition of the cyclin-dependent kinase inhibitor p27(Kip1) by Akt/mediated phosphorylation in breast cancer. Nat Med *8*, 1136-1144.

Xu, X., Sakon, M., Hiraoka, N., Yamamoto, H., Hayashi, N., Dono, K., Nakamori, S., Umeshita, K., Ito, Y., Matsuura, N., and Monden, M. (2004). Akt2 expression correlates with prognosis of human hepatocellular carcinoma. Oncol Rep *11*, 25-32.

Xuan Nguyen, T.L., Choi, J.W., Lee, S.B., Ye, K., Woo, S.D., Lee, K.H., and Ahn, J.Y. (2006). Akt phosphorylation is essential for nuclear translocation and retention in NGF-stimulated PC12 cells.*349*, 789-798.

Yamamoto, S., Tomita, Y., Hoshida, Y., Morooka, T., Nagano, H., Dono, K., Umeshita, K., Sakon, M., Ishikawa, O., Ohigashi, H., Nakamori, S., Monden, M., and Aozasa, K. (2004). Prognostic significance of activated Akt expression in pancreatic ductal adenocarcinoma. Clin Cancer Res *10*, 2846-2850.

Yang, Z.Z., Tschopp, O., Di-Poi, N., Bruder, E., Baudry, A., Dummler, B., Wahli, W., and Hemmings, B.A. (2005). Dosage-dependent effects of Akt1/protein kinase Bα (PKBα) and Akt3/PKBγ on thymus, skin, and cardiovascular and nervous system development in mice. Mol Cell Biol *25*, 10407-10418.

Yuan, Z.Q., Sun, M., Feldman, R.I., Wang, G., Ma, X.L., Jiang, C., Coppola, D., Nicosia, S.V., and Cheng, J.Q. (2000). Frequent activation of Akt2 and induction of apoptosis by inhibition of phosphoinositide-3-OH-kinase/Akt pathway in human ovarian cancer. Oncogene *19*, 2324-2330.

Zhan, M., and Han, Z.C. (2004). Phosphoinositide 3-Kinase/Akt in radiation responses. Histol Histopathol *19*, 915-923.Zong, H., Ren, J.M., Young, L.H., Pyapaert, M., Mu, J., Birnbaum, M.J., and Shulman, G.I. (2002). AMP kinase is required for mitochondrial biogenesis in skeletal muscle in response to chronic energy deprivation. Proc Natl Sci USA *99*, 15983-15987.

Zong, H., Ren, J.M., Young, L.H., Pypaert, M., Mu, J., Birnbaum, M.J., and Shulman, G.I. (2002). AMP kinase is required for mitochondrial biogenesis in skeletal muscle in response to chronic energy deprivation. Proc Natl Acad Sci USA *99*, 15983-15987.

7.0 ACKNOWLEDGEMENT OF CONTRIBUTORS

The acknowledgements below, apply to the work performed in Section 3.0 of the thesis:

Special thanks to Dr. J.M. Woodgett for supplying the Akt2 cDNA and to Ningning Li who performed the restriction digest and pECFP insertion. Stacey Hembruff and Dr. Amadeo Parissenti supplied the MDA-MB468, 293T, and MCF-7 cell lines. Dr. Carita Lanner supplied the MCF-10A cell line. Dr. Bill Stegman from Jackson Immunoresearch provided technical assistance with the triple staining protocol.

8.0 APPENDICES

APPENDIX I

```
Akt1    ATGAGCGACGTGGCTATTGTGAAGGAGGGTTGGCTGCACAAACGAGGGGAGTACATCAAG 60
Akt2    ATGAATGAGGTGTCTGTCATCAAAGAAGGCTGGCTCCACAAGCGTGGTGAATACATCAAG 60
Akt3    ATGAGCGATGTTACCATTGTGAAAGAAGGTTGGGTTCAGAAGAGGGGAGAATATATAAAA 60
        ****  ** **  *  *  * ** ** ** *** * ** **  * ** ** ** ** **

Akt1    ACCTGGCGGCCACGCTACTTCCTCCTCAAGAATGATGGCACCTTCATTGGCTACAAGGAG 120
Akt2    ACCTGGAGGCCACGGTACTTCCTGCTGAAGAGCGACGGCTCCTTCATTGGGTACAAGGAG 120
Akt3    AACTGGAGGCCAAGATACTTCCTTTTGAAGACAGATGGCTCATTCATAGGATATAAAGAG 120
        * **** ***** * ********  * ****  ** *** * ***** ** ** ** ***

Akt1    CGGCCGCAGGATGTGGACCAACGTGAGGCTCCCCTCAACAACTTCTCTGTGGCGCAGTGC 180
Akt2    AGGCCCGAGGCCCCTGATCAGACTCTACCCCCCTTAAACAACTTCTCCGTAGCAGAATGC 180
Akt3    AAACCTCAAGATGTGGATTTACCTTA---TCCCCTCAACAACTTTTCAGTGGCAAAATGC 177
           **  * *     **      *      *** * ******** ** ** **  * ***

Akt1    CAGCTGATGAAGACGGAGCGGCCCCGGCCCAACACCTTCATCATCCGCTGCCTGCAGTGG 240
Akt2    CAGCTGATGAAGACCGAGAGGCCGCGACCCAACACCTTTGTCATACGCTGCCTGCAGTGG 240
Akt3    CAGTTAATGAAAACAGAACGACCAAAGCCAAACACATTTATAATCAGATGTCTCCAGTGG 237
        *** * ***** ** **  * **    ** ***** **  * **  * ** ** ******

Akt1    ACCACTGTCATCGAACGCACCTTCCATGTGGAGACTCCTGAGGAGCGGGAGGAGTGGACA 300
Akt2    ACCACAGTCATCGAGAGGACCTTCCACGTGGATTCTCCAGACGAGAGGGAGGAGTGGATG 300
Akt3    ACTACTGTTATAGAGAGAACATTTCATGTAGATACTCCAGAGGAAAGGGAAGAATGGACA 297
        ** ** ** ** **  * ** ** ** ** **  **** ** **  **** ** ****

Akt1    ACCGCCATCCAGACTGTGGCTGACGGCCTCAAGAAGCAGG------AGGAGGAGGAGATG 354
Akt2    CGGGCCATCCAGATGGTCGCCAACAGCCTCAAGCAGCGGGCCCCAGGCGAGGACCCCATG 360
Akt3    GAAGCTATCCAGGCTGTAGCAGACAGACTGCAGAGGCAAG------AAGAGGAGAGAATG 351
           ** ******   ** **  ** * **  **  **  *        *****    ***

Akt1    GACTTCCGGTCGGGCTCACCCAGTGACAACTCAGGGGCTGAAGAGATGGAGGTGTCCCTG 414
Akt2    GACTACAAGTGTGGCTCCCCCAGTGACTCCTCCACGACTGAGGAGATGGAAGTGGCGGTC 420
Akt3    AATTGTAGTCCAACTTCACAAATTGATAATATAGGAGAGGAAGAGATGGATGCCTCTACA 411
         * *           ** *  * ***             ** ******** *   *

Akt1    GCCAAGCCCAAGCACCGCGTGACCATGAACGAGTTTGAGTACCTGAAGCTGCTGGGCAAG 474
Akt2    AGCAAGGCACGGGCTAAAGTGACCATGAATGACTTCGACTATCTCAAACTCCTTGGCAAG 480
Akt3    ACCCATCATAAA---AGAAAGACAATGAATGATTTTGACTATTTGAAACTACTAGGTAAA 468
          * *               *** ***** ** ** ** **  * ** ** ** ** **

Akt1    GGCACTTTCGGCAAGGTGATCCTGGTGAAGGAGAAGGCCACAGGCCGCTACTACGCCATG 534
Akt2    GGAACCTTTGGCAAAGTCATCCTGGTGCGGGAGAAGGCCACTGGCCGCTACTACGCCATG 540
Akt3    GGCACTTTTGGGAAAGTTATTTTGGTTCGAGAGAAGGCAAGTGGAAAATACTATGCTATG 528
        ** ** ** ** ** ** **  ****    ******** *  **    ***** ** ***

Akt1    AAGATCCTCAAGAAGGAAGTCATCGTGGCCAAGGACGAGGTGGCCCACACACTCACCGAG 594
Akt2    AAGATCCTGCGGAAGGAAGTCATCATTGCCAAGGATGAAGTCGCTCACACAGTCACCGAG 600
Akt3    AAGATTCTGAAGAAAGAAGTCATTATTGCAAAGGATGAAGTGGCACACACTCTAACTGAA 588
        ***** **   *** ********  * ** ***** ** ** ** *****  * ** **

Akt1    AACCGCGTCCTGCAGAACTCCAGGCACCCCTTCCTCACAGCCCTGAAGTACTCTTTCCAG 654
Akt2    AGCCGGGTCCTCCAGAACACCAGGCACCCGTTCCTCACTGCGCTGAAGTATGCCTTCCAG 660
```

```
Akt3    AGCAGAGTATTAAAGAACACTAGACATCCCTTTTTAACATCCTTGAAATATTCCTTCCAG 648
        * * * **  *  ***** * ** ** ** **  * **  *  **** **  * ******

Akt1    ACCCACGACCGCCTCTGCTTTGTCATGGAGTACGCCAACGGGGGCGAGCTGTTCTTCCAC 714
Akt2    ACCCACGACCGCCTGTGCTTTGTGATGGAGTATGCCAACGGGGGTGAGCTGTTCTTCCAC 720
Akt3    ACAAAAGACCGTTTGTGTTTTGTGATGGAATATGTTAATGGGGGCGAGCTGTTTTTCCAT 708
        **  * *****  * ** ***** ***** ** *  ** ***** ******** *****

Akt1    CTGTCCCGGGAGCGTGTGTTCTCCGAGGACCGGGCCCGCTTCTATGGCGCTGAGATTGTG 774
Akt2    CTGTCCCGGGAGCGTGTCTTCACAGAGGAGCGGGCCCGGTTTTATGGTGCAGAGATTGTC 780
Akt3    TTGTCGAGAGAGCGGGTGTTCTCTGAGGACCGCACACGTTTCTATGGTGCAGAAATTGTC 768
         ****  * ***** ** *** * ***** **  * ** ** ***** ** ** *****

Akt1    TCAGCCCTGGACTACCTGCACTCGGAGAAGAACGTGGTGTACCGGGACCTCAAGCTGGAG 834
Akt2    TCGGCTCTTGAGTACTTGCACTCGCGGG---ACGTGGTATACCGCGACATCAAGCTGGAA 837
Akt3    TCTGCCTTGGACTATCTACATTCCGGAA---AGATTGTGTACCGTGATCTCAAGTTGGAG 825
        ** **  * ** **  * ** **        *  * ** ***** **  ***** ****

Akt1    AACCTCATGCTGGACAAGGACGGGCACATTAAGATCACAGACTTCGGGCTGTGCAAGGAG 894
Akt2    AACCTCATGCTGGACAAAGATGGCCACATCAAGATCACTGACTTTGGCCTCTGCAAAGAG 897
Akt3    AATCTAATGCTGGACAAAGATGGCCACATAAAAATTACAGATTTTGGACTTTGCAAAGAA 885
        ** ** ********** ** ** ***** ** ** ** ** ** ** ** ***** **

Akt1    GGGATCAAGGACGGTGCCACCATGAAGACCTTTTGCGGCACACCTGAGTACCTGGCCCCC 954
Akt2    GGCATCAGTGACGGGGCCACCATGAAAACCTTCTGTGGGACCCCGGAGTACCTGGCGCCT 957
Akt3    GGGATCACAGATGCAGCCACCATGAAGACATTCTGTGGCACTCCAGAATATCTGGCACCA 945
        ** ****  ** *  ********** ** ** ** ** ** ** ** ** ***** **

Akt1    GAGGTGCTGGAGGACAATGACTACGGCCGTGCAGTGGACTGGTGGGGGCTGGGCGTGGTC 1014
Akt2    GAGGTGCTGGAGGACAATGACTATGGCCGGGCCGTGGACTGGTGGGGGCTGGGTGTGGTC 1017
Akt3    GAGGTGTTAGAAGATAATGACTATGGCCGAGCAGTAGACTGGTGGGGCCTAGGGGTTGTC 1005
        ****** * ** ** ******** ***** ** ** ********** ** ** ** ***

Akt1    ATGTACGAGATGATGTGCGGTCGCCTGCCCTTCTACAACCAGGACCATGAGAAGCTTTTT 1074
Akt2    ATGTACGAGATGATGTGCGGCCGCCTGCCCTTCTACAACCAGGACCACGAGCGCCTCTTC 1077
Akt3    ATGTATGAAATGATGTGTGGGAGGTTACCTTTCTACAACCAGGACCATGAGAAACTTTTT 1065
        ***** ** ******** **  *  * ** ***************** ***   ** **

Akt1    GAGCTCATCCTCATGGAGGAGATCCGCTTCCCGCGCACGCTTGGTCCCGAGGCCAAGTCC 1134
Akt2    GAGCTCATCCTCATGGAAGAGATCCGCTTCCCGCGCACGCTCAGCCCCGAGGCCAAGTCC 1137
Akt3    GAATTAATATTAATGGAAGACATTAAATTTCCTCGAACACTCTCTTCAGATGCAAAATCA 1125
        **  * **  * ***** ** **    ** ** ** ** **     * ** ** ** **

Akt1    TTGCTTTCAGGGCTGCTCAAGAAGGACCCCAAGCAGAGGCTTGGCGGGGGCTCCGAGGAC 1194
Akt2    CTGCTTGCTGGGCTGCTTAAGAAGGACCCCAAGCAGAGGCTTGGTGGGGGGCCCAGCGAT 1197
Akt3    TTGCTTTCAGGGCTCTTGATAAAGGATCCAAATAAACGCCTTGGTGGAGGACCAGATGAT 1185
         ***** * *****  * *  ***** ** **  *  * ***** ** **  *    **

Akt1    GCCAAGGAGATCATGCAGCATCGCTTCTTTGCCGGTATCGTGTGGCAGCACGTGTACGAG 1254
Akt2    GCCAAGGAGGTCATGGAGCACAGGTTCTTCCTCAGCATCAACTGGCAGGACGTGGTCCAG 1257
Akt3    GCAAAAGAAATTATGAGACACAGTTTCTTCTCTGGAGTAAACTGGCAAGATGTATATGAT 1245
        ** ** **  * ***   **  * *****     *  *    *****  * **     *

Akt1    AAGAAGCTCAGCCCACCCTTCAAGCCCCAGGTCACGTCGGAGACTGACACCAGGTATTTT 1314
Akt2    AAGAAGCTCCTGCCACCCTTCAAACCTCAGGTCACGTCCGAGGTCGACACAAGGTACTTC 1317
Akt3    AAAAAGCTTGTACCTCCTTTTAAACCTCAAGTAACATCTGAGACAGATACTAGATATTTT 1305
        ** *****    ** ** ** ** ** ** ** ** ** ***   ** ** ** ** **
```

```
Akt1    GATGAGGAGTTCACGGCCCAGATGATCACCATCACACCACCTGACCAAGATGACA----- 1369
Akt2    GATGATGAATTTACCGCCCAGTCCATCACAATCACACCCCCTGACCGCTATGACA----- 1372
Akt3    GATGAAGAATTTACAGCTCAGACTATTACAATAACACCACCTGAAAAATATGATGAGGAT 1365
        ***** ** ** ** ** ***   ** ** ** ***** *****     ****

Akt1    -GCATGGAGTGTGTGGACAGCGAGCGCAGGCCCCACTTCCCCCAGTTCTCCTACTCGGCC 1428
Akt2    -GCCTGGGCTTACTGGAGCTGGACCAGCGGACCCACTTCCCCCAGTTCTCCTACTCGGCC 1431
Akt3    GGTATGGACTGCATGGACAATGAGAGGCGGCCGCATTTCCCTCAATTTTCCTACTCTGCA 1425
          *  ***  *   ****    **     ** * ** ***** ** ** ******** **

Akt1    AGCGGCACGGCCTGA 1443
Akt2    AGCATCCGCGAGTGA 1446
Akt3    AGTGGACGAGAATAA 1440
        **       *  * *
```

Akt1 siRNA #1
Akt1 siRNA #2

Akt2 siRNA #1
Akt2 siRNA #2

Akt3 siRNA #1
Akt3 siRNA #2

Figure A1. Nucleotide alignment of the coding sequences of Akt1, Akt2 and Akt3 (alignment performed using Clustal W software). Sequences of the siRNAs used in the experiments within the thesis are denoted in coloured font.

```
Akt1    MSDVAIVKEGWLHKRGEYIKTWRPRYFLLKNDGTFIGYKERPQDVDQREAPLNNFSVAQC 60
Akt3    MSDVTIVKEGWVQKRGEYIKNWRPRYFLLKTDGSFIGYKEKPQDVDLP-YPLNNFSVAKC 59
Akt2    MNEVSVIKEGWLHKRGEYIKTWRPRYFLLKSDGSFIGYKERPEAPDQTLPPLNNFSVAEC 60
        *.:*:::****::*******.*********.**:******:*:  *    ********:*

Akt1    QLMKTERPRPNTFIIRCLQWTTVIERTFHVETPEEREEWTTAIQTVADGLKKQE--EEEM 118
Akt3    QLMKTERPKPNTFIIRCLQWTTVIERTFHVDTPEEREEWTEAIQAVADRLQRQE--EERM 117
Akt2    QLMKTERPRPNTFVIRCLQWTTVIERTFHVDSPDEREEWMRAIQMVANSLKQRAPGEDPM 120
        ********:****:****************::*:*****  *** **: *:::   *: *

Akt1    DFRSGSPSDNSGAEEMEVSLAKPKHRVTMNEFEYLKLLGKGTFGKVILVKEKATGRYYAM 178
Akt3    N[redacted]EMDASTTHHK-RKTMNDFDYLKLLGKGTFGKVILVREKASGKYYAM 176
Akt2    DYKCGSPSDSSTTEEMEVAVSKARAKVTMNDFDYLKLLGKGTFGKVILVREKATGRYYAM 180
        :    *  *.   ***:.: :: : : ***:*:****************:***:*:****

Akt1    KILKKEVIVAKDEVAHTLTENRVLQNSRHPFLTALKYSFQTHDRLCFVMEYANGGELFFH 238
Akt3    KILKKEVIIAKDEVAHTLTESRVLKNTRHPFLTSLKYSFQTKDRLCFVMEYVNGGELFFH 236
Akt2    KILRKEVIIAKDEVAHTVTESRVLQNTRHPFLTALKYAFQTHDRLCFVMEYANGGELFFH 240
        ***:****:********:**.***:*:******:***:***:*********.********

Akt1    LSRERVFSEDRARFYGAEIVSALDYLHSEKNVVYRDLKLENLMLDKDGHIKITDFGLCKE 298
Akt3    LSRERVFSEDRTRFYGAEIVSALDYLHSGK-IVYRDLKLENLMLDKDGHIKITDFGLCKE 295
Akt2    LSRERVFTEERARFYGAEIVSALEYLHSRD-VVYRDIKLENLMLDKDGHIKITDFGLCKE 299
        *******:*:*:***********:**** . :****:**********************

Akt1    GIKDGATMKTFCGTPEYLAPEVLEDNDYGRAVDWWGLGVVMYEMMCGRLPFYNQDHEKLF 358
Akt3    GITDAATMKTFCGTPEYLAPEVLEDNDYGRAVDWWGLGVVMYEMMCGRLPFYNQDHEKLF 355
Akt2    GISDGATMKTFCGTPEYLAPEVLEDNDYGRAVDWWGLGVVMYEMMCGRLPFYNQDHERLF 359
        **.*.**************************************************:**

Akt1    ELILMEEIRFPRTLGPEAKSLLSGLLKKDPKQRLGGGSEDAKEIMQHRFFAGIVWQHVYE 418
Akt3    ELILMEDIKFPRTLSSDAKSLLSGLLIKDPNKRLGGGPDDAKEIMRHSFFSGVNWQDVYD 415
Akt2    ELILMEEIRFPRTLSPEAKSLLAGLLKKDPKQRLGGGPSDAKEVMEHRFFLSINWQDVVQ 419
        ******:*:*****..:*****:*** ***::*****..****:*.* ** .: **.* :

Akt1    KKLSPPFKPQVTSETDTRYFDEEFTAQMITITPPD--QDDSMECVDSERRPHFPQFSYSA 476
Akt3    KKLVPPFKPQVTSETDTRYFDEEFTAQTITITPPEKYDEDGMDCMDNERRPHFPQFSYSA 475
Akt2    KKLLPPFKPQVTSEVDTRYFDDEFTAQSITITPPD--RYDSLGLLELDQRTHFPQFSYSA 477
        *** **********.******:***** ******:    *.:  :: ::*.*********

Akt1    SGTA 480
Akt3    SGRE 479
Akt2    SIRE 481
        *
```

Figure A2. Amino acid alignment of Akt1, Akt2 and Akt3 (alignment performed using Clustal W software). Red highlight denotes targeting of Akt3 antibody from Upstate Biotechnology (sequences for the other antibodies were unavailable).

APPENDIX II

Table A1. List of Antibodies and Dilutions used in the experiments

Primary Antibodies	Cat. Number	Company	Dilution	Application	Secondary Species	Lot Number	Thesis Section
Akt (pan)	9272	Cell Signal	1:1000	Western	Rabbit	10	3.0
Akt1 (2H10)	2967	Cell Signal	1:2000	Western/IP	Mouse	2, 3	Throughout
Akt1 (D-17)	sc-7126	Santa Cruz	1:10	IF	Goat	See Sec. 3.0	Throughout
Akt1	07-419	Upstate	1:1000	Western	Rabbit	24350	3.0
Akt2 (F-7)	sc-5270	Santa Cruz	1:100/1:10	Western/IP/ IF	Mouse	See Sec. 3.0	Throughout
Akt2	2962	Cell Signal	1:100	Western	Rabbit	1	3.0
Akt2	07-372	Upstate	1:500	Western	Rabbit	22444	3.0
Akt3	05-780	Upstate	1:1000	Western	Mouse	26827	Throughout
Akt3	07-383	Upstate	1:1000	Western	Rabbit	26508	3.0
Akt3	4059	Cell Signal	1:500	Western	Rabbit	1	3.0
Akt3 (M-14)	sc-11521	Santa Cruz	1:100/1:10	Western/IF	Goat	L1702	Throughout
p-Akt (S473)	9271	Cell Signal	1:1000	Western	Rabbit	7, 8, 9, 10	3.0 and 5.0
p-AMPKα(T172)	2535	Cell Signal	1:500	Western	Rabbit mAb	8	4.0
AMPKα	2532	Cell Signal	1:500	Western	Rabbit	4	4.0
Calnexin	sc-11397	Santa Cruz	1:10-1:20	IF	Rabbit	K2404	3.0
p-Cdc2p34 (T15)	sc-7989	Santa Cruz	1:200	Western	Goat	G1905	4.0
Cdk2	MS-617	Lab Vision	1:200/1:10	Western/IF	Mouse	617P508F	4.0
Cyclin A (H-432)	sc-751	Santa Cruz	1:200	Western	Rabbit	G0104	4.0
Cyclin D (H-295)	sc-753	Santa Cruz	1:200	Western	Rabbit	C2804	4.0
Cyclin E	sc-247	Santa Cruz	1:200	Western	Mouse	C2304	4.0
p-ERK (E-4)	sc-7383	Santa Cruz	1:1000	Western	Mouse	I1806	4.0
p-4E-BP1 (S65)	9456	Cell Signal	1:2000	Western	Rabbit mAb	1	4.0 and 5.0
4E-BP1	9644	Cell Signal	1:2000	Western	Rabbit mAb	2	4.0 and 5.0
p-FoxO1 (S256)	9461	Cell Signal	1:500	Western	Rabbit	5	4.0 and 5.0
FoxO1	9462	Cell Signal	1:500	Western	Rabbit	5	4.0 and 5.0
GSK-3β	9332	Cell Signal	1:500	Western	Rabbit	1	4.0
p-GSK3-α/β	9331	Cell Signal	1:500	Western	Rabbit	2A	4.0
Lamin B1	sc-20682	Santa Cruz	1:200/1:10	Western/IF	Rabbit	I1504, J2105	3.0
LC3B	2775	Cell Signal	1:500/1:50	Western/IF	Rabbit	2, 4	4.0
p21	sc-397	Santa Cruz	1:200	Western	Rabbit	G182	4.0
p27	sc-1641	Santa Cruz	1:200/1:10	Western/IF	Mouse	F1907	4.0
p-p27 (T187)	sc-16324	Santa Cruz	1:200	Western	Rabbit	E0407	4.0
p-p27 Kip1 T157	AF1555	R&D Systems	1:1000	Western	Rabbit		4.0
p-p27 Kip1 T198	AF3994	R&D Systems	1:1000	Western	Rabbit		4.0
p70S6K	9202	Cell Signal	1:500	Western	Rabbit	8	4.0 and 5.0
p-p70S6K T389	9206	Cell Signal	1:500	Western	Mouse	6, 7	4.0 and 5.0
PGC-1α	sc-13067	Santa Cruz	1:1000	Western	Rabbit	J2307	4.0
PDI (H-160)	sc-20132	Santa Cruz	1:10	IF	Rabbit	E1905	3.0
PTEN	9552	Cell Signal	1:500	Western	Rabbit	1	3.0
Skp2	4358	Cell Signal	1:500	Western	Rabbit	1	4.0
TGN38 (C-15)	sc-27680	Santa Cruz	1:10	IF	Goat	D2205	3.0
α-tubulin	T5168	Sigma	1:2000	Western	Mouse	016K4886	3.0
γ-tubulin	T6557	Sigma	1:20 000	Western	Mouse		Throughout
VDAC1 (D-16)	sc-32063	Santa Cruz	1:200	Western	Goat	C2306	3.0

Secondary Antibodies	Catalogue No.	Company	Dilution	Lot Number
Anti-mouse IgG peroxidase antibody (rabbit)	A9044	Sigma	1:5000	
Anti-rabbit ImmunoPure peroxidase conjugated	31460	Pierce	1:5000	AG605297/F18167610
Anti-goat IgG H+L Chain (rabbit) Peroxidase	401515	Calbiochem	1:10 000	D21183

Secondary Antibodies (Immunofluorescence)	Catalogue Number	Company	Dilution	Lot Number
AffiniPure Fab fragment rabbit anti-goat	305-007-003	Jackson Immunoresearch	100 µg/ml	64029
Fluorescein (FITC)-conjugated AffiniPure donkey anti-mouse IgG	715-095-150	Jackson Immunoresearch	1:100	66086
Cy5-conjugated AffiniPure donkey anti-rabbit IgG	711-175-152	Jackson Immunoresearch	1:500	63978
Donkey anti-goat IgG FITC	sc-2024	Santa Cruz	1:100	L3003
Donkey anti-goat IgG Rhodamine	sc-2094	Santa Cruz	1:100	I0303
Goat anti-mouse IgG FITC	sc-2010	Santa Cruz	1:100	C1004
Goat anti-mouse IgG Rhodamine	sc-2092	Santa Cruz	1:100	L1003
Goat anti-rabbit IgG FITC	sc-2012	Santa Cruz	1:100	D1504
Donkey anti-rabbit IgG Rhodamine	sc-20905	Santa Cruz	1:100	H0503

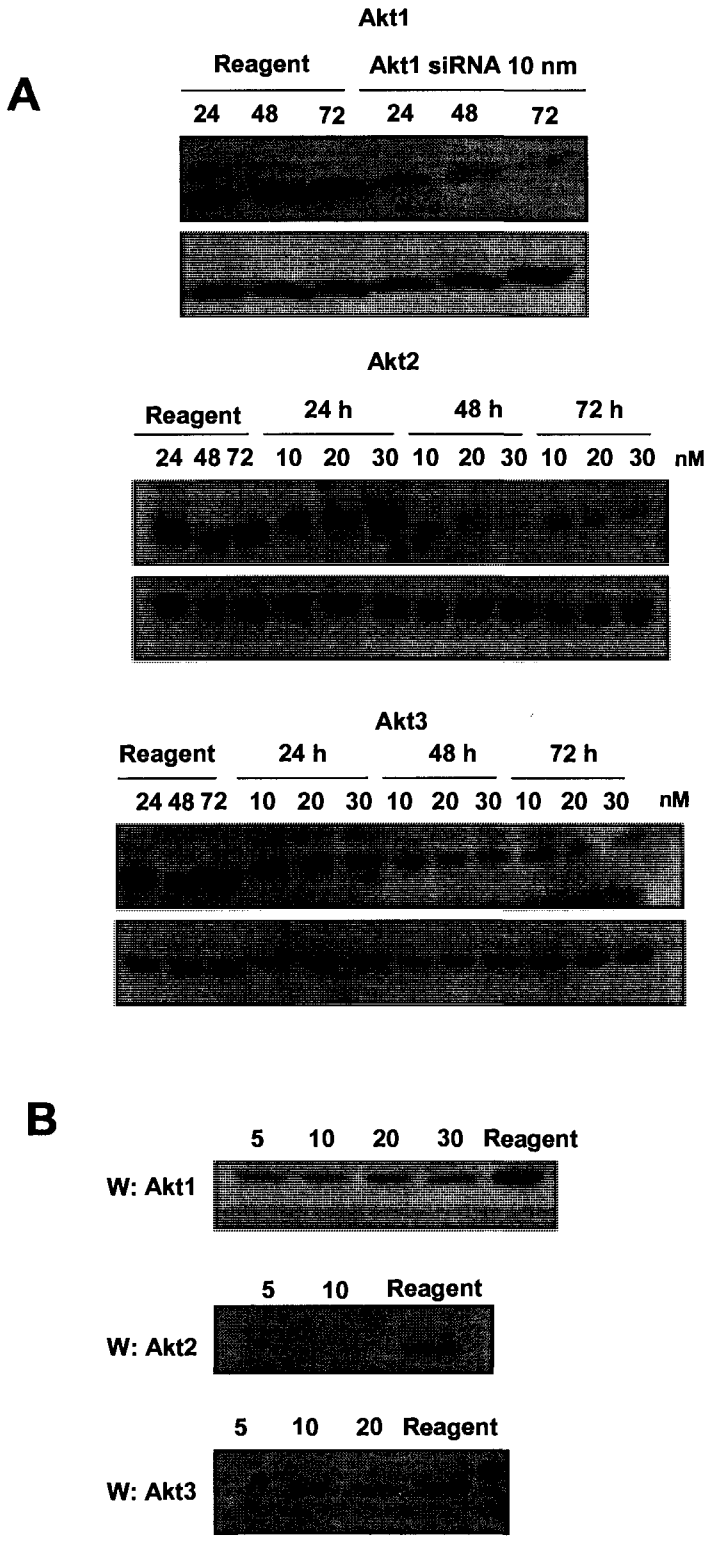

Fig. A3. Optimization/Dose curves for siRNA (A) siRNA Set #1 **(B)** siRNA Set #2

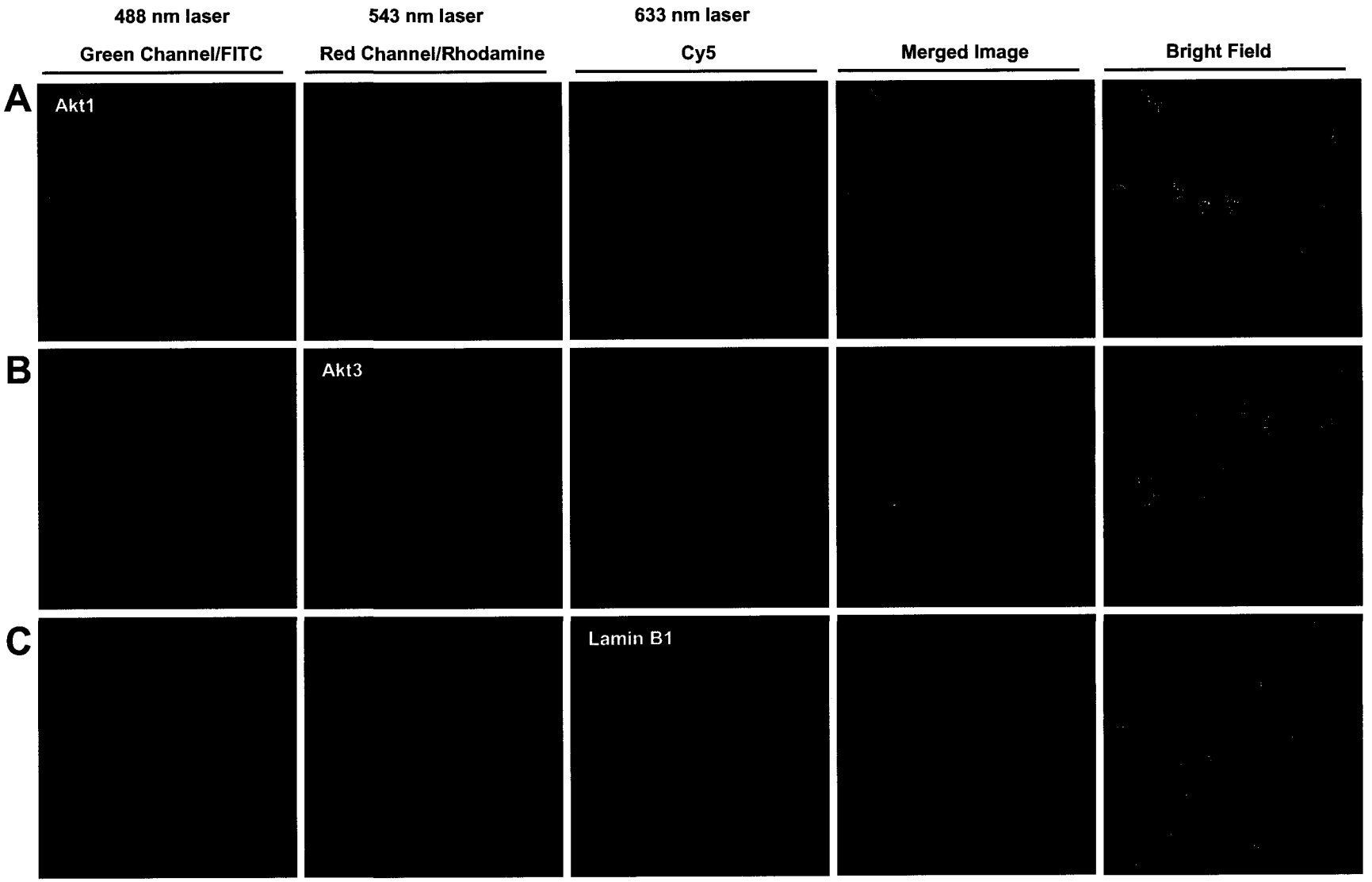
488 nm laser
Green Channel/FITC
543 nm laser
Red Channel/Rhodamine
633 nm laser
Cy5
Merged Image
Bright Field
A
Akt1
B
Akt3
C
Lamin B1

Fig. A4: Optimization of Confocal Microscopy Experiments: MDA-MB231 cells were plated onto glass coverslips and stained with (A) Akt1/FITC, (B) Akt3/Rhodamine, and (C) Lamin B1/Cy5. Images were captured with all channels open with the identical settings used for all the experiments in the thesis. These results show the stringent settings and filters used in the experiments and show that each fluorophore recognized the intended target with no bleedthrough into the other channels when captured simultaneously.

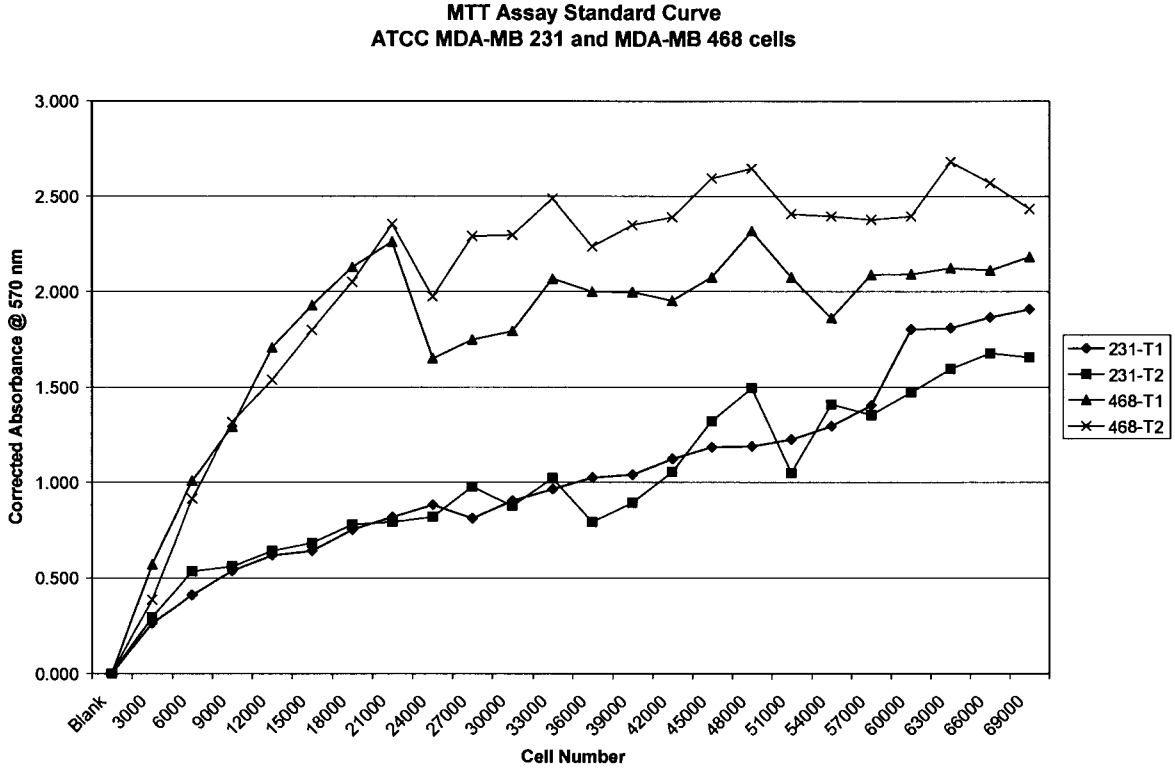

Figure A5. Optimization curves for MTT Assays. Determination of the plating number for the MTT assay. Cells were plated for all experiments in the linear portion of the curve based on the results from this test.

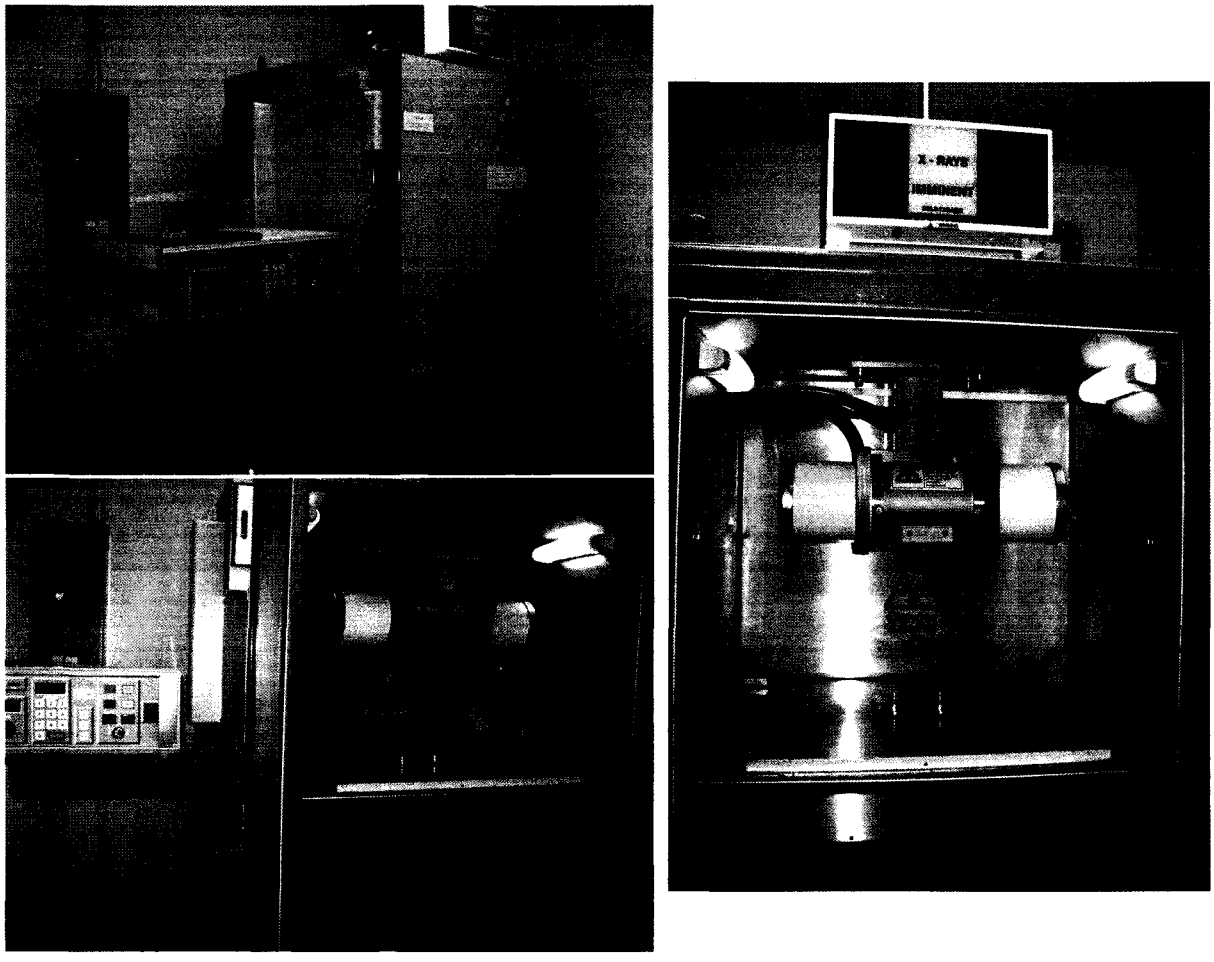

Fig. A6. Set-up of Gulmay X-ray Irradiation machine. Cells are placed on a Perspex plate, on the second lifting shelf.

APPENDIX III

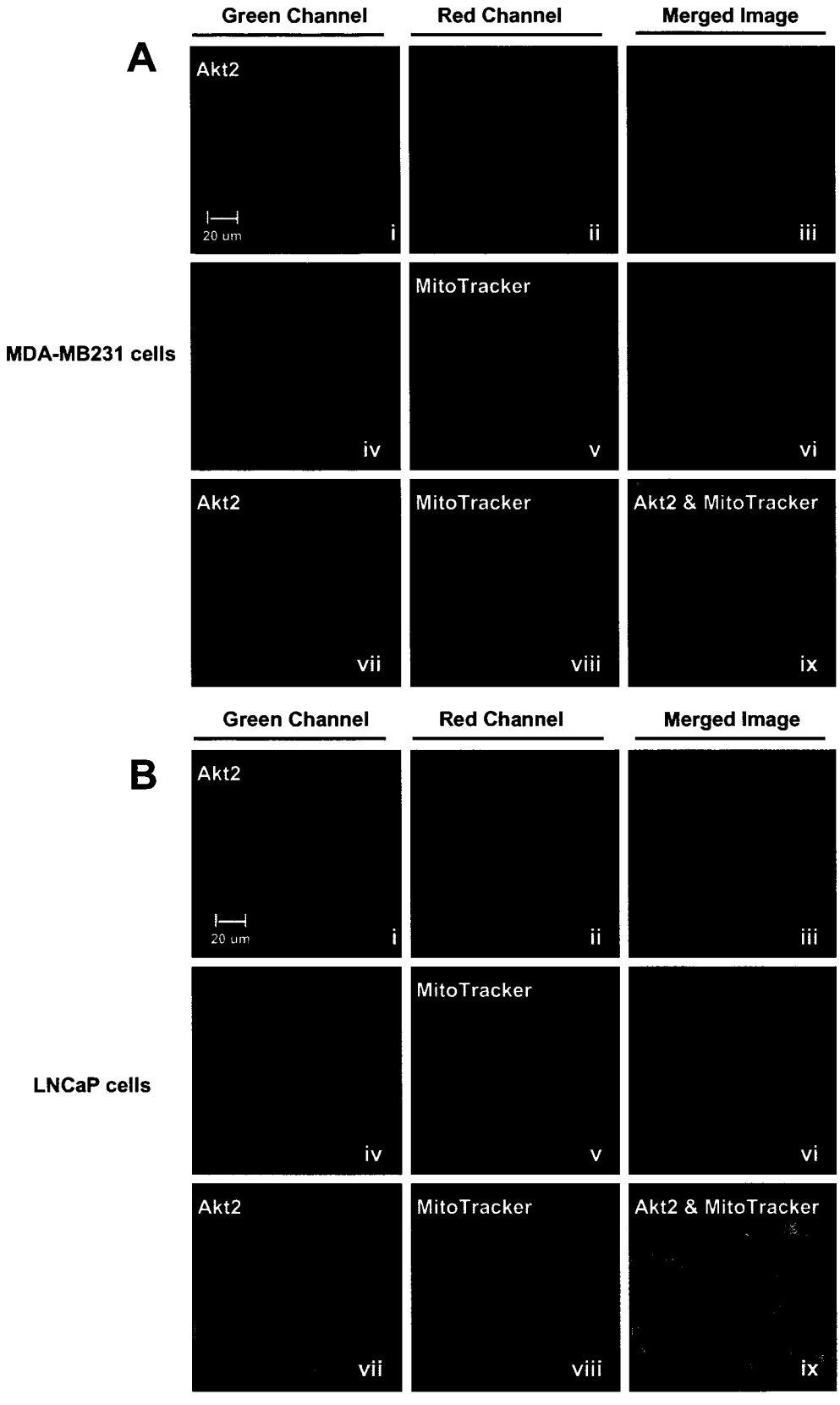
Green Channel
Red Channel
Merged Image
A
Akt2
20 um
i
ii
iii
MDA-MB231 cells
iv
MitoTracker
v
vi
Akt2
vii
MitoTracker
viii
Akt2 & MitoTracker
ix
Green Channel
Red Channel
Merged Image
B
Akt2
20 um
i
ii
iii
LNCaP cells
iv
MitoTracker
v
vi
Akt2
vii
MitoTracker
viii
Akt2 & MitoTracker
ix

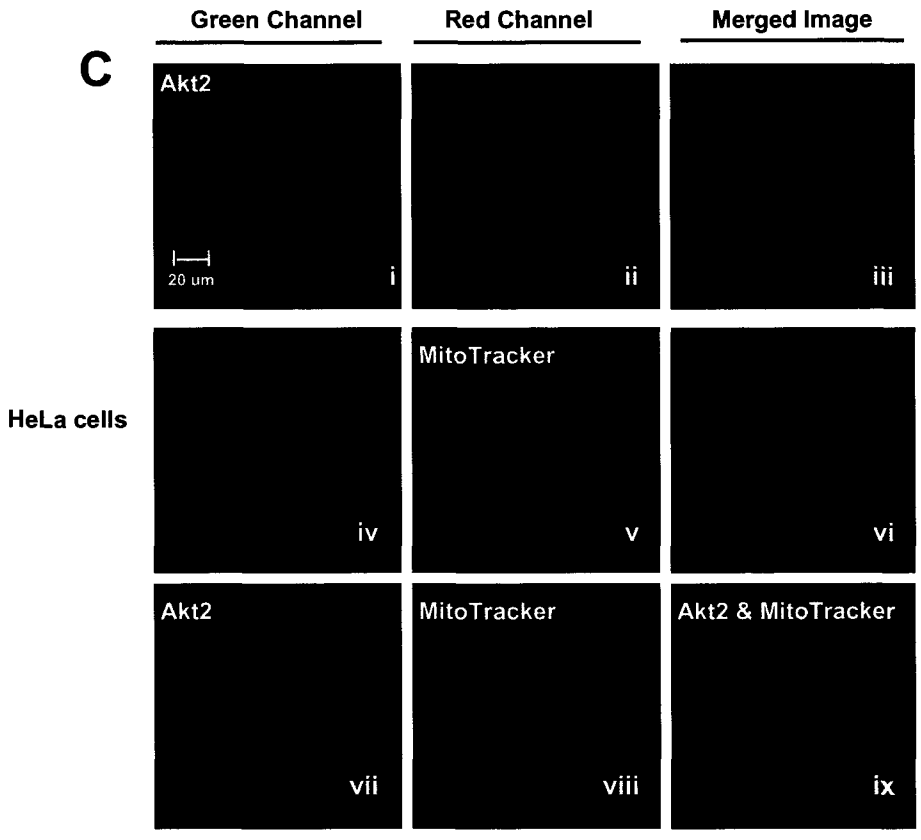

Fig. A7. Assessment of bleedthrough on MitoTracker experiments. Cells were fixed and permeabilized and labelled with either Akt2 (green) or MitoTracker (red), and both. (A) MDA-MB231 cells, (B) LNCaP cells, (C) HeLa cells. All MitoTracker loading was performed using 50 nM of MitoTracker. Note that the signal from MitoTracker alone in the red channel is stronger than when incorporated with the antibody staining (green). This is due to the fact that cells labelled with MitoTracker only were only fixed, and not permeabilized. Permeabilization results in a loss in the intensity of MitoTracker. All images were captured with the same filters and microscopy settings used in the experiments within the thesis.

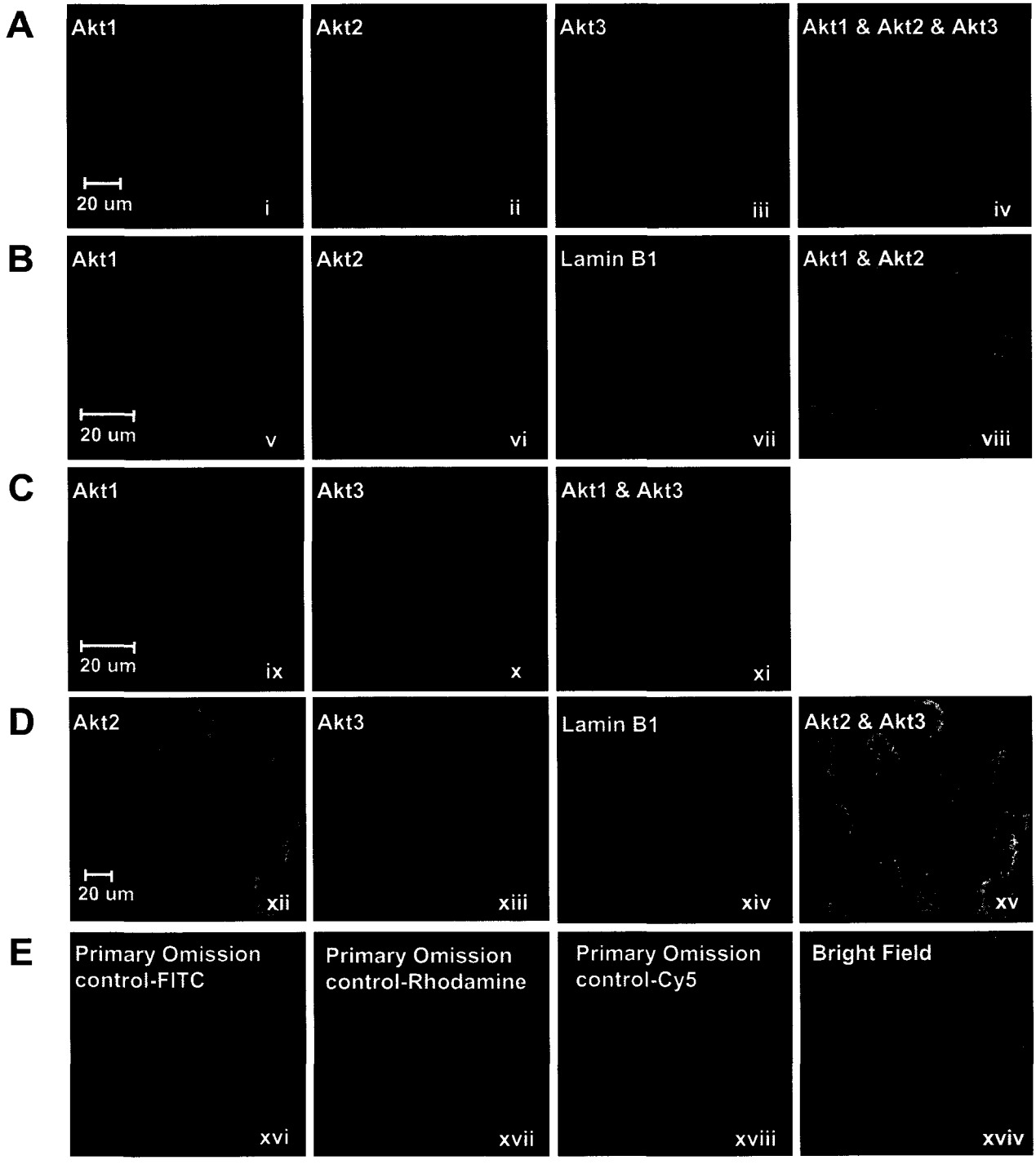
A
Akt1
20 um
i
Akt2
ii
Akt3
iii
Akt1 & Akt2 & Akt3
iv
B
Akt1
20 um
v
Akt2
vi
Lamin B1
vii
Akt1 & Akt2
viii
C
Akt1
20 um
ix
Akt3
x
Akt1 & Akt3
xi
D
Akt2
20 um
xii
Akt3
xiii
Lamin B1
xiv
Akt2 & Akt3
xv
E
Primary Omission control-FITC
xvi
Primary Omission control-Rhodamine
xvii
Primary Omission control-Cy5
xviii
Bright Field
xviv

Fig. A8. Alternate for Fig. 3.4 Panel D (Akt2/Akt3) has been replaced with an alternate image from the same trial. All other images are as presented in Fig. 3.4

A

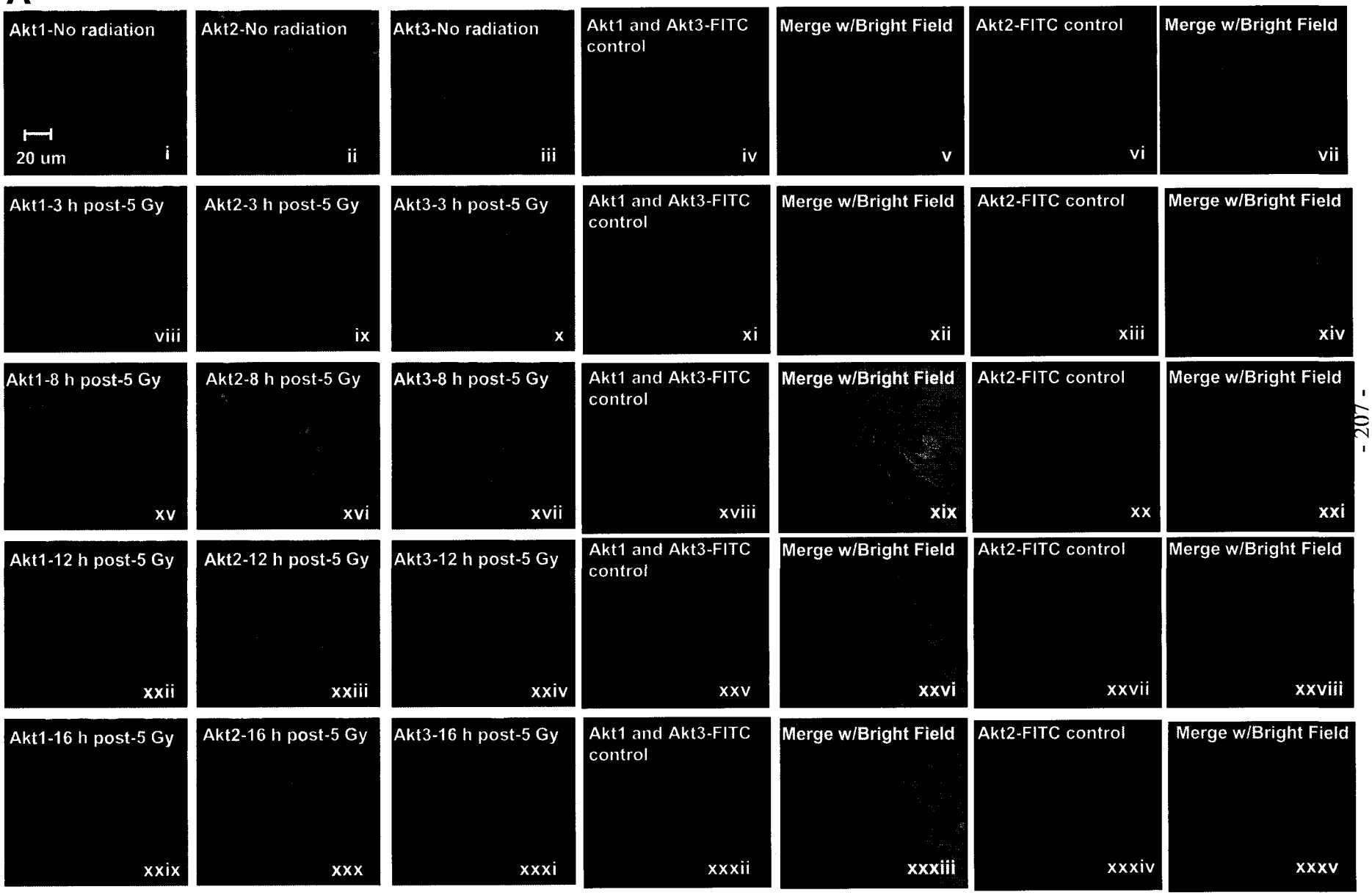
Akt1-No radiation
20 um
i
Akt2-No radiation
ii
Akt3-No radiation
iii
Akt1 and Akt3-FITC control
iv
Merge w/Bright Field
v
Akt2-FITC control
vi
Merge w/Bright Field
vii
Akt1-3 h post-5 Gy
viii
Akt2-3 h post-5 Gy
ix
Akt3-3 h post-5 Gy
x
Akt1 and Akt3-FITC control
xi
Merge w/Bright Field
xii
Akt2-FITC control
xiii
Merge w/Bright Field
xiv
Akt1-8 h post-5 Gy
xv
Akt2-8 h post-5 Gy
xvi
Akt3-8 h post-5 Gy
xvii
Akt1 and Akt3-FITC control
xviii
Merge w/Bright Field
xix
Akt2-FITC control
xx
Merge w/Bright Field
xxi
Akt1-12 h post-5 Gy
xxii
Akt2-12 h post-5 Gy
xxiii
Akt3-12 h post-5 Gy
xxiv
Akt1 and Akt3-FITC control
xxv
Merge w/Bright Field
xxvi
Akt2-FITC control
xxvii
Merge w/Bright Field
xxviii
Akt1-16 h post-5 Gy
xxix
Akt2-16 h post-5 Gy
xxx
Akt3-16 h post-5 Gy
xxxi
Akt1 and Akt3-FITC control
xxxii
Merge w/Bright Field
xxxiii
Akt2-FITC control
xxxiv
Merge w/Bright Field
xxxv

Fig. A9. Alternate for Fig. 3.14 showing all controls (primary omission and bright field) for every timepoint during the radiation timecourse.

APPENDIX IV

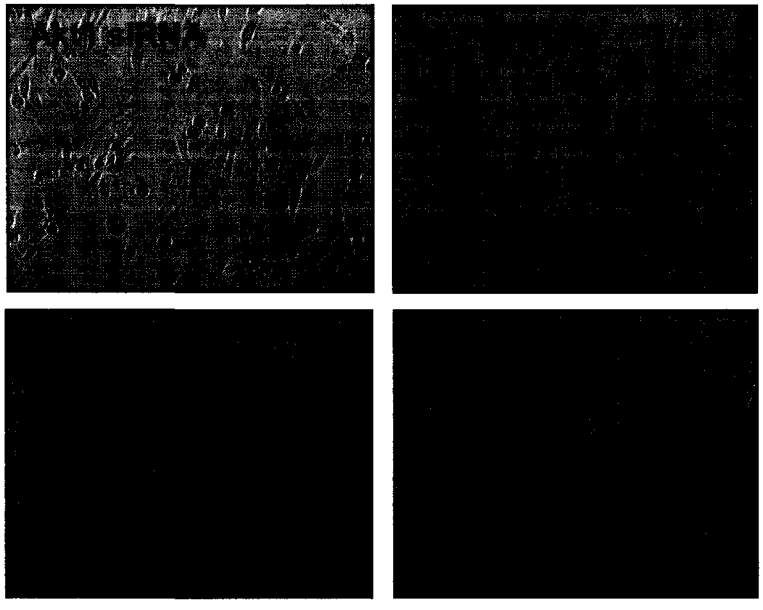

Fig. A10. Morphological changes in transfected cells 6-7 days post-transfection initiation (note the changes in Akt2).

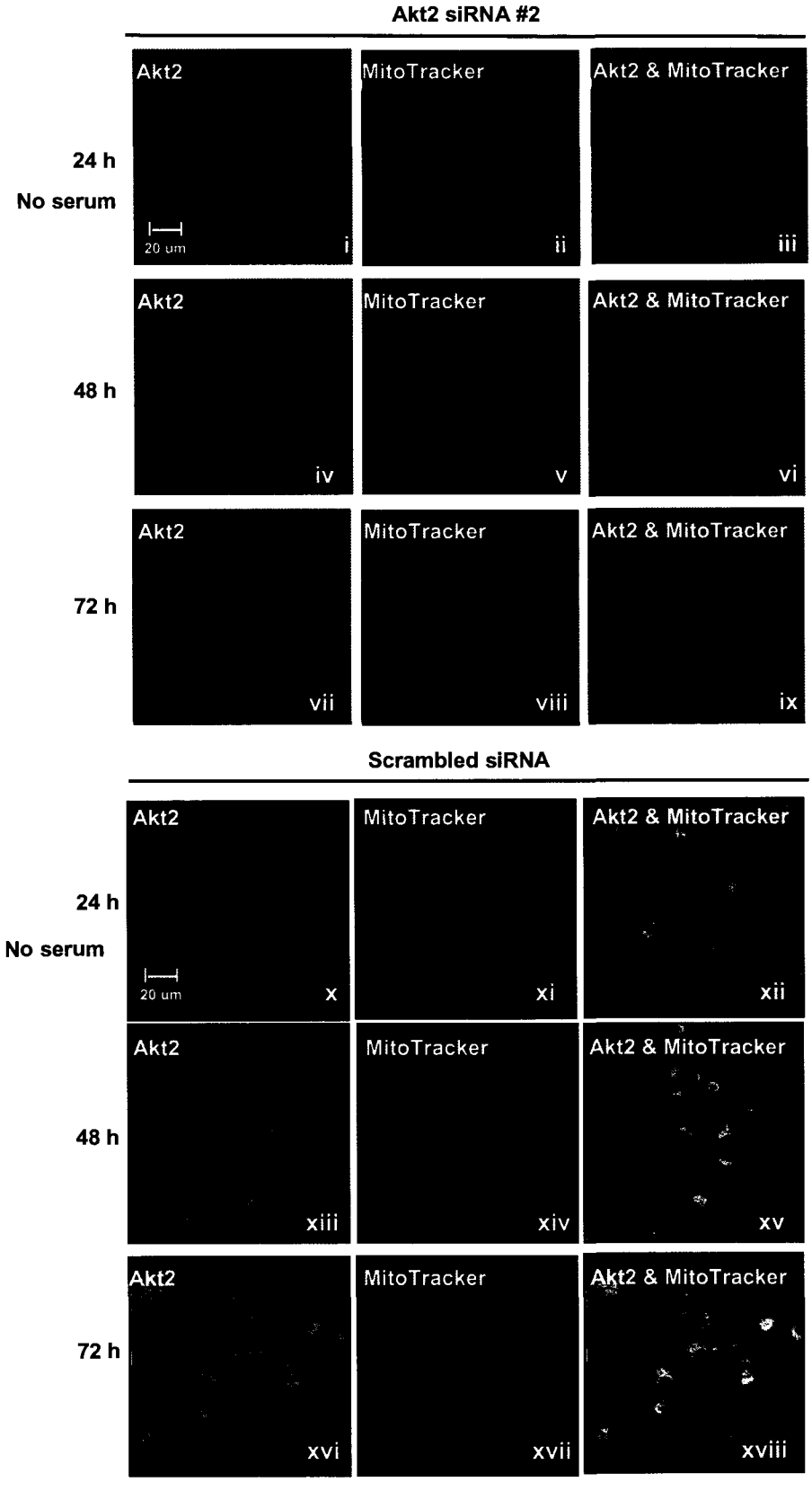

Fig. A11. Fig. 4.12 incorporating Akt2 siRNA #2 (top panel). Note that the controls were kept the same as in the original figure for comparison

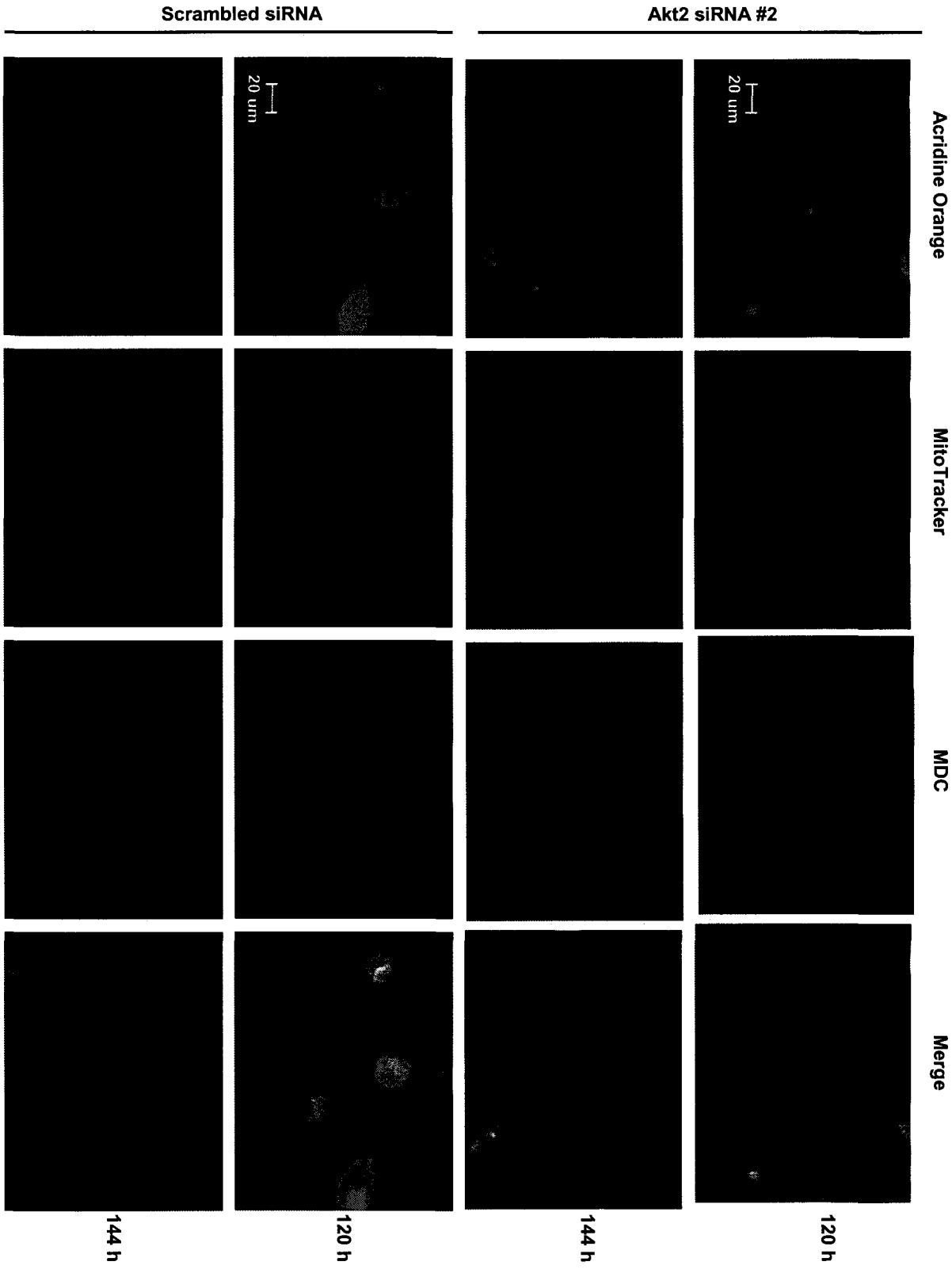

Fig. A12. Fig. 4.15 incorporating Akt2 siRNA #2 (top panel). Note that the controls were kept the same as in the original figure for comparison

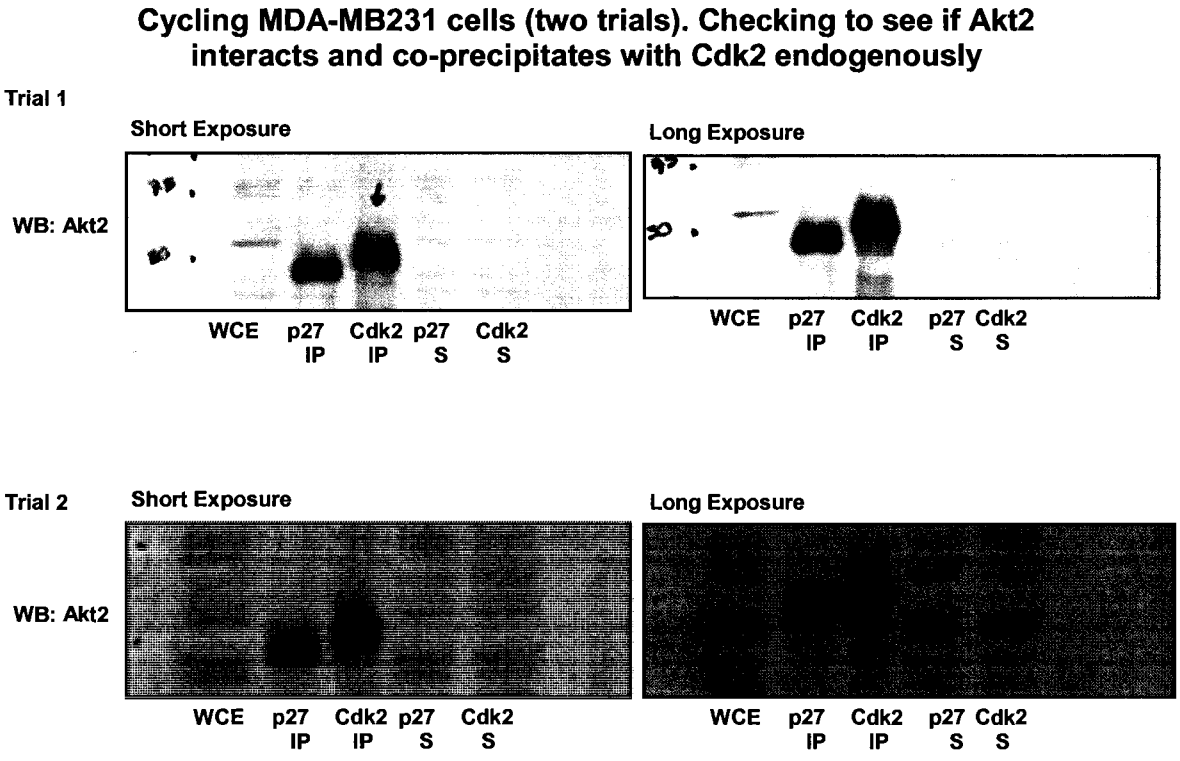

Fig. A13. Co-precipitation of Akt2 and Cdk2 in cycling MDA-MB231 cells. Preliminary results.

9.0 CURRICULUM VITAE

CURRICULUM VITAE

Stacey Assunta Santi

***Departmental Affiliation*:** Department of Biochemistry (BMI), University of Ottawa
Regional Cancer Program, Hopital Regional Sudbury Regional Hospital (HRSRH)

EDUCATION

Degrees:

2002- 2008
Ph.D (Biochemistry)
University of Ottawa, Ottawa ON
Department of BMI (Biochemistry, Microbiology & Immunology)
Thesis title: *The characterization and regulation of the Akt isoforms in a model of metastatic breast cancer.*

1999-2002
M.Sc. (Biology)
Laurentian University, Sudbury ON
Department of Biology
(Defended Dec. 2001, conferred June 2002)
Thesis title: *Studies on the geographic distribution, prevalence, intensity and bone pathology of sinus worm (Skrjabingylus SPP.) infection in mustelid species*

1996-1999
Hons. B.Sc.
Laurentian University, Sudbury ON
Concentration: Biomedicine (Biology)

1992-1996
Hons. B.A.
Laurentian University, Sudbury ON
Concentration: Psychology

ACADEMIC HISTORY:

Research Endeavors/Interests:

1. Signal transduction pathways in cancer
2. Tumor biology and cancer treatment
3. Epidemiology

SCHOLARLY AND PROFESSIONAL WORK:

Refereed Publications

2006 Prevalence, intensity, and geographic distribution of sinus worm (*Skrjabingylus nasicola*) infection in mink (*Mustela vison*) of central Ontario.

S.A. Santi, Glenn H. Parker, Natalie P. Schaffner, Liane Capodagli, and Michael A. Persinger. *Can J. Zoology* 2006, 84:1011:1018

2005 Chloroquine-mediated radiosensitization is due to the stabilization of the lysosomal membrane and subsequent induction of necrotic cell death.
H. Zhao, Y. Cai, S. Santi, R. Lafrenie, H. Lee, *Radiation Research* 2005 164:250-257

2001 Normal spatial memory following postseizure treatment with ketamine: Selective damage attenuates memory deficits in brain-damaged rodents.
S.A. Santi, L.L. Cook, M.A. Persinger, *International Journal of Neuroscience* 2001 Mar;107(1-2):63-75

Papers in Submission

2009 The ablation of Akt2 induces autophagy of the mitochondria through cell cycle arrest, downregulation of P70S6K, and deregulation of mitogenesis.
S.A. Santi and Hoyun Lee

2009 The Akt isoforms occupy distinct subcellular localizations within cells.
S.A. Santi and Hoyun Lee

Non-refereed Publications

1995 Collaborative Day Treatment Programs: Integrating Education and Mental Health Background Literature Review for the 1994-1995 Ruth Macmillan Center Year-End Report. Persi, J., Santi, S.A.

PRESENTATIONS AT PROFESSIONAL MEETINGS AND SYMPOSIA

Refereed

2004 The Akt/PKB survival pathway and radiation resistance: a role for isoform specificity?
S.A. Santi, H. Lee.
Presented at the *CARO-ACRO (Canadian Association of Radiation Oncology) Annual Scientific meeting*. Halifax, Nova Scotia, September 9-12, 2004

2003 The role of the phosphatidylinositol-3 kinase pathway in determining radiation sensitivity in the breast cancer cell line MDA-MB 231.
L. Falcioni, S.A. Santi, Hoyun Lee
Presented by Dr. Hoyun Lee (supervisor) at the *12th International Congress of Radiation Research.* Brisbane, Australia, August 17-22, 2003

2002 Studies on the distribution, prevalence and intensity of sinus worm infection (*Skrjabingylus nasicola*) in the American mink (*Mustela vison*) from Ontario, Quebec and Newfoundland
Santi, S.A.; Parker, G.H., Department of Biology, Laurentian University
Presented at the *41st Annual Meeting of the Canadian Society of Zoologists*, Lethbridge, Alberta, May 8th, 2002

2001 Sinus damage by *Skrjabingylus nasicola* and its effect on braincase capacity in the American mink (*Mustela vison*).
Santi, S.A.; Parker, G.H. Department of Biology, Laurentian University
Presented at the *40th Annual Meeting of the Canadian Society of Zoologists*

Scholarly/Academic Presentations (Non-refereed)

2008 Akt2 induces mitophagy through modulation of the mTOR pathway and cell cycle progression in breast cancer cells.
Tumour Biology Seminar Series, Northeastern Ontario Regional Cancer Centre (NEORCC), January 2008

2007 Akt/PKB and cell survival: A role for isoform specificity?
Santi, S.A. and Hoyun Lee
Annual Biochemistry Poster Day, University of Ottawa, May 2007

2007 Akt/PKB and cell survival: A role for isoform specificity?
Tumour Biology Seminar Series, Northeastern Ontario Regional Cancer Centre (NEORCC), March 2007

2005 Akt/PKB survival pathway in radiation treatment: a role for isoform specificity in breast cancer.
Santi, S.A.
Tumour Biology Seminar Series, Northeastern Ontario Regional Cancer Centre (NEORCC), April 2005

2005 The Akt/PKB survival pathway: a role for isoform specificity in breast cancer?
Santi, S.A., and Hoyun Lee
Annual Biochemistry Poster Day, University of Ottawa, March 2005

2003 The role of Akt/PKB in radiation-resistant breast cancer cells.
Santi, S.A.
Tumour Biology Seminar Series, Northeastern Ontario Regional Cancer Centre (NEORCC), October 2003

2003 The role of phosphatidylinositol-3-kinase (PI3-K) and CCAAT enhancer binding protein delta (C/EBPδ) in determining radiation sensitivity in breast cancer cells
Santi, S.A., Falcioni, L., Segura, T.M., Pearce, A.G. and Hoyun Lee
Annual Biochemistry Poster Day, University of Ottawa, April 2003

2001 Studies on the geographic distribution, prevalence, intensity and bone pathology of sinus worm (*Skrjabingylus* spp.) infection in mustelid species.
Santi, S.A., Department of Biology, Laurentian University
M.Sc. thesis defense, December 2001

2001 The prevalence and intensity of *Skrjabingylus* spp. in mustelids from Ontario, Quebec, Newfoundland and Pennsylvania.

Santi, S.A., Parker G.H., Department of Biology. Departmental Seminar, Laurentian University, March 2001.

2000 Prevalence and intensity of sinus worm infections in selected species of mustelids from various geographical regions.
Santi, S.A.; Parker, G.H.. Department of Biology, M.Sc thesis proposal Laurentian University, April, 2000.

1999 Prevalence and intensity of sinus worm (*Skrjabingylus nasicola)* infection in mink from various geographical regions of Ontario.
Santi, S.A., Parker, G.H., Department of Biology, Laurentian University
Presented at the 11th Annual Ontario Biology Day, McMaster University

1999 Prevalence and intensity of sinus worm (*Skrjabingylus nasicola)* infection in mink from various geographical regions of Ontario.
Santi, S.A., Parker, G.H., Department of Biology, Laurentian University
B.Sc. Honours thesis defense, Laurentian University, March 1999

1996 Critical thinking, hostility and physiological arousal: Differences in the Type A/B Behaviour Pattern. B.A. Honours thesis defense presented at Laurentian University, March 1996

RELEVANT TRAINING EXPERIENCE:

1999-2001 ***Teaching Assistant***
Description: Supervisors Dr. G.H. Parker and Dr. F.V. Clulow.
Courses taught: Vertebrate Physiology, Histology, Anatomy and Physiology, Embryology

1999 ***Research Assistant***
Description: Conducted under the supervision of Dr. G.H. Parker; research pertaining to parasitology and pathology; epidemiology of parasitic infections.

1997 ***Volunteer Research Assistant***
Description: Neuroscience Research Group (under the supervision of Dr. M.A. Persinger); conducted research experiments examining spatial memory in seizured rats.

1996-1997 ***Teaching Assistant***
Description: Developmental Psychology (Supervisor: Professor. B. Bourget) and Forensic Psychology (Supervisor: Dr. P.M. Valliant); assisted students, marked papers, helped set examinations and tests and compiled research relating to Canadian criminal law.

1994-1996 ***Research Assistant***
Description: Assisted Dr. J. Persi at Sudbury Algoma Hospital/Network North in research and compiling a final report on certain treatment programs relevant to the field of Developmental Psychology.

1993-1994 ***Volunteer Research Assistant***
Description: Developmental Psychology; supervised by Dr. B. Bigelow; compiled research data for a study with preschool children.

RELEVANT COURSEWORK/SKILLS:

Laboratory and Molecular Biology Techniques

Tissue cell culture (both cancer and non-transformed cell lines), cell assays (clonogenic assays, cell titer assays, as well as MTT and BrdU assays), siRNA technology, recombinant DNA technology (transfection and cloning), FACS analysis, quantitative RT-PCR/RT-PCR, protein chemistry (1D-gel electrophoresis, immunoprecipitation, western blotting, subcellular fractionation), immunohistochemistry, immunocytochemistry, confocal and fluorescent microscopy, signal transduction pathway analysis.

Statistics and Computer Software

SPSS (both VAX and Windows framework), as well as GraphPad Prism.

SUPERVISORY DUTIES:

2007-2008 Supervisor of project/lab work to undergraduate summer students
2005-2008 Deputy Safety Officer, HRSRH Regional Cancer Program

AWARDS/SCHOLARSHIPS:

2005-2006	University of Ottawa Doctoral Research Scholarship ($9000)
2005	Janice Skot Bursary ($1000), Northern Cancer Research Foundation
2004	University of Ottawa Travel Award ($500)
2004	CARO-ACRO Travel Award ($1000) Halifax, Nova Scotia.
2003	Dr. Randy Bissett Bursary, Northern Cancer Research Foundation ($1000)
2001	A. Murray Fallis Award for the Best Parasitology Student Oral Presentation. Presented by the Canadian Society of Zoologists ($150)
2001	American Society of Parasitologists Student Travel Award
2000-2001	Ontario Graduate Scholarship Institutional Award ($7000)
1992-1993	Laurentian University Tuition Scholarship ($2200)

VOLUNTEER WORK:

August 2005 Strokes for Hope Golf Tournament, sponsored by the Northern Cancer Research Foundation

October 2004 Northeastern Ontario Regional Cancer Centre (NEORCC) Annual Open House/Career Night

October 2004 Northern Ontario Surgical Oncology Meeting. Northeastern Ontario Regional Cancer Centre (NEORCC), Sudbury, ON

August 2004 Strokes for Hope Golf Tournament, sponsored by Northern Cancer Research Fund (NCRF)

October 2003 Northeastern Ontario Regional Cancer Centre (NEORCC) Annual Open House/Career Night

August 2003 Strokes for Hope Golf Tournament, sponsored by Northern Cancer Research Fund (NCRF)